ACCELERATOR PROJECTS AT KEK

K. Oide [KEK, Ibaraki, Japan]

Abstract

This is a short talk to introduce accelerator projects at KEK including the Super B-Factory (SuperKEKB), Photon Factory (PD/PF-AR) and the high-intensity proton machine J-PARC. Some R&D efforts for future such as the International Linear Collider (ILC/STF/ATF) and the Energy Recovery Linac will be also overviewed. It may briefly mention on critical issues related to beam instrumentation for each project.

CONTRIBUTION NOT RECEIVED

ISBN 978-3-95450-119-9

PROGRESS OF BEAM INSTRUMENTATION IN J-PARC LINAC

A. Miura# and the J-PARC Beam Instrumentation Group
J-PARC Linac, Japan Atomic Energy Agency, Tokai, Ibaraki, 319-1195, Japan

Abstract

J-PARC, one of the high intensity proton accelerators, achieved the output power of 300 kW at the downstream rapid cycling synchrotron with the beam energy 181 MeV and the beam current 15 mA. When an upgrade of an ion source which can provide 50 mA and the installation of the additional acceleration cavities for the energy upgrade up to 400 MeV are completed, output power reaches 1 MW. To meet with the requirements of the high intensity beam instruments, we prepare several measures against high intensity proton related issues. Following subjects have been reported among many subjects: development of strip-line type beam position monitors, beam current monitors, phase monitors and transverse profile monitors. And the subjects of the beam instruments for the energy upgraded Linac including the longitudinal beam profile monitor and the developing laser based profile monitor are mentioned. A big earthquake occurred on March 11, 2011. J-PARC had a big damage, but we successfully resumed a commercial operation. This paper also mentions the influence of the quake on the J-PARC Linac.

INTRODUCTION

J-PARC (Japan Proton Accelerator Research Complex) Linac aims to provide high intensity beams of peak current 50 mA, beam energy 181 MeV, pulse width 0.5 mA and repetition rate 25 Hz using an RFQ, three DTL cavities and 15 SDTL cavities and two beam transports which have two debuncher cavities include the matching points to inject the downstream rapid cycling synchrotron (RCS) [1]. Beam parameters of Linac are listed in table 1.

In the energy upgrade project since 2013, present two debuncher cavities are replaced to SDTL section as the 16th acceleration cavity. Twenty one ACS (Annular-Coupled Structure Linac) cavities will be installed in the present A0BT subsection. To meet with this project, the beam instruments for the future ACS and L3BT section for the beam commissioning are newly designed and fabricated [2]. The goal of 133 kW beam power and hand-on maintenance will place significant demands on the performance and operational reliability of accelerator diagnostics systems.

Table 1: Operational Beam Parameters of Present and Upgraded Linac

Particle	Negative hydrogen ion
Peak Beam Current	5 - 50 mA
Source Energy	180 - 400 MeV
Typical Bunch Length	1 - 2 deg. (rms)
Typical Transverse Side	1 - 2 mm (rms)
Pulse Width	0.5 msec
Bunch Repetition Frequency	324 MHz, 972 MHz for New ACS cavities
Operational Repetition Rate	1 - 25 Hz
Chopper beam-on ratio	56 %
Beam power	36 kW (133 kW after upgrade)

#akihiko.miura@j-parc.jp

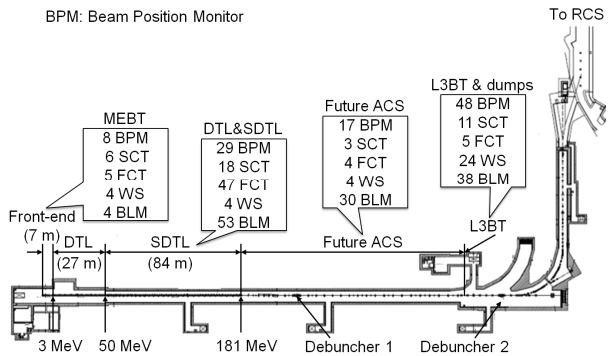

Figure 1: Delivery of beam instruments in the J-PARC Linac.

COMMISSIONING TOOLS

Number of the Commissioning Tools in Linac

As delivery of beam instruments and parts on the beam line are not at a time, the sensors of beam instruments are installed in the following order in subsection of LINAC.

(1) MEBT1 (Medium Energy Beam Transport)
(2) DTL (Drift-Tube Linac) & SDTL (Separated DTL)
(3) A0BT (Beam Transport from ACS to Beam Dump)
(4) L3BT (Beam Transport from Linac to RCS)

After the instruments had been tested in the DTL commissioning in KEK site, installation of all instruments had conducted. Each of the instruments is handled and supervised by J-PARC staffs all through the installation. In the present beam line, 38 beam current monitors (SCT: slow current transformer), 61 phase monitors (FCT: fast current transformers), 36 beam profile monitors (WSM: wire scanner monitor), 102 beam position monitors (BPM) and 124 beam loss monitors (BLM) are employed for the beam operation [3-4] (Fig. 1). In the upgrade project, 24 SCTs, 51 FCTs, 4 WSMs, 49 BPMs and 30 BLMs are replaced from those of present beam line. And three bunch shape monitors (BSM) are newly employed.

Beam Position Monitor (BPM)

J-PARC Linac employs over a hundred of BPMs which have about 40 - 180 mm diameter and 4-stripline electrodes with one end shorted by 50 Ω terminations [5]. Electrostatic computations are used to adjust the BPM cross-section parameters to obtain 50 Ω transmission lines. BPMs are sustained by pole edge of quadrupole magnet and designed to reduce the offset between quadrupole

ISBN 978-3-95450-119-9

BEAM INSTRUMENTATION FOR THE SUPERKEKB RINGS

M. Arinaga, J. W. Flanagan, H. Fukuma*, H. Ikeda, H. Ishii, S. Kanaeda,
K. Mori, M. Tejima, M. Tobiyama, KEK, Tsukuba, Japan
G. Bonvicini, H. Farhat, R. Gillard, Wayne State U., Detroit, MI 48202, USA
G.S. Varner, U. Hawaii, Honolulu, HI 96822, USA

Abstract

The electron-positron collider KEKB B-factory is currently being upgraded to SuperKEKB. The design luminosity of 8 x 10^{35} /cm^2/s will be achieved using beams with low emittance, of several nm and doubling beam currents to 2.6 A in the electron ring (HER) and 3.6 A in the positron ring (LER). A beam position monitor (BPM) system for the HER and LER will be equipped with super-heterodyne detectors, turn-by-turn log-ratio detectors with a fast gate to measure optics parameters during collision operation and detectors of BPMs near the collision point (IP) for orbit feedback to maintain stable collision. New X-ray beam profile monitors based on the coded aperture imaging method will be installed aiming at bunch by bunch measurement of the beam profile. A large angle beamstrahlung monitor detecting polarization of the synchrotron radiation generated by beam-beam interaction will be installed near IP to obtain information about the beam-beam geometry. The bunch-by-bunch feedback system will be upgraded using low noise front-end electronics and new 12-bit iGp digital filters. An overview of beam instrumentation for the SuperKEKB rings will be given in this paper.

INTRODUCTION

The electron-positron collider KEKB B-factory is currently being upgraded to SuperKEKB[1]. The design luminosity of 8 x 10^{35} /cm^2/s will be achieved using the so called nano-beam scheme[2]. Machine upgrades include the replacement of the current, cylindrical LER beam pipes to one with ante-chambers so as to withstand large beam currents and mitigate the electron cloud effect, a new final focus in the interaction region (IR) in order to adopt the nano-beam scheme and the construction of a positron damping ring for positron injection. The first beam is expected in the Japanese FY 2014. Machine parameters of SuperKEKB are shown in Table 1.

BEAM POSITION MONITOR SYSTEM

The number of beam position monitors (BPMs) in SuperKEKB is 445 in the LER and 466 in the HER. The closed orbit measurement system of KEKB utilized a VXI system[3]. The KEKB detector was a 1 GHz narrowband superheterodyne detector module. One module covered four beam position monitors (BPMs), two in the LER and two in the HER, by multiplexing the signals with switch modules. The main detector system of SuperKEKB follows that of KEKB. The narrowband detectors of KEKB are reused in the SuperKEKB HER. A new narrowband detector with a detection frequency of 509 MHz is being developed, since the cutoff frequency of the new LER ante-chamber is below 1 GHz. Additionally, turn by turn detectors will be installed at selected BPMs at the rate of three per betatron wave length to measure the optics during collision. Also, a special wideband detector is being installed for the four BPMs closest to the collision point (IP) for orbit feedback to maintain stable collision. Table 2 shows a list of detectors in SuperKEKB.

Table 1: Machine Parameters of SuperKEKB

	HER	LER
Energy (GeV)	7	4
Circumference (m)	3016	
Beam current (A)	2.6	3.6
Number of bunches	2500	
Single bunch current (mA)	1.04	1.44
Bunch separation (ns)	4	
Bunch length (mm)	5	6
Beta function @IP hor./ver. (mm)	25/0.30	32/0.27
Emittance (nm)	4.6	3.2
X-Y coupling (%)	0.28	0.27
Vertical beam size at IP (nm)	59	48
Damping time: trans./long. (ms)	58/29	43/22

Displacement sensors, which measure the mechanical displacement between a BPM head and a sextupole magnet, are installed at all BPMs neighboring the sextupole magnets, same as at KEKB.

Button Electrode and BPM Chamber

The BPM chambers and button electrodes in the HER are reused from KEKB. A button electrode with a diameter of 6 mm has been developed for the LER to reduce the beam power at the electrode[4]. The electrode is a flange type for easy replacement and for removal during the TiN coating process of the chamber to reduce the electron cloud. A pin-type inner conductor is used for tight electrical connection. The estimated longitudinal loss factor of a beam chamber with four electrodes is 0.16 mV/pC. The coupling impedance is 2 ohm at the center frequency of 14.8 GHz and the Q value is 38. The estimated growth time of the longitudinal coupled-bunch

*hitoshi.fukuma@kek.jp

ISBN 978-3-95450-119-9

A GENERIC BPM ELECTRONICS PLATFORM FOR EUROPEAN XFEL, SwissFEL AND SLS

Boris Keil, Raphael Baldinger, Robin Ditter, Waldemar Koprek, Reinhold Kramert, Goran Marinkovic, Markus Roggli, Markus Stadler, Daniel Marco Treyer, PSI, Villigen, Switzerland

Abstract

PSI is currently developing the 2nd generation of a generic modular electronics platform for linac and storage ring BPMs and other beam diagnostics systems. The first platform, developed in 2004 and based on a generic digital back-end with Xilinx Virtex 2Pro FPGAs, is currently used at PSI for proton accelerator BPMs, resonant stripline BPMs at the SwissFEL test injector facility, and a number of other diagnostics and detector systems. The 2nd platform will be employed e.g. for European XFEL BPMs, a new SLS BPM system, and the SwissFEL BPM system. This paper gives an overview of the architecture, features and applications of the new platform, including interfaces to control, timing and feedback systems. Differences and synergies of the different BPM and non-BPM applications will be discussed.

INTRODUCTION

As shown in Table 1, we will build an overall number of 720 BPM electronics of for different accelerators and BPM types in the next years. Moreover, we plan to use our new BPM digitizer and digital back-end electronics also for non-BPM applications.

Table 1: PSI BPM Activities and Related Accelerators

Accele-rator	***1st Beam***	***BPM Quantity***	***Status / Activity***
SLS	2000	~140(button, resonant stripline)	Digital BPM system since 2000. 2011: Start design of new BPM electronics.
SwissFEL Test Injector	2010	~25 (resonant stripline, …)	19 resonant stripline BPMs in operation. Test area for FEL cavity & button BPMs.
FLASH-II	2013	~20 (cavity)	PSI provides undulator cavity BPM electronics (E-XFEL pre-series).
E-XFEL	2014/15	~410 (button, cavity)	PSI provides electronics for ~290 button & ~120 dual-resonator cavity BPMs.
SwissFEL	2016	~150 (cavity)	Adaptation of E-XFEL cavity BPMs to lower charge & shorter bunch spacing.

European XFEL

PSI will provide the electronics for the European XFEL (E-XFEL) BPM system [1] as a Swiss in-kind contribution, with the exception of ~30 RF front-ends (RFFEs) for the re-entrant cavity BPMs in the cold E-XFEL linac that are designed by CEA/Saclay. First beam for the E-XFEL injector is scheduled for autumn 2014, beam in the main linac and undulators is expected one year later.

FLASH-II

A pre-series version of the E-XFEL undulator cavity BPM electronics will be used at FLASH-II [2], a 2nd undulator line for the VUV FEL facility FLASH to be commissioned mid 2013.

SwissFEL BPMs

SwissFEL [3] is a 0.1nm hard X-ray SASE FEL currently being developed at PSI. 1st beam in the undulators is expected mid 2016. PSI develops both the BPM electronics and the pickups for SwissFEL, based on the E-XFEL design but adapted to the lower charge (10-200pC vs. 100-1000pC) and shorter bunch spacing (28ns vs. 222ns) of SwissFEL.

SwissFEL Test Injector BPMs

In 2010, PSI commissioned the SwissFEL test injector facility (SITF), a 250MeV linac used for R&D and component development for SwissFEL. Since first prototypes of BPM electronics for E-XFEL and SwissFEL were still under development in 2010, the BPM system of SITF [4] is based on the previous generation of BPM electronics, using the same digital back-end board as the PSI proton cyclotron BPM system [5].

SLS BPM Upgrade

In 2011, PSI also started first developments for new SLS BPM electronics [6]. However, the present SLS BPM system that was commissioned 12 years ago [7] still has excellent mean time between failure (MTBF) and satisfies the present user requirements. Therefore the SLS upgrade activities have lower priority that our FEL projects where 1st beam milestones have to be met. Nevertheless, the timely development of a new SLS BPM system is motivated by long-term maintenance, growing user requirements, and the significant improvements in performance and functionality enabled by the latest analog and digital IC generations. Moreover, due to large synergies with the E-XFEL BPM systems, the development effort for the new SLS electronics is significantly reduced. As shown in Figure 1, FEL cavity and SLS button BPM electronics can use the same digital back-end mezzanine carrier FPGA board and same type of fast high-resolution (16-bit) ADC mezzanine. The main structural difference of the RFFEs is the lack of a mixer and local oscillator (LO) for the SLS, where the lower BPM pickup signal frequency of 500MHz allows direct undersampling.

ISBN 978-3-95450-119-9

MODELING AND PERFORMANCE EVALUATION OF DCCTS IN SSRF*

Zhichu Chen†, Yongbin Leng, Yun Xiong, Weimin Zhou, SSRF, SINAP, Shanghai, China

Abstract

Direct Current Current Transformer (DCCT) is the most commonly used high precision current monitor in modern particle accelerators including Shanghai Synchrotron Radiation Facility (SSRF). Three types of noise have been observed in the output signal of the DCCT in the storage ring of SSRF: power line noise, beam current related narrow band noise and random square wave noise from nowhere. This article will discuss the noise removal algorithms in SSRF and the performance of the DCCTs afterwards.

INTRODUCTION

As the biggest science research facility in China, SSRF has started user run with 7 beam lines since March, 2009. The whole facility contains a 150 MeV LINAC, a full energy booster and a 3.5 GeV storage ring and has offered 77200 hours' user time. Since the demand for the beam quality is being increasing with the growth of the user group, the accuracy of the measurement of the direct current (DC) component of the beam current has become particularly important.

According to the design requirements of the SSRF as a third generation light source, a high precision DC beam current monitor with the ranger greater than 400 mA and the resolution requirements for booster and storage ring are 50 μA@10 Hz and 10 μA@1 Hz respectively. The refresh rate of the DC beam current and the corresponding lifetime should not be lower than 1 Hz in order to keep the machine to operate normally.

The New Parameter Current Transformer (NPCT) sensor from the Bergoz Instrumentation has been evaluated at the SPEAR3.[1] NPCT175 with a resolution of 1 $\mu A/\sqrt{Hz}$ was chosen to meet the design requirements. Two DCCTs were positioned at section 15 and 17 and were named DCCT15 and DCCT17 respectively. The sensor is designed to be sensitive to the electromagnetic fields so that a shielding system is needed to isolate the sensor from the outside fields. The design of the shielding system was borrowed from SPEAR3 (see the exploded view in Fig. 1) since it seems rational enough and it is proved to perform competently on that machine.

The PXI bus industrial computer was selected as the input-output (IO) controller platform for its compatibility, stability, availability for various of IO boards and the CPU computing capability. In order to choose a proper digital voltmeter (DVM) module from the 4070 series of National Instrumentation (NI), a noise test was made between NI4070 (6.5 bit) and NI4071 (7.5 bit). Another test using the NPCT175 and NI4070 as a whole system was also processed. The result is shown in Fig. 2 and we can see that:

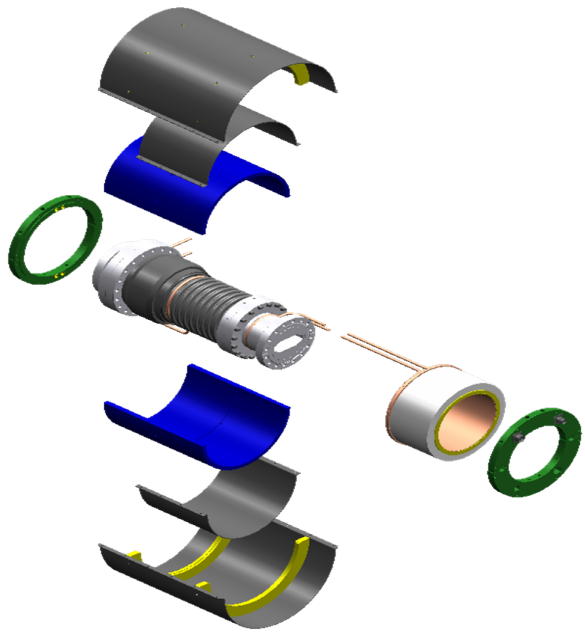

Figure 1: Exploded view of the shielding system designed by SPEAR3.

- The performances of NI4070 and NI4071 are quite close when the sampling rate is higher than 200 Hz;
- The noise of the DVMs—both NI4070 and NI4071—is much less than the NPCT-DVM system when the sampling rate is lower than 40 Hz which means the noise of the sensor has a great contribution to it;
- The performance of the NPCT-DVM system is close to that of the DVMs when the sampling rate is higher than 40 Hz.

The sampling rate was chosen to be a relatively high value of 10 kHz because showing more details of the beam current waveform was preferred, especially during the commisioning. NI4070 DVM was selected as the data acquisition module of the DC beam current monitor system since the performance of NI4071 wouldn't be significantly

* Work supported by National Natural Science Foundation of China (No. 11075198)

† chenzhichu@sinap.ac.cn

ISBN 978-3-95450-119-9

VERTICAL EMITTANCE MEASUREMENTS USING A VERTICAL UNDULATOR

K.P. Wootton*, M.J. Boland, G.N. Taylor, R.P. Rassool,
School of Physics, University of Melbourne, VIC, Australia
M.J. Boland, B.C.C. Cowie, R. Dowd, Y.-R.E. Tan, Australian Synchrotron, Clayton, VIC, Australia
Y. Papaphilippou, CERN, BE Department, Geneva, Switzerland

Abstract

We have reported on initial work to measure vertical emittance using a vertical undulator. Using simulations, we motivate the important experimental subtleties in the application of this technique. Preliminary measurements of undulator spectra are presented that demonstrate the high sensitivity of vertical undulators to picometre vertical emittances. Finally, possible future applications of this technique are explored.

INTRODUCTION

Electron storage ring light sources and damping rings continue to produce beams of increasingly small vertical emittance. With the recent report of the minimum observed vertical emittance of $\varepsilon_y = 0.9 \pm 0.4$ pm rad at the SLS [1], we require techniques sensitive to sub-micrometre electron beam sizes. At the Australian Synchrotron, we have developed a technique for measuring the vertical emittance of electron beams that we call vertical undulator emittance measurement [2].

In these proceedings, we assess undulators as a beam diagnostic. In contrast to horizontal undulators being largely insensitive to picometre vertical emittance, we highlight the sensitivity of vertical undulators to the vertical emittance. We present preliminary results and simulations, as well as ideas for future vertical emittance diagnostics.

THEORY

Undulators have been used as diagnostics of storage ring emittance. Horizontal undulators – undulators that deflect the electron beam in the orbit plane of the ring – have been demonstrated to give excellent measurement of the horizontal beam size and energy spread [3–7]. Where the electron beam emittance is close to fully-coupled, the brilliance of horizontal undulators exhibits some sensitivity to the vertical emittance [4]. Electron storage and rings typically design for transverse emittance ratios less than a few percent, with damping ring designs aiming for minimum vertical emittance. In this low vertical emittance limit horizontal undulators are identified as particularly insensitive to vertical emittance, limited by the single-electron opening angle of undulator radiation [3].

* k.wootton@student.unimelb.edu.au

Photon Beam Brilliance

Modelled in SPECTRA [8], the sensitivity of horizontal and vertical undulators to vertical emittance is illustrated in Figure 1 below.

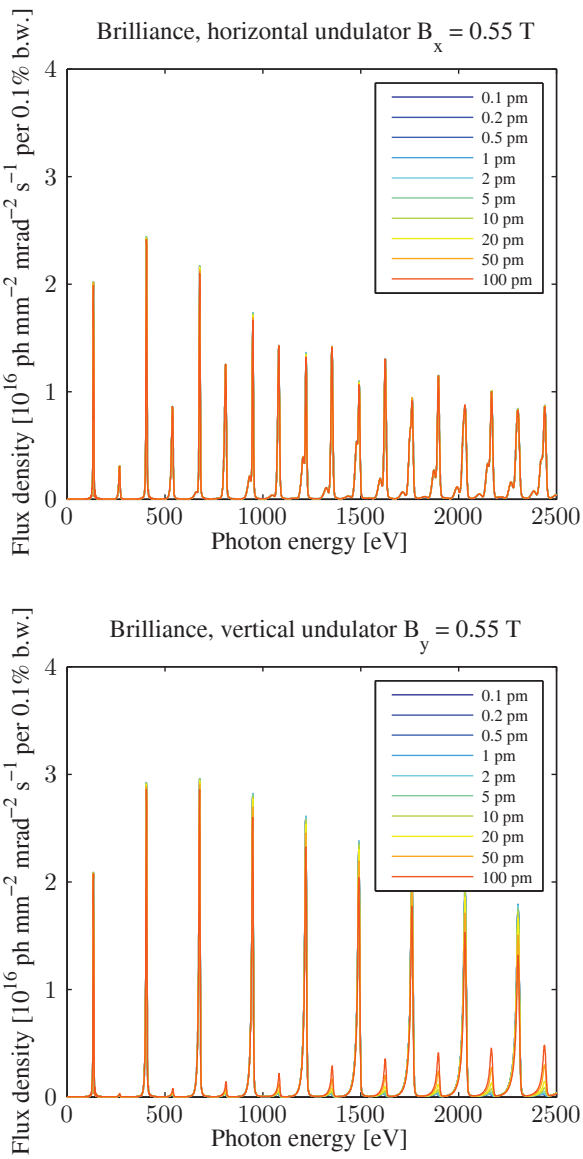

Figure 1: Photon beam brilliance, for horizontal undulator and vertical undulator of deflection parameter $K = 3.85$, for ASLS user lattice with $\eta_x = 0.1$ m in the insertion [9].

ISBN 978-3-95450-119-9

UV/X-RAY DIFFRACTION RADIATION FOR NON-INTERCEPTING MICRON-SCALE BEAM SIZE MEASUREMENT

L. Bobb *, N. Chritin, T. Lefevre CERN, Geneva, Switzerland
P. Karataev, JAI at RHUL, Egham, Surrey, UK
M. Billing, CLASSE, Ithaca, New York, USA

Abstract

Diffraction radiation (DR) is produced when a relativistic charged particle moves in the vicinity of a medium. The electric field of the charged particle polarizes the target atoms which then oscillate, emitting radiation with a very broad spectrum. The spatial-spectral properties of DR are sensitive to a range of electron beam parameters. Furthermore, the energy loss due to DR is so small that the electron beam parameters are unchanged. Therefore DR can be used to develop non-invasive diagnostic tools. The aim of this project is to measure the transverse (vertical) beam size using incoherent DR. To achieve the micron-scale resolution required by CLIC, DR in UV and X-ray spectral-range must be investigated. During the next few years, experimental validation of such a scheme will be conducted on the CesrTA at Cornell University, USA. Here we present the current status of the experiment preparation.

INTRODUCTION

Over the last 30 years Optical Transition Radiation (OTR) [1] has been widely developed for beam imaging and transverse profile measurement. However OTR based systems are invasive and do not permit the measurement of high charge density beams without risking damage to the instrumentation. Beam diagnostics using Diffraction Radiation [2, 3] has been proposed as an alternative [4, 5].

In the optical wavelength range the use of diffraction radiation (ODR) as a high-resolution non-invasive diagnostic tool for transverse beam size measurement has been widely investigated; at the Advanced Test Facility at KEK in Japan [6], at the FLASH test facility at DESY [7] and at the Advanced Photon Source at Argonne, USA [8]. At ATF2 the achieved beam size sensitivity was as small as 14 µm [9].

For next generation linear colliders such as the Compact Linear Collider (CLIC) [10], transverse beam size measurements must have a resolution on the micron-scale. Currently, laser wire scanners [11] are the main candidate for non-invasive high resolution measurements. However, over a distance of more than 40 km many laser wire monitors would be required. This is both costly and difficult to maintain- DR could offer a simpler and cheaper alternative. However as expected theoretically [12], the DR sensitivity to beam size becomes negligible at extreme beam energies. Our aim is to develop a non-invasive beam size monitor with micrometer resolution for electron and positron beams of a few GeV energy. In the CLIC machine layout [15], these devices would then be used both from the Damping ring exit to the entrance of the Main beam linac and in the CLIC Drive beam complex (2.4 GeV).

Table 1: Phase 1 Experiment Parameters for CesrTA [13] and Comparison with the CLIC Damping Ring Complex [14]

	E (GeV)	σ_H (µm)	σ_V (µm)
CesrTA	2.1	320	∼9.2
	5.3	2500	∼65
CLIC	2.86	∼10-200	∼1-50

The Cornell Electron Storage Ring, with beam parameters as shown in Table 1 was primarily reconfigured as a test accelerator (CesrTA) [16] for the investigation of beam physics for the International Linear Collider damping rings. An experimental program was recently proposed to develop and test a Diffraction Radiation monitor to be installed in the straight section of the ring where small beam sizes can be achieved. The sensitivity to beam-size is improved at shorter observation wavelengths, so the experimental program has been divided into two consecutive phases. The first phase, we are currently implementing at the moment aims to measure the beam size in the 20–50 µm range using visible and UV light. If successful a second phase will be launched in order to push the detector sensitivity down to few micrometers using shorter wavelengths in the soft x-ray range. This paper presents the current status of our work.

SIMULATIONS

ODR Model and the PVPC

The ODR model considers the case when a charged particle moves through a slit between two tilted semi-planes i.e. only DR produced from the target is considered. The author of [17] has shown that the vertical polarisation component is sensitive to beam size. In [18], the expression for the ODR vertical polarisation component convoluted with a Gaussian distribution is given and shown here in Eq. 1 where α is the fine structure constant, γ is the Lorentz factor, θ_0 is the target tilt angle, $t_{x,y} = \gamma\theta_{x,y}$ where $\theta_{x,y}$ are the radiation angles measured from the mirror reflection direction, λ is the observation wavelength, σ_y is the rms vertical beam size, a is the target aperture size, $\overline{a_x}$ is the

* lorraine.bobb@cern.ch

ISBN 978-3-95450-119-9

THE FIRST ELECTRON BUNCH MEASUREMENT BY MEANS OF DAST ORGANIC EO CRYSTALS

Y. Okayasu
JASRI, 1-1-1 Koto, Sayo-cho, Sayo-gun, Hyogo, Japan
H. Tomizawa, S. Matsubara, T. Sato, K. Ogawa and T. Togashi
RIKEN Harima Institute, 1-1-1 Koto, Sayo-cho, Sayo-gun, Hyogo, Japan
E.J. Takahshi
The Institute of Physical and Chemical Research (RIKEN),
Wako Main Campus, 2-1 Hirosawa, Wako, Saitama, Japan
H. Minamide and K. Matsukawa
RIKEN ASI Tera-photonics Laboratory,
519-1399 Aoba, Aramaki, Aoba-ku, Sendai, Miyagi, Japan
M. Aoyama
Japan Atomic Energy Agency, 8-1-7 Umemidai, Kizugawa city, Kyoto, Japan
A. Iwasaki and S. Owada
The University of Tokyo, 7-3-1 Hongo, Bunkyo-ku, Tokyo, Japan

Abstract

A pilot user experiment with the seeded FEL have been demonstrated at the Prototype Test Accelerator (EUV-FEL), SPring-8 from July, 2012. A precise measurement of the electron bunch charge distribution (BCD) is crucial key to keep both spatial and temporal overlaps between high-order harmonic (HH) laser pulses and electron bunches. In addition, R&D of a 3D-BCD monitor with a single-shot detection has been extensively promoted at SPring-8. The monitor adopts a spectral decoding based Electro-Optic (EO) sampling technique that is non-destructive and enables real-time reconstruction of the 3D-BCD with temporal resolution of 30 to 40 fs (FWHM). So far, such EO sampling based BCD monitors have been developed by using inorganic EO crystals such as ZnTe or GaP and their temporal resolutions are limited by 110 $\sim$ 130 fs (FWHM). As a part of this project, the first BCD measurement with an organic EO crystal; DAST has been successfully demonstrated at the facility. Signal intensities, temporal resolutions and radiation related issues for both ZnTe and DAST are discussed.

INTRODUCTION

In general, XFEL (X-ray Free Electron Laser) accelerator drives ultra-short electron bunches such as $\sim$100 μm (rms) for transverse and $\sim$30 fs (FWHM) for longitudinal directions. In order to drive such ultra-short electron bunches, it is required not only to measure bunch length with a few tens of femtoseconds temporal resolution, but also to simultaneously measure transverse bunch charge distribution (BCD) with real-time, non-destructive, and shot-by-shot measurement. For example, for SACLA (SPring-8 Angstrom Compact Free Electron Laser), RF deflectors have been utilized to measure the temporal distribution of electron bunches, so far [1, 2]. However, since this method is beam-destructive, real-time reconstruction and shot-by-shot detection of the electron bunch cannot be realized during the operation of SASE-FEL oscillation.

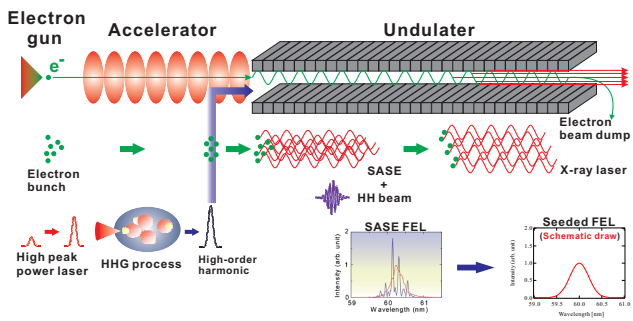

Figure 1: A schematic drawing of SASE-FEL and seeded FEL operation.

Furthermore, for user experiment with HHG-seeded FEL, both high-order harmonics (HH) laser pulse and electron bunch are required to be spatially and temporally overlapped at all times as shown in Fig. 1. Therefore, both longitudinal and transverse BCD measurements, i.e., 3D-BCD measurements with probe laser, that is split from the HHG process, realizes to make shot-by-shot feedback to the HHG-seeded FEL operation.

The Electro-Optic (EO) sampling is one of the practical techniques to realize the 3D-BCD measurements [3, 4]. In this method, the Coulomb field distribution of a relativistic electron bunch is encoded on to a probe laser pulse as modulation of polarization due to phase retardation by EO effect. Intensity spectrum of the probe laser is modulated after a polarized splitter. In case we measure the intensity spectrum modulation with a multi-channel spectrom-

ISBN 978-3-95450-119-9

IMPROVEMENT OF SCREEN MONITOR WITH SUPPRESSION OF COHERENT-OTR EFFECT FOR SACLA

S. Matsubara [#, A)], H. Maesaka [A, B)], S. Inoue [C)], and Y. Otake [A, B)]
[A)] Japan Synchrotron Radiation Research Institute, 1-1-1 Kouto, Sayo-cho, Sayo-gun, Hyogo, 679-5198, Japan
[B)] RIKEN SPring-8 Center, 1-1-1 Kouto, Sayo-cho, Sayo-gun, Hyogo-ken, 679-5148, Japan
[C)] SPring-8 Service Co., Ltd., 1-20-5 Kouto, Shingu-cho, Tatsuno-shi, Hyogo, 679-5165, Japan

Abstract

The construction of SACLA (SPring-8 Angstrom Compact free electron LAser) was already completed and it is under operation. A screen monitor (SCM) system has been developed and was installed in order to obtain a direct image of a transverse beam profile with a spatial resolution of about 10 μm, which is required to investigate electron-beam properties, such as a beam emittance. The SCM originally has a stainless steel target as an OTR radiator or a Ce:YAG crystal as a scintillation target. At the beginning of SACLA operation, strong coherent OTR (COTR), which provides incorrect beam profile image, was observed after full bunch compression to make a peak-current of over 1 kA. In order to suppress the COTR effect on the SCM, the stainless steel target was replaced to the Ce:YAG scintillation target. Since the COTR was still generated from the Ce:YAG target, a spatial-mask was employed. The mask was mounted on the optical axis around the center of the SCM image, because the COTR light is emitted forward within ~1/γ radian, while the scintillation light almost has no angular dependence. Clear beam profiles with a diameter of a few tens of micrometre are observed by means of the SCM with this simple improvement.

INTRODUCTION

In the SPring-8 site, construction of SACLA, which is an XFEL facility, was already completed and it is under operation [1,2]. For SACLA to stably generate a high-intense X-ray laser pulse of shorter than 0.1 nm wavelength, the electron-beam injected into the undulator section is demanded to have a high peak-current of more than 3 kA and a low-emittance of less than 1 π mm mrad. The 1 ns width electron-beam, which is generated from a thermionic gun with a low emittance of 0.6 π mm mrad and is formed from a 3 μs width (FWHM) at the gun by a beam chopper, is compressed to nearly 10 fs by the velocity bunching process of an injector part and three bunch compressors without emittance growth. The electron-beam for generating high-intense X-ray laser pulses is made by fine tuning of the accelerator, investigating the beam properties. In SACLA, a monitor system for a beam profile and a beam bunch length is indispensable for the SASE operation of the XFEL.

A large number of screen monitors (SCM) have been installed along the accelerator and the undulator line for measuring beam profiles [3,4]. Especially after the third bunch compressor (BC3), the values of the emittance and bunch length of the beam should be obtained. The emittance is measured by the Q-scan method [5] with the SCM. For the bunch length measurement, a temporal beam profile is monitored by converting the temporal structure to a spatial profile using the RF-deflector in order to achieve a temporal resolution of 10 fs [6]. In these measurements, the transverse beam size of a few 10 μm (rms) should be observed with the SCM. Therefore, the SCM is demanded to have a spatial resolution of 10 μm for SACLA.

At the beginning of SACLA operation, however, some of the spatial profiles were not correctly able to be monitored by the SCM on account of strong coherent OTR (COTR), which made an incorrect beam profile image, after the BC3. The COTR is also observed at LCLS, FLASH, and other facilities [7,8,9], when an electron-beam is compressed over a certain pulse width. Our SCMs, nevertheless, did not have a countermeasure against the COTRt, because the COTR has not been observed in the SCSS test accelerator [10], which is a small-scaled machine of SACLA.

Therefore, the SCM has been improved for mitigation of the COTR effect to increase availability of the SCMs placed downstream of the accelerator.

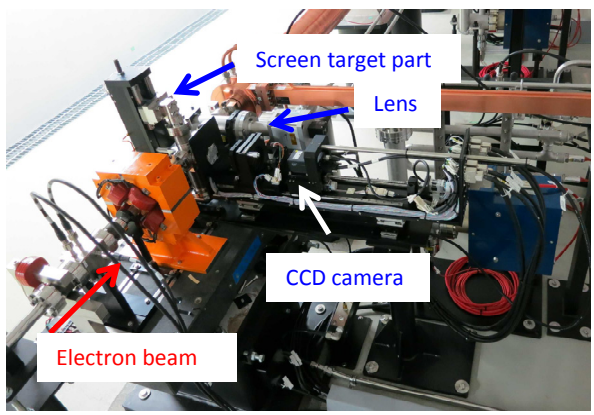

Figure 1: Setup of the SCM system.

#matsubara@spring8.or.jp

ISBN 978-3-95450-119-9

ELECTRON BEAM DIAGNOSTIC SYSTEM FOR THE JAPANESE XFEL, SACLA

H. Maesaka#, H. Ego, C. Kondo, T. Ohshima, H. Tomizawa, Y. Otake,
RIKEN SPring-8 Center, Kouto, Sayo-cho, Sayo-gun, Hyogo, Japan
S. Matsubara , T. Matsumoto, K. Yanagida,
Japan Synchrotron Radiation Research Institute, Kouto, Sayo-cho, Sayo-gun, Hyogo, Japan

Abstract

We present the design and performance of the beam diagnostic instruments for the Japanese x-ray free electron laser (XFEL) facility, SACLA. XFEL radiation is generated by self-amplified spontaneous emission (SASE) process in SACLA, which requires a highly brilliant electron beam with a normalized emittance of less than 1 mm mrad and a peak current of more than 3 kA. To achieve this high peak current, 1 A beam with 1 ns duration from a thermionic electron gun is compressed down to 30 fs by means of a multi-stage bunch compression system. Therefore, the beam diagnostic system for SACLA was designed for the measurements of the emittance and bunch length at each compression stage. We developed a high-resolution transverse profile monitor and a temporal bunch structure measurement system with a C-band rf deflecting cavity etc. In addition, the precise overlapping between an electron beam and radiated x-rays in an undulator section is necessary to ensure XFEL interaction. Therefore, we employed a C-band sub-μm resolution rf cavity BPM to fulfill the demanded accuracy of 4 μm. All the performances of our developed beam monitors reached the demanded resolutions. By using these beam diagnostic instruments, the first x-ray lasing at a wavelength of 0.12 nm was achieved and SACLA has been stably operated for user experiments since March, 2012 in the wavelength region from 0.08 nm to 0.25 nm.

INTRODUCTION

The x-ray free electron laser (XFEL) facility, SACLA (SPring-8 Angstrom Compact Free Electron LAser) [1], was successfully commissioned and the first x-ray lasing was observed in June, 2011 at an x-ray wavelength of 0.12 nm. SACLA has been stably operated for various user experiments since March, 2012 in the wavelength region from 0.08 nm to 0.25 nm. In SACLA, XFEL radiation is generated by a self-amplified spontaneous emission (SASE) process. The SASE process in the x-ray region requires a high peak current of more than 3 kA and a small normalized emittance of less than 1 mm mrad [2].

To achieve these requirements, we designed and constructed a low-emittance injector, an 8 GeV C-band accelerator and a short-period in-vacuum undulator beamline, as shown in Fig. 1. An electron beam is generated by a thermionic electron gun with a CeB_6 cathode. The normalized emittance of the electron beam is 0.6 mm mrad, the initial current is 1 A and its pulse width is 1 ns (FWHM) formed from 3 μs (FWHM) by a high-voltage chopper. The beam is accelerated to 8 GeV by the following series of rf accelerator cavities: 238 MHz pre-buncher, 476 MHz booster, L-band (1428 MHz), S-band (2856 MHz) and C-band (5712 MHz) accelerators. In the meantime, the bunch length is shortened from 1 ns to 30 fs by using a velocity bunching process through the sub-harmonic acceleration cavities and a bunch compression process by means of three magnetic chicanes. The peak current is finally boosted up to 3 kA without substantial emittance growth. The electron beam is then fed into in-vacuum undulators with a period of 18 mm and the maximum K-value of 2.2, and XFEL light is finally generated.

In order to maintain the high gain SASE process at an x-ray wavelength, we need to monitor a beam position, a transverse beam profile, beam arrival timing and a temporal bunch structure at each acceleration stage. The resolution of the beam-position monitor in the undulator section is required to be less than 1 μm so as to maintain the overlap between the electron beam and radiated x-rays within 4 μm precision [3]. The transverse beam profile should be measured with a spatial resolution of less than 10 μm in order to measure a normalized emittance less than 1 mm mrad. The required resolution of the temporal bunch structure measurement is 10 fs at a position after the full compression, since the bunch length becomes 30 fs. In addition, since the initial bunch length is 1 ns, temporal profile monitors with a wide time scale from 1 ns to 10 fs are demanded. Therefore, we developed

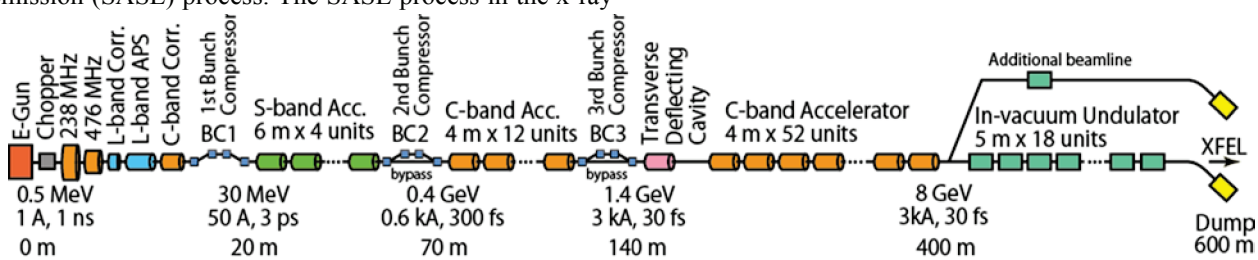

Figure 1: Schematic layout of SACLA.

maesaka@spring8.or.jp

ISBN 978-3-95450-119-9

DESIGN STUDY OF THE STRIPLINES FOR THE EXTRACTION KICKER OF THE CLIC DAMPING RINGS*

C. Belver-Aguilar, A. Faus-Golfe, IFIC (CSIC-UV), Valencia, Spain
M.J. Barnes, CERN, Geneva, Switzerland
F. Toral, CIEMAT, Madrid, Spain

Abstract

Pre-Damping Rings (PDRs) and Damping Rings (DRs) are needed to reduce the beam emittance and, therefore, to achieve the luminosity requirements for the CLIC main linac. Several stripline kicker systems will be used to inject and extract the beam from the PDRs and DRs. Results of initial studies of the stripline cross-section and the beam coupling impedance, for a non-tapered beam pipe, have previously been reported. In this paper, we present the analysis to study the final choice of the cross-section design, based on impedance matching and field homogeneity requirements, the power reflected in the transition between an electrode and the input coaxial feedthrough, and the predicted beam coupling impedance. Mechanical tolerances for the stripline manufacturing process are presently being studied. The striplines are planned to be prototyped by December 2012.

GEOMETRIC DESIGN STUDY

The stripline kicker proposed for the extraction kicker of the CLIC DRs consists of two parallel electrodes of 1.7 m length inside a cylindrical vacuum pipe: each electrode is powered by an inductive adder [1]. The two electrodes are charged to opposite polarity; there is a virtual ground midway between the electrodes. The striplines will be powered, via coaxial feedthroughs, from the beam exit end: the upstream feedthroughs will be connected to resistive loads, see Fig. 1. The stripline kicker operates as two coupled transmission lines, each of which should ideally have a characteristic impedance matched to 50 Ω. Coupled transmission line theory shows two operating modes for the stripline kicker, since three conductors are involved in the signal transmission, i.e. both electrodes and the vacuum beam pipe. These modes are known as odd and even mode: odd mode when the electrodes are excited with opposite polarity voltages, and even mode when the electrodes are excited by the unkicked circulating beam when passing through the aperture of the striplines [2].

Flat and Half-moon Electrode Cross-sections

The electrode cross-section was previously selected by studying several shapes for the striplines and optimizing them in order to achieve 50 Ω even mode characteristic impedance, and $\pm 0.01\%$ of field inhomogeneity over a circle of 1 mm radius at the center of the aperture [2]. An additional constraint was to achieve an odd mode characteristic impedance as close as possible to 50 Ω. Flat electrodes allowed for an optimum characteristic impedance and field homogeneity with a minimum stripline beam pipe radius of 25 mm. A small stripline beam pipe radius diminishes the non-desirable effects of the wakefields and results in closer values of even and odd mode characteristic impedances.

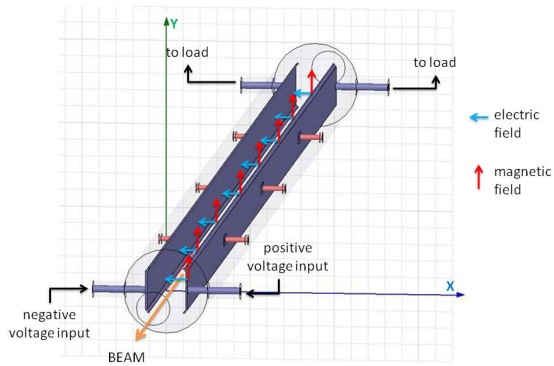

Figure 1: 3D model of a stripline kicker [4].

Recent studies have shown that a modified half-moon electrode, with a reduced coverage angle (see Fig. 2), allows for a better optimization of the odd mode characteristic impedance with a stripline beam pipe radius of 20 mm.

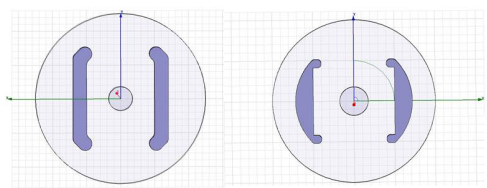

Figure 2: Cross-section of the striplines for flat electrodes (left) and modified half-moon electrodes (right). The circle drawn in the center is 3.5 mm radius in both striplines.

For flat electrodes with 50 Ω even mode characteristic impedance, an odd mode characteristic impedance of 36.8 Ω was achieved with a stripline beam pipe radius of 25 mm [2]; for the newly studied modified half-moon electrode the odd mode characteristic impedance is 40.9 Ω. To increase this value closer to 50 Ω, the capacitance between

* Work supported by IDC-20101074 and FPA2010-21456-C02-01

ISBN 978-3-95450-119-9

270° ELECTRON BEAM BENDING SYSTEM USING TWO SECTOR MAGNETS FOR THERAPY APPLICATION

Shahzad Akhter, V.N. Bhoraskar, S.D. Dhole*,
Department of Physics, University of Pune, Ganeshkhind, Pune, India
B.J. Patil, Department of Physics, Abasaheb Garware College, Karve Road, Pune, india
S.T. Chavan, S.N. Pethe, R. Krishnan, SAMEER, IIT Powai Campus, Mumbai, India

Abstract

The 270 degree doubly achromatic beam bending magnet system using two sector magnets has been designed mainly for treating cancer and skin diseases. The main requirements of the design of two magnet system is to focus an electron beam having a spot size less than 3 mm × 3 mm, energy spread within 3% and divergence angle ≤ 3 mrad at the target. To achieve these parameters the simulation was carried out using Lorentz-3EM software. The beam spot, divergence angle and energy spread were observed with respect to the variation in angles of sector magnets and drift distance. From the simulated results, it has been optimized that the first and second magnet has an angle 195 degree and 75 degree and the drift distance 64 mm. It is also observed that at the 1396, 2878 and 4677 A-turn, the optimized design produces 3324, 6221 and 9317 Gauss of magnetic field at median plane require to bend 6, 12 and 18 MeV electron beam respectively. The output parameters of the optimized design are energy spread 3 %, divergence angle ∼ 2.8 mrad and spot size 2.6 mm.

INTRODUCTION

Radiotherapy using electron and photon represent a most diffused technique to treat tumor diseases. With the advent of high energy linear and circular accelerators, electron / photon have become a viable option in treating superficial tumors up to the depth of about 5-10 cm. In such case, the dose of radiation absorbed correlates directly with the energy of the beam and its deposition of energy in tissues, which results in damage to DNA strands and diminishes the cell's ability to replicate indefinitely. For the last several years, electron accelerators are extensively being used in the medical field with special applications of photon and electron beam for cancer therapy and various skin diseases [1].

High energy medical electron linacs are usually mounted horizontally because of larger length of linac tube. The emergent electron beam from the accelerating tube is deflected magnetically through 90° or 270° into a vertical plane to hit an X-ray target or electron scatterer [2]. A small, stable, and axially symmetric beam spot on the target is needed. For fully rotational medical electron linacs, it is necessary both to minimize physical height of the machine and to maintain 100 cm distance between the x-ray target and rotational centre. In addition, it is also a basic requirement that the bending magnet is doubly achromatic i.e. the position and angle of the output beam is independent of input beam energy.

The 90° deflection system can bend a mono-energetic beam on axis to a point at the X-ray target, but the spread of energies of the actual beam results in a spread of such focal point at the X-ray target. Also, the radial displacement and angular divergence of the entrant beam results in spread of exit beam. To overcome the above problems a 270° bending magnet system is used. This system is doubly achromatic and can be made using one, two and three magnets [3]. Based on the orbit dimension and size, two dipole bending magnet system is advantageous. Therefore, an objective of the present paper is to provide a 270° beam bending using two dipole magnet system in which first bend is with 195° and other bend is with 75° to minimize the height of the orbit above the accelerator beam line.

MATERIALS AND METHOD

The linear electron accelerator available at Society of Applied Microwave Electronics and Engineering Research, Mumbai having energies 6,9,12, 15 and 18 MeV [4], average current 80 μA, pulsed current 130 mA, pulsed width 6 μs, repetition rate 150 PPS is going to be used for the present study. The linear accelerator produces beam of 6 to 20 MeV with energy spread of 7%.

The Lorentz-3EM software has been used for studying the trajectory of charged particles through electric and/or magnetic fields in three dimensional geometry. The magnetic field between the poles and trajectory for various electron energies have been calculated with the help of Lorentz-3EM software for better accuracy.

MAGNET DESIGN

In order to take advantage of the low height of an elementary single dipole and at the same time take advantage of achromatic system, a double focusing doubly achromatic magnet system was designed. It consists of two dipole magnets which are used to bend the 6 to 20 MeV

* sanjay@physics.unipune.ac.in

ISBN 978-3-95450-119-9

AN ELECTRON BEAM PROFILE MONITOR FOR THE RACE-TRACK MICROTRON

S.D. Dhole*, V.N. Bhoraskar, N.S. Shinde
Department of Physics, University of Pune, Ganeshkhind, Pune, India
B.J. Patil, Department of Physics, Abasaheb Garware College, Karve Road, Pune, India

Abstract

In electron irradiation experiments on materials such as semiconductors, solar cells etc., an uniformity and the charge distribution in the electron beam is very important. Therefore, an electron beam current monitor and its electronic system have been designed and built to measure the distribution of a beam current either in the horizontal or vertical direction along with the beam dimensions. To obtain X-Y beam profile, a special type of Faraday Cup was designed which mainly consists of charge collecting electrodes made up of thin copper strips. Each strip having dimensions 0.5 mm wide, 4 mm thick and 20 mm long were fixed parallel to each other and separation between them was $\sim$ 0.5 mm. This multi electrode Faraday was mounted at the extraction port of the Race Track Microtron, where 1 MeV electron beam allowed to fall on it. The beam characterization in the form of current and uniformity were measured. The current from each strip were measured using an electronic circuit developed based on the multiplexing principle. The uniformity of the beam can be measured with an accuracy of 10%. The minimum and maximum dimensions which can be measured are 3 mm and 15 mm respectively.

INTRODUCTION

The MeV energy range electron beams have gained importance due to their applications in space technology and tailoring of device parameters. In several cases, approximate beam dimensions are required for controlled irradiation. The electron beam delivered by an electron accelerator called 'Race-Track Microtron' [1, 2] has pulse duration 1.6 s with repetition rate 50 PPS. Normally, at 1 MeV electron energy, the beam size obtained is around 6 mm $\times$ 4 mm. The beam dimension can further be increased by using scattering mechanism which is required to irradiate samples of large dimensions. The dimension of the beam may vary due to several factors such as variations in the magnetic field configuration, electron beam injection conditions, microwave cavity field, etc. Similarly, when the beam is passed through a bending magnet, the beam shape at the magnet exit is very much different from that at the magnet entrance. It is not always possible to know the uniformity of the electron beam using scintillator and therefore it was thought appropriate to design and fabricate a beam current monitor, which can provide intensity distribution over the beam area at different points along horizontal and vertical directions. Such a monitor along with an electronic system has been designed, fabricated and put into operation in the laboratory.

* sanjay@physics.unipune.ac.in

EXPERIMENT

Multielectrode Faraday Cup

This consist of charge collecting electrodes in the form of thin copper strips. Such fifteen numbers of copper strips, each of 0.5 mm wide, 4 mm thick and 20 mm long were fixed parallel to each other with adhesive on a Perspex sheet. The separation between two strip was kept $\sim$ 0.5 mm. The thickness of copper strip was calculated on the basis of range of 1 MeV electron in copper [3]. Therefore, the thickness of copper strip was chosen such that all the incident electron can stop inside the strip. The assembly was enclosed in an aluminum box having length 50 mm, width 50 mm and depth 30 mm. For charge measurement, each copper strip was connected to a BNC connector. Front side of the box is closed with a 50 μm aluminized mylar to provide shielding against external electrical noise. This beam profile measurement assembly was kept in the electron beam line and each of the BNC connector was connected to an electronic circuit specially made for this monitor.

Electronic System

An electronic circuitry [4, 5, 6, 7, 8, 9] has been designed, built and assembled to obtain visual display of the charge distribution of an electron beam on a CRO as well as on a digital display. The block diagram of the circuit used for this work is shown in Figure 1, whereas the circuit details are shown in Figure 2. Eight strips of the beam current monitor were connected to multiplexer of type 4051B. This multiplexer is 8 to 1 type multiplexer, which has a facility of eight independent input bits or channels, three control bits and one output bit. This is also sometimes called as data selector, because output bit is depends on the input data bit that is selected. For instance, if the control signal ABC is 000, then the information from the first copper strip of the Faraday cup is transmitted to the output. However, if the control signal ABC is change to 111, then the information from the eight strips is transmitted to the output. From the circuit one can see that the multiplexer can be operated in the mode of transmit information, which is available at one of the eight inputs to the corresponding output terminals, sequence of which can be preset through a programme

ISBN 978-3-95450-119-9

VIMOS, NEW CAPABILITIES FOR AN OPTICAL SAFETY SYSTEM

K. Thomsen, J. Devlaminck, PSI, 5232 Villigen, Switzerland

Abstract

VIMOS is a dedicated safety system developed at the Spallation Neutron Source SINQ at the Paul Scherrer Institut, PSI, in Switzerland. VIMOS very directly monitors the correct current density distribution of the proton beam on the target by sampling the light emitted from a glowing mesh heated by the passing protons. The design has been optimized for obtaining maximum sensitivity and timely detection of beam irregularities relying on standard well-proven components. Recently it has been demonstrated that technical boundary conditions like radiation level and signal strength should allow for upgrading the system to a sensitive diagnostic device delivering quantitative and image-resolved values for the proton current density distribution on the SINQ target. By determining the temperature of the glowing mesh from the signals in two separate wavelength bands the temperature distribution over the mesh can be derived und subsequently the incident proton beam current density distribution. Work aimed at investigating the feasibility of adding these diagnostic abilities to VIMOS shows initial promising results.

VIMOS, SAFETY SYSTEM

One of the outstanding features of the SINQ neutron spallation source at PSI is its vertical insertion with the proton beam impinging on the target from directly below. Whereas this design is favourable with respect to the circulation inside a liquid metal (LM) target, it entails the severe risk of major facility damage in case of a leak. To minimize the risk of burning a hole through the liquid metal container with the beam and subsequently perforating the lower target enclosure of the MEGAPIE LM target, a new and additional safety system named VIMOS has been devised and successfully installed [1,2].

VIMOS is based on a most simple and direct approach, i.e. it monitors the glowing of a tungsten mesh inserted into the proton beam closely spaced in front of the target. This mesh is heated by the passing protons, and VIMOS watches for deviations from the expected visual signal. In case that any hot spot due to unintended beam concentration is detected, an alarm is triggered and the accelerator is switched off in less than 100 ms. In order to react most quickly to any unexpected increase of the glowing signal from the mesh, VIMOS has purposely been designed with a strongly non-linear response function [2].

VIMOS works reliable since its installation before the MEGAPIE target irradiation started and it has proven its value actually already in the commissioning phase. Now it is routinely used for beam monitoring during normal operations by the operators of the accelerator also with SINQ's standard solid state targets.

Aim of an Upgrade

In the light of the proven reliability and usefulness of VIMOS, the wish for additional capabilities of the system has emerged. One demand was to somehow calibrate the system for a display of beam current density. The other request is for enhanced sensitivity, i.e. responding also at lower current (-densities), to provide more information for set up, in particular at phases when the beam at low current is newly directed onto the SINQ target.

As the original safety goal of reacting only to hot spots imposes some limitations and inherent difficulties for obtaining more detailed diagnostics' information on beam profile during normal operations, a comprehensive upgrade of the system has been envisioned [3].

IMPLEMENTATION OF DIAGNOSTICS

One stringent boundary condition right from the start was that the safety function of VIMOS should stay untouched, new features should only come on top and as far as possible without interfering with the well-proved safety relevant installation.

Following a stepwise approach, several pre-conditions and key issues have first been identified and scrutinized before designing added diagnostic capabilities.

Enabling Conditions

Originally, VIMOS employed a radiation resistant camera, which was directly mounted in the focus of the colleting mirror and thus exposed to irradiation by back-streaming protons and high energy neutrons [4]. Epithermal neutrons in particular caused damage to the semiconductors in the camera as, after being moderated by scattering in the shielding in the surroundings, they changed the doping and thus impaired proper functioning after several months of operational exposure.

In order to increase the lifetime of the expensive cameras and also in anticipation of possible future upgrades, the camera position has been moved 3 meters further away. The light is now transmitted to the new camera position on a wall of the SINQ beam vault by means of a radiation resistant image guide [5].

With the improved possibility of packing substantial graded shielding around the sensor, the original tube-based camera has been replaced by a more standard off-the shelf CCD camera [6].

A light guide and the first shielded CDD camera have been installed in November 2008 and work since then as expected. The camera shows only acceptable damage in the form of increased noise, which does not impede the proper functioning of the system. Little and not quantified radiation damage meaning increased attenuation is seen in the image fiber.

ISBN 978-3-95450-119-9

DEVELOPMENT OF PHASE PROBE FOR THE NIRS SMALL CYCLOTRON HM-18

Satoru Hojo#, Ken Katagiri, Akira Goto, NIRS, 4-9-1 Anagawa, Inage, Chiba, Japan
Yuichi Takahashi, Toshihiro Honma, AEC, 3-8-5 Konakadai, Inage, Chiba, Japan

Abstract

The small cyclotron HM-18 of the National Institute of Radiological Sciences (NIRS) allows us to accelerate H^- and D^- ion at fixed energies of 18 and 9 MeV, respectively. It has four trim coils for generation of the isochronous fields. Until recently, currents of the four trim coils had been adjusted only by monitoring the output beam intensity. In order to exactly produce the isochronous fields, a phase probe has been newly installed in the HM-18. The phase probe has a simple structure in which four copper electrode plates of 55~76 mm x 68 mm in area are glued to a copper base plate with a polyimide insulator sheet sandwiched between them. The thicknesses of the copper plates and the polyimide are 0.1 mm. This structure has an advantage that it can be easily installed in the cyclotron; only one part of a pair of upper and lower electrodes, which is usually adopted in cyclotrons, is simply attached on the surface of the (lower) sector pole. The development of the phase probe and some results of a preliminary beam test using it are reported.

INTRODUCTION

The small cyclotron HM-18 of the NIRS has been operated for use in RI production since 1994[1]. The HM-18 cyclotron is a negative-ion accelerator that was purchased from Sumitomo Heavy Industry, Ltd. A layout of the HM-18 is shown in Figure 1. Two carbon-foil strippers are located at a radius of 435 mm for beam extraction; they are located in the opposite sides to each other. In one side beams are delivered to a beam transport line, which is jointed to that of the NIRS-930 cyclotron. In the other side four target ports are attached directly to the beam chamber for production of short-lived radio isotopes such as ^{11}C and ^{18}F. The HM-18 has an internal cold-cathode ion source that produces H^- and D^- ions, which are accelerated up to 18 and 9 MeV, respectively, with the acceleration frequency of 45 MHz. The acceleration harmonics are 2 and 4 for H^- and D^- ions, respectively. Four trim coils are used for generation of the isochronous fields. Until recently, currents of the four trim coils had been adjusted only by monitoring the output beam intensity; the isochronous field was indefinite because the beam phase was not able to be measured. Therefore, a phase probe has been newly installed in order to exactly produce the isochronous fields in the HM-18.

s_hojo@nirs.go.jp

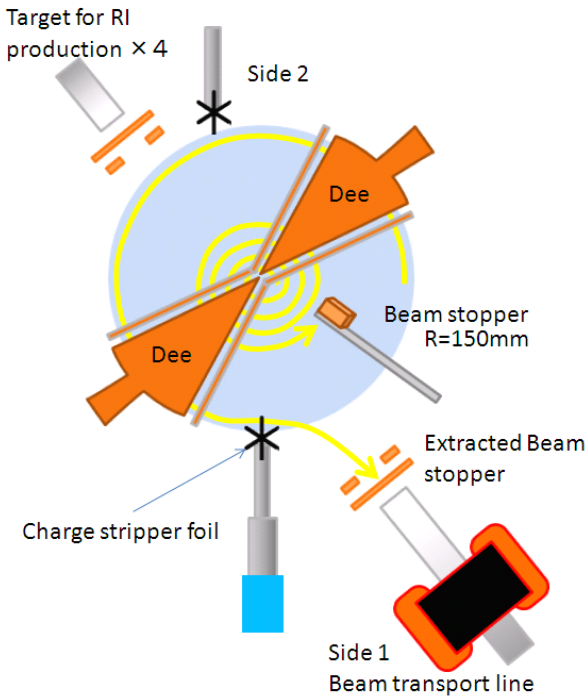

Figure1: Schematic layout of the HM-18 cyclotron.

STRUCTURE OF PHASE PROBE

Photograph and cross-sectional view of the new phase probe is shown in Figure 2. This phase probe has a simple structure. Usually, a phase probe is composed of a pair of upper and lower electrodes, but the new phase probe for the HM-18 is composed only of lower part. It consists of four copper plates of 55~76 mm (azimuthal width) x 68 mm (radial length) in area glued to a copper base plate with a polyimide insulator sheet sandwiched between them. Adhesive double-coated tapes are used for the attachment of them. The thicknesses of the copper plates and the polyimide sheet are 0.1 mm. Semi-rigid coaxial cables are used for transport of beam signals in the beam chamber. The outer conductor of the cable is made of copper tube with 1.2 mm in diameter. The ends of the inner and outer conductor are soldered to the fins of the pickup electrodes and the grounded copper plate, respectively, as shown in Figure 2.

This structure has an advantage that it can be easily installed in the cyclotron. Photograph of the phase probe installed in the HM-18 is shown in Figure 3. The phase probe and signal cables are simply attached on the surface of the lower sector pole with adhesive aluminium tapes.

ISBN 978-3-95450-119-9

VARIOUS USAGES OF WALL CURRENT MONITORS FOR COMMISSIONING OF RF SYSTEMS IN J-PARC SYNCHROTRONS

Fumihiko Tamura*, Masanobu Yamamoto, Alexander Schnase, Masahito Yoshii, Chihiro Ohmori, Masahiro Nomura, Makoto Toda, Taihei Shimada, Keigo Hara, Katsushi Hasegawa
J-PARC Center, KEK & JAEA, Tokai-mura, Naka-gun, Ibaraki-ken, Japan

Abstract

Wall current monitors (WCM) for rf system commissioning are installed in the J-PARC synchrotrons, the RCS and the MR. The WCM signals are used as the input of the beam loading compensation system, and also used for diagnostics to adjust the rf system parameters. Since the rf and beam frequencies are in the range of a few MHz and several ten MHz, direct measurement of the WCM signals is possible. For the diagnosis, the WCM signals are taken by an oscilloscope with the revolution clock signal generated by the low level rf (LLRF) control system, and slices of the WCM waveform with lengths of the revolution periods are generated. By stacking the slices, one can get a mountain plot, which shows motions of bunches and variations of the bunch shapes. Also, time variations of the bunching factor, which are important for acceleration of high intensity proton beams, are obtained. The harmonic analysis is performed on the WCM signal and the cavity voltage monitor signal. By using complex amplitudes of them, one can calculate the impedance seen by the beam. We show examples of the analyzes described above. The rf parameters for high intensity beams have been successfully adjusted by using these analysis methods.

INTRODUCTION

The Japan Proton Accelerator Research Complex (J-PARC) is a multi-purpose high intensity proton accelerator facility, which consists of the linac, the rapid cycling synchrotron (RCS), and the main ring synchrotron (MR). At present, the maximum output beam power of the RCS and the MR is 300 kW and 200 kW, respectively.

In the RCS and the MR, wall current monitors (WCM) dedicated for rf system commissioning are installed [1, 2]. The WCMs are designed to have a high cut-off frequency more than a few 100 MHz, which is high enough compared to the beam frequency up to several ten MHz.

The low level rf (LLRF) control systems of the J-PARC RCS and MR are implemented by digital circuits to realize precise and reproducible rf control. The WCM signals are used as the input of the beam loading compensation [3], and used for diagnostics to adjust the rf parameters and patterns.

For the high power commissioning of the RCS and the MR, the information from the WCM is important and indispensable. The analysis of the WCM waveforms taken by a long memory oscilloscope is performed on a PC. In this paper, we show examples of the various analysis results of the WCM waveforms.

* fumihiko.tamura@j-parc.jp

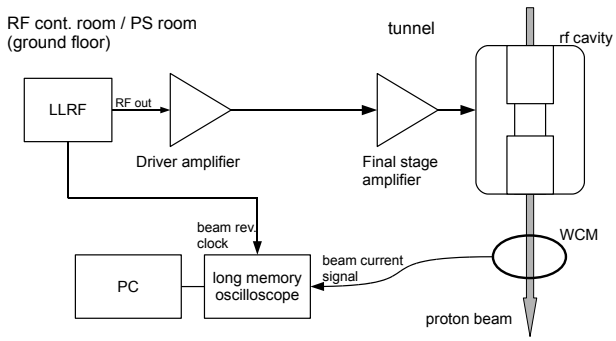

Figure 1: Measurement setup.

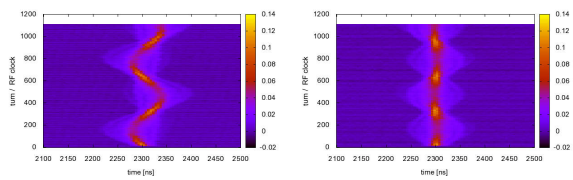

Figure 2: Mountain plots of the injected bunch. (Left) in case $f_{\mathrm{rf}} = 1.671650$ MHz, the momentum of the injected beam and the rf frequency are not matched. (Right) in case $f_{\mathrm{rf}} = 1.671750$ MHz, they are matched well.

BEAM CURRENT ANALYSIS USING WCM WAVEFORM SLICES

Since the beam frequencies are in the range up to several ten MHz, direct measurement of the WCM beam signal by using an oscilloscope is possible. As shown in Fig. 1, the WCM signal is taken together with the revolution clock signal, which is generated by the digital LLRF control system and precisely follows the accelerating frequency sweeps. The signals are recorded by a long memory oscilloscope and the waveforms are analyzed on a PC. Slices of the WCM waveform with lengths of the revolution period, which is calculated by using the revolution clock signal, are generated. Since the revolution clock signal follows the frequency pattern change, no additional information is necessary to generate the slices. By stacking the slices, one can obtain a mountain plot. Mountain plots are used to analyze the motions of bunches and variations of the bunch shapes. Figure 2 shows an example of the in-

ISBN 978-3-95450-119-9

COMPARISON OF THREE DIFFERENT CONCEPTS OF HIGH DYNAMIC RANGE AND DEPENDABILITY OPTIMISED CURRENT MEASUREMENT DIGITISERS FOR BEAM LOSS SYSTEMS

W. Viganò, B. Dehning, E. Effinger, G. G. Venturini, C. Zamantzas, CERN, Geneva, Switzerland

Abstract

Three Different Concepts of High Dynamic Range and Dependability Optimised Current Measurement Digitisers for Beam Loss Systems will be compared on this paper.

The first concept is based on Current to Frequency Conversion, enhanced with an ADC for extending the dynamic range and decreasing the response time. A summary of 3 years' worth of operational experience with such a system for LHC beam loss monitoring will be given. The second principle is based on an Adaptive Current to Frequency Converter implemented in an ASIC. The basic parameters of the circuit are discussed and compared with measurements. Several measures are taken to harden both circuits against single event effects and to make them tolerant for operation in radioactive environments. The third circuit is based on a Fully Differential Integrator for enhanced dynamic range, where laboratory and test installation measurements will be presented. All circuits are designed to avoid any dead time in the acquisition and have reliability and fail safe operational considerations taken into account.

STRUCTURE OF THE COMPARISON

Each concept will be described by means of specifications, implementation and performance. In the conclusion a summary of the three methods will be given.

CURRENT TO FREQUENCY CONVERTER

Specifications

LHC protection requires a high reliability Beam Loss Monitoring system. The Front End card, referred to as the CFC card, has been designed to be exposed to a maximum of 500Gy integrated dose for 20 years LHC life-time.

To achieve a reliability level SIL3 (10^{-7} to 10^{-8} failure/h) of the system, several different test modes, status information, protection circuits and a redundant data transmission are implemented. For the verification, different tests have been performed, such as irradiation, temperature, magnetic field, and burn-in tests.

A summary of the System Specification is given in Table 1.

Table 1: CFC Specifications

Measurement range	2.5pA to 1mA
Error range from 10pA to 1mA	-50% to +100%
Error range from 1nA to 1mA	±25%
Maximum input current	561mA
Minimum acquisition period	40us
Input range with minimum acquisition period	5nA to 1mA
Input voltage peak	1500V @ 100us
Radiation Total Dose	500Gy in 20yr

Implementation

To measure a current over this high dynamic range, a Current to Frequency Converter (CFC – Figure 1) based on the balanced charge integrating techniques, has been chosen. In comparison with other switching techniques, the CFC has the advantage that it is without dead times and with no loss of charges.

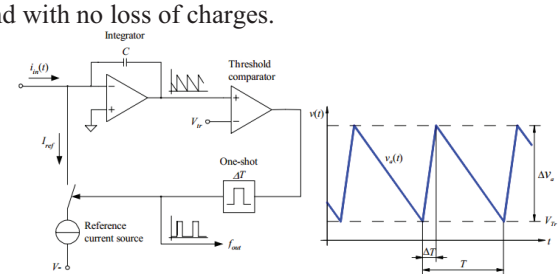

Figure 1: CFC block diagram.

Since the output frequency depends on the input current (where a small current corresponds to a very low frequency), an additional analogue to digital converter (ADC) is added to measure the output voltage of the integrator and to calculate partial counts in the Threshold Comparator card, named BLETC. This measurement decreases the response time and increases the dynamic range. The integration time window of the system is 40µs. The data, including the counted CFC pulses and the integrator output voltage, are transmitted every 40µs to the BLETC. Figure 2 shows the CFC circuit diagram.

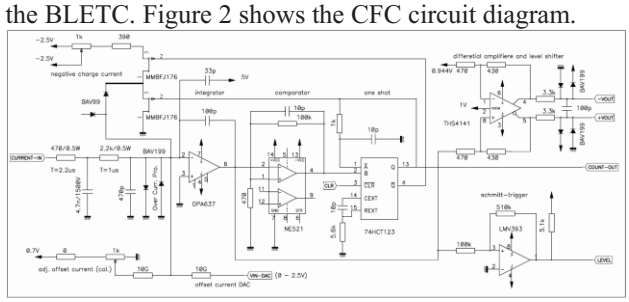

Figure 2: CFC circuit diagram.

To ensure the system is working according to specification and to increase the reliability, several tests, test modes and error detection systems have been added on the CFC card, as shown in Table 2.

Table 2: CFC Tests List

N	Description
1	Before the installation, a calibration and an initial test are performed using a dedicated setup, which performs an

ISBN 978-3-95450-119-9

DIAMOND DETECTORS FOR LHC

Erich Griesmayer, Pavel Kavrigin, CIVIDEC Instrumentation, Vienna, Austria
Bernd Dehning, Ewald Effinger, Tobias Baer, Maria Hempel, Heinz Pernegger, Daniel Dobos, CERN, Geneva, Switzerland

Abstract

Diamond detectors are installed at the LHC as fast beam loss monitors. Their excellent time resolution [1] make them a useful beam diagnostic tool for bunch-to-bunch beam loss observations [2], which is essential for the understanding of fast beam loss scenarios at the LHC [3, 4].

INTRODUCTION

Diamond is probably the most versatile, efficient and radiation-tolerant material available for use in beam detectors. Correspondingly, it has a wide range of applications in beam instrumentation and in beam diagnostics. Currently ten diamond detectors are in use as fast beam loss monitors at the LHC at CERN. The nanosecond time response in combination with the sensitivity to single particles makes them ideal for use in fast beam loss detection. A beam dump caused by a so called UFO, an "unidentified falling object", is shown. UFOs are believed to be dust particles with a typical size of a few micrometers, which lead to beam losses, which last about ten revolutions of the proton beam.

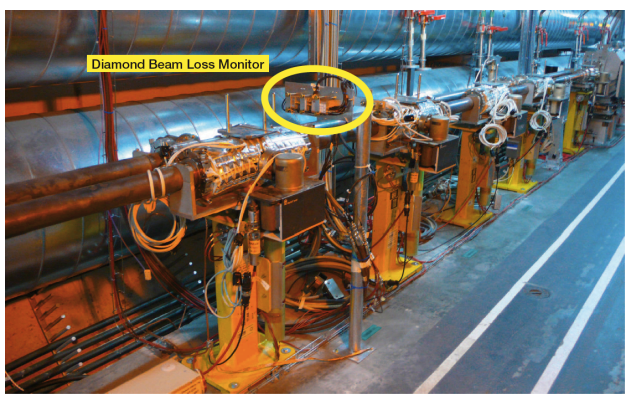

Figure 1: Installation of a Diamond Beam Loss Monitor in the LHC tunnel in IP 7.

THE DIAMOND MONITORS

The diamond monitors were provided by CIVIDEC Instrumentation and installed at TCLA.D6L7.B2. They are composed of a diamond detector (pCVD diamond material, substrate size 10 mm x 10 mm x 0.5 mm, gold electrodes 8 mm x 8 mm, operated at 500 V bias voltage), a 4 GHz AD-DC splitter, and a 2 GHz, 40 dB RF amplifier. A CK50 cable with a length of about 300 m connects the beam loss monitor the readout instrumentation. A LeCroy oscilloscope was used for the digital readout (Waverunner 104MXi, 1 GSPS, 1 GHz, 8 bit ADC). The installation of the diamond beam loss monitor in point 7 is shown in Figure 1.

SPACIAL LOSS PROFILE

A beam abort, which was obviously caused by an UFO event in the injection area in point 4, was recorded on the 27th of August 2012 with a diamond beam loss monitor, which was located in the cleaning area in point 7. Figure 2 shows the spacial loss profile of this event, i.e. the recorded loss amplitude versus the 89 μs turn period of the LHC.

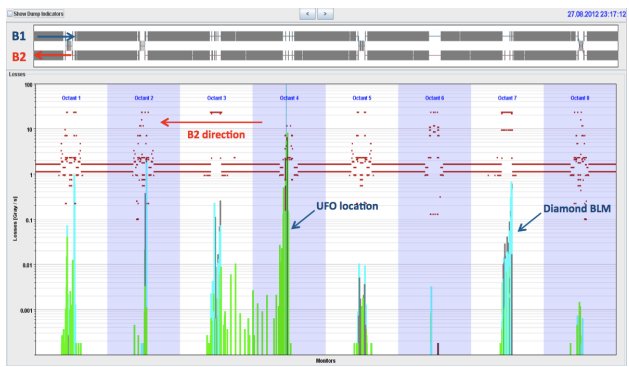

Figure 2: Spatial loss profile versus the LHC turn period of 89 μs. Beam abort event caused by an UFO.

In the following figures, data of the beam abort event, taken with the diamond beam loss monitor, are shown. Starting with a buffer size of 500 μs, a zoom into the memory in four stages is provided. Each zoom reveals insights into the loss structure of the LHC.

The 500 μs Zoom

The Figure 3 shows the loss profile in a time window of 500 μs. The beam losses increase over a period of some microseconds and the dump causes a high pulse at the end of the loss pattern. The tree beam abort gaps define the revolution period of the LHC.

ISBN 978-3-95450-119-9

CHARACTERIZATION OF A WIDE DYNAMIC-RANGE, RADIATION-TOLERANT CHARGE-DIGITIZER ASIC FOR MONITORING OF BEAM LOSSES

Giuseppe Guido Venturini*, CERN / EPFL, Switzerland
Francis Anghinolfi, CERN, Geneva, Switzerland
Bernd Dehning, CERN, Geneva, Switzerland
Maher Kayal, EPFL, STI IEL GR-KA, Lausanne, Switzerland

Abstract

An Application Specific Integrated Circuit (ASIC) has been designed and fabricated to provide a compact solution to digitize current signals from ionization chambers and diamond detectors, employed as beam loss monitors at CERN and several other high energy physics facilities. The circuit topology has been devised to accept positive and negative currents, to have a wide dynamic range (above 120 dB), withstand radiation levels over 10 Mrad and offer different modes of operation, covering a broad range of applications. Furthermore, an internal conversion reference is employed in the digitization, to provide an accurate absolute measurement. This paper discusses the detailed characterization of the first prototype: linearity, radiation tolerance and temperature dependence of the conversion, as well as implications and system-level considerations regarding its use for beam instrumentation applications in a high energy physics facility.

INTRODUCTION

A Beam Loss Monitoring (BLM) system is employed throughout the accelerators at CERN. The aim of the system is threefold: ensure machine protection, provide diagnostics information and aid machine setup. Different kinds of radiation monitors are employed, depending on the accelerator, measurement and expected signal, among them ionization chambers and diamond detectors. The monitors are exposed to the secondary particles shower that is initiated when a high-energy particle escapes from the beam and impacts against the vacuum chamber. The number of particles that are lost from the beam and the energy deposited in the machine components – such as the LHC superconducting magnets – are reconstructed from the output signal provided by the monitors, which are situated in studied locations along the rings, injection and extraction lines, and dump targets.

The BLM system for a large accelerator like the LHC has several channels – over 4000 – and it extends over a significant distance. The system is built in layers: the analog output signal of the monitors is digitized by data acquisition cards located in the tunnel, implementing a Current to Frequency Converter (CFC) and providing a conversion code every 40 µs. The front-end acquisition boards transmit the data to the Threshold Comparators (TC), located in VME crates on the surface, via double redundant optical links. The TCs collect, analyze the data and optionally trigger a beam abort, when losses that could potentially compromise the machine are detected. A Combiner and Survey (CS) card installed in the same VME crate receives and handles the beam abort signals. The data are then forwarded for logging and display [1].

In this context, this contribution discusses the state of the research that has been carried out at CERN, regarding the first step of the data processing outlined above: data acquisition from the monitors.

Table 1: Specifications

Parameter	
Dynamic range	1×10^6
Input polarity	double
Minimum detected current	1 nA
(through averaging)	1 pA
Linearity error	$< \pm 10\,\%$
Integration window	40 µs
Total ionizing dose	10 Mrad in 20 years

REQUIREMENTS

The requirements for the BLM front-end acquisition are listed in Table 1.

The intensity of the ionizing radiation detected by the particle monitors can span several decades, as a consequence of the characteristics of the accelerator, the operational status of the machine, the location in which the monitor is installed and the background radiation. For this reason, the different kinds of beam loss monitors designed and employed at CERN are able to provide a linear response over a wide dynamic range (DR) [2].

Since before the beginning of operation of the LHC, an effort has been made in the BE/BI/BL section to study and design a single-gain acquisition board, able to cover the whole dynamic range of the input signal [3]. This work follows the same approach as the currently operational LHC

* giuseppe.guido.venturini@cern.ch

ISBN 978-3-95450-119-9

REAL-TIME CALCULATION OF SCALE FACTORS OF X-RAY BEAM POSITION MONITORS DURING USER OPERATION

C. Bloomer, G. Rehm, Diamond Light Source, Oxfordshire, UK

Abstract

Photoemission based X-ray Beam Position Monitors (XBPMs) are widely used at 3rd generation light sources to both monitor and stabilise the photon beam to sub-micron precision. Traditionally, finding the geometric scale factors requires either systematic stepper motor movements of the XBPM or well controlled electron beam displacements to measure the response of the XBPM. For each Insertion Device gap it is required to repeat this in order to build up a complete set of scale factors covering all possible operating conditions. Elliptically Polarising Undulators further complicate matters by having multiple operating modes which would require multi dimensional lookup tables. Presented in this paper is a method for retrieving the geometric scale factors of an XBPM in real time by making use of the intrinsic small random movements of the electron beam and finding the correlation in synchronous measurements from Electron BPMs and XBPMs at kHz sample rates.

INTRODUCTION

Diamond Light Source utilizes two photoemission X-ray Beam Position Monitors (XBPMs) on most front ends in order to monitor and improve the stability of the photon beam. XBPMs for Insertion Device (ID) beamlines are mounted on stepper motors with micron-precision encoders, and traditionally the XBPMs are calibrated by using known stepper motor offsets to emulate real X-ray beam movements. Alternatively, controlled electron beam bumps through the ID straight can also be used to calibrate the XBPMs [1, 2]. A scale factor is calculated by comparing the measured response from the four XBPM blades to the known magnitude of the controlled movements. This gives a scale factor measured for a selection of ID gaps, which is saved into an EPICS database. During user operation the scale factor database is interpolated to give a factor for the current ID gap and used to convert the dimensionless position given by the XBPM signal into a position in mm. The dimensionless response of the XBPM, Δ/Σ, is defined as follows:

$$(\Delta/\Sigma)_x = \frac{A - B - C + D}{A + B + C + D}$$

$$(\Delta/\Sigma)_y = \frac{A + B - C - D}{A + B + C + D}$$

where A,B,C,D are the four XBPM blade signal currents.

There are several limitations to both of these calibration methods. Both require dedicated beamline time, during which the beamline is not able to accommodate users: if stepper motor movements are utilised then users may see X-ray beam shadowing as the XBPM moves across the beam; if electron beam bumps are used then the changing X-ray beam position and angle causes changes to the measured intensity and photon energy at the sample-point.

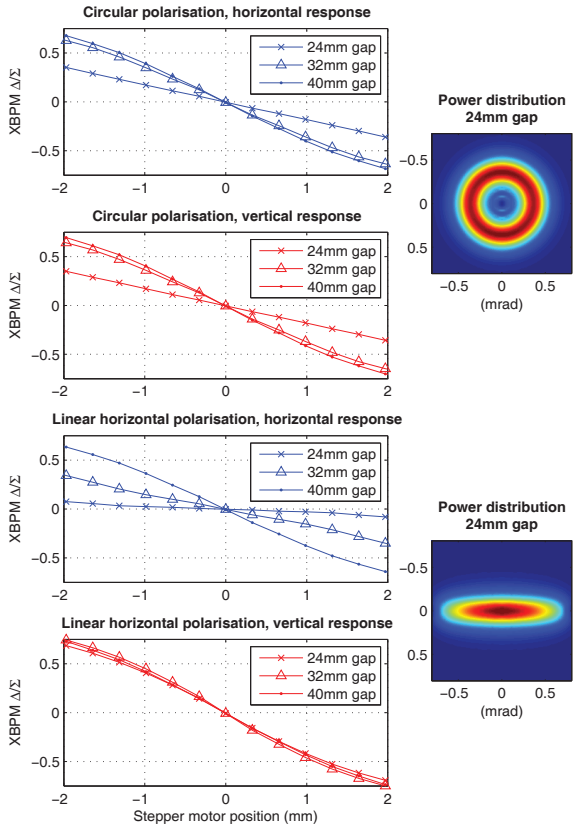

Figure 1: XBPM response to stepper motor movements for the I06 beamline at Diamond. The simulated power distribution of circular and linear horizontal polarised light are shown on the right to give an indication of the different photon distributions. Each gap and phase requires a different scale factor.

A second limitation is that a scale factor must be measured for each ID setting that a beamline could use, as different ID gaps produce different spatial distributions of radiation and thus require different scale factors. Elliptically polarising undulators, such as APPLE II devices, also require a different scale factor value for each different polarisation, as seen in Fig. 1. It is possible to create a look-up table for each individual ID setting, but populating such a table is a time consuming process. Typically at Diamond, a single XBPM stepper motor scan in one axis would take

ISBN 978-3-95450-119-9

NEW ELECTRONICS DESIGN FOR THE EUROPEAN XFEL RE-ENTRANT CAVITY MONITOR

C. Simon#, CEA-Saclay/DSM/Irfu, Gif sur Yvette, France
N. Baboi, DESY, Hamburg, Germany
R. Baldinger, B.Keil, R. Kramert, G. Marinkovic, M. Roggli, M. Stadler, PSI, Villigen, Switzerland

Abstract

About one third of the beam position monitors (BPMs) in the European XFEL (E-XFEL) cryomodules will be re-entrant cavities. The BPM mechanics and Radio-Frequency front-end (RFFE) electronics are developed by CEA/Saclay. Two RFFEs and a digital back-end with two ADC mezzanines are integrated into a compact standalone unit called MBU (modular BPM unit) developed by PSI.

The signal processing uses hybrids and a single stage down conversion to generate the signals sum and delta. Every RF/analog component of the re-entrant BPM electronics has been simulated with a Mathcad model and tested independently on test benches. The very low Q of the cavity monopole mode allows the new electronics to filter this mode at the dipole mode frequency, and an I/Q demodulation for delta and sum channels allow the digital back-end to determine the sign of the beam position just by comparing the phases of the channels, independently of beam arrival time jitter and external reference clock phase. This paper describes the design and architecture of a new re-entrant BPM electronics, including results of beam tests at FLASH that were performed to validate the chosen design.

INTRODUCTION

The European XFEL [1] is an X-ray free electron laser user facility currently under construction in Hamburg, Germany. This accelerator has a superconducting 17.5GeV main linac and its parameters are summarized in Tab 1.

Table 1: E-XFEL Accelerator Parameters

Parameter	Value
Normalized projected emittance	1-2 mm mrad
Typical beam sizes (RMS)	20 – 200 µm
Nominal bunch charge	0.1 – 1 nC
Bunch spacing	≥ 222 ns
Macro-pulse length	600 µs
Number of bunches within macro-pulse	1 - 2700
Nominal macro-pulse repetition rate	10 Hz
Maximum macro-pulse repetition rate	25 Hz

The BPM system is developed by a collaboration of CEA/Saclay/Irfu, DESY and PSI. Each cryomodule is equipped with a beam position monitor connected to a quadrupole at the high-energy end of the cavity string. 31 cold BPMs will be re-entrant RF cavities which have to operate in a clean and cryogenic environment. Pickup realisation and mounting in the cryomodule are a CEA/DESY collaboration but are not discussed here [2].

#claire.simon@cea.fr

MODULAR BPM UNIT CONCEPT

The electronics of the European XFEL BPM system [3] follows a modular design approach [4]. This customized crate, called Modular BPM Unit (MBU) (Fig. 1), contains a generic digital back-end (GPAC = generic PSI ADC carrier) with two ADC mezzanine boards, and either four button [3] or two re-entrant or undulator cavity [3] BPM RFFEs, or any combination of those types, as well as power supplies, fans, and a rear IO module with digital and multi-gigabit fiber optic IOs.

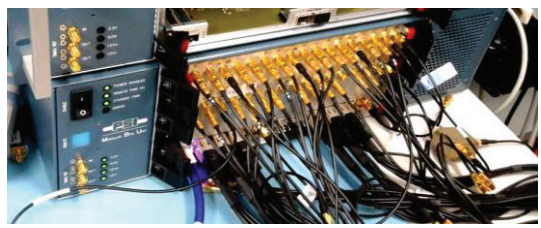

Figure 1: Modular BPM Unit.

RF/ANALOG ELECTRONICS

The signal processing of the re-entrant BPM uses a single stage down conversion to obtain Δ/Σ. The difference Δ and sum Σ signals are obtained from a passive 4- ports 180° hybrid which will be installed in a box mounted at the side of the cryomodule. Each coupler is connected to each pair of opposite antennas and transmits the signals to the radio-frequency front-end (RFFE) electronics via some 30 m long semi-rigid cables. This RFFE electronics, based on a Printed Circuit Board (PCB) with surface mount components, uses the VME64x form factor as required by the Modular BPM Unit. A first electronics was realized in 2010 and tested with beam [2], and a new RFFE with additional functionality is currently being developed.

New Design

The new RFFE analog electronics design, presented Fig. 2, has three channels to perform single-stage downconversion of X position, Y position and reference (charge) RF signals from L-band to an intermediate (IF) frequency. Because of the low external quality factor, the

ISBN 978-3-95450-119-9

DESIGN AND CHARACTERIZATION OF A PROTOTYPE STRIPLINE BEAM POSITION MONITOR FOR THE CLIC DRIVE BEAM*

A. Benot-Morell, CERN, Geneva, Switzerland and IFIC (CSIC-UV), Valencia, Spain
L. Søby, M. Wendt, CERN, Geneva, Switzerland
J.M. Nappa, J. Tassan-Viol, S. Vilalte, IN2P3-LAPP, Annecy-le-Vieux, France
S. Smith, SLAC National Accelerator Lab, Menlo Park CA, USA

Abstract

The prototype of a stripline Beam Position Monitor (BPM) with its associated readout electronics is under development at CERN, in collaboration with SLAC, LAPP and IFIC. The anticipated position resolution and accuracy are expected to be below 2µm and 20µm respectively for operation of the BPM in the CLIC drive beam (DB) linac. This paper describes the particular CLIC DB conditions with respect to the beam position monitoring, presents the measurement concept, and summarizes electromagnetic simulations and RF measurements performed on the prototype.

INTRODUCTION

CLIC, a Compact electron-positron LInear Collider proposed to probe high energy physics (HEP) in the TeV energy scale, is based on a two-beam scheme. RF power, required to accelerate a high energy luminosity beam is extracted from a high current Drive Beam (DB), whose decelerator requires more than 40000 quadrupoles, each holding a BPM. These BPMs face several challenges, as they will be operated in close proximity to the Power Extraction and Transfer Structures (PETS), while the accuracy requirements are demanding (20µm). They have to be compact, inexpensive and operate below the waveguide (WG) cut-off frequency of the beam pipe to ensure locality of the position signals, which rules out the signal processing at the 12GHz bunch frequency. Also wakefields, and hence the longitudinal impedance, must be kept low. This first proposed solution is a compact, conventional stripline BPM utilizing a signal processing scheme operating below 40MHz. Before installation into the CLIC Test Facility (CTF3), the manufactured prototype has been characterized in detail on an RF bench setup. In parallel, the design of a readout system is progressing.

CONCEPTUAL BPM PICKUP DESIGN

The CLIC DB stripline BPM pickup is compact and fits into the quadrupole vacuum chamber. Each of the four electrodes spans an angular coverage of 45º, having a characteristic impedance of 50Ω and a physical electrode length of L=25mm. As of the proximity of 12GHz high power accelerating structures (PETS), L was chosen to utilize one of the notches in the transfer function ($nc/2L$, n=2, where c is the speed of light in vacuum) to be at 12GHz, which is also the bunch frequency. Therefore, in the time domain, the idealized response to a multi-bunch train will only show the first and last pair of bunches, all other bunches in-between will be cancelled (Fig. 1). Other relevant design parameters are listed in Table 1.

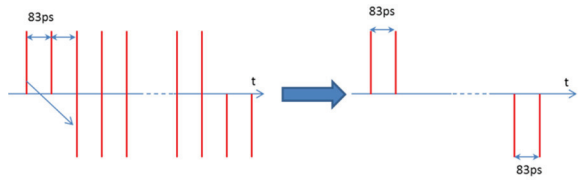

Figure 1: Idealized BPM multi-bunch train response.

Table 1: Drive Beam Stripline BPM Parameters

Parameter	Value	Comment
Diameter	24 mm	stripline ID
Stripline length	25 mm	
Width	12.5 %	of circumference (45^0)
Ch. Impedance	50 Ω	
Duct aperture	23 mm	In decelerator
Resolution	2 µm	Full train
Accuracy	20 µm	
Temporal resolution	10 ns	BW > 20 MHz

The signal processing will be performed at baseband frequencies ranging 4 to 40MHz, to avoid non-local confounding signals, mainly coming from the PETS, starting at 7.6GHz, the cut-off frequency of the TE_{11} mode for a circular waveguide of 23mm pipe aperture.

The position signal sensitivity of a stripline BPM detector is based on the image charge model, and is approximately $pos=(r/2)\Delta/\Sigma$, being r the beam pipe radius, Δ and Σ the difference and sum of the opposite electrode signals, and pos the horizontal (x) or vertical (y) beam position. A thorough description of the readout electronics and further details of the design can be found in [1] and [2].

PROTOTYPE CHARACTERIZATION

Position Characteristics and Linearity

The full system was tested using the procedure described in [2] to check its performance. The position characteristic was analysed using a stretched wire fed by an RF excitation signal, while being moved in 1mm steps in the range ±6mm. Table 2 shows the results for the position sensitivity at the origin, the electrical offset and the RMS linearity error for both planes. Although the performance of the electronics was satisfactory, showing the expected signal shape and levels, [2], the obtained

*Work supported by MINECO contract FPA2010-21456-C02-01, SEIC-2010-00028 and U.S. Department of Energy contract DE-AC02-76SF00515

ISBN 978-3-95450-119-9

MODULAR LOGARITHMIC AMPLIFIER BEAM POSITION MONITOR READOUT SYSTEM AT THE UNIVERSITY OF HAWAI'I*

B. T. Jacobson, M. R. Hadmack, J. M. J. Madey, P. Niknejadi
Department of Physics & Astronomy, University of Hawai'i, Honolulu, HI 96826, USA

Abstract

High brightness electron beams for inverse Compton photon sources driven by thermionic microwave guns require real-time position measurements in order to achieve the spatial and temporal coincidence necessary to ensure statistically measurable signals. True logarithmic amplifiers are more adequately suited to signal comparison than are sigma-delta methods. A low-cost, modular and scalable readout and data acquisition system for strip-line beam position monitors utilizing the AD640 log-amp is being developed at University of Hawai'i MkV Linear Accelerator and Free Electron Laser Lab. Initial measurements and prototyping of the hardware is complete with commissioning and deployment of the system currently ongoing. We present the methodology and early results of this project.

INTRODUCTION

The University of Hawai'i (UH) MkV Linear Accelerator facility and Free Electron Laser (FEL) Lab utilizes a thermionic LaB_6 cathode electron source in a microwave gun injector followed by a single section of traveling wave S-Band linear accelerator to produce a ∼200 mA average macro-pulse current 40 MeV electron beam. This beam drives a hybrid NdFeB planar undulator and Michelson interferometer phase-locked resonator based infrared FEL. Constructed on UH campus and occupying roughly one-third of the first floor of the physics department, the accelerator beamline was commissioned by 2009 and the lab produced first laser light in 2010; current experiments are focused on initial demonstration of inverse Compton x-ray photon production via FEL laser output and electron beam collision. A pico-second resolution x-ray detector and multi-gigabit per second sampling electronics are also being developed in parallel by collaborators in the University of Hawai'i Instrumentation Development Lab (IDLab) for measurement of the resulting micro-bunch x-ray train.

The electron beam transport system configuration for these experiments requires strong focusing to achieve small transverse size of the e-beam (and similarly for the optical beam used in the collision) in order to achieve optimum x-ray flux. One of the machine upgrades underway in support of the objective of a well-centered beam in the quadrupole magnets of the transport system and measurement of the electron beam transverse position for injection into the x-ray interaction point (IP) is the instrumentation of the beam position monitors (BPM's) installed along the UH MkV beamline.

Two varieties of BPM's are installed along the MkV beamline, a stripline type and a wall current variety. The stripline BPM's (shown installed on beamline in Fig. 1) consist of a stainless steel body with four copper electrodes oriented with $\frac{\pi}{2}$ symmetry mounted on standard $2\frac{3}{4}$ inch conflat flanges and are surplus from the SPEAR project at SLAC[1]. These stripline BPM's are installed in four locations along the diagnostic chicane transport system, which transports the e-beam from the linac to the FEL, as well as injects the e-beam into the scattering chamber where the x-ray IP is located.

The so-called "tin-can" wall current BPM's contain an FR-4 printed circuit board (PCB) sandwiched between a pair of conflat-type knife edge flanges that make vacuum seal against the copper plating on the board, routed with traces which carry induced wall current at four cardinal positions around the beam pipe with a minimum of temporal distortion to a 4-port connector block at the perimeter of the PCB. A suitably placed toroid provides a large inductance that forces all of the image currents that otherwise might flow along the outside of the beam pipe to instead flow along the impedance-matched PCB traces, insuring that all the components of the wall currents so sampled will emerge on the inner conductors of the coaxial output ports of the BPM. The frequency response of these wall current BPM's is nearly flat from below 100 kHz to beyond 20 GHz. Figure 2 shows one of the two wall current beam position monitors that have been installed in the MkV beamline (one at the linac output and one at the input to the FEL). Further description of these devices will be published separately.

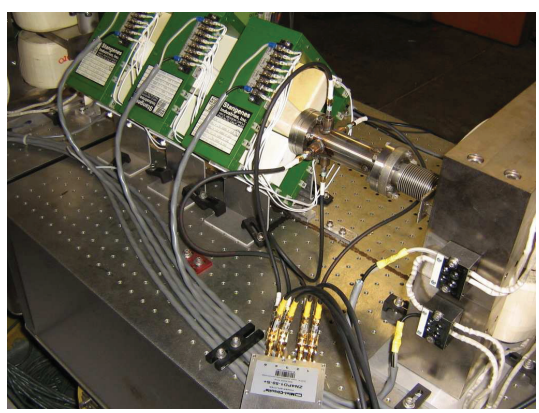

Figure 1: Stripline BPM installed on University of Hawai'i MkV FEL beamline.

* Work supported by DHS Agreement Number: 2010-DN-077-AR1045-02, Amendment 2

ISBN 978-3-95450-119-9

A PROTOTYPE CAVITY BEAM POSITION MONITOR FOR THE CLIC MAIN BEAM*

F. Cullinan†, S.T. Boogert, N. Joshi, A. Lyapin, JAI at Royal Holloway, Egham, UK
D. Bastard, E. Calvo, N. Chritin, F. Guillot-Vignot, T. Lefevre, L. Søby, M. Wendt, CERN, Geneva
A. Lunin, V.P. Yakovlev, Fermilab, Batavia, USA
S. Smith, SLAC, Menlo Park, California

Abstract

The Compact Linear Collider (CLIC) places unprecedented demands on its diagnostics systems. A large number of cavity beam position monitors (BPMs) throughout the main linac and beam delivery system (BDS) must routinely perform with 50 nm spatial resolution. Multiple position measurements within a single 156 ns bunch train are also required. A prototype low-Q cavity beam position monitor has been designed and built to be tested on the CLIC Test Facility (CTF3) probe beam. This paper presents the latest measurements of the prototype cavity BPM and the design and simulation of the radio frequency (RF) signal processing electronics with regards to the final performance. Installation of the BPM in the CTF3 probe beamline is also discussed.

INTRODUCTION

The CLIC design for 3 TeV centre of mass energy includes a 40 km long main linac and a 6 km long beam delivery system which require precise beam position monitoring for operation. This will be achieved using close to 4800 cavity beam position monitors, one for each of the 4196 quadrupole magnets in the main linac and a further 600 in the BDS. These must have a good spatial resolution of 50 nm and a time resolution of 50 ns in order to provide multiple, accurate position measurements within a single bunch train. They must also operate in an environment where large shifts in temperature are expected [1].

A prototype cavity BPM has been designed and built to be tested on the CTF3 probe beam later this year. It consists of two cavities, a position cavity and a reference cavity. The position cavity is a cylindrical pillbox with rectangular waveguides that strongly couple to the first resonant dipole mode in two polarisations (TM_{110}). The amplitude of each polarisation is proportional to the beam offset in one transverse dimension. The dipole mode frequency of 14.99 GHz is close to 14 GHz which will be used for CLIC. It was chosen so that signals from consecutive bunches, separated by 0.667 ns (0.5 ns for CLIC), add constructively and dominate signals from other modes excited by the beam. The reference cavity is re-entrant and its first monopole mode (TM_{010}) is used for bunch charge normalisation and as a reference beam arrival phase. It has the same frequency as the position cavity first dipole mode so that the same signal processing can be applied to both for improved stability. Both cavities are designed to have low quality factors in order to achieve a good time resolution. The beam pipe through the assembly has the same 4 mm radius as the CLIC main linac [2].

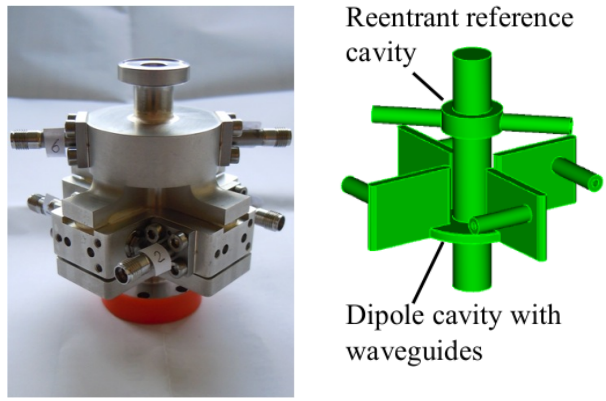

Figure 1: The brazed prototype pick-up assembly (left) and the vacuum geometry (right) with fitted feedthroughs.

A photograph of the two cavity assembly, which consists of four stainless steel parts brazed together, is shown in Fig. 1. The signals are extracted via feedthrough antennas in the re-entrant part of the reference cavity and in the case of the position cavity, at the end of the waveguides where there are also tuning bolts. These push against the wall of each waveguide opposite the antenna to tune the antenna coupling to the dipole mode resonant frequency. Each opposing pair of feedthrough antennas in the position cavity measure the same dipole mode polarisation. Combination of the two signals is not intended but having two means a lower external quality factor and leaves the option to suppress the TM_{210} quadrupole mode using a 180° hybrid or to compensate for cross coupling with adjustable short-circuit terminations. The signal from one of the two feedthrough antennas in the reference cavity could also be diode rectified for timing measurements [3].

The prototype pick-up was brazed at the end of April and the feedthroughs, which are aligned with dowel pins and sealed with silver-coated copper gaskets, were fitted afterwards by hand. The assembly then successfully passed a vacuum test. This paper describes the latest RF measurements of the cavity, progress towards developing down-conversion electronics and finally, beam test plans.

* The research leading to these results has received funding from the European Commission under the FP7 Research Infrastructures project EuCARD, grant agreement no.227579, DITANET under EU contract PITN-GA-2008-215080 and the STFC; Computing time with ACE3P provided by US DOE at NERSC

† Francis.Cullinan.2010@live.rhul.ac.uk

ISBN 978-3-95450-119-9

DEVELOPMENT OF 3D EO-SAMPLING SYSTEM FOR THE ULTIMATE TEMPORAL RESOLUTION

K. Ogawa and H. Tomizawa
RIKEN Harima Institute, 1-1-1 Kouto, Sayo-cho, Sayo-gun, Hyogo, Japan
Y. Okayasu and S. Matsubara
JASRI/SPring-8, 1-1-1 Kouto, Sayo-cho, Sayo-gun, Hyogo, Japan

Abstract

We have developed a set of key components for ultrafast electron-bunch measurement using Electro-Optic (EO) sampling technique. The key components are a highly-qualified EO-probe laser pulse with an octave bandwidth, an ultrafast organic EO crystal, and a spectrographic EO-demultiplexing (EO-decoding) system. In addition, we developed three-dimensional bunch charge distribution (3D-BCD) monitor with arrival timing for an FEL seeded with a high-order harmonic (HH) pulse. A 3D-BCD monitor is used multiple EO crystal. In our EUV-FEL accelerator, we prepared a seeded FEL with an EO-sampling based feedback system for user experiments. For obtaining a higher seeding hit rate, 3D overlapping between the electron bunch and the seeding HH-pulse must be maximized and kept at a constant optimal seeding condition. Keeping the peak wavelength of EO signals at the same wavelength with our feedback system, we provided seeded FEL pulses (intensity >4σ of SASE) with a 20-30% hit rate during pilot user experiments. For achieving the upper limit of temporal resolution, we are planning to combine high-temporal-response EO-detector crystals and an octave broadband laser pulse with a linear chirp rate of 1 fs/nm. We are developing the EO-probe laser pulse with ~10 μJ pulse energy and bandwidth over 300 nm (FWHM). In 2011, we successfully demonstrated the first electron bunch measurement with an ultrafast organic EO crystal in the FEL accelerator at SPring-8.

INTRODUCTION

Since 2010 at SPring-8, we have been demonstrating a seeded free-electron laser (FEL) in the extreme ultra violet (EUV) region by high-order harmonics (HH) generation from an external laser source in a prototype test accelerator (EUV-FEL) [1]. In FEL seeding as a full-coherent high-intensive light source for EUV user experiments, high hit rates of successfully seeded FEL pulses are required. Precise measurements of the electron bunch charge distribution (BCD) and its arrival timing are crucial keys to maximize and keep 3D (spatial and temporal) overlapping between the high-order harmonics (HH) laser pulse and the electron bunch. We constructed a timing drift monitor based on EO-sampling, which simultaneously measures the timing differences between the seeding laser pulse and the electron bunch using a common external pulsed laser source (Ti:Sapphire) of both the HH-driving and EO-probing pulses (Fig. 1). The EO-sampling system can use timing feedback for continuous operation of HH-seeded FELs.

The R&D of a non-destructive 3D-BCD monitor (proposed by H. Tomizawa in 2006 [2]) with bunch-by-bunch detection and real-time reconstructions has been investigated at SPring-8. This innovative monitor is based on an EO-multiplexing technique that resembles real-time spectral decoding and enables simultaneous non-destructive measurements of longitudinal and transverse BCDs. This part of the monitor was simultaneously materialized for probing eight EO crystals that surround the electron beam axis with a radial polarized, hollow EO-probe laser pulse. In 2009, we verified the concept of a 3D-BCD monitor through electron bunch measurements in the photoinjector test facility at SPring-8 [3].

As part of the Self-Amplified Spontaneous Emission (SASE) XFEL project at SPring-8, an additional target of temporal resolution is ~30 fs (FWHM), which utilizes an ultrafast organic EO crystal (DAST) instead of conventional inorganic EO crystals (ZnTe, GaP, etc.). EO sampling with DAST crystals is expected to measure a bunch length that is less than 30 fs (FWHM). In 2011, we demonstrated the first EOS bunch measurements with DAST crystal in the EUV-FEL accelerator.

In this paper, we describe the development status of ultrafast EO-sampling decoding system and octave broadband EO-probe laser pulse for application of 3D-BCD as a 3D-overlapping monitor for FEL seeding.

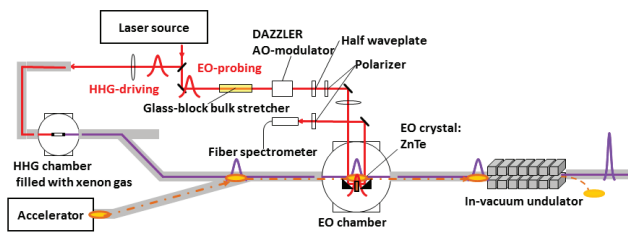

Figure 1: Experimental setup of seeded FEL with EO-sampling feedback at EUV-FEL accelerator: relative positioning in transverse and timing in longitudinal of electron bunch with respect to arriving timing of a seeding HH pulse are monitored at entrance of the first in-vacuum undulator to keep in a best seeding condition.

3D-BCD MONITOR

EO-sampling measures a probe-pulse's retardation by changing the refraction index of a non-linear optical crystal by the radial Coulomb field of relativistic electron bunch slices. The EO-probe laser pulse is injected into the EO crystal at the same time as the electron bunch arrives at the EO crystal. The BCDs are bunch-by-bunch encoded

ISBN 978-3-95450-119-9

IMPROVEMENT OF THE SIAM PHOTON SOURCE STORAGE RING BPM SYSTEM

S. Klinkhieo, P. Sudmuang, S. Krainara, N. Suradet, S. Tesprasitte, S. Boonsuya, P. Klysubun, SLRI, 111 University Ave., Muang, Nakhon Ratchasima 30000, Thailand
Yung-Hui Liu, Hsin-Pai Hsueh, June-Rong Chen, NSRRC, 101 Hsin-Ann Road, Hsinchu Science Park, Hsinchu 30076, Taiwan
P. Songsiriritthigul, School of Physics, Suranaree University of Technology, Muang, Nakhon Ratchasima 30000, Thailand

Abstract

This report describes the improvement of the Beam Position Monitor (BPM) system of the 1.2 GeV storage ring of the Siam Photon Source (SPS). Systematic studies and investigations to improve the machine performance, and storage ring BPM system have been carried out in the last few years. Major technical problems have been found and solved. The causes of the unreliability of the original BPM system were also identified. It was mainly caused by the low quality and improper installation of BPM signal cables. Detailed descriptions of the replacement with higher quality (lower loss and better interference shielding) BPM cables and implementation of a separate cable trays for the BPM cables, as well as the work on BPM electronic board calibration will be described. The measurement results before and after the improvement of the BPM system will also be presented.

INTRODUCTION

The Siam Photon Source storage ring routinely operates at 1.2 GeV with a nominal current of 150 mA. The ring circumference is 81.3 meters. Its lattice is Double Bend Achromat (DBA). The ring has, among other components, 20 button-type BPMs. [1, 2]

As the number of users increases, so does the demand for better quality beam. Our first efforts focused on investigation and improvement of the existing BPM system since the BPM is the most important diagnostic tool for both machine studies and routine machine operation. In addition, it will be an indispensable part of our orbit feedback system in the near future. In the beginning of 2011, major problems of the original BPM system were indentified and fixed by the machine group and visiting machine physicists from NSRRC, Taiwan. The improved BPM system shows reliable performance and exhibits accuracy of measurement in micron-scale resolution.

In the following sections, we first describe the status of the original SPS storage ring BPM system. We then present our work on replacing BPM signal cables and calibrating the BPM electronic modules. Finally, measurement results before and after the improvement of the BPM system are presented.

*supat@slri.or.th

ORIGINAL SPS STORAGE RING BPM SYSTEM

Back in the year 2000, the SPS storage ring was just installed and commissioned. The ring incorporated a set of 20 button-type BPMs, with each BPM comprised of a BPM block, position sensors, coaxial cables, and detector electronics board. The signals from each individual board were collected and processed by the control system. The BPM block is directly welded on the storage ring vacuum chambers without flanges or bellows.

BPM Electronic Modules

The BPM pick-up system uses four electrodes as position sensors. Beam position is a function of the amplitude difference of these electrodes' signals. These signals are fed into the BPM electronic modules where they are processed sequentially to provide simultaneously two outputs: horizontal (X) and vertical (Y) beam positions. [3, 4]

The MX-BPM-118.00MHz electronic modules of the BPMs were made by Bergoz Instrumentation. All the modules and data acquisition equipments are distributed into two groups, the housing of which are located outside the radiation shielding wall on the opposing sides of the storage ring (Fig. 1).

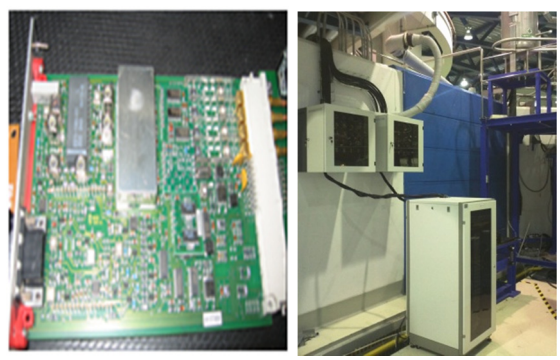

(a) (b)

Figure 1: (a) Bergoz BPM electronic module. (b) Electronic device rack.

BPM Cables

The old system uses HUBER&SHUNER GX03272 coaxial cables, with one layer of electromagnetic shielding, mounted with N-type and SMA-type connectors on each end. The BPM electrode signal is

ISBN 978-3-95450-119-9

PHOTON BEAM POSITION MONITOR AT SIAM PHOTON SOURCE

P. Sudmuang, S. Chaichual, N. Suradet, S. Boonsuya, N. Sumano, S. Krainara, H. Nakajima, S. Rugmai, P. Klysubun
Synchrotron Light Research Institute, 111 University Avenue, Muang District, Nakhon Ratchasima 30000, Thailand

Abstract

Photon beam position monitors (PBPM) have been designed and installed in the beamline front-ends at Siam Photon Source (SPS). Up till now, these blade-type PBPMs have been successfully installed at three bending magnet and an insertion device (planar undulator) beamlines. Their performance has been tested and compared with that of the electron beam position monitor. The achieved resolution is found to be better than 3 μm. The obtained PBPM data proved to be extremely invaluable in the investigation of the sources of the observed beam positional fluctuation, and for compensation of the orbit perturbation caused by undulator gap change. In this paper, the details of the calibration procedure will be presented. Various factors affecting reading of the signal such as undulator gap change effect, choice of bias voltage, and temperature variation have been investigated and the results will be discussed herewith.

INTRODUCTION

The Siam Photon Source (SPS) is a dedicated 1.2 GeV synchrotron light source in Thailand [1]. Currently, there are seven photon beamlines in operation, with three more under commissioning. In addition, there are three new photon beamlines under construction. As the number of experiments increases, coupled with the fact that more complicate experiments are being carried out, there is more demand from the users for higher quality beam, especially with regards to the beam positional stability aspect. In recent years the machine group has focused its effort to achieve this goal [2]. To investigate the sources of the beam position fluctuation and observe the subsequent improvement quantitatively, Photon Beam Position Monitors (PBPMs) have been developed and installed. Several types of PBPMs have been developed at synchrotron facilities around the world [3-4]. For SPS, the 4-blade type PBPM is chosen.

In this paper, the PBPM structure together with the criteria for blade spacing determination are presented, followed by the details of the calibration procedure, and various factors affecting the sensitivity and linearity threshold of the PBPM. In addition, the experiments for testing PBPM performance are described.

PBPM DESIGN

PBPM Structure

Figure 1(a) shows the design of the 4-blade type PBPM structure. The blades are triangular and were made of 0.2 mm-thick tungsten. The upper pair was affixed to a water-cooled copper block at the front facing the beam, while the lower pair was placed at the rear end. The blades were slotted in sapphire plates for electrical insulation and thermal conduction. A biased photoelectron collector was installed on each side of the copper block to remove the scattered photoelectrons. The PBPM block is attached to an XY translation stage for alignment and calibration processes. The schematic layout of the whole PBPM setup is shown in Figure 1(b). Generated photocurrent is measured by a picoammeter (Keithley 6485). To investigate thermal effect on the measured photocurrent, a thermocouple was installed on the copper block.

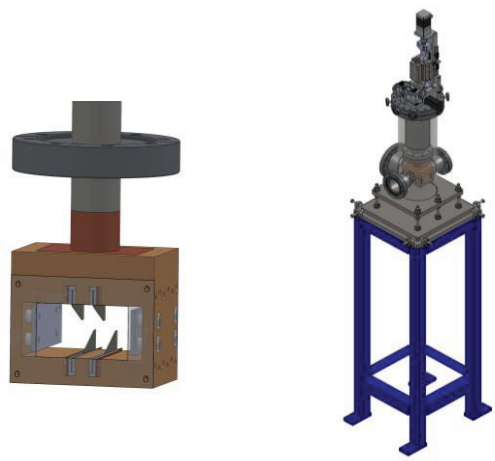

(a) (b)

Figure 1: 3D drawings of (a) the 4-blade type PBPM block, and (b) the whole PBPM setup.

Determination of the Blade Spacing

The spacing between the blades (G_x , G_y), as shown in Figure 2, are determined by the photon beam power densities at the location of the PBPM. In order to optimize the sensitivity and linearity range, the spacing should be two times the Gaussian width, i.e. $G = 2\sigma$, except for G_x of the bending magnet PBPM, which is specified by the horizontal opening angle of a particular photon beamline. To avoid cross-talk among the blades, the upper and lower blades were shifted by 2 mm (D) apart.

ISBN 978-3-95450-119-9

PERFORMANCE AND UPGRADE OF BPMS AT THE J-PARC MR

T. Toyama[1], Y. Hashimoto[1], K. Hanamura[3], S. Hatakeyama[2,3], M. Okada[1], M. Tejima[1]
J-PARC/KEK[1], J-PARC/JAEA[2], Mitsubishi Electric System & Service Co.,Ltd[3], Tokai, Naka, Japan

Abstract

Since recovery from the great earthquake 2011.3.11, proton beams, more than 10^{14} ppp (protons/pulse), are accelerated up to 30 GeV at the J-PARC MR. For higher intensity beams the following two tasks need to finish: signal attenuation and re-allocation of the BPMs. The attenuator and switchable LPF are attached just before the BPMC (a processing circuit for the BPM). In connection with the MR collimator upgrade to get much more intensity, some BPMs are re-allocated with the steering magnets.

INTRODUCTION

The BPMs in the J-PARC MR were originally designed with the external capacitors [1, 2]. The aim was to improve a position response by mitigating the capacitive coupling between electrodes, and to get an adequate output voltage at the design intensity, $4x10^{13}$ ppb (protons/bunch) with the lowered cut-off frequency. However, we decided to abandon the idea of adding the capacitors. With the external capacitors the signal would have been too small at low intensity beams of the initial beam commissioning. On the contrary in the present configuration without capacitors the signal is too large with the design intensity beam. We have added the small box consisted of an attenuator and a switchable LPF just before the BPMC (a processing circuit for the BPM). This paper describes the design and test results on those additional backend-circuits.

To reach higher intensities, we have to admit more controlled beam losses localized at the MR collimator than the original design [3, 4]. The original lattice element order:

Quad. – Drift / Collimator – Steering – [BPM+Quad]

was changed to

Quad. – Drift / Collimator – Additional collimator – Quad. – [Steering+BPM].

The design and procedure of the re-allocation is reported.

ATTENUATOR PLUS SWITCHABLE LPF FOR MR BPMS

There are 186 BPMs in the MR. A drawing and a photograph of the regular size BPM are depicted in Fig. 1. The electrodes are cut diagonally, which result in linear position response. According with the recent intensity increase, Fig. 2, we need to set the signal attenuators before the present BPMC (Fig.3).

One of the diagonal-cut electrode pair with the inner diameter of ϕ130 mm and the length of 100 mm is estimated to produce the signals as shown with a red line in Fig. 3. The design intensity of ~$4x10^{13}$ protons per bunch and the bunching factor (B_f) of ~0.045 (flat top) are assumed.

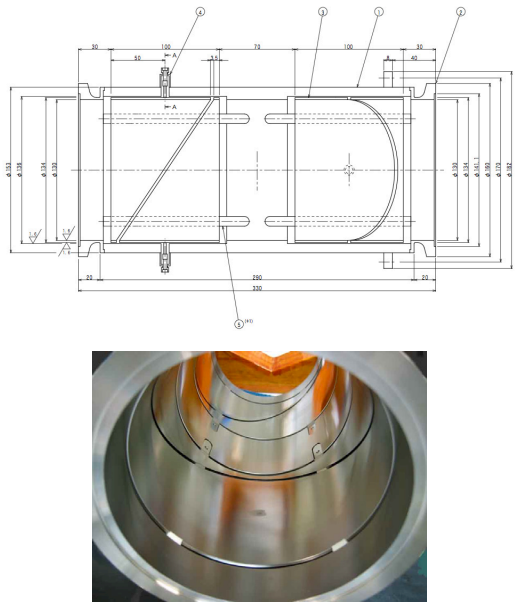

Figure 1: Beam position monitor of the MR.

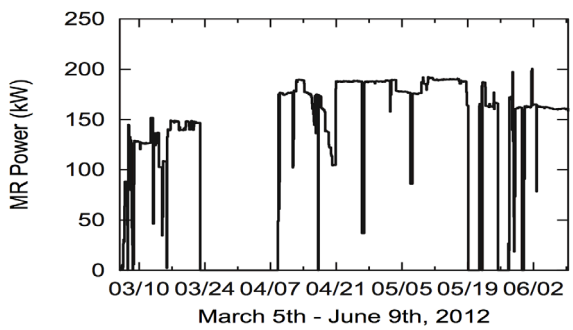

Figure 2: MR beam power history of the fast beam extraction in the first half of FY2012 [5].

Due to the high-pass frequency characteristics of the BPM, higher frequency dominated beam of smaller B_f tends to produce higher BPM output voltage, 108 V at maximum. The peak beam current variation due to adiabatic change of the longitudinal motion during acceleration from 3 GeV to 30 GeV is exaggerated by the high-pass frequency response of the BPM, and the signal variation due to B_f change from 0.3 to 0.045 is ~30 times (Fig. 4). Adopting LPF with the cut-off of 796kHz, we obtain the signal voltage for the BPM circuit as 9.25 V at maximum with a 10 dB attenuator as shown in Fig. 3 and 4, which is well below the acceptable input level of the BPM circuits. Moreover the signal voltage variation is reduced to the ratio of ~8.

ISBN 978-3-95450-119-9

TURN-BY-TURN BPM SYSTEM USING COAXIAL SWITCHES AND ARM MICROCONTROLLER AT UVSOR

Tomonori Toyoda, Kenji Hayashi, and Masahiro Katoh, IMS, Okazaki, Japan

Abstract

A major upgrade of the electron storage ring at UVSOR facility (Institute for Molecular Science, Japan) started from April 2012. To assist the commissioning procedure, we have developed a turn-by-turn Beam Position Monitor (BPM) system which consists of a signal switching circuit, a digital oscilloscope and software. Using this system, we have been able to determine not only the orbit but also the betatron tune. The system was very powerful to achieve the beam storage at the commissioning.

OUTLINE OF UVSOR

A 750 MeV synchrotron light source, UVSOR (Fig. 1), has been operational since 1983. In 2003, the ring had a major upgrade to reduce the emittance and increase the straight sections available for insertion devices. Since then, the ring has been called UVSOR-II. Since 2010, the storage ring had been operated for users fully in the top-up injection mode, in which the beam current is kept constant at 300 mA.

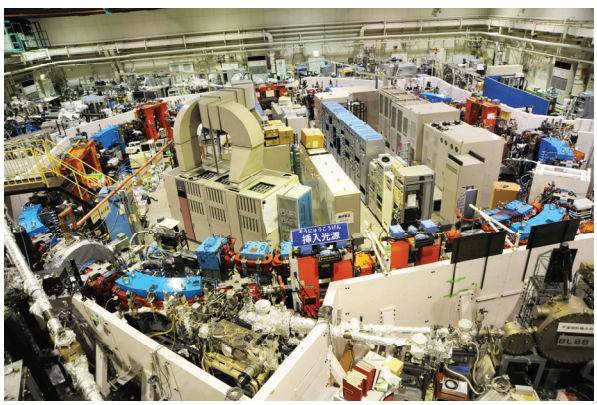

Figure 1: UVSOR-III electron storage ring.

In 2012, a new upgrade program is in progress. The bending magnets were replaced with combined-function ones to reduce the emittance by about a factor of two. A new in-vacuum undulator was installed in the last straight section reserved for insertion devices. A pulse sextupole magnet for injection without a bump orbit was constructed and is ready for commissioning. After this upgrade, the ring is called UVSOR-III. Parameters of UVSOR-III are shown in Table 1.

Table 1: Main Parameters of UVSOR-III

Electron Beam energy	750MeV
Circumference	53.2m
Straight Sections	4m x 4, 1.5m x 4
Emittance	17nm-rad
Energy Spread	5.4m x 10^{-4}
Betatron Tunes	(3.70, 3.20)
Momentum Compaction Factor	0.033
XY Coupling(presumed)	3%
RF Accelerating Voltage	100kV
RF Frequency	90.1MHz

BPM AT UVSOR

UVSOR-III storage ring has 24 BPMs (Fig. 2), each of which consists of 4 button electrodes (Fig. 3 and 4). We use a commercial signal processing system (Bergoz Co. [1]) for regular operation.

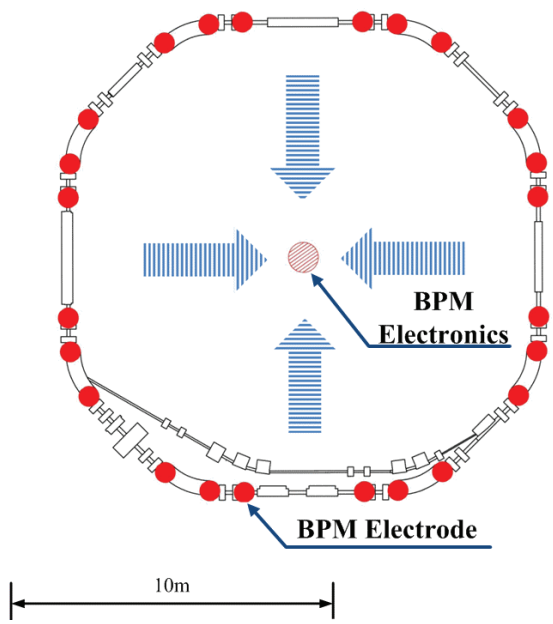

Figure 2: Layout of the BPM heads along the ring.

Position of the electron beam is calculated using the equations:

$$X = K_X \frac{V_A - V_B - V_C + V_D}{V_A + V_B + V_C + V_D} \qquad (1)$$

ISBN 978-3-95450-119-9

APPLICATION OF EMMA BPMS TO THE ALICE ENERGY RECOVERY LINAC

A. Kalinin#, D. Angal-Kalinin, F. Jackson, J. K. Jones, P. H. Williams,
ASTeC, STFC Daresbury Laboratory, Warrington, U.K

Abstract

The ALICE Energy Recovery Linac Arc1 button pickups have been recently equipped with EMMA BPM electronics. These EPICS VME BPMs give bunch-by-bunch information about charge and position, allowing investigation of beam dynamics in ALICE in different modes of operation. A Mathematica program is designed to monitor statistically individual bunches (spacing 61.54ns) as well the train as a whole (up to 1625 bunches), allowing the study of jitter and position stability of the beam through the Arc1. The Arc1 has been designed to be isochronous, with the bunch compression achieved through a separate dedicated bunch compressor chicane. The Arc1 incorporates two sextupoles for correcting non-linear longitudinal matrix terms and experimental evidence suggests that the off-centred beam in the sextupoles breaks the linear isochronicity. We present some beam measurement results collected in 2012 using these BPMs.

INTRODUCTION

The ALICE (Accelerators and Lasers In Combined Experiments) facility, shown in Fig.1, is an energy recovery test accelerator operated at Daresbury Laboratory since 2006 [2].

The accelerator consists of: a photoinjector with DC gun (up to 350 keV); buncher and superconducting booster (typically 6.5 MeV beam energy); an energy-recovery loop (typically 26 MeV beam energy) containing a superconducting linac module; a bunch compression chicane; and an FEL undulator.

The main demands on the ALICE beam dynamics and beam quality come from the IR-FEL and the coherent THz emission from the compression chicane used for dedicated experiments. By design the ALICE lattice consists of an isochronous first arc (Arc1), a bunch compressor with R_{56}= –0.28m, and a second arc with R_{56} = +0.28m. The arc design is based on triple bend achromats (TBA) [3], and the R_{56} is tuneable by the strengths of quadrupoles within the arc.

The R_{56} of Arc1 strongly influences the post linac bunch compression. This has been consistently observed in both THz as well as FEL setups. Due to a previous lack of reliable beam diagnostics in Arc1, it has not been possible to investigate beam dynamics in detail, especially through the sextupoles, which are needed to provide second order correction. It has consistently been observed that the two sextupoles steer the beam and modify the transverse optics, making Arc1 non-isochronous and affecting the beam dynamics in the transverse as well as longitudinal planes. FEL lasing was found to be very sensitive to the setting of the first sextupole, whereas the second sextupole has never demonstrated any improvement in either the FEL or THz setups.

In order to understand the beam dynamics in Arc1 and the chicane, the pickups 01 to 06 in Arc1 (see inset of Fig. 1), and an additional pickup in the chicane, have been recently equipped with EMMA BPM electronics. It is possible to connect any five (from seven) pickups to the electronics at a time. These BPMs provide information about misalignments and trajectory errors in Arc1 as well as providing bunch-by-bunch and train-to-train information about charge and position.

Additional information from the time-of-flight (ToF) measurements [4] combined with these observations should be able to provide a better understanding of beam dynamics, and help in explaining the current performance limitations.

We present here the first experimental results obtained using these BPMs, and describe the details of BPM capabilities and the Mathematica processing program used for analysis.

BEAM POSITION MONITORS

One of the ALICE functions is to deliver beam to a NS-FFAG EMMA. EMMA's BPMs [1] are designed for turn-by-turn measurements (turn is 55.2ns). Four of them of the same type are used in the ALICE to EMMA Injection Line to monitor a single bunch train from ALICE. These BPMs were modified to work with ALICE many-bunch trains, which is useful for injection tuning and opens the possibility to apply these BPMs to ALICE as well. The ALICE train bunch rate can be set to (1.3GHz/16)/N, where N=1, 2, ... is an integer. For most of ALICE experiments, N=5 (bunch spacing T=61.54ns). This rate has been used for the BPM measurements below. The train length was up to 1625 bunches (which is typical for IR-FEL operation). The bunch charge was in the range (30 to 60)pC.

The Arc1 and chicane pickups are rectangle pickups with two pairs of horizontal buttons symmetrically spaced from the x, y planes. In the measurements below we calculated the beam offset in the simplest way using a formula $((V11-V12\mp V21\pm V22))/\Sigma$, and the charge simply as $\Sigma=V11+V12+V21+V22$. The pickups have no fiducials, so the relative positions of the BPM centres to the quadrupole centres, or the beam pipe, are unknown.

Each two-plane BPM (see [1]) comprises two Front-Ends placed near the pickup. Each of them works with two opposite button signals. It first converts them into

#alexander.kalinin@stfc.ac.uk

ISBN 978-3-95450-119-9

DESIGN AND FABRICATION OF THE STRIPLINE BPM AT ESS-BILBAO

S. Varnasseri, I. Arredondo, D. Belver, F.J. Bermejo, J. Feuchtwanger, N. Garmendia,
P.J. Gonzalez, L. Muguira, ESS-Bilbao, Leioa, Spain
V. Etxebarria, J. Jugo, J. Portilla, University of the Basque Country, UPV/EHU, Leioa, Spain

Abstract

A stripline-type BPM has been designed and built at the ESS-Bilbao premises. The design is based on traveling wave electrodes principles to detect the transverse position of the beam enclosed within the vacuum chamber. In the design of stripline setup, it has been considered to keep the comparison conditions with previously used pick-ups as similar as possible. The length of strip electrodes is 200 mm and the coverage angle is 0.952 rad. The structure is rotationally $\pi/2$ symmetric and the alignment of electrodes are $\pi/4$, $3\pi/4$, $5\pi/4$ and $7\pi/4$. The design is optimized for a frequency of 352 MHz, however it can function on a wide range of frequencies out coming from the measurement results. Striplines in general have well defined behavior even for low beta and low intensity beams as well as functionality at low and high frequencies. A report on the design and characteristics measurement of stripline is presented which includes the frequency range, the effect of insulation of electrodes, the electrode response as well as their sensitivity to beam power and position.

INTRODUCTION

The ESS-Bilbao (ESSB) project comprises a light-ion linear accelerator feeding a low-energy neutron source. Beam Position Monitors (BPMs) are some of the diagnostic systems under current development. A first stage in such an endeavor was the full development of a Button Pick-up BPM prototype [1] which attained full performance specification. The main drawback of button pick-ups concerns their weak sensing response at low energy and low beta beams such are the ones already under consideration within ESS-Bilbao. To overcome such difficulty, in collaboration with the Department of Electricity and Electronics of the University of the Basque Country (UPV/EHU), we have designed, built and tested a stripline monitor consisting of four electrodes as schematically shown in Fig.1. The implementation of this BPM system includes the pick-ups and stripline BPMs, the test stand for simulating beam conditions, the analog and digital electronic units and the control system [1]. The control system integrates the BPM system into the Experimental Physics and Industrial Controls System (EPICS) [2] network of the accelerator.

GENERAL DESIGN AND CONSIDERATIONS

The electromagnetic structure of the stripline BPM was separated into two smaller structures for the ease of the electromagnetic simulation [3]. One structure includes the tube and electrode strips and the second structure comprises the transitions and feedthroughs. The criteria of maximum sensitivity at the ESSB RF frequency of 352 MHz and the 50 Ω impedance for the elements are taken as constraints to the design. The rigid N-type feedthrough with long signal pin is chosen as also the signal feed out from stripline to the electronics via coaxial cables. The transition from the strip electrode to the feedthrough was simulated and optimized in order to minimize the signal reflection in both ways. The optimum length of electrode, for which the sensitivity of the signal to the beam displacement is maximum, occurs at a signal walk equal to one quarter of wavelength of the exit beam. The stripline tube inner diameter is 57 mm and the length of strip electrodes is 200 mm, while the azimuthal coverage angle is 0.952 rad. Increasing the coverage angle could result in signal integrity deterioration due to coupling between adjacent strip electrodes. The assembly angles of strip electrodes are $\pi/4$, $3\pi/4$, $5\pi/4$ and $7\pi/4$. This corresponds to a $\pi/4$ rotation of the stripline block around the beam axis in order to be fitted easily on the test stand.

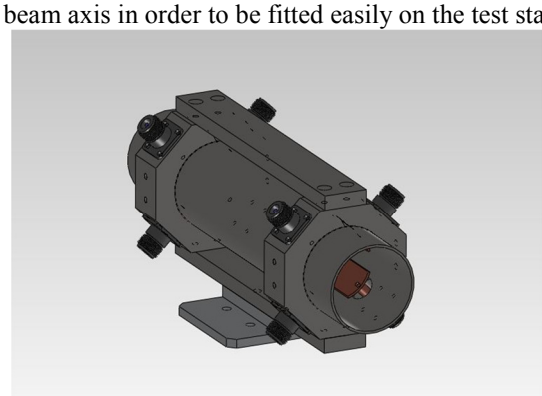

Figure 1: 3D schematic of the stripline BPM.

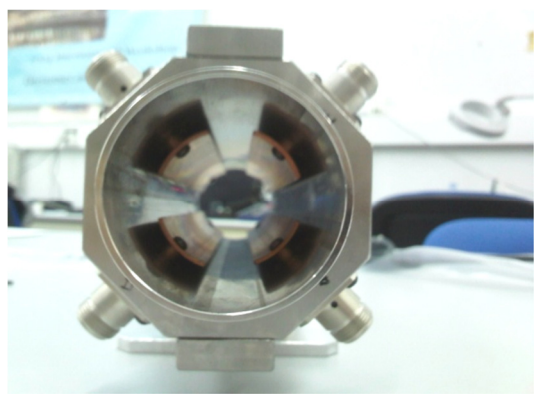

Figure 2: Stripline BPM fabricated electrodes configuration.

ISBN 978-3-95450-119-9

IMAGE PROFILE DIAGNOSTICS SOLUTION FOR THE TAIWAN PHOTON SOURCE

C. Y. Liao#, C. H. Kuo, C. Y. Wu, Y. S. Cheng, Demi Lee, P. C. Chiu, K. H. Hu, K. T. Hsu
NSRRC, Hsinchu 30076, Taiwan

Abstract

TPS (Taiwan Photo Source) is a third generation 3 GeV synchrotron light facility, featuring ultra-high photon brightness with extremely low emittance which will be a state-of-the-art synchrotron radiation facility and is being in construction at National Synchrotron Radiation Research Center (NSRRC) campus. Beam image profile and its analysis play an important role in beam diagnostics of a particle accelerator system. However, due to the CCD image collection devices are distributed around the linac, booster, and storage ring, a distributed EPICS system based image profile diagnostics solution was proposed, which are based on GigE Vision camera with PoE support. This solution provides an easy way for cabling, and delivery adequate performance. Implementation plan for the TPS and results of prototype test at existed facility to examine functionality of hardware and software will be summarized in this report.

INTRODUCTION

The TPS is a state-of-the-art synchrotron radiation facility featuring ultra-high photon brightness with extremely low emittance [1]. Civil construction was started from February 2010. The building will be finished in 2012. Machine commissioning is scheduled in late 2013. User service will start from 2014. The TPS accelerator complex consists of a 150 MeV S-band linac, linac to booster transfer line (LTB), 0.15–3 GeV booster synchrotron, booster to storage ring transfer line (BTS), and 3 GeV storage ring. The storage ring has 24 DBA lattices cells with 6-fold symmetry configuration. The latest generation diagnostic systems will equip to help TPS achieve its design goals.

To optimize the machine operation and diagnostic applications, the beam profile and its analysis play an important role in the beam diagnostics of a particle-accelerator system. The use of a destructive (fluorescent screen, YAG:Ce, $Y_3Al_5O_{12}$ [2]) or non-destructive (Microchannel plate, MCP [3]) screen monitor, or a synchrotron radiation monitor [4] to measure the beam profile is a simple mechanism that has been widely used in synchrotron facilities. The beam-profile image conveys extensive information about beam parameters, including the beam centre, sigma, tilt angle etc. As is customary, the beam profile as a two-dimensional (2D) image is recorded with cameras. The fluorescent screens that convert the flux density of the beam into a measurable signal as a function of position, and a charge-coupled device (CCD) camera for image acquisition, are used in applications of this kind. Thanks to inexpensive CCD cameras and the availability of computer technology, the obtaining, storage and analysis of 2D images has become easier and quicker. The images of the beam as recorded with cameras are most conveniently represented as light intensity with 2D circular or elliptical Gaussian distributions.

In this report, a distributed EPICS system based image profile diagnostics solution was proposed, which are based on Gigabit PoE (Power over Ethernet) embedded vision system with PoE camera. This solution provides an effective way to simplify wiring, and increased performance, load independence and reliability, which can be used at various places such as screen monitor, synchrotron radiation monitor, ICCD, and streak camera, as a standalone image acquisition and processing system.

OVERVIEW OF INFRASTRUCTURE

The infrastructure is developed by using a Gigabit PoE embedded vision system installed the EPICS IOC and integrated with Matlab program to build up a data acquisition and processing system. For the beam diagnostic application, this system is responsible for the beam profile acquisition from fluorescent screen, gated ICCD or streak camera, and used to analysis to find the beam characteristic data. The infrastructure employed can be divided into hardware and software components as described in the following subsections.

Vision System and Camera

In the image profile diagnostics solution, a Gigabit PoE embedded vision system (ADLINK, EOS-1200 [5]), as shown in Fig. 1, was used instead of traditional computer and switch. This device is a rugged and compact embedded vision system equipped with the 2nd generation CPU (i7) and four independent PoE ports. It also supports a rich I/O capability, including four serial ports (RS232/422/485), two USB 3.0 ports, 32 PNP/NPN isolated digital I/Os, which make it ideal to integrate, and deploy with other subsystem for system development.

Figure 1: Gigabit PoE embedded vision system.

#liao.cy@nsrrc.org.tw

ISBN 978-3-95450-119-9

IMPROVEMENT OF HARDWARE AND SOFTWARE SETUP FOR THE ACQUISITION AND PROCESSING OF SIAM PHOTON SOURCE BPM SIGNAL

N. Suradet, S. Klinkhieo, P. Sudmuang, S. Krainara, C. Preecha, S. Boonsuya, P. Klysubun
SLRI, 111 University Avenue, Muang District, Nakhon Ratchasima, 30000, Thailand

Abstract

Data acquisition and processing system has been developed for the Siam Photon Source (SPS) storage ring BPM system in order to improve monitoring and logging performances. BPM readout, i.e. scanning of BPM electrode voltage outputs and subsequently converting to X-Y position values, is now performed by an upgraded Programmable Logic Controller (PLC) with higher bit resolution (16-bit) analog-to-digital converter (ADC). Moving averaging is then performed on the obtained BPM data utilizing a LabVIEW code to reduce background noise during on-line measurement. All data is then stored on a dedicated computer serving as a central data logging system, which can be remotely accessed via a network communication link. In this report, details of the new setup will be presented, and comparison will be made between the performance of the new and previous setups, together with suggestions on further improvements.

INTRODUCTION

The Siam Photon Source (SPS) is the first synchrotron light source of Thailand. The accelerator complex consists of a 40 MeV electron linac, a 1.0-GeV injector and a 1.2 GeV electron storage ring, the configuration of which is based on a four-fold symmetric double bend achromat (DBA) lattice. [1-3] In recent years, the demand for better beam position stability has continually increased. To address this issue, the machine group has undertaken a number of coordinated efforts, for e.g., improving sensor systems in the storage ring, stabilizing ambient and cooling water temperatures, improving the diagnostic beamline setup, developing a slow orbit feedback system, among others. One of the most important tasks in this undertaking is undoubtedly the improvement of the orbit measurement and monitoring systems.

The improved SPS storage ring BPM system has provided the machine group with the possibility to improve the beam quality by providing accurate and reliable reading, assisting the group in making correct analyses. The new logging and retrieval systems also help making the correlation between the monitored beam fluctuation and any machine parameters easier. It is also a vital part of the slow orbit feedback system, which had not been possible to implement since the machine produced its first synchrotron light. [4, 5]. This report describes the improvement of BPM data acquisition and processing system, the development of a new logging system, along with the upgraded hardware and software configurations. The measurement results before and after the improvement will be presented and discussed.

HARDWARE CONFIGURATION

Figure 1 shows a schematic block diagram of the developed BPM signal processing for the SPS storage ring. The BPM electrode signals processed by the BPM electronic modules are passed to the programmable logic controllers (PLC). Signal averaging and data logging are then performed by two dedicated computer servers.

BPM System

BPM pickups are installed in 20 locations next to the quadrupole magnets along the 81.3 meters long circumference of the SPS storage ring. Each BPM block consists of four electrodes. Raw signals from the electrodes will be sent to the *BPM electronic modules* where they are processed to provide horizontal (X) and vertical (Y) beam position outputs, simultaneously [4, 5].

Programmable Logic Control

The PLC has to accomplish several tasks. First, the output signals from BPM electronic modules are converted by a new 16-bit ADC (Allen Bradley 1756-IF6I) in the PLC's module at 40 Hz sampling frequency. The X-Y beam positions are calculated and subsequently fed into the PC-Average and PC-Logger computers. All PLC and BPM modules, as well as all electronic devices for data acquisition are installed in the same rack, situated just outside the storage ring in the experimental hall area.

Computers

The two processing computers are located in the machine control room. The data processing server (PC-Average) and the data acquisition server (PC-Logger) are connected to each other via a LAN network.

SOFTWARE CONFIGURATION

As mention in the previous section, the software development and implementation are divided into two parts: (i) the data processing (moving average) part on PC-Average computer, and (ii) the data acquisition (data logging) part on PC-Logger computer.

ISBN 978-3-95450-119-9

DESIGN STATUS OF THE EUROPEAN X-FEL TRANVERSE INTRA BUNCH TRAIN FEEDBACK

Boris Keil, Raphael Baldinger, Carl David Beard, Micha Markus Dehler, Waldemar Koprek, Goran Marinkovic, Markus Roggli, Martin Rohrer, Markus Stadler, Daniel Marco Treyer,
PSI, Villigen, Switzerland
Vladimir Balandin, Winfried Decking, Nina Golubeva, DESY, Hamburg, Germany

Abstract

The European X-Ray Free Electron Laser (E-XFEL) [1] will have a fast transverse intra-bunch train feedback (IBFB) system [2] to stabilize the beam position in the SASE undulators. E-XFEL bunch trains consist of up to 2700 bunches with a minimum bunch spacing of 222ns and typ. 10Hz train repetition rate. The IBFB will measure the positions of each bunch in the bunch train, and apply intra-train feedback corrections with fast kickers, in addition to a feed-forward correction for reproducible trajectory perturbations. By achieving a feedback loop latency in the order of one microsecond, the IBFB will allow the beam position to converge quickly to the nominal orbit as required for stable SASE operation. The latest conceptual design of the IBFB and the status of IBFB components will be presented.

INTRODUCTION

The E-XFEL has a superconducting 17.5GeV main linac, with 0.1-1nC nominal bunch charge, and N·111ns bunch spacing, where N is an integer > 1. One distinct feature of the accelerator is its ability to generate bunch trains of up to 600µs length with arbitrary bunch patterns for the SASE undulators, where different parts of the same bunch train can be distributed to different undulator lines by means of a beam distribution system [3].

Transverse Beam Stability

In order to achieve sufficient and reproducible intensity and pointing stability of the X-ray photon pulses generated in the E-XFEL SASE undulators, the electron beam should deviate less than ~σ/10 from its nominal (ideally straight) trajectory in the undulators, with typical beam sizes of σ=30µm or less depending on beam charge and resulting emittance. However, due to a number of transverse perturbations sources, deviations of more than ~σ/10 from this trajectory are expected to occur without operational IBFB. Perturbations that are random, i.e. not reproducible, will be corrected by a fast intra bunch train feedback (IBFB) system can measure and correct the trajectory individually for each bunch. In addition, for perturbations that are reproducible from bunch train to bunch train (or change sufficiently slow) the IBFB will apply a static (or adaptive) feed-forward correction.

Perturbation Sources, Frequencies, and Feedback Loop Latency

Table 1 shows the presently expected main horizontal (X) and vertical (Y) perturbation sources, their estimated worst-case peak amplitudes and necessary correction kicks [4], normalized to 30m beta function both at the location of position measurement and of the kicker. Since no significant random perturbations with very high frequencies are expected, we aim for a feedback loop latency of <1.5µs, allowing to correct non-reproducible perturbations up to a maximum (0dB) frequency of ~70kHz. Although a lower latency is possible, we favour a latency that is somewhat larger that the technically feasible minimum value, because this allows to use e.g. ADCs with higher resolution (having higher latency) for the BPMs, or more advanced FPGA algorithms to correct BPM RF front-end IQ imbalance and X/Y-coupling, thus reducing BPM-noise dominated perturbations that the IBFB adds to the beam. Since the IBFB kickers can apply arbitrary individual kicks for each bunch, the additional feed-forward corrections applied by the IBFB allow to correct reproducible perturbations of any frequency from several MHz down to DC within the available kick range.

Table 1: E-XFEL beam trajectory perturbation sources, estimated worst-case peak amplitudes, and frequencies

	X [µm]	Y [µm]	Frequency [kHz]	Plane	Perturbation Type	Kick(X) [µrad]	Kick(Y) [µrad]
Magnet Vibrations	±28	±28	<1	X/Y	Random	±1.0	±1.0
Power Supply Noise	±12.6	±12.6	<1	X/Y	Random	±0.5	±0.5
Vibration-Induced Dispersion Jitter	±2.5	±2.5	<1	X/Y	Random	±0.1	±0.1
Beam Distribution Kicker Drift	±0	±1	<1	Y	Repetitive	±0	±0.04
Beam Distribution Kicker Noise	±0	±1	<5000	Y	Random	±0	±0.04
Spurious Dispersion (3% Energy Chirp)	±15	±15	<1	X/Y	Repetitive	±0.5	±0.5
Nonlinear Dispersion (3% Energy Chirp)	±15	±0	<1	X	Repetitive	±0.5	±0
Spurious Dispersion (1E-4 Energy Jitter)	±0.5	±0.5	<5000	X/Y	Random	±0.02	±0.02
Nonlinear Dispersion (1E-4 Energy Jitter)	±0.15	±0	<5000	X	Random	±0.005	±0
Wakefields	±25	±25	<5000	X/Y	Repetitive	±0.9	±0.9
Sum Of Peak Values	**±98.8**	**±85.6**				**±3.5**	**±3.1**

ISBN 978-3-95450-119-9

DEVELOPMENT OF BUNCH CURRENT AND OSCILLATION RECORDER FOR SuperKEKB ACCELERATOR

Makoto Tobiyama# and John W. Flanagan,
KEK Accelerator Laboratory, 1-1 Oho, Tsukuba 305-0801, Japan

Abstract

A High-speed digital signal memory has been developed for the bunch current and oscillation recorder for SuperKEKB. It consists of an 8-bit ADC and a FPGA daughter card consists of Spartan-6 and DDR2 memories commercially available on a double width VME card. The block-RAM on the FPGA is used to transfer bunch current data with low latency for prompt bunch current measurements, and the large DDR2 memory is used for long-duration position recording, such as post-mortem bunch oscillation recording. The performance of the board, including data transfer rate, will be presented.

INTRODUCTION

The construction of the SuperKEKB accelerators to upgrade the KEKB B-factory has started in FY 2010 and in progress almost on schedule up to now. On SuperKEKB rings, we almost double the stored current, reduce the beam emittance down to about 1/10, squeeze betatron functions at the interaction point to achieve 40 times larger luminosity than KEKB. As the physical and dynamic aperture of the rings will be much smaller than that of KEKB, a positron damping ring is under construction to reduce the beam size of the injected beam. Table 1 shows the main parameters of the SuperKEKB accelerators (High Energy Ring: HER, Low Energy Ring: LER and Damping Ring: DR).

Since the luminosity of a collider is proportional to the bunch current product of each beam, and it is almost normal that they push the bunch currents as near as available to the beam-beam limit, it is fairly important to measure the bunch currents and to keep the filling pattern as flat as possible for stable operations and effective tunings. In other rings such as the damping ring or storage rings for SR use, though the priority of measuring prompt bunch current to flat the filling pattern is not so high, it is still meaningful to record or control the bunch filling information to understand the beam behaviour such as to study the collective effects.

In KEKB, we have used the bunch current monitor and the bunch oscillation recorder based on the hardware two-tap filter for the bunch feedback systems[1]. It had an 8-bit ADC (MAX101), fast data demultiplexer which demultiplex the 8-bit data to 16 ways, and 20MB SRAMS, controlled by the extended VME interface. During injection, the injection trigger signal interrupted the bunch current recorder to stopped the recording, then initiate the data transfer process using the VME interrupt to transfer the bunch current information to a reflective memory board on the same VME bus. One of the other reflective memory board connected with the optical fibre was placed at the gun control rack of the linac (~600 m far from the bunch current monitor) to select the injection bunch from the bunch current information[2]. This bucket selection system (bunch current equalizer) has worked very well to stabilize the bunch filling pattern fairly flat even after large loss of bunches due to beam-beam kick or beam instability. This enabled us to make fine tuning of the colliding condition to get higher and stable luminosity. Actually, when we had trouble on the bunch current monitor such as jumping the timing and couldn't use the bunch current equalizer, the operation of the ring was fairly difficult and the peak and integrated luminosity of such period was obviously lower than other time.

We have developed a new bunch current recorder based on current FPGA technology (18K10). With the aid of the great flexibility and the capacity of the FPGA, the board supports the harmonic number of h=5120 for SuperKEKB-LER and HER, h=230 for SuperKEKB Damping Ring, h=640 for PF-AR and h=312 for PF ring just by setting the DIP-switch on the board. Also, we have designed the board to be usable for the large-scale memory board which records all the bunch oscillations over long time, 0.16 s for SuperKEKB rings. The performance of the board, including data transfer rate will be shown.

Table 1: Main parameters of SuperKEKB rings (HER: electron, LER: positron, DR: positron damping ring)

	LER	HER	DR	
Energy	4.0	7.0	1.05	GeV
Circumference	3016	3016	135	m
RF frequency	508.886	508.886	508.886	MHz
Revolution	0.0994	0.0994	2.2	MHz
Beam current	3.8	2.6	0.08	A
H. number	5120	5120	230	
Bunch number	2500	2500	4	
Bunch length	6	5	5	mm
H emittance	3	5	13	nm rad
Coupling	0.4	0.3	10	

OUTLINE OF THE SYSTEM

Hardware Design

The block diagram of the bunch current recorder board (18K10) is shown in Fig. 1. It has an trigger input, an revolution input, an RF clock input and two complementary DATA inputs. Both trigger and revolution

#makoto.tobiyama@kek.jp

ISBN 978-3-95450-119-9

RELIABLE BEAM-INTENSITY CONTROL TECHNIQUE AT THE HIMAC SYNCHROTRON

K. Mizushima#, T. Furukawa, T. Shirai, S. Sato, Y. Iwata, K. Katagiri, Y. Hara, K. Noda,
National Institute of Radiological Sciences, Chiba, Japan

Abstract

Short extraction called preliminary extraction has been added before irradiation in order to avoid an overshoot of the beam spill. A fast beam shutter was developed and installed in the extraction line to prevent the beam delivering to the patient during preliminary extraction. The fast shutter enables us to switch from preliminary extraction to irradiation in 100 ms, and the reliability of the beam-intensity control system was drastically improved by the preliminary extraction technique.

INTRODUCTION

In raster scan irradiation for charged particle cancer therapy, an upper limit of the beam intensity depends on the magnetic scan speed. The beam intensities beyond the limit cause extra dose deposition, which must be avoided for reducing the damage to normal tissues. Some therapy facilities, therefore, employ the feedback control system of the extracted beam intensity [1], and National Institute of Radiological Sciences (NIRS) in Japan is also one of them.

NIRS has carried out carbon-ion therapy with beam scanning [2] since May 2011. The carbon-ion beam is slowly extracted from the Heavy Ion Medical Accelerator in Chiba (HIMAC) synchrotron using the third-order resonance with the RF-knockout method [3]. The intensity of the extracted beam is kept constant by controlling the amplitude of the transverse RF-field with the feedback system [4]. In the beam-off period, the transverse RF-field is turned off, and the betatron tune is moved away from the resonance by exciting fast quadrupole magnets. Their magnets are also turned off at the start of extraction. However, then some particles having large betatron amplitude go out of the stable region at a stroke, and they are observed as a spill overshoot. At the HIMAC synchrotron, it was often induced by a slight variation of the beam emittance in operation cycles. A typical figure of the spill overshoot is shown in Fig. 1. The high overshoot of the beam spill is capable of bringing dose hot spot inside the target volume, because the tolerable beam-intensity in scanning irradiation is low.

It is impossible to avoid the spill overshoot with the feedback control of the transverse RF-field amplitude, because the spill overshoot occurs even if the transverse RF-field remains turned off. Although the fundamental solution of this problem is the improvement of the operation repeatability, it is difficult to maintain the beam emittance with high accuracy on a long-term basis.

#mizshima@nirs.go.jp

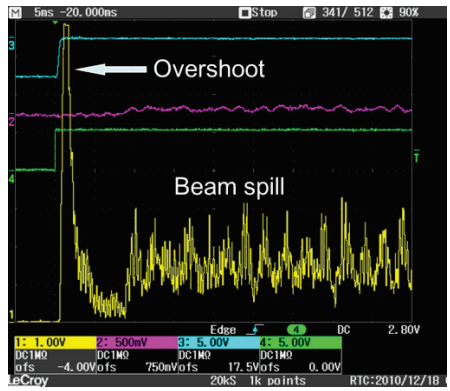

Figure 1: Typical overshoot of the beam spill at the start of extraction.

Accordingly, the required solution is a repeatability-independent way, such as the one which removes the uncontrollable spilled particles selectively.

We have added short extraction, called preliminary extraction (pre-extraction), as a technique for avoiding the spill overshoot. Before irradiation, the particles causing the spill overshoot are removed unfailingly from the synchrotron by pre-extraction. It is necessary to prevent the beam delivering to the patient during pre-extraction. In addition, for reducing the dead time, it is desirable that the switching between pre-extraction and irradiation performs in a short time. Therefore, a fast beam shutter was developed and installed in the HIMAC extraction line.

The spill overshoot was prevented in the experiment at the HIMAC, and the reliability of the beam-intensity control system was drastically improved by the pre-extraction technique. In this paper, we describe the pre-extraction system including the developed fast shutter and the experimental results.

PRE-EXTRACTION SYSTEM

System Layout

The pre-extraction system has been incorporated into a beam-intensity control system of the HIMAC synchrotron. A block diagram of the beam-intensity control system is shown in Fig. 2. An RF-knockout controller works as the generator and feedback amplifier of the low-level RF voltage. The reference and actual values of the beam intensity are provided from an irradiation control unit to this controller. The actual value is measured by an ionization chamber.

The pre-extraction control unit is a Programmable Logic Controller. This unit carries out the control of the

ISBN 978-3-95450-119-9

DEVELOPMENT OF THE SYSTEM FOR LONGITUDINAL COUPLED BUNCH MODES MEASUREMENT AT INDUS-2

S. Yadav#, A.C. Holikatti, Avanish Ojha, Y.Tyagi, T.A. Puntambekar, C.P. Navathe
Raja Ramanna Centre for Advanced Technology, Indore, India

Abstract

In a circular accelerator, beam instabilities are intensity-dependent collective effects that arise because of the electromagnetic wake fields generated by the beam as it interacts with its environment. These instabilities limit the high current operation in the accelerator and degrade the performance of synchrotron radiation beam. Indus-2 is a synchrotron radiation source at RRCAT, Indore having design beam current of 300 mA and 2.5 GeV beam energy. Beam intensity signal obtained from wall current monitor (WCM) is used to measure the longitudinal coupled bunch modes (CBM). To study the beam instabilities, an automated software has been developed which acquires the beam intensity spectrum for measurement of coupled bunch modes. The software has option of complete CBM scan, scanning near the significant RF cavity higher order modes (HOM) and scanning of user-selected modes. The scanning time for complete 291 modes is ~5 minutes. In this paper, we describe the measurement system, features of the developed software and some measurement results on Indus-2 machine.

INTRODUCTION

To achieve high luminosity and brightness in a circular accelerator, intense particle beam with number of bunches is required. Collective effects or collective instabilities must be taken into the account where higher beam intensity is desired. Indus-2 is a synchrotron radiation source at RRCAT, Indore, India having design beam current of 300 mA and 2.5 GeV beam energy. Presently Indus-2 is being operated at 100 mA beam current and 2.5 GeV beam energy. Study and detailed understanding of the nature and cause of collective instabilities with corrective measures are important for the successful operation of accelerator. Coupled bunch collective effects include the effects which are associated with electromagnetic fields generated by the collection of all particles in a beam [1]. In a circular accelerator, if the interaction of particle beam with the environment increases the collective effects, the particle beam becomes unstable and these instabilities are called as coupled bunch instabilities. The effects of coupled bunch instabilities on synchrotron machine performance are increased emittance of beam, increased beam size, possibility of beam loss, saturation of maximum beam current and lifetime reduction etc.

Collective instabilities can be measured by the amplitude of transverse and longitudinal oscillations of charged particle beam by analyzing the beam spectral components. The transverse (betatron) and longitudinal (synchrotron) oscillation are normally damped by natural damping mechanism. The equation of motion of particle in circular accelerator is given as

$$\ddot{x}(t) + 2D\dot{x}(t) + \omega^2 x(t) = 0 \qquad (1)$$

Where, D is the natural damping factor and ω is synchrotron or betatron frequency. The solution of the above equation is a damped oscillation for ω >> D as shown in the Fig.1. This is the condition of a stable beam.

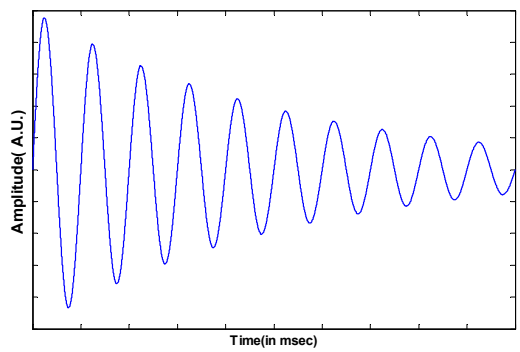

Figure 1: Natural damping of beam oscillation.

The electromagnetic fields created by the interaction of bunches of charged particle with metallic surroundings in an accelerator are called wake fields. The wake fields act back on the bunches and increases growth of longitudinal and transverse oscillations. In the presence of wake fields the equation of motion of particle in circular accelerator can be written as

$$\ddot{x}(t) + 2(D - G)\dot{x}(t) + \omega^2 x(t) = 0 \qquad (2)$$

Where, G is growth rate factor because of wake fields and D is the natural damping factor. The solution of the equation in the presence of wake fields depends on the growth rate. If growth rate is less than damping rate the resultant oscillation will be damped as shown in Fig.1. If growth rate is higher than damping rate the resultant oscillation starts growing and the beam becomes unstable [2]. Figure 2 shows the condition of unstable oscillations. These instabilities can be observed by longitudinal and transverse oscillation frequency in the beam spectrum.

syadav@rrcat.gov.in

ISBN 978-3-95450-119-9

INTRODUCTION OF PHOTON BPMS IN SOLEIL GLOBAL ORBIT FEEDBACK SYSTEMS

N. Hubert#, L. Cassinari, L. Nadolski

Synchrotron SOLEIL, Saint Aubin, BP 34, 91192 Gif-sur-Yvette, France

Abstract

SOLEIL global orbit feedback systems (slow and fast), based on 122 electron Beam Position Monitor (e-BPM) readings, are in operation since 2008 and give very satisfying performances (0.1Hz-500Hz vertical noise below 300 nm RMS and long term (8h) drifts below 1µm RMS).

Whereas each straight section is equipped with an upstream and downstream e-BPM, there is no e-BPM next to a dipole magnet. For that reason, photon BPMs (x-BPMs) in the dipole beamline frontends give additional information that can be used to better stabilize the source point in the dipoles. In fact x-BPMs provide also a better position angular measurement resolution, as they are located at 4 meters from the source point.

Results presented in this paper show that vertical position stability on bending magnet beamlines can be improved by including their x-BPM measurements in the global orbit feedback systems.

As a first step x-BPMs have been introduced in the Slow Orbit FeedBack system (SOFB) that corrects the orbit with a repetition rate of 0.1Hz. In a second step x-BPMs will be introduced in the Fast Orbit FeedBack system (FOFB) running at a repetition rate of 10 kHz.

INTRODUCTION

SOLEIL synchrotron is a third generation light source in operation since 2006. Orbit stability is a key parameter for the beam quality delivered to the 26 beamlines. Very good performances have already been achieved for long term and short term stability as reported in Ref. [1]. Combined slow and fast orbit feedback systems [2] keep the horizontal and vertical position and angle within the standard stability requirement: less than 10 % of the beam size and divergence, respectively. Nevertheless, continuous effort is done to improve even more the SOLEIL beam orbit stability taking into account new demands for stabilizing the closed orbit. Currently, integration of the photon beam position monitors (x-BPMs) in the feedback loops is being studied. Two x-BPMs are located several meters away from the source point and have a better sensitivity than the electron beam position monitors (e-BPMs). Moreover, bending magnet beamline x-BPMs can give additional information for the orbit stability, since the SOLEIL lattice does not have any e-BPM next to a bending magnet source point (Fig. 1).

nicolas.hubert@synchrotron–soleil.fr

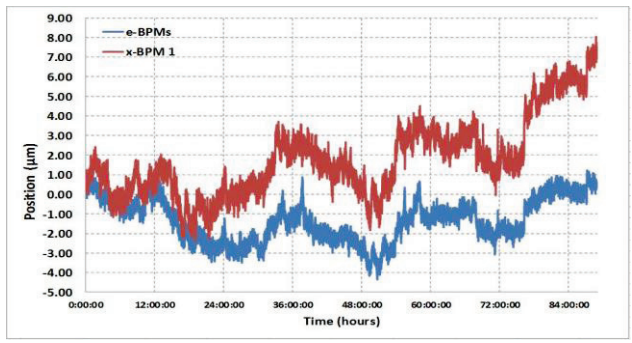

Figure 1: Vertical beam position measured by a dipole x-BPM at 4.7m from the source point (red curve). As a comparison, the projection of the position calculated from position and angle of the electron beam at source point is plotted in blue. The stability observed on the x-BPM is not as good as the one observed on e-BPMs.

CONTEXT

Orbit Feedback Systems

The SOLEIL beam orbit is stabilized using two interleaved orbit feedback systems based on the reading of the 122 e-BPMs of the machine. The slow system acts every 10 seconds on a set of 57 corrector coils located in the sextupole magnets (arcs). The fast system acts every 100 µs on a different set of 50 air-coil correctors located upstream and downstream of every straight section. Both systems are global, that is to say that the information from all e-BPMs is taken into account to compute the setting values for each corrector. An interaction process [2] allows having both systems efficient on a common frequency range: from DC to 0.05Hz for the slow orbit feedback (SOFB) and from DC to 200 Hz for the fast orbit feedback (FOFB).

Photon BPMs

SOLEIL beamlines frontend are equipped with blade x-BPMs, manufactured by FMB [3] after a design from BESSY. The position measurement given by this kind of x-BPM is based on the beam halo detection and thus is strongly dependent on the photon beam shape. On bending magnet source points, the beam shape is constant whereas for the insertion devices, it hugely depends on its configuration (gap, phase, photon polarisation …). For this very reason, only x-BPMs on bending magnet beamlines can be included at the moment in the orbit feedback loops (vertical plane only).

ISBN 978-3-95450-119-9

MEASUREMENTS OF MARTIN-PUPLETT INTERFEROMETER LIMITATIONS USING BLACKBODY SOURCE

P. Evtushenko#, M. J. Klopf, JLab, Newport News, USA

Abstract

Frequency domain measurements with Martin-Puplett interferometer is one of a few techniques capable of bunch length measurements at the level of ~ 100 fs. As the bunch length becomes shorter, it is important to know and be able to measure the limitations of the instrument in terms of shortest measurable bunch length. In this paper we describe an experiment using a blackbody source with the modified Martin-Puplett interferometer that is routinely used for bunch length measurements at the JLab FEL, as a way to estimate the shortest, measurable bunch length. The limitation comes from high frequency cut-off of the wire-grid polarizer currently used and is estimated to be 50 fs RMS. The measurements are made with the same Golay cell detector that is used for beam measurements. We demonstrate that, even though the blackbody source is many orders of magnitude less bright than the coherent transition or synchrotron radiation, it can be used for the measurements and gives a very good signal to noise ratio in combination with lock-in detection. We also compare the measurements made in air and in vacuum to characterize the very strong effect of the atmospheric absorption.

MOTIVATION

At the JLab IR/UV Upgrade FEL facility the bunch length measurements are made with a modified Martin-Puplett interferometer (MPI) [1]. The measurements are made at full bunch compression at the beam energy of up to 135 MeV. When the IR FEL is operated with the bunch charge of 135 pC the bunch is routinely compressed down to 130 fs RMS. This value assumes that our data evaluation procedure is reasonable accurate. A procedure that operates in the frequency domain is described elsewhere [2]. A good quantitative agreement between the IR FEL performance and its 1D model was found when such bunch length measurements were used as the input to the model [3]. The other measured beam parameters used as an input for the model are energy spread, emittance and Twiss parameters at the wiggler. Since the beam parameters other that bunch length are relatively straight-forward to measure, the agreement gave us some confidence that the bunch length evaluation procedure is working reasonably well. However, when UV FEL was commissioned a much higher small signal gain was measured than the 1D model predicted [4]. When trying to explain the disagreement by hypothesizing, that some electron beam parameters were measured incorrectly, one comes to the conclusion that the error in the measurements would have to be very large, and only a combination of different parameters measured incorrectly could explain the disagreement between the measurements and the model. Since the bunch length is the least straightforwardly measured beam parameter it drew the most suspicion. The UV FEL is operated with the bunch charge of 60 pC and bunch length of 100 fs was measured at full compression.

In addition, the Coherent Transition Radiation (CTR) source used for the bunch length measurements in the UV FEL appears to be much brighter that the one used in the IR FEL. The same Golay cell detector was used with both beamlines. Besides the interferometric measurements we minimize the bunch length by maximizing the amplitude of the Golay cell. The measurements are averaged over the tune-up beam macro pulse due to the detector's time constant. With comparable bunch length, according to the MPI measurements, we had to reduce the integrated macro pulse charge by a factor of ~ 30, to have the same Golay cell signal amplitude. The macro pulse was shortened from 250 to 20 μs and the bunch charge was reduced from 135 to 60 pC. Since the power of the coherent radiation is proportional to the charge squared, the reduction of the charge actually reduces the CTR power by the factor of ~5. One possibility to explain the difference in efficiency of two setups is the better alignment of the one at the UV FEL beam line, which we indeed have. Yet, factor of 60 in brightness seemed to be too large to explain only by the alignment. These observation has contributed to the need to evaluate our MPI in terms of its applicability the bunch length of 100 fs and shorter.

A shorter bunch length corresponds to a broader spectrum and one might expect that the measurements become easier as the spectrum is affected less by the low frequency cutoff. The bandwidth of the MPI measurements with CTR is limited on the low frequency side by the size of the CTR radiator [5], and on the high frequency side by performance of the freestanding wire-grid polarizer beam splitter and analyzer. As the frequency becomes higher the wavelength of the radiation becomes smaller than the gap between the wires such that the wire-grids performance degrades. Hence, the MPI, whose operation relies of on the polarization, does not function properly. Therefore, our goal of the interferometer evaluation was to measure the high frequency limit of the overall setup.

FREE-STANDING WIRE-GRIDS

The wire-grids, used in our modified MPI, are made of Tungsten wires with diameter of 20 μm with period of 50 μm. There are a large number of publications dedicated to the subject, both theoretical [6,7] and experimental [8-10], to name just a few. Two dimensionless parameters are usually introduced. The first one is the ratio of the wire diameter to the grid period $S = d/p$. The second one is the ratio of the grid period to the radiation wavelength $\varkappa = p/\lambda$. There are several quite different mathematical

Pavel.Evtushenko@jlab.org

ISBN 978-3-95450-119-9

RF FRONT END FOR HIGH BANDWIDTH BUNCH ARRIVAL TIME MONITORS IN FREE-ELECTRON LASERS AT DESY

A. Penirschke#, A. Angelovski, M. Hansli, R. Jakoby, Institut für Mikrowellentechnik und Photonik, TU Darmstadt, Darmstadt, Germany
C. Sydlo, M. K. Czwalinna, M. Bousonville, H. Schlarb, DESY, Hamburg, Germany
A. Kuhl, Universität Hamburg, Institut für Experimentalphysik Gruppe Beschleunigerphysik, Hamburg, Germany
S. M. Schnepp, Laboratory for Electromagnetic Fields and Microwave Electronics, ETH Zürich, Switzerland
T. Weiland, Institut für Theorie Elektromagnetischer Felder, TU Darmstadt, Darmstadt, Germany

Abstract

High gain free-electron lasers (FELs) can generate ultra short X-ray pulses in the femtosecond range. For a stable operation of the FEL, the precise knowledge of the bunch arrival time is crucial. The bunch arrival time monitors (BAMs) at FLASH achieve a resolution less than 10 fs for bunch charges higher than 500 pC which is sufficient for the beam based stabilization system of the Free-Electron Laser in Hamburg FLASH [1]. Increased demands for low bunch charge operation mode down to 20 pC at FLASH II and the European X-ray free-electron laser XFEL require an upgrade of the existing beam diagnostic equipment. A new high bandwidth BAM with new developed cone shaped pickups [2] promises sub-10 fs resolution for both, the high and low bunch charge operation mode. This paper adresses the RF signal path of the high bandwidth BAMs for FLASH II and XFEL. It comprises radiation resistant coaxial cables, combiners and limiters up to a frequency of 40 GHz from the pickup electrodes to the Mach Zehnder Modulator (EOM). Detailed investigations of the signal path using measurements and simulations with AWR Microwave Office allows for a good prediction of the signal quality and shape at the EOM.

INTRODUCTION

In order to achieve femtosecond stability in the synchronization process, the Free Electron Laser in Hamburg (FLASH) is equipped with Bunch Arrival-time Monitors (BAM) which are part of the electro-optical detection system [1]. The BAM comprises an RF-pickup, an electro-optical front-end and read-out electronics [3].

The resolution of the BAM is proportional to the slope steepness at the zero crossing of the pickup signal [4]. The slope steepness is a function of the peak-to-peak voltage and the duration of the voltage response. These two parameters are related to the geometrical parameters of the pickup structure such as the diameter of the cone-shaped pickup and the diameter of the cut-out.

*Work supported by the Federal Ministry of Education and Research (BMBF).
penirschke@imp.tu-darmstadt.de

CONE-SHAPED PICKUP DESIGN

In [5] a cone-shaped pickup was introduced which allows the detection of the arrival time with sub-fs resolution for the low charge operation mode in FLASH II and XFEL. The simulated BAM pickup system has a slope at the zero crossing of approximately 382 mV/ps and operates in the frequency range of DC - 40 GHz. Figure 1 shows a sketch of the cross-section of the cone-shape pickup.

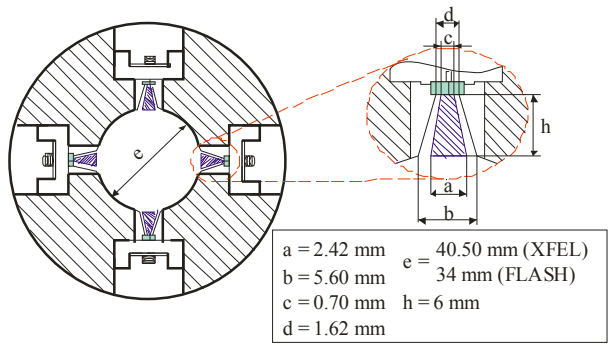

Figure 1: Cross-section of the cone-shaped pickup [5].

The cone represents a continuous transition from the button to the pin of the connector matched to the cable impedance of 50 Ω.

BAM RF-FRONT END

Due to higher operation frequencies the RF front end of the current BAM needs to be upgraded for the high bandwidth BAM. A sketch of the proposed RF front end is shown in Figure 2.

For high- and low-charge operation, two different channels are necessary. The low charge and the high charge channel consist of two opposite arranged pickups (either horizontally or vertically arranged) which are connected to a combiner via phase-matched rf-cables.

ISBN 978-3-95450-119-9

STUDY OF BEAM LENGTH MEASUREMENT BASED ON TM010 MODE

Renxian Yuan, Weimin Zhou, Luyang Yu, Yongbin Leng

SSRF, Shanghai, 201800 China

Abstract

Beam length measurement in frequency domain is a familiar method, and the resolution is seriously limited by the system signal-noise-ratio (SNR) and the beam length measured. Usually this method can only obtain the resolution about ~10*ps* with beam length ~30*ps* when using signal from button or stripline BPM. But in FEL case, the beam length is the *ps* or sub–*ps* order. The paper discusses the probability of beam length measurement based on the TM010 mode in FEL case. When adopting High Order Mode(HOM) reject and system gain control, the system SNR can arrive at 112*dB* and the resolution can achieve 30*fs* with beam length *ps* or sub-*ps* order.

INTRUDUCE

The measurement area and resolution of beam length measurement in frequency domain is seriously limited by the system SNR. So obtaining the system SNR up to 100*dB* is the decisive factor of beam length measurement in frequency domain in FEL case. It is well known that cavity BPM can achieve the position measurement resolution up to ~10*nm* because the signal from TM011 mode having a very high R/Q. The amplitude ratio of TM010 mode and TM011 mode of the same cavity can be written as:

$$K_r = \frac{(R/Q)_{010}^{0.5}}{(R/Q)_{110}^{0.5}} = \sqrt{\frac{2f_{110}}{f_{010}}} \cdot \frac{J_0(rk_{010})J_0(R_c k_{011})}{J_1(rk_{011})J_1(R_c k_{010})} \quad (1)$$

Where f is the harmonic frequency of TM_{010} mode and TM_{011} mode, and J_0 and J_1 is the 0-order and 1-order Bessel function respectively, r is the beam position from the cavity centre, R_c is the cavity's radius, k is the wave number of TM_{010} mode and TM_{011} mode. It is reported that the cavity BPM's resolution can achieve 0.05μm when beam charge is 1nC [1][2]. It means that the measurement system noise equals the output TM_{011} mode signal with beam condition 0.05μm@1nC. In the case, K_r is up to 4×10^5. So the system SNR of TM_{010} mode can be inferred up to 112*dB*.

When the beam is a Gaussian distribution bunch, the signal amplitude of TM_{010} mode can be written as:

$$V=\pi q \cdot f_{010} \cdot \sqrt{\frac{Z}{Q_L}\left(\frac{R}{Q}\right)_{010}} \exp\left(-\frac{2\pi^2 f_{010}^2 \cdot \sigma_L^2}{c_0^2}\right) \quad (2)$$

Where q is the beam charge, Z is output impedance, Q_L is the quality factor, σ_L is the beam length, $(R/Q)_{010}$ is the normalized shunt impedance of TM_{010} mode. So if used two cavities which working as TM_{010} mode at different frequency, the output signal can be written as:

$$V_1=\pi q \cdot f_{010,1} \cdot \sqrt{\frac{Z}{Q_{L,1}}\left(\frac{R}{Q}\right)_{010,1}} \exp\left(-\frac{2\pi^2 f_{010,1}^2 \cdot \sigma_L^2}{c_0^2}\right) \quad (3)$$

$$V_2=\pi q \cdot f_{010,2} \cdot \sqrt{\frac{Z}{Q_{L,2}}\left(\frac{R}{Q}\right)_{010,2}} \exp\left(-\frac{2\pi^2 f_{010,2}^2 \cdot \sigma_L^2}{c_0^2}\right) \quad (4)$$

So the coupling of beam charge can be eliminated by the outputs division. Then the beam length can be getting as:

$$\sigma_L^2 = \frac{c_0^2}{2\pi^2(f_{010,2}^2 - f_{010,1}^2)}\left(\ln\left(\frac{V_1}{V_2}\right) + \ln\left(\frac{f_{010,2}}{f_{010,1}}\right) + 0.5\ln\left(\frac{Q_{L,1}(R/Q)_2}{Q_{L,2}(R/Q)_1}\right)\right) \quad (5)$$

In the Eq.(5), the second and the third term is constant decided by the two cavities, so the sum of the two terms can be defined as $\ln(R_1/R_2)$, then:

$$\sigma_L = \sqrt{\frac{c_0^2}{2\pi^2(f_{010,2}^2 - f_{010,1}^2)}} \cdot \sqrt{\ln\left(\frac{V_1 R_2}{V_2 R_1}\right)} \quad (6)$$

And when the beam deviates the Gaussian distribution, the *rms* beam length can get from a similar equation [3]. When the beam length is very shorter than c/f_{010}, the resolution can be written as:

$$\Delta\sigma_L \simeq \frac{c_0^2}{2\pi^2(f_{010,2}^2 - f_{010,1}^2)} \cdot \frac{SNR_V}{\sigma_L} \quad (7)$$

Where SNR_V is the signal-noise-ratio of the TM_{010} mode. From the Eq.(7), it can be seen that the resolution of the beam length measurement is seriously limited by the SNR of diagnostic system and beam length itself. Supposing the SNR 112*dB*, $f_{010,1}$ and $f_{010,2}$ equal 3*GHz* and 8*GHz* respectively, Fig.1 shows the relation between the resolution and beam length. It can be seen that the resolution can achieve 3.5μm@1nC even the beam length is only 0.1*ps*.

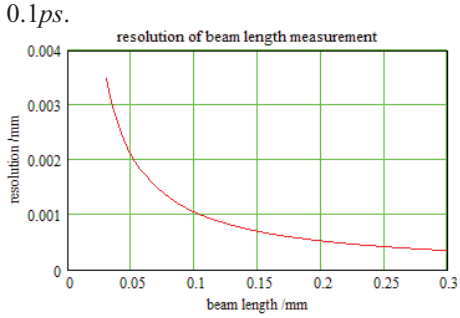

Figure 1: Relation between the resolution and bunch length.

ISBN 978-3-95450-119-9

REALIZATION AND MEASUREMENTS OF CONE-SHAPED PICKUPS FOR BUNCH ARRIVAL-TIME MONITORS FOR FLASH AND XFEL*

A. Angelovski#, M. Hansli, A. Penirschke, R. Jakoby, Institut für Mikrowellentechnik und Photonik, TU Darmstadt, Darmstadt, Germany
C.Sydlo, M.K. Czwalinna, H. Schlarb, M. Bousonville, DESY, Hamburg, Germany
A. Kuhl, Universität Hamburg, Institut für Experimentalphysik
Gruppe Beschleunigerphysik, Hamburg, Germany
S. M. Schnepp, Laboratory for Electromagnetic Fields and Microwave Electronics, ETH Zürich, Switzerland
T. Weiland, Institut für Theorie Elektromagnetischer Felder, TU Darmstadt, Darmstadt, Germany

Abstract

At the Free Electron Laser FLASH at DESY, the state of the art Bunch Arrival-time Monitors (BAMs) have a time resolution better than 10 fs for bunch charges of more than 500 pC [1]. With the extension of FLASH II and the European X-ray Free Electron Laser Project (XFEL) a low charge operation mode with 20 pC bunch charge is planned. The time resolution of the BAMs significantly drops as the bunch charge reduces [2]. High bandwidth BAMs are essential for a femto-second time resolution of the measured arrival-time in case of low charge and high charge operation mode of the free-electron lasers (FELs). The proposed cone-shaped pickup electrodes with bandwidth up to 40 GHz are manufactured and measured. Due to the different beam pipe apertures for FLASH and XFEL, two hermetic bodies are manufactured. The RF properties of the pickups are measured and compared to the simulation results obtained by CST MICROWAVE STUDIO®.

INTRODUCTION

For providing an optimal operation of the free-electron lasers (FELs), which generate ultra short X-ray pulses, the arrival-time of the electron bunches has to be measured with femtosecond precision. For that purpose Bunch Arrival-time Monitors (BAMs) are developed and installed at the Free Electron Laser FLASH at DESY. These arrival-time monitors combine the beam induced signal with an electro-optical detection scheme as described in [1]. The time resolution of such a detection scheme depends on the steepness of the pickup voltage slope at the first zero-crossing. The state of the art BAMs have an intrinsic time resolution better than 10 fs for bunch charges of more than 500 pC [1]. With the extension of FLASH II and the XFEL, a low charge operation mode with bunch charge of 20 pC is planned. The slope steepness reduces with lower bunch charges leading to significant performance degradations [2]. This can be compensated by increasing the bandwidth of the BAM components. The BAMs comprise RF-pickups, an electro-optical front-end and read-out electronics [3].

In this paper we present the realization and the measurements of cone-shaped pickups for the BAMs with bandwidth up to 40 GHz proposed in [4]. The pickups are characterized by scattering parameters and the results are compared to the simulations performed with CST MICROWAVE STUDIO®.

HIGH BANDWIDTH CONE-SHAPED PICKUPS FOR BAM

In order to achieve sub-10 fs time resolution for bunch charges of 20 pC or lower, the bandwidth of the BAM pickups should be increased up to 40 GHz. With this bandwidth the voltage slope at the first zero crossing of the pickup signal is more than 300 mV/ps at 20 pC [6].

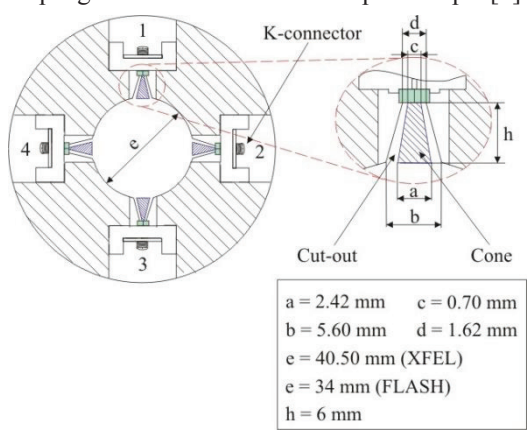

Figure 1: Cross-section of the cone-shaped pickups with the denoted ports.

Figure 1 shows the cross-section of the high bandwidth cone-shaped pickups. The design details can be found in [4 - 6]. Eight pickups have been produced by Orient Microwave Corp [7]. The pickups are mounted in the stainless steel hermetic body. Due to the different beam pipe apertures for FLASH and XFEL, two hermetic

*Work supported by the Federal Ministry of Education and Research (BMBF) within FSP 301 under the contract numbers 05H10GU2 and 05K10RDA
angelovski@imp.tu-darmstadt.de

ISBN 978-3-95450-119-9

PLANAR TRANSMISSION LINE BPM FOR HORIZONTAL APERTURE CHICANE FOR XFEL

A. Angelovski#, A. Penirschke, R. Jakoby, Institut für Mikrowellentechnik und Photonik, TU Darmstadt, Darmstadt, Germany
U. Mavrič, C.Sydlo, C. Gerth, DESY, Hamburg, Germany

Abstract

In order to obtain ultra short bunches in the Free Electron Laser FLASH at DESY, the electron beam is compressed in magnetic chicanes. Precise knowledge of the beam position in the chicane allows for non-destructive energy measurements of each individual bunch in the beam. In the current implementation, the Energy Beam Position Monitor (EBPM) pick-ups are coaxial pick-up striplines mounted perpendicularly to the beam. One can determine the horizontal beam position by measuring the phase difference of the beam induced signal at opposite ends of a pick-up. Due to the different electrical and mechanical requirements for the European XFEL a new EBPM has to be developed.

In this paper, we present the design and analysis of a planar transmission line structure which is planned to be used as an EBPM in the European XFEL. The planar design of the pick-ups can provide for a proper impedance match to the subsequent electronics as well as sufficient mechanical stability along the aperture when using alumina substrate.

INTRODUCTION

The European XFEL will need a zoo of diagnostic tools for the study of the longitudinal properties of the electron beam. The Electron Beam Position Monitor (EBPM) will be used as part of longitudinal diagnostic tools for the European XFEL. It is composed of the pick-up structure and detection electronics.

The EBPM is an instrument used for bunch energy measurements [1] and it will be used at three different locations along the European XFEL LINAC. The energy measurement is done by means of position measurements, where the transformation from position to bunch energy is defined by the formalism of the bunch compressor [2]. As opposed to a standard BPM, the energy BPM measures phases to define the absolute position of the bunch in the dispersive section of the bunch compressor. Figure 1 shows the current EBPM installed at FLASH and the principle of phase detection [1]. Two coaxial pick-up striplines are mounted perpendicular to the beam. At both ends of the pick-up ceramic disks are placed for mechanical support and the pick-ups are tapered towards the connectors. The difference between the measured phases of the pulses coming from the left and from the right side of the pick-up is proportional to the position (dx in Fig. 1) of the bunch.

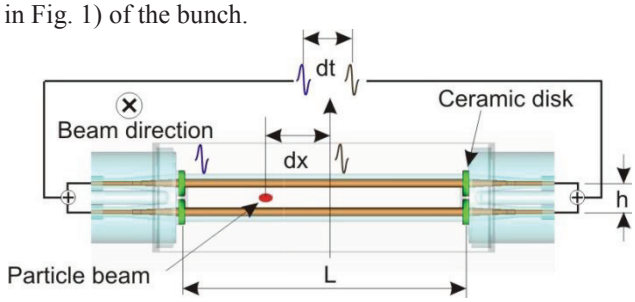

Figure 1: CAD model of the EBPM installed in the second bunch compressor at FLASH.

The measurement resolution of the bunch position, hence energy, depends on the frequency of the detection. Therefore it is advisable to have the phase detection at a rather high frequency. The upper limit is defined by the manufacturing limitations of the pick-up, limitations of the detection electronics and size of the chicane which imposes the wavelength, below which the phase detection might become ambiguous [3]. The resolution of the instrument also depends on the signal spectral density that the pick-up structure transfers from the beam to the output connector.

As the requirements for the future EBPM at the European XFEL (mechanical and electrical) differs significantly from the ones at FLASH, a new EBPM needs to be designed. Table 1 summarizes a comparison between the design parameters for FLASH and the European XFEL.

angelovski@imp.tu-darmstadt.de

ISBN 978-3-95450-119-9

MEASUREMENT OF TEMPORAL RESOLUTION AND DETECTION EFFICIENCY OF X-RAY STREAK CAMERA BY SINGLE PHOTON IMAGES

A. Mochihashi*, M. Masaki, S. Takano, K. Tamura, H. Ohkuma,
JASRI/SPring-8, 1-1-1 Kouto, Sayo, Hyogo, 679-5198 Japan

Abstract

In the third generation and the next generation synchrotron radiation light sources, the electron beam bunch length of ps∼sub-ps is expected to be achieved. An X-ray streak camera (X-SC) can directly measure the temporal width of X-ray synchrotron radiation pulse. The temporal resolution of X-SC depends on the initial velocity distribution of the photoelectrons from a photocathode which converts the X-ray photons to the photoelectrons. To measure the temporal resolution of the X-SC, we have observed 'single photon' streak camera images and measured the temporal spread of the images. We have also tried to evaluate the dependence of the temporal resolution and the detection efficiency on the thickness of the photocathode. For this purpose, we have developed a multi-array type CsI photocathode with 3 different thickness of the photocathodes. The experimental setups, and the results of the measurements of the temporal spread and the detection efficiency of the single photon events are presented.

INTRODUCTION

An X-ray streak camera (X-SC) can measure directly X-ray pulses whose lengthes are nano to pico seconds. In case of a single shot observation, the temporal resolution of the X-SC depends on an initial velocity distribution of photoelectrons at an X-ray incident photocathode and a space charge effect of the photoelectrons on the photocathode. A conversion process in which incident photons change to the photoelectrons at the photocathode creates primary electrons whose energy is ∼ keV because of the incident photon energy. On the other hand, secondary electrons which have typically the energy of several ten eV and the energy spread of several eV are also created. Because the secondary electrons contribute formation of the streak images, the initial velocity distribution of the secondary electrons affects the temporal resolution of the X-SC. The temporal spread due to the initial velocity distribution of the secondary electrons can be observed as a temporal spread of the streak image when single photon hits the photocathode. We have observed the temporal spread of the streak images of the single photon events by decreasing intensity of the incident photons up to single photon counting level. By changing the incident photon energy, we have observed the dependence of the temporal resolution of the X-SC on the photon energy. Because the secondary electrons which are created by multiple scattering process of the photoelectrons in the photocathode contribute the formation of the streak image, it is supposed that the detection efficiency and the temporal resolution depend on the thickness of the photocathode. To investigate this, we have developed a multi-array CsI photocathode which can set three different thickness of the photocathodes simultaneously and oserved the dependence of the temporal resolution and the detection efficiency on the thickness of the photocathode.

* mochi@spring8.or.jp

EXPERIMENTAL SETUP

Figure 1 shows the block diagram and the timing setup of the single photon experiment. In the experiment, we have used a streak camera system (Hamamatsu, C5680-06) with a synchroscan unit(Hamamatsu, M5675) and dual sweeping unit (Hamamatsu, M5679). The RF signal (508.58MHz) of the SPring-8 storage ring is transferred from the RF station to the beamline station via optical cable, and the optical signal is converted to the electronic signal by O/E module. The timing signal of the synchroscan unit is generated by the frequency divider which generates 7th subharmonics of the RF frequency (72.65MHz). The timing signal is used for the input signal of the delay unit (Hamamatsu, C6878) which can adjust timing delay of the synchroscan unit. The reference signal from the synchroscan unit is used for the reference input of the delay unit.

The timing signal of the dual sweeping unit is generated by the frequency divider and the streak trigger unit (Hamamatsu, C4547). The streak trigger unit generates 9Hz repetition signal synchronized with the RF signal and the signal is used for the trigger of the digital delay pulse generator (Stanford Research Systems, DG535). The pulse generator generates 3 timing signals: (A)exposure trigger for CCD camera, (B)gate signal for image intensifier (I.I.) and (C)trigger signal for the dual sweeping unit. Because the CCD camera has internal delay (11μs) for the external trigger, the CCD trigger signal precedes in 11μs for both the I.I. gate trigger and the sweeping trigger. The fluorescent substance at the end of the streak tube is P43[1] for C5680-06; the 100%→10% decay time of the fluorescence is 1ms. Because of the decay time, it is necessary for identification of each single photon event on the fluorescent screen to provide timing gate shorter than 1ms for the photoelectrons which hit the screen. We have used the dual sweeping unit as a timing gate for the photoelectrons which hit the screen: we have operated the dual sweeping unit whose operation

ISBN 978-3-95450-119-9

EO-SAMPLING-BASED TEMPORAL OVERLAP CONTROL SYSTEM FOR AN HH SEEDED FEL

S. Matsubara[#,1], A. Iwasaki[2], S. Owada[2], T. Sato[3], K. Ogawa[3], T. Togashi[1], E.J. Takahashi[4], M. Aoyama[5], Y. Okayasu[1,3], T. Watanabe[1,3], and H. Tomizawa[1,3]
[1]SPring-8/Japan Synchrotron Radiation Research Institute (JASRI), 1-1-1, Kouto, Sayo-cho, Sayo-gun, Hyogo 679-5198, Japan
[2]Department of Chemistry, School of Science, The University of Tokyo, 7-3-1 Hongo, Bunkyo-ku, Tokyo 113-0033, Japan
[3]RIKEN Harima Institute, RIKEN SPring-8 Center, 1-1-1, Kouto, Sayo-cho, Sayo-gun, Hyogo 679-5148, Japan
[4]RIKEN Advanced Science Institute, Hirosawa 2-1, Wako, Saitama 351-0198, Japan
[5]Kansai Photon Science Institute (Kizu), Japan Atomic Energy Agency, 8-1-7 Umemidai, Kizukawa-shi, Kyoto 619-0215, Japan

Abstract

FELs have been greatly interested as intense light source in short-wavelength region. However, their temporal profile and frequency spectra have shot-to-shot fluctuation originated from a SASE process. One of the promising approached to the problems is a seeded FEL scheme by introducing full-coherent light pulses. It is important for the high order harmonics (HH) seeded FEL scheme to synchronize the seeding laser pulses to the electron bunches. The difference of their arrival timing is drifting at the meeting point in the first undulator. On the other hand, the spatial pointing of the seed laser must be smaller than transverse overlapping between HH-pulse and electron bunch. Therefore, an arrival time feedback system and non-destructive monitor are necessary to achieve seeded FEL operation continuously. We have constructed the arrival timing monitor based on Electro-Optic (EO) sampling which measures the arrival time difference of the seeded laser pulses with respect to the electron bunches simultaneously while the seeded FEL operation, in which the probe laser pulses for the EO-sampling is from the same laser source using as FEL-seeding. The EO-sampling system has been used for the arrival time feedback with less than 500 fs adjustability for continual operation of the HH-seeded FEL. The continual operation of the seeded FEL is feasible for day-long user experiments.

INTRODUCTION

SCSS test accelerator in SPring-8 Center has been operated as the HH-seeded FEL several times for the extreme ultraviolet (EUV) wavelength region [1]. The HH-seeded FEL is very powerful method to generate intense full-coherent and narrow-band pulses in short wavelength region. The HH-seeded FEL operation has been performed by synchronizing and spatial overlapping between the seeding laser pulse, which is generated from an ultra-short pulsed Ti:Sapphire laser pulses, and the electron bunches.

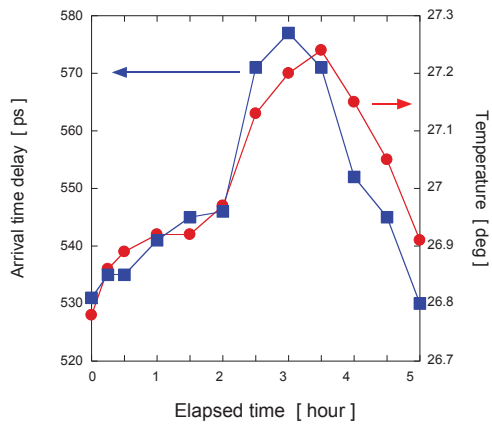

Figure 1: Drift of the arrival timing between the electron bunch and the laser pulse and the temperature in the facility for elapsed time.

We found that our seeding laser source has large drift of the arrival-time about 50 ps for a day as shown in Fig. 1. The drift was measured by the EO-sampling system and temporal delay control system described following section. The arrival timing drift was correlated with a variation in the environmental temperature at the accelerator facility as shown in Fig. 1. The electron bunch length (~600 fs) and seeding laser pulse length (~50 fs) are less than 1 ps. Therefore, it is necessary to achieve the temporal overlap between them within ~500 fs accuracy for the continual operation of the seeded FEL. The temporal overlap is indispensable for the arrival time monitor in real time without disturbing seeded FEL operation. EO-sampling measurement is one of the best methods to monitor the arrival time difference between the seeding laser pulses and the electron bunches [2, 3].

We built the temporal control system based on the EO-sampling technique employing the same external laser source for seeding.

matsubara@spring8.or.jp

ISBN 978-3-95450-119-9

DESIGN AND OPERATION OF THE HIGH INTENSITY LUMINOSITY MONITORS OF THE LHC*

H.S. Matis,# S. Hedges, M. Placidi, A. Ratti, W. C. Turner, LBNL, Berkeley, CA, U.S.A.
R. Miyamoto, ESS, Lund, Sweden, E. Bravin, CERN, Geneva, Switzerland

Abstract

We have built a high-pressure ionization chamber (BRAN) for the IR1 (ATLAS) and IR5 (CMS) regions of the LHC. This chamber is designed to measure the relative bunch-by-bunch luminosity of the LHC from beam commissioning all the way up to the expected full luminosity of 10^{34} cm^{-2}s^{-1} at 7.0 TeV.

INTRODUCTION

The BRAN, which is used as a high intensity gas ionization detector has been described in several recent papers [1-4]. It is located in the TANs, which are absorbers made up of steel and copper and are located on either side of the IR1 and IR5 interacting regions. It measures the neutrons and photons from the collisions in the forward direction. The detector (currently running at 7 bar) has four quadrants, which are distributed around the center of each IR.

MODELING

Method

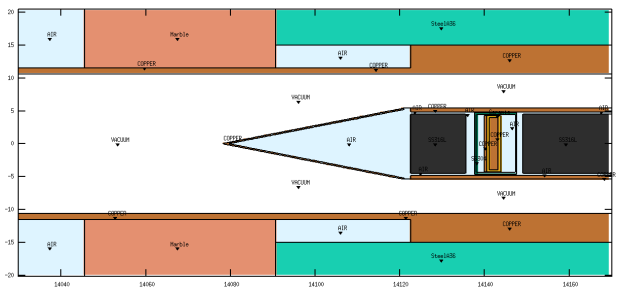

Figure 1: Top view of the BRAN in the CMS TAN. The color white indicates the regions of vacuum.

We have used the modeling program called FLUKA [5-6] to simulate collisions in the LHC. The model simulates half of the IP. The full detail of the beam line is included up to the TAN in which the detector rests. The geometry of the TAN is shown in Figure 1. The TAN is an absorber, which shields the first LHC dipole from the forward neutral particles produced at the intersecting region (IR). The TAN is about 140 m from the IR. The model includes the materials in the TAN at the beginning of the 2012 run.

Using the DPMJET [7] option of FLUKA, we have simulated the following reactions pp, pPb and PbPb over the expected operating range of the LHC. We can see how the shower forms by looking at Figure 2.

This figure shows how the shower develops for pp (which is dominated by gamma ray showers) and PbPb (which is dominated by neutron showers).

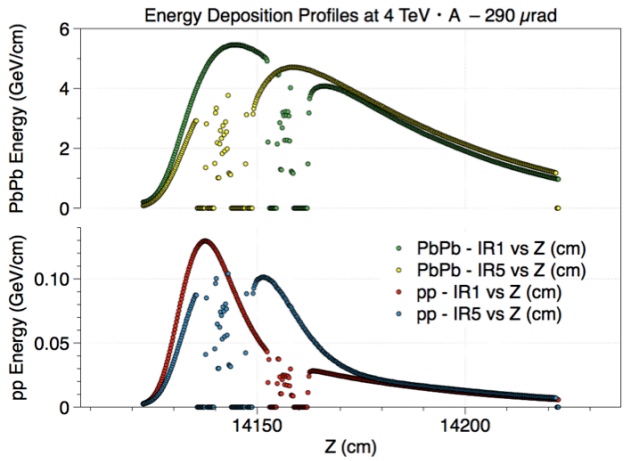

Figure 2: Energy deposited in the TAN for pp and PbPb collisions. The region in the center for each detector is where the BRAN is located. The different material in from of the BRAN produces the difference between the shower deposition between the IR regions.

The simulations show how the energy is deposited in the detector as a function of energy and crossing angle of the beams. For instance, Figure 3 shows the predicted behavior at the nominal full crossing angle of 290 μrad, which is used for the 2012 LHC run. Figure 4 shows the sensitivity to crossing angle for both pp and PbPb collisions. The crossing angle ratio, χ_r is the difference in energy between the top and bottom quadrants divided by the total energy. Note, the simulation predicts that the quantity χ_r is higher in PbPb collisions.

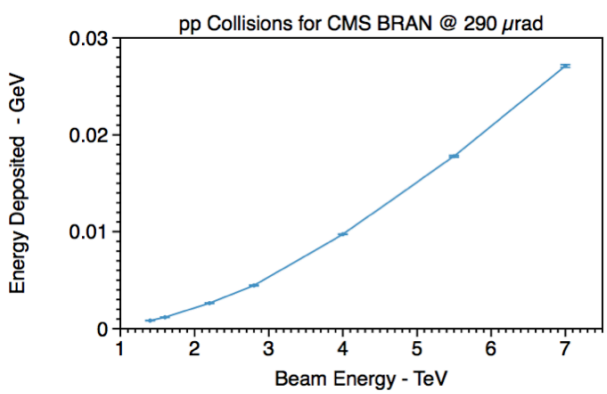

Figure 3: Energy deposited in the IR5 BRAN as a function of the energy of one of the beams in pp collisions.

*Work supported by the US-LARP program.
#hsmatis@lbl.gov

ISBN 978-3-95450-119-9

BEAM MONITORS OF NIRS FAST SCANNING SYSTEM FOR PARTICLE THERAPY

T. Furukawa, T. Inaniwa, S. Sato, E. Takeshita, K. Mizushima,
K. Katagiri, Y. Hara, T. Shirai, and K. Noda
National Institute of Radiological Sciences, Chiba, Japan

Abstract

At National Institute of Radiological Sciences (NIRS), more than 6500 patients have been successfully treated by carbon-ion beams since 1994. The successful results of treatments have led us to construct a new treatment facility equipped with three-dimensional pencil beam scanning irradiation system. The commissioning of NIRS fast scanning system installed into the new facility was started in September 2010, and the treatment with scanned ion beam was started in May 2011. In the scanning delivery system, beam monitors are some of the most important components to safely deliver the dose to the patient. In this paper, the design and the commissioning of beam monitors in the delivery system are described.

INTRODUCTION

Since 1994, more than 6500 patients have been successfully treated with carbon-ion beams delivered from Heavy Ion Medical Accelerator in Chiba (HIMAC). To make optimal use of these characteristics and to achieve accurate treatment, three-dimensional (3D) pencil beam scanning [1-3] is one of the sophisticated techniques in use. For implementation of this irradiation technique, at HIMAC, a new treatment facility [4] was constructed. Figure 1 shows the treatment room of a new treatment facility. After intense commissioning and quality assurance tests, the treatment with scanned ion beam was started in May 2011.

Figure 1: Treatment room of the new treatment facility.

The beam delivery with beam scanning can be used to achieve the desired dose distribution by magnetically deflecting the beam across the target and by changing the beam penetration depth. Thus, scanning irradiation method requires sophisticated beam monitoring and control system to deliver well defined dose throughout the target volume safely with sufficient accuracy. In order to measure and control the dose of each spot, the main and the sub ionization chambers are placed separately as flux monitors. For monitoring of the scanned beam position, a beam position monitor, which is multi-wire proportional chamber, is installed just downstream from the flux monitors. This monitor can output not only the beam position but also the 2D fluence distribution using dynamic fast convolution algorithm.

In this paper, the design and the commissioning of these monitors in the delivery system are described.

NIRS FAST SCANNING SYSTEM

Layout of the scanning system [5] is shown in Fig. 2. It consists of the scanning magnets, main and sub flux monitors, position monitor, mini-ridge filter and range shifter. To achieve the fast beam scanning at the isocenter, the distances from scanning magnets to the isocenter are designed to be 8.4 and 7.6 m, respectively. The vacuum window is made of 0.1mm-thick kapton and located 1.3 m upstream from the isocenter. Beam monitors, mini-ridge filter and range shifter are installed downstream of the vacuum window. Since the required field size is 220×220 mm^2 for the transverse directions, the effective area of the monitors are designed to be 240×240 mm^2. Further, these monitors are designed to measure the beam having energies between 80 and 430 MeV/u, and having intensities between $1 \cdot 10^7$ and $1 \cdot 10^9$ particles per second (pps).

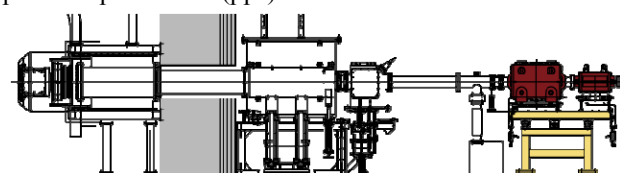

Figure 2: Delivery system of the new treatment facility. Beam monitors described in this paper are assembled in the region highlighted by red dot curve.

FLUX MONITORS

Configuration of Flux Monitor

The flux monitors, which are parallel-plate ionization chambers, are placed just after the exit window of the vacuum duct, and they are operated in air at atmospheric pressure. Each flux monitor consists of a signal foil

ISBN 978-3-95450-119-9

STATUS AND ACTIVITIES OF THE SPRING-8 DIAGNOSTICS BEAMLINES

S. Takano*, M. Masaki, A. Mochihashi, H. Ohkuma, M. Shoji, and K. Tamura
JASRI/SPring-8, Hyogo 679-5198, Japan
H. Sumitomo, and M. Yoshioka, SPring-8 Service Co. Ltd. (SES), Hyogo 679-5165, Japan

Abstract

At SPring-8 synchrotron radiation (SR) in both the X-ray and the visible bands is exploited in the two diagnostics beamlines. The diagnostics beamline I has a dipole magnet source. Recently, the transfer line of the visible light has been upgraded. A new in-vacuum mirror was installed to increase the acceptance of the visible photons. A new dark room was built and dedicated to the gated photon counting system for bunch purity monitoring. To improve the performance, the input optics of the visible streak camera was replaced by a reflective optics. Study of the power fluctuation of visible SR pulse is in progress to develop a diagnostic method of short bunch length. At the diagnostics beamline I, the size of the electron beam is measured by imaging with the zone plate X-ray optics. The diagnostics beamline II has an insertion device (ID) light source. To monitor stabilities of the ID photon beam, a position monitor for the white X-ray beam based on a CVD diamond screen was installed. A turn-by-turn diagnostics system using the monochromatic X-ray beam of the ID was developed to observe fast phenomena such as beam oscillation at injection for top-up and beam blowups caused by instabilities. Study of temporal resolution of the X-ray streak camera is also in progress at the diagnostics beamline II.

INTRODUCTION

Synchrotron radiation (SR) is a nondestructive probe to diagnose relativistic electron beams in high-energy accelerators. At SPring-8 SR in both the X-ray and the visible bands is exploited in the two diagnostics beamlines [1]. The diagnostics beamline I has a dipole magnet source, and the diagnostics beamline II has an insertion device (ID) light source. In this paper we will report present status and activities of the SPring-8 diagnostics beamlines.

DIAGNOSTICS BEAMLINE I (BL38B2)

The diagnostics beamline I (BL38B2) has a bending magnet light source with critical photon energy of 28.9 keV. In 2011, the transfer line of the visible light was upgraded. The schematic layout of the beamline after the upgrade is shown in Fig. 1. The beamline has an optics hutch and two dark rooms on the experimental hall. The visible synchrotron light is separated from the X-ray beam by two in-vacuum mirrors in the optics hutch. The mirror below the photon beam axis is the original one and the other one above the photon axis has been added in the upgrade. The X-rays pass through the gap of the two mirrors. The separated visible light is transported in a bent shielded pipe out of the optics hutch to the darkrooms. The visible light separated by the lower

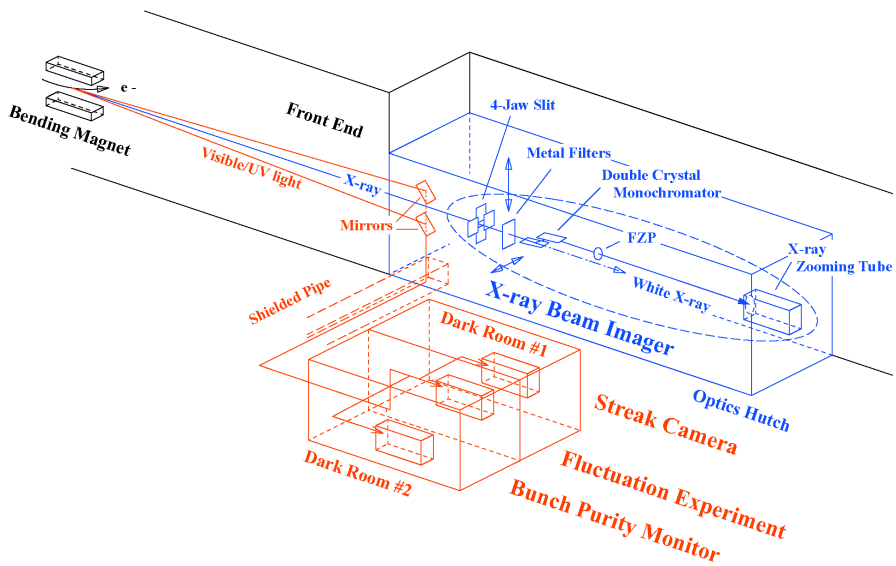

Figure 1: The schematic layout of the SPring-8 diagnostics beamline I (BL38B2).

*takano@spring8.or.jp

ISBN 978-3-95450-119-9

HARTMANN SCREEN AND WAVEFRONT SENSOR SYSTEM FOR EXTRACTING MIRROR AT SSRF*

J. Chen, K.R. Ye, Y.B. Leng, SINAP, Shanghai, China

Abstract

A Be mirror was used to extract visible synchrotron radiation light from bending magnet at SSRF. The surface of mirror was deformed because of X-ray heat. A set of Hartmann Screen Test was used to measure the surface of the mirror. Another equipment named The Shack-Hartmann wavefront sensor system was introduced to get more precision data. The result of two kind of test match each other well.

GENERAL OVERVIEW

There are two diagnostic beam lines in the storage ring of Shanghai Synchrotron Radiation Facility, one of them adopt interferometer to measure the transverse electron beam size of storage ring using visible light. The visible light was extract from synchrotron radiation by a Be mirror. The Be mirror was special designed to reflect visible light from vacuum and let x-ray pass through. Part of the energy of x-ray was absorbed by the Be mirror and the heat cause deformation of the mirror. The impact of mirror deformation to measurement of interferometer was analyst and the deformation was measured by Hartmann Screen and Shack-Hartmann wavefront sensor. The result of deformation measurement was used to correct the measurement of beam size by interferometer.

DESIGN OF THE Be MIRROR

Beryllium is the best metal to conduct x-ray with high melting point (1287°C) and high specific heat (1925 J·kg−1·K−1) and with low absorption of x-ray.[1] As shown in Fig. 1(a), the shape of mirror back is paraboloid with equation y=0.05x2+2. Center of the mirror is thin to absorb less energy of x-ray. Water flow across two hole to take heat away. Although these method are implemented to reduce the heat deformation, it can't be avoided. In simulation, the distribution of temperature is displayed in Fig. 1(b), the highest temperature is 65°C locate in the center of the mirror and the lowest temperature is 35.3°C. The deformation of mirror is shown in Fig. 1(c), height of the peak is 5.16μm, height of the bottom is 2.68μm, peak to valley is 7.84μm.[2]

A thermal-mechanical analysis with electron beams show: the thermal distortion values for metals between 0°C to 400°C, these effects were especially good in Beryllium mirrors .The deformation of Be mirror is simulated by ANSYS and XOP for varying the shape, size, and diameter of cooling tube. We fixed outer-dimension of beryllium mirror is 80mm(wide), 60mm(high), 12mm(thickness). With the diameter of water-cooling tube will 8mm, the centric deformation of mirror surface results 3.9μm with inlet water temperature 26°C. The highest temperature of mirror will be 56°C.

*Work supported by Shanghai Institute of Applied Physics

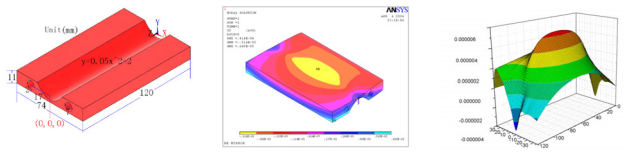

(a)Shape of Be mirror (b)Temperature distribution (c)Deformation distribution

Figure 1: Design and simulation of the Be mirror.

INFECT TO BEAM SIZE MEASUREMENT

Beam size is measured by interferometer[3], the optics layout is shown in Fig. 2(a), the optical system include some relay mirrors to transport and split light, one double slits to split the wavefront and a focus mirror to make two light beam from two slits intersect at the surface of CCD sensor. [4]

The formula to calculate beam size is shown as Eq. 1, in which σ means the size of beam, λ is wave length of light, D is preparation of double slits, and γ is spatial coherence. The coherence is measured by Levenberg–Marquardt fitting of intensity distribution of interference fringe(shown in Fig. 2(b), Fig. 2(c)), and the other parameters can be measured by simple way.

$$\sigma = \frac{\lambda R}{\pi D}\sqrt{-\frac{\ln\gamma}{2}} \qquad (1)$$

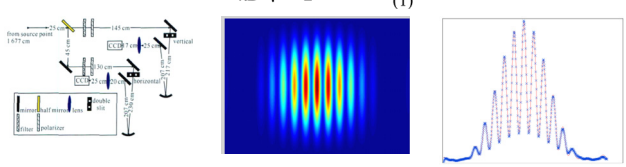

(a)Optics layout of interferometer (b)interference fringe (c)L-M fitting to calculate spatial coherence

Figure 2: Measurement of beam size.

As design shape of the Be mirror, it tend to bend in vertical direction and the deformation in horizontal can be ignored. As shown in Fig. 3, the distance from source point to Be mirror A and the distance from Be mirror two double slits B and the separation of double slits D_{real} are known. Assuming the deformation lead mirror shift angle is b, D_{ideal} is the ideal separation of double slits which means the separation of double slits should be used without deformation. In Eq.1, the parameter D should be D_{ideal} instead of D_{real}. In Eq.2, A, B, D_{real} are known, if we measure the mirror deformation to get shift angle b, the ideal separation of double slits can be calculate like this:

$$h = \frac{D_{real}}{2} - B * \tan(2b) \Rightarrow a = \arctan\left(\frac{h}{A}\right) \qquad (2)$$

$$\Rightarrow D_{real} = 2(A+B)\tan(a)$$

ISBN 978-3-95450-119-9

DEVELOPMENT OF THE NEW TYPE MLIC WITH PMMA PLATES AND GRAPHITE ELECTRODES

S. Iwata, N. Shinozaki, A. Takubo, C. Kobayashi, AEC#, Chiba, Japan
S. Fukuda, NIRS, Chiba-shi, Japan
T. Kanai, Gunma University, Heavy-Ion Medical Center, Maebashi-Gunma, Japan

Abstract

The MLIC (Multi-Layer Ionization Chamber) that has a lot of ionization chambers stacked in the depth direction is a useful detector for measuring the depth dose distribution (DDD). By using the MLIC, the measurement time and the amount of beam for dosimetry are drastically decreased. In HIMAC (Heavy-Ion Medical Accelerator in Chiba), the MLIC has been effectively used for QA (Quality Assurance) measurement of heavy-ion therapeutic beam since 2002. We are developing a new type MLIC that has electrodes made of graphite on the surface of the polymethyl-methacrylate (PMMA) plates for particle therapy. The purpose is to obtain the same results as the DDD measured in water. We will report on the progress of the development.

INTRODUCTION

In heavy ion therapy, the quality of the beam has to be checked every day. The DDD is an important indicator of the beam condition. However, the DDD measurement needs much time with the existing method that used the dosimeter moving step by step in the depth direction. The MLIC can measure the DDD at once. It has a lot of measurement points regularly arranged in the depth direction. Therefore, it does not need time for changing the depth position of the dosimeter. In addition, the amount of the beam used for the measurement of the DDD could be reduced.

In HIMAC, the MLIC has been used since 2002. It has contributed to the increase of the number of treatment by shortening the measuring time of the DDD. More specifically, the measuring time was reduced to about 3 minutes from about 20 minutes. It does not include the time to set up and to put away the detector.

From the experience in using the MLIC, it has been recognized as useful means for quality assurance of the heavy-ion therapeutic beam in HIMAC. On the other hand, it was found necessary to improve the accuracy of the dosimetry with the MLIC. In external beam therapy, the dose distribution in water is treated as a reference. Therefore, it is preferable that the output of the MLIC closes in the DDD in water. However, the MLIC used in HIMAC is not so because it has the electrode substrates made of glass epoxy plate (FR4) and copper foil. These electrode substrates also have been used for an energy absorber of the heavy-ion beam. The materials of them are composed of higher atomic number elements than water. The varieties of the fragmented particles generated by these materials are different from ones generated in water, under irradiation of the heavy-ion beam. In such effect, it is expected that the measurement result of the existing MLIC is different from that of the DDD in water.

We are developing the new type MLIC (See Figure 1) that can output the equivalent data of the DDD in water. This MLIC has the electrode substrates made of PMMA and graphite. The constituent atoms of these materials are only hydrogen, carbon, and oxygen. Therefore, the effect of the fragmented particles generated inside the new type MLIC will be close to the water phantom. However, we have not yet reached that make a specific assessment for the results of the new type MLIC, for now. In this paper, the progress of its development is described.

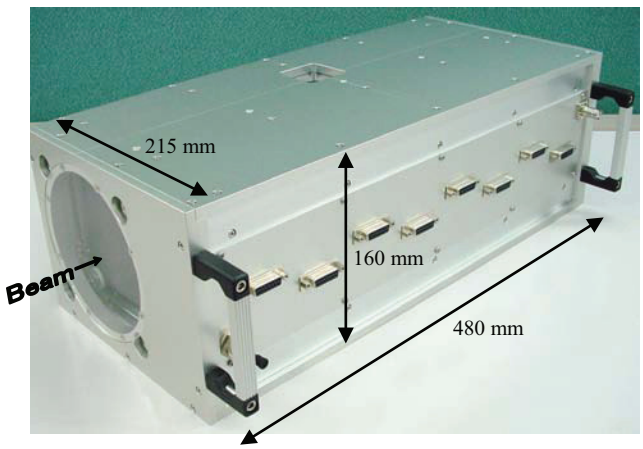

Figure 1: The picture of the new type MLIC.

DESIGN OF THE NEW TYPE MLIC

The MLIC has a lot of ionization chambers stacked in the depth direction. The ion chambers of the new type MLIC are parallel plate type. Each electrode substrates are placed orthogonal to the beam traveling direction. The momentum of the beam particles are lost by passing through the electrode substrates. In essence, progresses to the back side of the MLIC, the beam particles slow down. The amount of charge collected by each stacked ionization chambers has varies depending on the depth position. Therefore, we will get the DDD as the Bragg peak. The measuring range of the new type MLIC is about 280 mmWEL (Water Equivalent Length) that corresponds to 400 MeV/u carbon beam.

Figure 2 shows the structure of the new type MLIC. And, Table 1 is the specification of it made for Gunma University Heavy Ion Medical Center.

http://www.aec-beam.co.jp

ISBN 978-3-95450-119-9

ELECTRON CLOUD MEASUREMENTS USING SHIELDED PICKUPS AT CESRTA*

J.P. Sikora†, J.A. Crittenden, J.S. Ginsberg, D.L. Rubin, CLASSE, Ithaca, New York, USA

Abstract

The Cornell Electron Storage Ring has been reconfigured as a test accelerator (CESRTA) with positron or electron beam energies ranging from 2 GeV to 5 GeV. An area of research at CESRTA is the study of the growth, decay and mitigation of electron clouds in the storage ring. Electron Cloud (EC) densities can be measured with a Shielded Pickup (SPU), where cloud electrons pass into the detector through an array of small holes in the wall of the beam-pipe. The signals produced by SPU have proved to be very useful in establishing the mitigating effect of different vacuum chamber surfaces - including differences in quantum efficiency as well as secondary and elastic yield. This has been accomplished through the careful comparison of observed signals with the output of the EC simulation code ECLOUD. We present example comparisons of data and simulation that show the sensitivity of the measurements to secondary and elastic yield. In addition, some data has been acquired using a solenoid to produce a longitudinal magnetic field at the SPU. We will also present our current understanding of the effect of a longitudinal magnetic field on SPU signals.

INTRODUCTION

An important feature of the Shielded Pickup (SPU) are the holes that connect its vacuum space to the that of the beam-pipe, as shown in Fig. 1. The holes have a depth to diameter ratio of about 3:1 that is effective in reducing the strength of the direct beam signal [1]. The holes also limit the angular acceptance of the detector, so that it is sensitive primarily to electrons with vertical trajectories.

Initial cloud electrons are generated when synchrotron radiation strikes the walls of the vacuum chamber producing photo-electrons. These electrons will then strike the wall and produce secondary electrons. There are three categories of secondary electrons [2]. The first is that of the true secondaries – where the incident electron interacts with the material in a non-trivial way and secondaries are produced. The two other categories are from scattering of an incident electron: elastics – where the energy of the secondary is equal to that of the incoming electron – and rediffused – electrons with energies up to the incident electron energy. Each of the categories has a corresponding secondary emission yield value, denoted by: δ_{ts}, δ_e and δ_r for true secondaries, elastic and rediffused respectively.

*This work is supported by the US National Science Foundation PHY-0734867, PHY-1002467 and the US Department of Energy DE-FC02-08ER41538, DE-SC0006505.

† jps13@cornell.edu

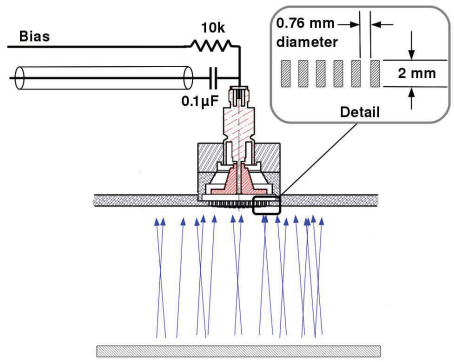

Figure 1: Cloud electrons enter the SPU through an array of small holes in the beam-pipe wall. The pickup is biased at +50 V and the signal amplified by +40 dB before being recorded by a digital oscilloscope.

Signals from the SPU are amplified and sent to an Agilent DSO6054 oscilloscope where they are digitized and averaged for 8k traces. The accelerator timing system provides triggers to the oscilloscope [3].

COMPARING DATA AND SIMULATION

Most of our experiments have focused on two bunch data, where bunches of equal population are injected into the storage ring with different spacings. As shown in Fig. 2, the signal from the second bunch is much larger than the first. The second bunch signal is dominated by electrons that were generated by the first bunch being kicked into the detector by the second bunch. So the signal after the second bunch represents a sample of the electron cloud that was produced by the first bunch.

The decay of the electron cloud is revealed by the superposition of a number of measurements with different bunch spacings. Through a comparison of these signals with simulations, the different spacings have shown different sensitivities to the three categories of secondary electrons.

Synchrotron radiation is simulated at the locations of the SPU with the program Synrad3D [4] that includes beam-pipe geometry and multiple diffuse scattering of photons throughout the CESR lattice. The simulation program ECLOUD [5, 6] uses the azimuthal photon absorption distribution to generate photo-electrons based on a parameterization of quantum efficiencies and photo-electron energies. The production of secondary electrons is based on the relative contributions from the three categories: true, rediffused and elastic. The vacuum chamber geometry and detector response is included in the model.

ISBN 978-3-95450-119-9

ELECTRON CLOUD MEASUREMENTS USING A TIME RESOLVED RETARDING FIELD ANALYZER AT CESRTA*

J.P. Sikora†, M.G. Billing, J.V. Conway, J.A. Crittenden, J.A. Lanzoni,
X. Liu, Y. Li, D.L. Rubin, C.R. Strohman, CLASSE, Ithaca, New York, USA
M.A. Palmer, Fermilab, Batavia, Illinois, USA
K. Kanazawa, KEK, Ibaraki, Japan

Abstract

The Cornell Electron Storage Ring has been reconfigured as a test accelerator (CESRTA) with positron or electron beam energies ranging from 2 GeV to 5 GeV. An area of research at CESRTA is the study of the growth, decay and mitigation of electron clouds in the storage ring. With a Retarding Field Analyzer (RFA), cloud electrons pass into the detector through an array of small holes in the wall of the beam-pipe. The electrons are captured by several collectors, so that the electron flux can be measured as a function of horizontal position. Up to now, we have time averaged the collector currents to provide DC measurements. We have recently designed and constructed a new Time Resolved RFA (TR-RFA), where the collector currents can be observed on the time scale of nanoseconds. We present a summary of the design, construction and commissioning of this device, as well as initial beam measurements at CESRTA.

INTRODUCTION

The Time Resolved Retarding Field Analyzer (TR-RFA) is a natural extension of two other instruments that have been very successful in the study of electron clouds (EC): Shielded Pickups (SPU) and Retarding Field Analyzers (RFA).

The SPU is simple device for sampling the time resolved growth and decay of the electron cloud [1, 2]. The SPU measures the flux of cloud electrons into the beam-pipe wall by allowing a sample of this current to pass into the detector through an array of small holes. The holes also isolate the SPU electrode from the direct beam signal – the depth to diameter ratio of the holes of about 3:1 provides significant attenuation [3]. This is especially important when recording time domain data. Time domain information has been used to map the growth and decay of the electron cloud, measure the effectiveness of mitigation techniques and to constrain the parameters used in electron cloud simulations [4].

In the case of a Retarding Field Analyzer (RFA), cloud electrons also enter the detector through an array of holes. In addition, a retarding grid can be biased negatively to suppress low energy electrons from reaching the collectors [5]. The current of electrons into the detector is time averaged and recorded. The devices installed at CESRTA have segmented collectors that allow this electron current to be measured as a function of horizontal position [6]. These devices have been useful in measuring the effectiveness of mitigation techniques, the horizontal distribution of the electron cloud and in constraining EC model parameters [7].

The Time Resolved RFA (TR-RFA) combines the properties of these two devices by providing a time resolved collector signal and a grid that can be used to obtain additional energy information. Figure 1 shows a cross section of the beam-pipe with a TR-RFA detector. The middle of three grids is used to provide the retarding field. There are nine collectors, each 0.6 cm wide and 7.5 cm long, etched on a kapton flex circuit that are connected directly to individual SMA feed-throughs as shown in Fig. 2. During data taking, the collectors are biased at +50 V to prevent secondary electrons from leaving the collector surface.

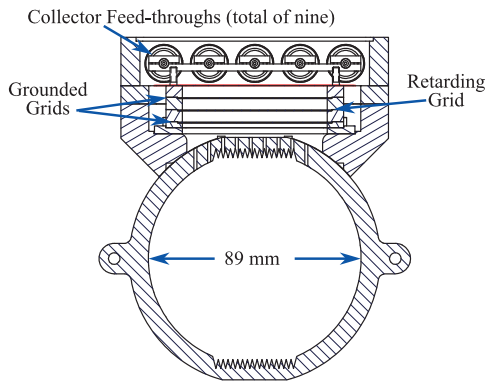

Figure 1: A cross section of the TR-RFA shows the geometry of the grooved beam-pipe extrusion and the relative location of grids and collectors.

INITIAL BEAM TESTS

Early in 2012, two prototype TR-RFAs were installed at CESRTA in beam-pipe of round cross section, one made of bare aluminum, the other with the vacuum surface coated with TiN. They were located in two of four chicane dipole magnets, replacing standard RFAs that had been in use previously. A bias of +50V was applied both to the retarding grid and the collectors during initial data taking. Cables 25 cm long route each collector signal to cascaded pairs of

* Work supported by the US National Science Foundation PHY-0734867, PHY-1002467, the US Deptartment of Energy DE-FC02-08ER41538, DE-SC0006505, and the Japan/US Cooperation Program
† jps13@cornell.edu

ISBN 978-3-95450-119-9

OVERVIEW OF BEAM INSTRUMENTATION AND TUNING AT RIKEN RI BEAM FACTORY

N. Fukunishi*, M. Fujimaki, M. Kase, M. Komiyama, J. Ohnishi, H. Okuno, N. Sakamoto, H. Watanabe, T. Watanabe, K. Yamada, O. Kamigaito, RIKEN Nishina Center for Accelerator-Based Science, 2-1 Hirosawa, Wako, Saitama 351-0198, Japan
R. Koyama, SHI Accelerator Service Ltd., 1-17-6 Ohsaki, Shinagawa, Tokyo 141-0032, Japan

Abstract

The RIKEN Radioactive Isotope Beam Factory (RIBF) has been successfully producing the world's most intense medium-energy heavy-ion beams, such as 0.42-pμA-^{48}Ca and 24-pnA-^{124}Xe beams. Several types of beam monitor have played a vital role in attaining current performance levels, though many are of conventional design. This article gives an overview of RIBF beam instrumentation and introduces beam-tuning methods adopted by RIBF.

RI BEAM FACTORY

The Radioactive Isotope Beam Factory (RIBF) [1,2] started operation at the end of 2006 as the first second-generation radioactive beam facility. The RIBF experimentally investigates unknown areas of the nuclear chart, especially candidate nuclei essential to nucleosynthesis, by producing the world's most intense RI beams. For this purpose, beam intensities of 1 pμA are required for all stable ions, from hydrogen to uranium.

Table 1: Beam Intensities Obtained by RIBF

Ion	Energy (A MeV)	Beam Intensity	Acceleration Mode
^{4}He	320	1 pμA	Variable energy
^{18}O	290	0.45 pμA	AVF injection
^{18}O	345	1 pμA	Variable energy
^{48}Ca	345	0.42 pμA	Variable energy
^{124}Xe	345	24 pnA	Fixed energy
^{238}U	345	3.6 pnA	Fixed energy

The RIBF accelerator complex consists of two injector linac complexes (RILAC [3] and RILAC2 [4]), an injector AVF cyclotron [5] and four ring cyclotrons (RRC [6], fRC [7], IRC [8], and SRC [9]), including the world's first superconducting ring cyclotron SRC. Three acceleration modes are available in RIBF. The first is AVF injection mode, which is suitable for accelerating very light ions such as ^{4}He and ^{18}O. Here, AVF, RRC, and SRC are used in series. For medium-heavy elements such as ^{48}Ca and ^{70}Zn, a variable energy mode using RILAC, RRC, IRC, and SRC is employed. The third mode is a fixed energy mode where the new injector RILAC2 is utilized with all four ring cyclotrons, producing high intensity, very heavy ion beams such as ^{124}Xe and ^{238}U. Table 1 summarizes recent beam intensities. We have already extracted 1-pμA beams from SRC for light ions, and are steadily approaching 1 pμA for ^{48}Ca. The new RILAC2 injector was recently commissioned, and various RIBF upgrade programs are in progress to improve ^{124}Xe and ^{238}U beam intensities.

RIBF BEAM INTENSITY RANGE AND BEAM INSTUMENTATION

The typical beam intensity from SRC, the final-stage RIBF accelerator, is several microamperes. This corresponds to several tens of microamperes in the injector and intermediate-stage accelerators, because RIBF employs two-step charge-stripping schemes [10]. RIBF beam monitors also measure beams with intensities of 100 nA or less, because we begin beam tuning with an intensity-attenuated beam to avoid unnecessary hardware damage caused by poor accelerator optimization. The maximum beam power already obtained is 6.9 kW for a 345-MeV/nucleon-^{48}Ca beam, which requires careful beam tuning.

RIBF beam monitors are required to cover a wide beam-intensity region ranging from a few tens of nanoamperes to 100 μA. RIBF mainly uses conventional destructive beam monitors because they are suited to low-intensity beam operations. RIBF beam monitors are divided into two groups: monitors specific to cyclotrons, which include phase probes and radial probes, and monitors installed in beam lines and the two linac compexes, such as Faraday cups and beam profile monitors.

PROBES USED IN CYCLOTRONS

A typical cyclotron beam tuning procedure is as follows. Ions are injected into the cyclotron through a bending magnet, magnetic channels, and an electrostatic channel. Baffle slits at channel entrances detect beam loss, allowing best-fit determination of an ion injection orbit. Ions are accelerated if proper phases of accelerating RF fields are chosen under reasonable starting values for the cyclotron's isochronous magnetic fields. Step by step, ions are accelerated to higher energies by adjusting magnetic and RF fields. A radial probe plays an essential role in this procedure. The ions at last reach the cyclotron design energy, but the isochronous magnetic fields are still imperfect and are significantly improved by using a phase probe. After magnetic field tuning, RF phases are optimized with the use of the radial probe. Finally, ions are extracted from the cyclotron through an electrostatic

*fukunisi@ribf.riken.jp

ISBN 978-3-95450-119-9

BEAM QUALITY ENSURING INSTRUMENTS AT THE GUNMA UNIVERSITY HEAVY-ION MEDICAL CENTER

E. Takeshita#, T. Kanai, S. Yamada, K. Yusa, M. Tashiro, H. Shimada,
K. Torikai, A. Saito, Y. Kubota, A. Matsumura, M. Kawashima,
Gunma University Heavy-Ion Medical Research Center
3-39-22, Showa, Maebashi, Gunma 371-8511 JAPAN

Abstract

Since carbon beam based cancer therapy started at the Gunma University Heavy-ion Medical Center in the year 2010, the total number of treated patients increased to 306 by the end of 2011. This fiscal year, already 164 patients have been treated. In order to control the medical beam qualities, i.e., position, size and intensity of the beam, monitoring devices were mounted on the high-energy beam transport line. The beam position and size can be measured and tuned with a screen monitor, which consists of a fluorescent screen and a CCD camera. Just before starting the treatment, the operators check for a proper beam position by strip-line monitor measurements placed close to the isocenter. The irradiation dose is controlled using two secondary electron emission monitors placed before wobbling magnets. This dose monitor is helpful as for high beam intensities it's less affected by the recombination effect. The technical layout of all beam monitors are described.

INTRODUCTION OF GHMC

The Gunma University Heavy Ion Medical Center (GHMC) [1] is located at the Gunma University Hospital. Basic and accelerator building designs started in April and July 2006, respectively. The construction works started in February 2007 and were completed in October 2008. The facility's dimension is about 65 m × 45 m, approximately 1/3 of the Heavy Ion Medical Accelerator in Chiba (HIMAC) [2]. The layout of the bottom floor is shown in Figure 1. The facility contains three treatment rooms with four irradiation ports (horizontal; Room A, horizontal + vertical; Room B, and vertical; Room C) and a room with a vertical port intended for R&D of beam delivery system and biology experiments.

Accelerator Complex

The injection part consists of a compact ECR ion source and two linear accelerators, which are the radio frequency quadrupole linac (RFQ linac) and the alternating phase focusing linac (APF linac) [3]. The RFQ linac accelerates the carbon ion beam up to 600 keV/u

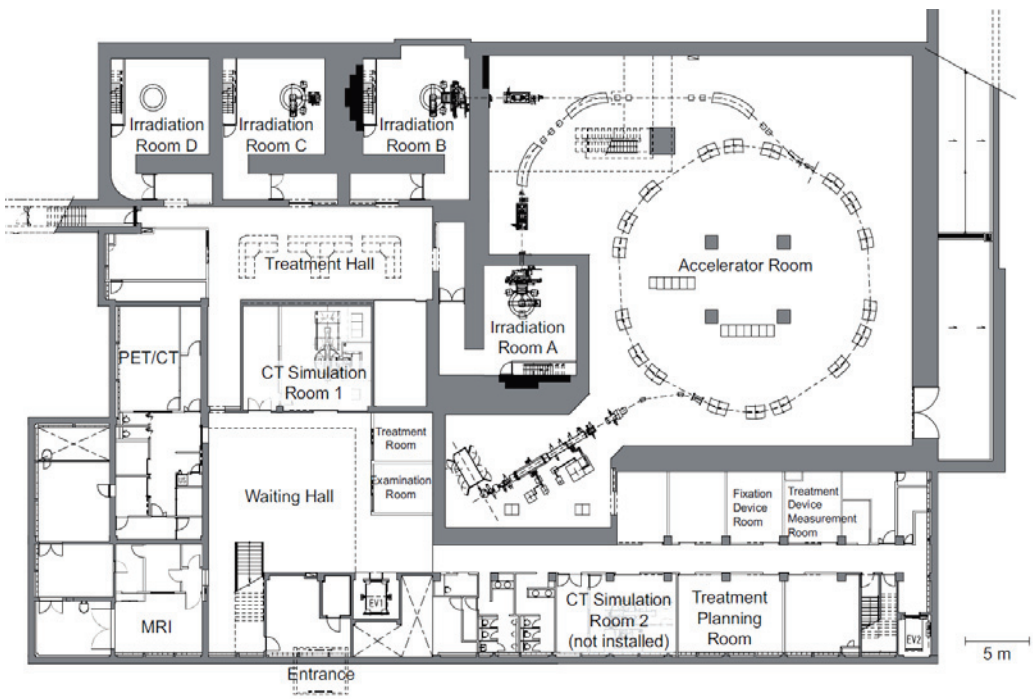

Figure 1: Layout of B1 floor in GHMC.

#eriuli@gunma-u.ac.jp

ISBN 978-3-95450-119-9

BEAM DIAGNOSTICS FOR AREAL RF PHOTOGUN LINAC

K. Manukyan#, G. Zanyan, B. Grigoryan, A. Sargsyan, V. Sahakyan, G. Amatuni,
CANDLE, Yerevan, Armenia

Abstract

Advanced Research Electron Accelerator Laboratory (AREAL) based on photocathode RF gun is under construction at CANDLE. The basic approach to the new facility is the photocathode S-band RF electron gun followed by two 1 m long S-band travelling wave accelerating sections. Linac will operate in single bunch mode with final beam energy up to 20 MeV and the bunch charge 10 –200 pC. In this paper the main approaches and characteristics of transverse and longitudinal beam diagnostics are presented.

INTRODUCTION

The beam diagnostic section for AREAL linac [1] can be divided into two sections

- Gun section diagnostics
- Linac diagnostics

The commissioning of the AREAL linac will proceed in two stages: in a first step (phase 1), the gun section with additional diagnostics will be put into operation. For phase 2 the full accelerator will be assembled.

The beam transport line between the electron gun and the first accelerating structure (energy < 4 MeV) has a length of almost 0.95 m, which is completely occupied by diagnostic devices. In this diagnostic line electron beam charge, position, transverse profile, emittance (phase 1), energy and energy spread must be measured. In a gun commissioning phase the gun section with additional diagnostics (pepperpot) will be put into operation. The schematic layout of the gun section with diagnostics is presented in Fig. 1.

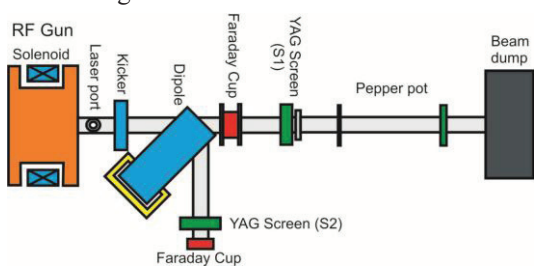

Figure 1: Layout of AREAL gun section with diagnostics (phase 1).

After gun commissioning the pepperpot will be moved to the end of the linac. Also high resolution Cavity BPM will be installed in the straight arm of the gun section. In linac diagnostics it is foreseen to measure electron beam charge, position, emittance, energy, energy spread and longitudinal profile. The schematic layout of the linac with diagnostics is presented in Fig. 2.

BEAM CHARGE

The task for the beam current and charge measurement is to verify that the charge produced at the cathode is completely transported along the whole beamline to the beam dumps. In AREAL linac the charge of individual bunches will be measured using Faraday Cups and Integrating Current Transformers (ICT) [2] (see Fig. 1, 2). Three Faraday cups are intended to be used to collect and measure the beam charge. Two of them will be installed in the end of the spectrometer arms. The third one is an insertable faraday cup which will be installed in the gun section. Electrical connections are made to the base of the Faraday cups, terminating in a BNC connector. The output signal is integrated on the oscilloscope and divided by the termination to give a reading of the charge.

Specifications of Faraday cups are presented in Table 1.

Table 1: Specifications of ARIAL linac Faraday cups.

	Non insertable	Insertable
Cup Diameter (mm)	15.1	9.5
Cup Length (mm)	75	69.5
Maximum Power (W)	10	4
Impedance	50 Ω	
Signal Output	BNC	

Also two in-air ICTs are planned to be used as non-destructive devices for electron bunch charge monitoring. Typical installations include bellows, a wall current bypass and an electromagnetic shield covering the ICT completely.

BEAM POSITION

Three BPMs are intended to be installed in AREAL linac. High resolution Cavity BPM (CBPM) will be installed in the gun diagnostic line in phase 2. It will provide about 1~3 μm resolution for electron beam trajectory measurements.

A cylindrical "pillbox" with conductive walls of length l and radius R resonates at its eigenfrequencies

$$f_{mnp} = \frac{1}{2\pi\sqrt{\mu_0\varepsilon_0}}\sqrt{\left(\frac{j_{mn}}{R}\right)^2+\left(\frac{p\pi}{l}\right)^2},$$

with j_{mn} - the n-th zero of the Bessel function J_m of order m, p is an integer number. For the application as BPM the lowest transverse magnetic fundamental TM_{010} monopole and TM_{110} dipole modes are of interest. The X and Y

ISBN 978-3-95450-119-9

EMITTANCE MEASUREMENT USING X-RAY BEAM PROFILE MONITOR AT KEK-ATF

T. Naito*, H. Hayano, K. Kubo, S. Kuroda, T. Okugi, N. Terunuma, J. Urakawa, H.R. Sakai,
N. Nakamura High Energy Accelerator Research Organization(KEK), Tsukuba, 305-0801, Japan

Abstract

The X-ray profile monitor (XPM) is used for the beam size measurement in the KEK-ATF damping ring(ATF-DR) at all times. The XPM consists of a crystal monochromator, two Fresnel zone plates(FZPs) and X-ray CCD camera. Two FZPs make the imaging optics. The design resolution of the selected wavelength 3.8nm is less than 1μm, which is sufficiently small for the emittance measurement of the ATF-DR. However, the measured results at the early stage were affected by the mechanical vibration. This paper describes the improvement of the resolution and the measurement results.

INTRODUCTION

The damping ring(DR) of the KEK-ATF has been designed to produce extremely low emittance beam for future accelerator technologies, especially focus on the International Linear collider(ILC).[1][2] The beam energy is 1.3GeV. The design horizontal emittance(ε_x), we call "emittance" as "un-normalized emittance", at a zero current is 1.1 x 10^{-11}m. The vertical emittance(ε_y) is 1x10^{-11}m when assuming 1% coupling. The expected beam size for the vertical is 5.5μm, at the location of the beam size monitor. The beta function at the location is 3m for the vertical. The beam size monitor needs to have enough resolution for 5.5μm measurement. The recent tuning effort of the DR is aiming to reduce the vertical emittance less than 1x10^{-11}m. In this case, the vertical beam size reduces to 4μm(ε_y=5x10^{-12}m) or 3μm(ε_y=3x10^{-12}m).

The X-ray profile monitor(XPM) was constructed by Tokyo University group[3][4] to measure the beam size in the DR. The XPM is a long-distance X-ray microscope, which consists of a crystal monochromator, two Fresnel zone plates(FZPs) and an X-ray CCD camera. The X-ray of the synchrotron radiation from the bending magnet is monochromatized by a crystal monochromator with the wavelength of 0.38nm(3.235keV). The two FZPs constitute imaging optics and the magnification ratio from the source to the CCD camera is 20. The estimated resolution of the XPM is less than 1μm, which is enough to measure the vertical DR emittance. The detail of the design parameter and the specification of the FZPs are described in [3].

At the beginning of the system commissioning, the measured beam size could not be less than 6μm in vertical, which correspond to 1.2 x 10^{-11}m of the vertical emittance. However, the emittance evaluated from other beam size monitors, a laser wire profile monitor(LW)[5] and a SR interferometer(SRI)[6] was less than 1.0 x 10^{-11}m. We investigated the reason of the discrepancy among the XPM, the LW and the SRI. We found that the mechanical vibration of the crystal monochromator deteriorated the minimum spot size. The minimum beam size 4μm was measured after reduced the mechanical vibration.

A standalone video analyser was used, which didn't have an interface to connect the accelerator control system. To synchronize the beam profile data with the other DR parameters, an online video analysis system was constructed. The new video analysis system can be controlled from the accelerator control system and can monitor the beam profile synchronized with the other machine parameters.

SYSTEM DESCRIPTION

The layout of the XPM is shown in Figure 1. The synchrotron radiation (SR) from the bending magnet(BH1R.27) located just before the long straight section is used for the XPM. The SR parameters are summarized in Table 1.

Table 1: Parameters of the SR of BH1R.27

Beam energy	1.3 GeV
Magnetic field of BH1R.27	0.75 T
Bending radius	5.4m
Critical energy of the SR	0.816 keV

The SR is monochromatized by a Si monochromater with crystal lattice plane Si(220), Bragg angle 86.35° and spectral resolution 5.6 x 10^{-5} for the wavelength 0.38nm(3.235keV). The two FZPs (Condenser Zone Plate : CZP, Micro Zone Plate : MZP) make the imaging optics. The CZP and the MZP have 0.91m and 24.9mm of the focal length, respectively. The magnification ratio of the CZP and the MZP are 0.1 and 200, respectively.

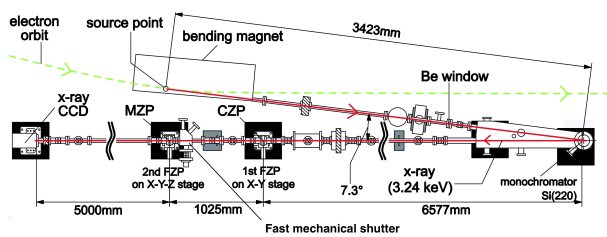

Figure 1: Layout of the XPM.

The image of the source point is magnified 20 times on the X-ray CCD. The X-ray CCD camera (HAMAMATSU C4742-98-KWD) is a direct incident type with a

*Work supported by US/Japan Sci. and Tech. Collaboration program.
#takashi.naito@kek.jp

ISBN 978-3-95450-119-9

MEASUREMENT OF SUB-PICOSECOND BUNCH LENGTH WITH THE INTERFEROMETRY FROM DOUBLE DIFFRACTION RADIATION TARGET*

J.B. Zhang, S.L. Lu, T.M. Yu, H.X. Deng, Shanghai Institute of Applied Physics, China
D.A. Shkitov, M.V. Shevelev, A.P. Potylitsyn#, G.A. Naumenko, Tomsk Polytechnic University, Russia

Abstract

Reliable and precise methods for non-invasive diagnostics of sub-picosecond electron bunches are required for new accelerator facilities (FEL, LWFA, et al.). Measurements of spectral characteristics of coherent radiation generated by such bunches using interferometer allow to determine a bunch length [1].

Here we present a compare experimental study between the measurement from the double diffraction radiation target interferometry and the measurement from the Michelson interferometer.

INTRODUCTION

Non-invasive methods of the sub-picosecond bunch length diagnostics are very important nowadays for such accelerator facilities as free electron lasers with typical bunch lengths of some hundreds of femtoseconds.

One of the ways to measure the electron bunch length is based on coherent radiation that is generated at wavelengths comparable to, or longer than, the bunch length, when all electrons in the bunch irradiate more or less in phase. The intensity of coherent radiation is proportional to the square of the bunch population. The spectral distribution of the coherent radiation contains information about the electron bunch distribution. Coherent diffraction radiation (CDR) is suggested as the mechanisms for coherent radiation generation due to their non-invasive nature.

DR appears when a charged particle moves rectilinearly in a vacuum in the vicinity of a medium. If the particle passes through a slit between two semi planes, it induces time-varying currents on both semi planes. These currents generate radiation. Two cones propagate in the direction of specular reflection producing an interference pattern.

The interference pattern obtained by two diffraction radiation beams from two shifted plates (double DR target) may be used instead an interferometer [2]. Recently, the coherent DR interferometry scheme was established [3] on the femtosecond accelerator facility at SINAP [4, 5].

* Work supported by the joint Russian-Chinese grant (RFBR No. 11-02-91177 and NSFC No. 11111120065) and partially by the Program of Russian Ministry of Education and Science "Nauka" and Chinese NSFC grant No. 11175240.
# Corresponding author. Email: pap@interact.phtd.tpu.ru

EXPERIMENTAL SETUP

Our experimental equipments were consisted of a linear accelerator, a vacuum chamber with targets driven by motion-control system, a Michelson interferometer and a detector.

Accelerator

The accelerator providing femtosecond electron bunch facility consists of an S-band thermionic cathode rf-gun, an alpha magnet and a SLAC-type accelerating tube. The electron beam emerges from an APS type 1.6 cell π/2 mode thermionic rf-gun. After pre-accelerated at the rf-gun, the electron beam is transported to the alpha-magnet via a beamline consisting of the focusing, steering, scraping and beam monitoring components. The alpha-magnet is used to compress the electron beam from a few hundreds of ps to few hundreds of fs in longitudinal length. A SLAC-type accelerating tube is used to accelerate the electron beam up to high energy to minimize the lengthening force in the drift space. The design parameters of electron beam are listed in Table 1.

Table 1: Parameters of Electron Beam

Beam energy	20 – 30 MeV
Beam charge	0.068 nC
Normalized emittance	~ 10 mm·mrad
Macro-bunch repetition frequency	3.125 – 12.5 Hz
Micro-bunch repetition frequency	2856.2 MHz
Macro-bunch duration	2 – 3 μs
Micro-bunch duration (FWHM)	0.3 – 3 ps

Interferometer

To measure the interferograms of the coherent diffraction radiation from ordinary DR target the typical Michelson interferometer was employed (see in Fig. 1). The interferometer consists of a beam splitter, which is made from a 2-μm-thick nitrocellulose and comes with a metallic coating, providing consistent 30% reflection and 30% transmission over a very wide bandwidth, a stationary Au-coated hollow reflector mirror, a moving Au-coated hollow reflector stepped by remote control system capable of sub-micron steps, and a off-axis parabolic mirror that focus the re-combined light into the a pyroelectric detector.

ISBN 978-3-95450-119-9

DEVELOPMENT OF OFFNER RELAY OPTICAL SYSTEM FOR OTR MONITOR AT 3-50 BEAM TRANSPORT LINE OF J-PARC

M. Tejima#, Y. Hashimoto, T. Toyama, KEK/J-PARC, Tokai, Ibaraki, Japan
T. Mitsuhashi, KEK, Tsukuba, Ibaraki, Japan
S. Otsu, Mitsubishi Electric System & Service Co. Ltd., Japan

Abstract

An extremely wide aperture relay optical system based on Offner system has been developed for Optical Transition Radiation (OTR) monitor at 3-50 beam transport line (3-50BT) from RCS to MR in J-PARC. Diagnostics for beam profile and halo at the 3-50BT are very important to optimize the injection of MR. For this purpose, an OTR monitor is planned to install for an observation of image of the beam and halo after the beam collimators in the 3-50BT. Since the opening of OTR is very wide due to small Gamma; 4.2, extremely wide aperture (500 mrad) optics will necessary to efficient extraction of OTR. We developed Offner type relay optics for the effective extraction of OTR. As a result, we obtained a clear aperture which covers 100 × 100 mm aria on the target screen. An optical design of OTR monitor and results of optical testing are presented in this paper.

INTRODUCTION

Japan Proton Accelerator Research Complex (J-PARC) is composed of three accelerators which are a 400 MeV (currently operating at 180 MeV) linear accelerator (LINAC), a 3 GeV rapid cycling synchrotron (RCS), a 50 GeV (currently 30 GeV) main ring (MR) [1]. The MR provides 30 GeV proton beams to beamlines in the Hadron Experimental Hall for hadron physics and to the neutrino beam line. The produced neutrino beams are sent to the Kamiokande facility which is located in Kamioka, 300km apart from J-PARC. Figure 1 shows the schematic drawing for the layout of beam transport line from RCS to MR.

14 Beam Position Monitors (BPMs), 50 Beam Loss Monitors (BLMs), 5 Fast Current Transformers (FCTs) and 9 Multi Wire Profile Monitors (MWPMs) are installed in the 3-50BT [2]. Those beam diagnostics systems are used for the measurement and regulation of the beam orbit, the beam loss and the beam size of the 3-50BT. In summer 2013, the linac energy will upgrade from 181 MeV to 400 MeV, and the intensity of protons those extracted from the RCS will be increased by double. For this upgrade, we will have a plane to diagnostic the two-dimensional profile of the beam core and the beam halo to reduce radio-activation of the MR as small as possible. For this purpose, we plane to install a new profile monitor in the 3-50BT to observe the two-dimensional beam profile.

Since the beam aperture of the MR was designed to 81π mm mrad, the permissible emittance of the injection beam is 54π mm mrad [3]. On the other hand, we estimated that the beam from the RCS should have a large halo surrounding of the beam core. Including the beam halo, the emittance of the beam in 3-50BT is estimated up to 216π mm mrad. The collimators those set in the 3-50BT is designed to removes the halo surrounding of the beam core to reduce pollution of the residual radioactivity of the MR. The effective diagnostic for the beam halo is very important to eliminate it by the beam collimator. The optical profile monitor using the OTR is suitable for this purpose, because the OTR is emitted from the surface of thin metal target (typically 10 μm thickness), and we can reduce radiation from the metal target as discussed in after.

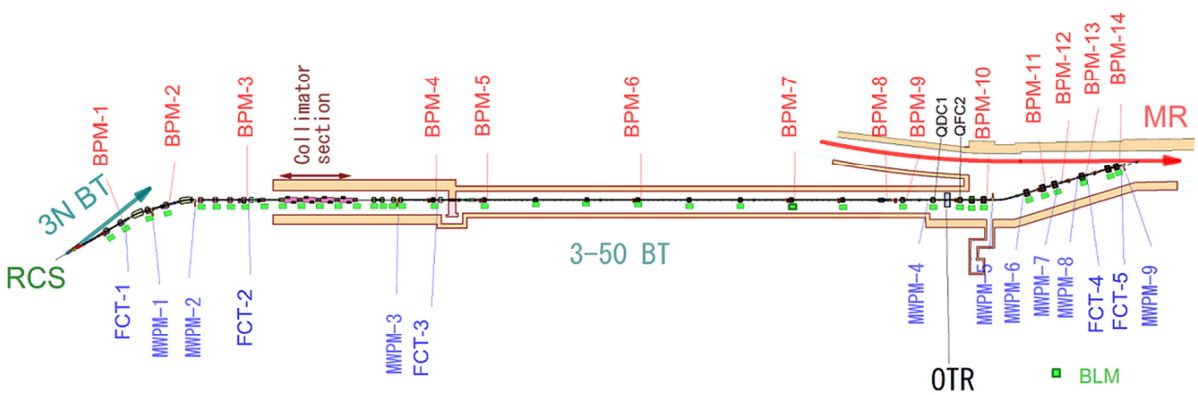

Figure 1: A schematic drawing for layout of beam instrumentations for 3-50BT in J-PARC. New beam profile monitor using the OTR is planed to set between QDC1 and QFC2. The collimator section locates between BPM3 and BPM4.

#masaki.tejima@kek.jp

ISBN 978-3-95450-119-9

DEVELOPMENT OF PROFILE MONITOR SYSTEM FOR HIGH INTENSE SPALLATION NEUTRON SOURCE

Shin-ichiro Meigo*, Motoki Ooi, Kiyomi Ikezaki, Atsushi Akutsu, Shinichi Sakamoto and Masatoshi Futakawa, J-PARC center, Japan Atomic Energy Agency (JAEA), Japan

Abstract

At the JSNS in J-PARC, a mercury target is employed as the neutron production target. It is well known that the damage on the mercury target is proportional to the 4th power of the peak current density of the primary proton beam on the target. For the high intense neutron source, the profile on the target is important to drive the neutron source with the continuously observation of the profile. We have developed to Multi Wire Profile Monitor System (MWPM). During beam operation, when the abnormally of the beam is found, the beam is cut out by the Machine Protection System (MPS). For the measurement of the two dimension observation on the target, we have developed the system based on the residual radiation measurement by using an imaging plate (IP). It is found that the beam width observed by the MWPM and the IP shows good agreement.

INTRODUCTION

In the Japan Proton Accelerator Research Complex (J-PARC) [1], an MW-class pulsed neutron source, the Japan Spallation Neutron Source (JSNS) [2], and the Muon Science facility (MUSE) [3] will be installed in the materials and life science facility (MLF) shown in Fig. 1. The 3-GeV proton beam is introduced to the mercury target for a neutron source and to a carbon graphite target of 20 mm thickness for a muon source. In order to utilize the proton beam efficiently for particle productions, both targets are aligned in a cascade scheme, where the graphite target is located 33 m upstream of the neutron target.

For both sources the 3-GeV proton beam is delivered from a rapid cycling synchrotron (RCS) to the targets by the 3NBT [4, 5, 6]. Before injection to the RCS, the proton beam is accelerated up to 181MeV by a LINAC. The beam is accumulated in short two bunches having width about 150 ns and accelerated up to 3 GeV in the RCS. After extraction, the 3-GeV proton beam is transferred to the muon production target and the spallation neutron source.

Recently it became evident that pitting damage appears in the target container of the mercury target [7]. Several facilities are studying the effect; Alternating Gradient Synchrotron (AGS) and Weapon Neutron Research facility (WNR) are pursuing off-beam experiments [8]. It has been reported that the damage is proportional to the 4th power of the peak current density of the beam [8]. Beam profile monitoring plays an important role in comprehending the damage to the target. Therefore it is very important to watch continuously the status of the beam at the target at the JSNS especially for the peak current density. We have developed a reliable beam profile monitor for the target by using Multi Wire Profile Monitor (MWPM). In order to watch the two dimensional profile on the target, we have also developed the profile monitor based on the imaging of radiation of the target vessel after beam irradiation.

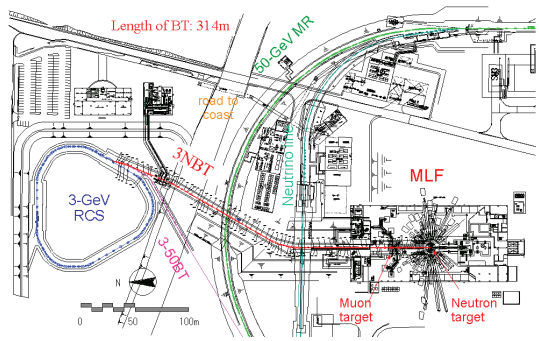

Figure 1: Layout of JSNS and MUSE at J-PARC. The beam transport line (3NBT) introduces the beam to both facilities located in the MLF building.

MULTI WIRE PROFILE MONITOR

Silicon Carbide (SiC) Wire

In order to obtain the characteristics of the proton beam, diagnostic system based on a Multi Wire Profile Monitor (MWPM) is developed. Principle of the MWPM is simple to observe the amount of the electron emission due to the interaction of the beam at the wire. As a material of sensitive wire, usually tungsten wire is selected due to large emission amount of the electron and having high temperature melting point. In the present system, silicon carbide (SiC)is chosen due to the high resistance of the radiation. Due to the interaction, the beam loss is caused, which is one of issues of the high intensity proton accelerator and the optimization of the beam loss is important. The angular differential cross section of Rutherford scattering is proportional to square of atomic number of wire material. Therefore wire material with low atomic number has advantage for beam loss. Here, we compare property between tungsten and SiC. Since the average atomic number of SiC is 10, the differential cross section of SiC becomes 1/55 times of the cross section of tungsten. In order to obtain the angular distribution after scattered by the wire is calculated with DECAY-TURTLE [9] modified at PSI [10]. It is recognized that SiC wire than tungsten gives less influence on the beam. In order to estimate of the lifetime

* meigo.shinichiro@jaea.go.jp

ISBN 978-3-95450-119-9

THE SYNCHROTRON RADIATION DIAGNOSTIC LINE AT SSRF*

J. Chen, Z.C. Chen, Y.B. Leng, G.Q. Huang, W.M. Zhou, K.R. Ye,
SINAP, Shanghai, 210200, China

Abstract

The synchrotron radiation photon beam line has been operated since 2009 at Shanghai Synchrotron Radiation Facility. There are two diagnostic beam lines of the storage ring behind bending magnet, which is employed conventional X-ray and visible imaging techniques. A synchrotron radiation (SR) interferometer using visible light region in order to measure the small transverse electron beam size (about 22μm), low emittance and a low coupling. A small off-axis mirror is set for the convenience of the observation. Wave front testing is used for interferometer to calibrate the deformation effect of optical components. An X-ray pin-hole camera is also employed in the diagnostics beamline of the ring to characterize beam. Typically the point spread function of the X-ray pinhole camera is calculated via analytical or numerical method. Those two methods check each other. As a result, the measurement with SR system has quite enough resolution of itself even though the absolute beam size acquired. This existed system suffices with dynamic problem for beam physics studies. It has been measured 2.8nm.rad in small emittance mode at SSRF.

GENERAL OVERVIEW

For SSRF 3.5Gev storage ring, the emittance is 3.9 (nm.rad). The Beam profile size, horizontal σx is 53μm and vertical σy is 22μm by the use of 1% vertical coupling. The monitor should be able to measure a small transverse beam dimension and motion.[1] So interferometer is one of better equipment to measure this order beam size. It is located at the 3^0 end of the $2^{\#}$ bending magnet of the first cell in the ring. A unique diagnostics line has been working. We also have imaged the beam profile at the SSRF using x-ray synchrotron radiation (XSR) at the $(0.8)^0$ end of same magnet, a selectable pinhole aperture. A unique synchroscan and dual-sweep features of visible streak camera has been used since 2009. Both transverse beam size and bunch length have been determined by this beamline.

The vertical opening angle of visible SR is roughly 3mrad. 4mrad opening will be available in the horizontal direction. The visible part of the synchrotron radiation is reflected by water-cooled Beryllium mirror. Using those two lines, we can characterize the electron beam size, phase-space ellipse and emittance. X-ray has been fetched directly from Al window. Synchrotron radiation monitor measures beam profile and beam size of the synchrotron radiation light source for performance optimization, routine operation check and various beam physics study. It is described those dedicated diagnostics beam lines, and measurement equipments such as SR interferometer, x-ray pinhole and streak camera etc. in this paper. There are the general design of the SRM, extraction mirror design, and measurement equipments. Using this monitor, we can characterize the electron beam size, phase-space ellipse and emittance. It will be shown some results also.

INSTRUCTION

The source point of SRM is bending magnet near injecting point. The synchrotron light is extracted by a water-cooled beryllium mirror. Then three mirrors guide the light to the dark room. The synchrotron light interferometers [2] [3] is set in the dark room and they measure horizontal and vertical beam sizes. Also a focusing system is applied to obtain the image of beam profile. The setup of all diagnostic beam line, it is include interferometer, x-ray pinhole camera and streak camera.

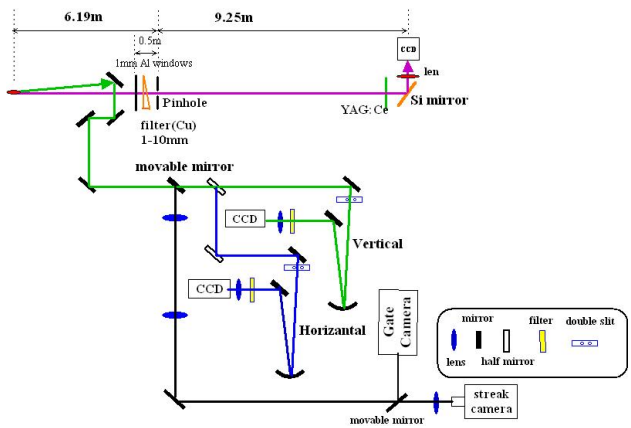

Figure 1: Schematic layout of the Optical Diagnostic Beamline viewed.

The basic layout and main components of the SSRF diagnostic beam line are shown in Fig. 1.

About this system detailed described is in the follows.

INTERFEROMETER & APPLICATION

The first mirror is set 9m apart from the source point, which reflects the visible light by 90° downward. Thermal distortion of the Be mirror for a given absorbed heat load by X-rays is simulated using the technique of finite-element analysis. We designed the mirror shape having a parabolic shape in the backside. Most of the X-ray will pass through the central thin part of the mirror.

The deformation of the mirror has been studied in detail in comparison with other materials. The result shows Be is best material for the extraction mirror.

*Work supported by Shanghai Institute of Applied Physics

ISBN 978-3-95450-119-9

FIRST MEASUREMENTS WITH CODED APERTURE X-RAY MONITOR AT THE ATF2 EXTRACTION LINE

J.W. Flanagan, M. Arinaga, H. Fukuma, H. Ikeda, T. Mitsuhashi, KEK, Tsukuba, Japan
G.S. Varner, U. Hawaii, Honolulu, HI USA

Abstract

The ATF2 extraction line is used as a test-bed for technologies needed for the ILC final-focus region. An x-ray extraction beam line has been constructed at the final upstream bend before the extraction line straight section, for development and testing of optics and readout systems for a coded aperture-based imaging system. The x-ray monitor is expected to eventually be able to measure single-shot vertical bunch sizes down to a few microns in size at its source location in the ATF2 extraction line. Preliminary scanned measurements have been made with beams in the ~15 micron range, and it is planned to make more measurements with further-tuned beam, and with fast read-out electronics. The details of the layout, expected performance, and preliminary measurement results will be presented.

INTRODUCTION

Coded aperture imaging is a technique well-developed among x-ray astronomers, which consists of using a pseudorandom array of pinholes, which project a mosaic of pinhole camera images onto a detector[1]. This image is then decoded using the known mask pattern to reconstruct the original image. One example of such a pattern is the Uniformly Redundant Array (URA)[2], which features an open aperture of 50% with an even sampling of spatial frequencies in the non-diffractive limit. This provides the spatial resolution somewhat better than that of a pinhole camera, but with much greater x-ray photon collection efficiency for single-shot measurements. Coded aperture x-ray imaging has been tested at CesrTA, with beam sizes down to about ~10 microns[3], and it is planned to use it at SuperKEKB[4]. An x-ray beam line has been constructed in the ATF2 extraction line, with the goal of testing coded aperture measurements with beam sizes down to ~4-5 μm.

BEAMLINE LAYOUT

The beamline is located off the last bend (BH3X) after the extraction point from the ATF ring, at the upstream end of the ATF2 line, as shown in Fig. 1. The bending radius of this magnet is 4.3 m, and the beam energy is 1.28 GeV, for a critical energy of 1.1 keV. The beam size at this bend is typically around 20 microns, but can be reduced, by lowering the beta function, to around 4-5 microns.[5] This bend is also used as the source for a visible-light SR monitor.

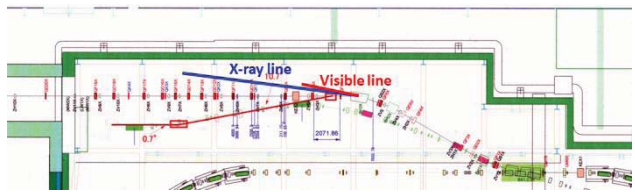

Figure 1: Location of x-ray beamline in the ATF2 extraction line.

The extraction chamber for the x-ray line has a 200 μm thick, polished beryllium window, with ATF2 vacuum on one side and atmosphere on the other side. Just downstream of the beryllium window is the coded aperture mask mounted on a rotating stage, which is then mounted on a 2-axis translational stage. Downstream of the mask is a vacuum chamber with 25 μm thick kapton at both the entrance and exit. There is a 6.4 cm air gap between the beryllium window, and entrance window of the second vacuum chamber, and a 1.5 cm air gap between the second chamber and the detector at the far downstream end, which is, like the mask, mounted on a rotating stage and 2-axis translational stage, on an optical table. Mask and detector mounts are shown in Fig. 3. The distance between the source point and the mask is 193.5 cm, and the distance from the mask to the detector is 835.7 cm.

Figure 2: Views from downstream (left) and upstream (right) during construction of x-ray beamline at ATF2.

The downstream vacuum chamber is only pumped down to a few tens of Pa with a scroll pump; its function is to provide a low-loss path for the x-ray beam, and it is separate from the accelerator beam vacuum. The total effective air path length, including the air gap around the mask and between the downstream kapton window and the detector, is ~10 cm.

ISBN 978-3-95450-119-9

BEAM SIZE AND INTENSITY DIAGNOSTICS FOR A SRF PHOTOELECTRON INJECTOR

R. Barday*, A. Jankowiak, T. Kamps, A. Matveenko, M. Schenk, F. Siewert, J. Völker,
Helmholtz-Zentrum Berlin für Materialien und Energie GmbH, Germany
J. Teichert, Helmholtz-Zentrum Dresden-Rossendorf, Germany

Abstract

A high brightness photoelectron injector must be developed as a part of the BERLinPro ERL program [1, 2]. The injector is designed to produce an electron beam with 100 mA average current and a normalized emittance of 1 mm·mrad. Prior to reaching the final gun/cathode design a staged SRF gun development program has been undertaken which began with the operation of a fully superconducting injector utilizing a lead photocathode. This will be followed by a normal conducting CsK_2Sb cathode capable of generating high current beams. In the first stage we have measured the fundamental beam parameters bunch charge, beam energy and energy spread with a special focus on the measurement of the transverse beam profiles. We will also discuss our plans for the beam characterization at high currents.

INTRODUCTION

In the first stage of the high brightness photoinjector R&D [3, 4] the electron beam is produced from a Pb photocathode in a superconducting RF gun cavity operating at 1.3 GHz. A superconducting lead photocathode was initially directly deposited on the back wall of the gun cavity and irradiated by a UV laser operated at 258 nm with 2-3 ps pulse duration. The maximum average beam current extracted from this gun was 50 nA corresponding to a bunch charge of about 6 pC. The maximum beam energy of about 2.0 MeV was achieved at a peak field on the cathode of 22 MV/m.

In the second version of this type of the SRF gun, a thin layer of lead with a diameter of 5 mm and a thickness of about 400 nm was deposited on a Nb plug, which can be inserted into the backplane of the cavity. The plug is vacuum sealed with an indium gasket. The advantage of this design is a possibility to change the photocathodes and to test different deposition methods. The gun cavity with the coated plug was tested up to the peak fields on the cathode of 35 MV/m without laser irradiation [5].

DIAGNOSTICS BEAMLINE

A schematic overview of the diagnostics beamline is shown in Fig. 1. A dipole spectrometer magnet is used to measure the beam energy and the energy spread. To improve the energy resolution we installed a vertical slit made of copper in the dispersive arm with a width of 2 mm and a thickness of 4 mm.

Measuring the low energy electrons utiliting a Faraday cup can be challenging due to backscattering of primary electrons and secondary electron emission. The number of backscattered electrons per incident electron for primary electrons with energy of 1 MeV impinging on a copper target is about 0.23 [6]. The secondary and backscattered electrons can be trapped if the Faraday cup has a sufficient large ratio of length to diameter, which is commonly not practical. Alternatively the Faraday cup can be electrically biased to suppress low energy electrons, which is the case in our beamline. The bunch charge is measured with an integrating current transformer (ICT).

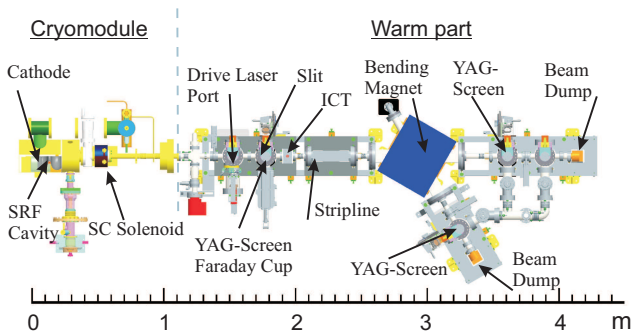

Figure 1: Schematic view of the diagnostics beamline.

An electron beam is visualized by the image of the scintillation light emitted by the cerium-doped yttrium aluminium garnet (YAG:Ce) crystal with Ce-doping concentration of 0.2 %. YAG is a vacuum friendly material with a short decay time and high light output of ∼35 photons per keV of absorbed energy. In order to avoid accumulation of the absorbed electric charge in the crystal, a thin, 10 nm, Indium Tin Oxide (ITO) coating was applied. ITO has high electrical conductivity and is optically transparent. Initial tests with an uncoated YAG crystal irradiated by low energy electrons showed damage, which look like fine scratches shown in Fig. 2.

To provide a better control of the electron beam and to avoid collisions between the Faraday cup and the view screen (which happened in the first version of the beamline with a YAG screen installed perpendicular to the Faraday cup), the YAG:Ce was incorporated into the Faraday cup (Fig. 3). In this design the free standing view screen with a diameter of 32 mm and a thickness of 100 μm was mounted at a 45 degree angle with respect to the incoming

* roman.barday@helmholtz-berlin.de

ISBN 978-3-95450-119-9

REAL-TIME BEAM PROFILE MEASUREMNT SYSTEM USING FLUORESCENT SCREENS

Takahiro Yuyama, Yosuke Yuri, Tomohisa Ishizaka, Ikuo Ishibori, and Susumu Okumura
Takasaki Advanced Radiation Research Institute, Japan Atomic Energy Agency
1233 Watanuki-machi Takasaki, Gunma, Japan, 370-1292

Abstract

An irradiation technique of a large-area uniform ion beam formed by multipole magnets is developed at the TIARA azimuthally-varying-field (AVF) cyclotron facility in Japan Atomic Energy Agency (JAEA). It is indispensable to perform uniform-beam tuning in real time for efficient operation. Therefore, we developed a real-time beam profile measurement system, composed of CCD cameras, fluorescent screens and an image analysis program based on LabVIEW. In order to measure the transverse intensity distribution of the beam through the fluorescence map converted from a camera image, the irradiation response of two fluorescent screens, DRZ-High (Gd_2O_2S:Tb) and AF995R (Al_2O_3:Cr), were investigated using several species of ion beams. The available fluence rate of the screens was found in the present system. The relative transverse intensity distribution could be obtained from the fluorescence in real time. It was also confirmed that the intensity distribution measured in this system agreed well with the relative intensity distribution obtained with a Gafchromic radiochromic film.

INTRODUCTION

The JAEA AVF cyclotron with a *K* number of 110 MeV accelerates and provides various species of ion beams at different energies for researches in the fields of biological and materials science, such as plant breeding, production of functional polymers and radiation hardness tests of space-use devices [1]. Various irradiation techniques have been developed for providing useful beams. In recent years, a large-area uniform beam irradiation technique using the nonlinear focusing force of octupole magnets has been developed [2]. In the technique, a Gaussian-like beam, obtained by multiple Coulomb scattering through a thin metallic foil, is transformed into a uniform beam on the target by folding the beam tail the by the nonlinear magnetic field. It is possible to irradiate the whole of a large-area sample uniformly at a constant fluence rate.

It is indispensable to form and evaluate the beam quickly for the efficient utilization of the uniform beam. The real-time measurement system of the beam profile based on the beam fluorescence was, therefore, configured and tested.

Table 1: Main Components of the Real-time Beam Profile Measurement System

Image analysis PC (PXI)	Chassis	PXI-1031	National Instruments Co.
	CPU	PXI-8106	
	Image capture device	PXI-1411	
	Chassis	PXI-1042Q	
	CPU	PXI-8106	
	Image capture device	PXIe-8234	
Fluorescent screen	Al2O3:Cr	AF995R	Desmarquest Co.
	Gd2O2S:Tb	DRZ-high	Mitsubishi chemical Co.
Measurement hardware	Horizontal camera	ICD42VP	Ikegami tsushinki Co.
	Vertical camera	scA1390-17gc	BASLER AG

SYSTEM CONFIGURATION

The real-time beam profile measurement system is composed of CCD cameras and fluorescent screens. The fluorescent data is processed using a computer (PXI, National Instruments) with LabVIEW. Two different types of fluorescent screens, DRZ-High (Gd_2O_2S:Tb, 0.5 mm thick, Mitsubishi chemical) and AF995R (Al_2O_3:Cr, 1 mm thick, Desmarquest) have been chosen. The active layer (310 μm thick) of DRZ-High is put on a 190-μm plastic base. The DRZ-High screen is more sensitive and has lower afterglow as compared with AF995R. The main devices used in the present system and their layout are shown in Table 1 and Fig. 1, respectively.

The fluorescent screen is mounted on the target in a vacuum chamber where the large-area uniform intensity distribution of the beam is formed by octupole magnets. The target size is as large as 20 cm square at the maximum. When the large-area screen is monitored diagonally using a camera, the distortion of the fluorescent image is inevitable. As shown in Fig. 1, the camera A (B), therefore, monitors the screen from the below (from the right side) diagonally for the horizontal

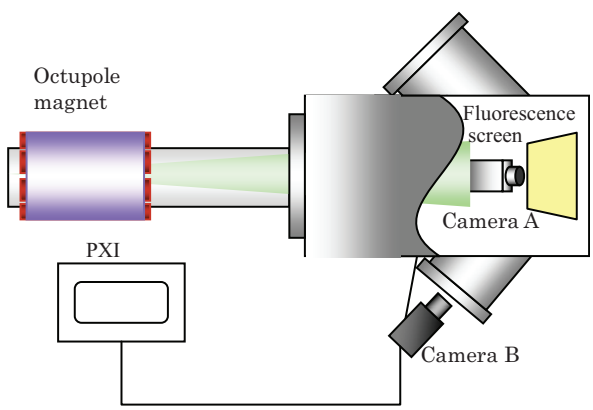

Figure 1: Schematic layout of the main components for the real-time beam profile measurement. The CCD cameras A and B monitor the beam fluorescence vertically and horizontally, respectively.

* E-mail: yuyama.takahiro@jaea.go.jp

ISBN 978-3-95450-119-9

EVALUATION OF A FLUORESCENT SCREEN WITH A CCD SYSTEM FOR QUALITY ASSURANCE IN HEAVY-ION BEAM SCANNING IRRADIATION SYSTEM

Y. Hara#, T. Furukawa, K. Mizushima, S. Sato, T. Inaniwa, T. Shirai and K. Noda,
National Institute of Radiological Sciences, Chiba, JAPAN
E. Takeshita, Gunma University Heavy-Ion Medical Center, Gunma, JAPAN

Abstract

Two-dimensional dosimetry system was developed for quality assurance (QA) of therapeutic scanned ion beams at HIMAC. This system consists of a fluorescent screen and a charge coupled device (CCD) camera. To evaluate the performance of this system, we carried out a few experiments for QA procedures. The verification of this system was also carried out by comparing the film dosimetry. As a result, we confirmed that this system could be used as the system for QA procedures of therapeutic scanned ion beams.

INTRODUCTION

Heavy-ion beams such as carbon-ion beams have attracted growing interest for cancer treatment due to their high dose localization and high biological effect at the Bragg peak. To make the best use of these characteristics and provide flexible dose delivery, three-dimensional (3D) pencil beam scanning [1-3] is an ideal irradiation technique. At the Heavy Ion Medical Accelerator in Chiba (HIMAC), it has been utilized for treatment since 2011 [4]. In a dynamic delivery system using the 3D scanning system, it requires additional quality assurance (QA) procedures to ensure a consistent and safe dose prescription, as compared with broad-beam delivery system. Since the accuracy and quality of the planned dose for the treatment depends on the accurate deposition of individually weighted pencil beams, any change of scanned beams will result in a significant impact on the irradiation dose. Thus, the QA procedures and tool for making refined measurements for the verification of the position and size of pencil beams must be developed. For this purpose, a few types of QA tool have been developed, such as an ionization chamber array and a radiographic film. These systems allow an efficient check of the absorbed dose in the treatment field at many points and perform a direct comparison with the planned dose at these points. However, the spatial resolution of the ionization chamber array is not so high. Although radiographic film is a very useful tool due to its high spatial resolution and suit for the measurement of the integral dose, overall data processing with the system is time consuming. Instead of these systems, we developed a quick verification system using a fluorescent screen with a charge coupled device (CCD) camera, which we called the QA-SCN [5], originally proposed by Boon et al [6, 7].

#y-hara@nirs.go.jp

In this paper, the results of the QA measurements obtained by using the QA-SCN are described. The performance of the QA-SCN is evaluated from the viewpoints of utility as the system for QA procedures of therapeutic scanned ion beams. The verification of the QA-SCN was also carried out by comparing the film dosimetry.

MATERIALS AND METHODS

The technical details of the QA-SCN system, e.g., design of the QA-SCN, the control system and the off-line image processing, was reported previously [5]. A simplified explanation only is given here.

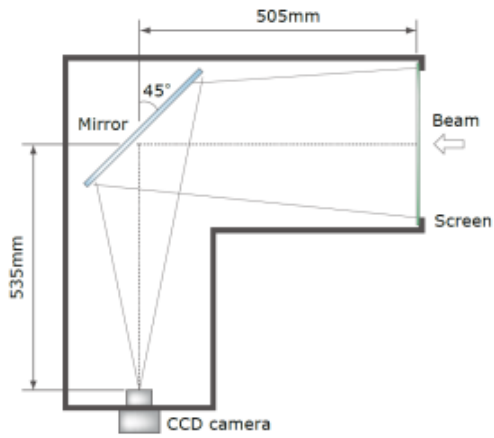

Figure 1: Schematic of the QA-SCN system layout.

The QA-SCN system was used to verify the 2D irradiation field deduced from the relative fluence on the isocenter without the water phantom. Figure 1 shows a schematic layout of the QA-SCN system. The QA-SCN consists of a fluorescent intensifying screen (Type HG-M2, Gd_2O_2S:Tb, Fujifilm Corp., Japan), a CCD camera (Type BU-41L, 1360×1024 pixels, Bitran Corp., Japan), a mirror, camera controllers and a dark box to protect against surrounding light. The CCD camera allows the measurements of 2D light output with a large dynamic range and low thermal noise, due to a decrease of the operating temperature of the CCD by a cooling unit. The QA-SCN is set at the isocenter. The distribution of fluorescent light is reflected by the mirror, located at 45 degrees relative to beam axis, and is observed by the CCD camera, which was installed at 90 degrees relative to the beam axis to reduce the background from the radiation. The distance between the fluorescent screen

ISBN 978-3-95450-119-9

ADJUSTABLE OPTICS FOR A NON-DESTRUCTIVE BEAM PROFILE MONITOR BASED ON SCINTILLATION OF RESIDUAL GAS

V. Kamerdzhiev, A. Pernizki, K. Reimers#, FZ-Jülich, Germany

Abstract

The scintillation profile monitor (SPM) is being developed at COSY in addition to the existing ionisation profile monitor (IPM). Contrary to the IPM it does not require in-vacuum components, making it a robust and inexpensive instrument. The SPM is suitable for high intensity operation rather than operation with low intensity polarised beams. A multichannel PMT is used to detect scintillation light. The rate of detectable scintillation events is about three orders of magnitude lower compared to the rate of ionisation events. To boost the photon yield, small amounts of nitrogen are injected into the SPM vacuum chamber. An adjustable light focusing system is being built to optimise the SPM performance for different machine operation modes. The new system allows using a variety of optical components ranging from single lenses to high-grade camera objectives. Cylindrical lenses are considered to further boost the sensitivity by better fitting the beam image to the detector geometry. The latest experimental results and the new design of the optical system are presented.

INTRODUCTION

The cooler synchrotron COSY is equipped with a low energy electron cooler and a stochastic cooling system. While the electron cooler is typically used at injection energy stochastic cooling is operated at higher energies. A 2 MeV electron cooler built by BINP is expected to be installed in a few months. The new cooler will allow electron cooling in the entire energy range of COSY [1].

Non-destructive beam diagnostics, in particular profile monitors are essential for the operation of circular accelerators with beam cooling. At COSY two profile monitors are installed. The ionisation profile monitor (IPM) relies on the beam particles ionising residual gas. The IPM is routinely used and delivers beam profiles with high sensitivity down to $1{\cdot}10^{8}$ protons in the ring at typical vacuum pressure of $1{\cdot}10^{-9}$ mbar [1]. It provides beam profiles in both transverse planes. The IPM became a very valuable tool for setting up beam cooling. However, high cost and components prone to aging triggered a search for alternatives.

The scintillation profile monitor (SPM) detects light emitted by the residual gas atoms and molecules after their excitation by the beam particles. This method is typically used in beamlines [3, 4]. The SPM is a robust and inexpensive instrument aimed at operation at high beam intensities. At COSY the much lower event rate compared to the IPM is coped with by creating a local pressure bump. Nitrogen [5, 6, 7] is injected directly into the SPM vacuum chamber using a commercially available piezo-electric dosing valve. The vacuum chamber is blackened inside to avoid light reflections. It is equipped with two DN100 viewports for light extraction and two DN40 ports for vacuum monitoring and gas injection. A 32-channel photomultiplier (PMT) is used to detect scintillation light.

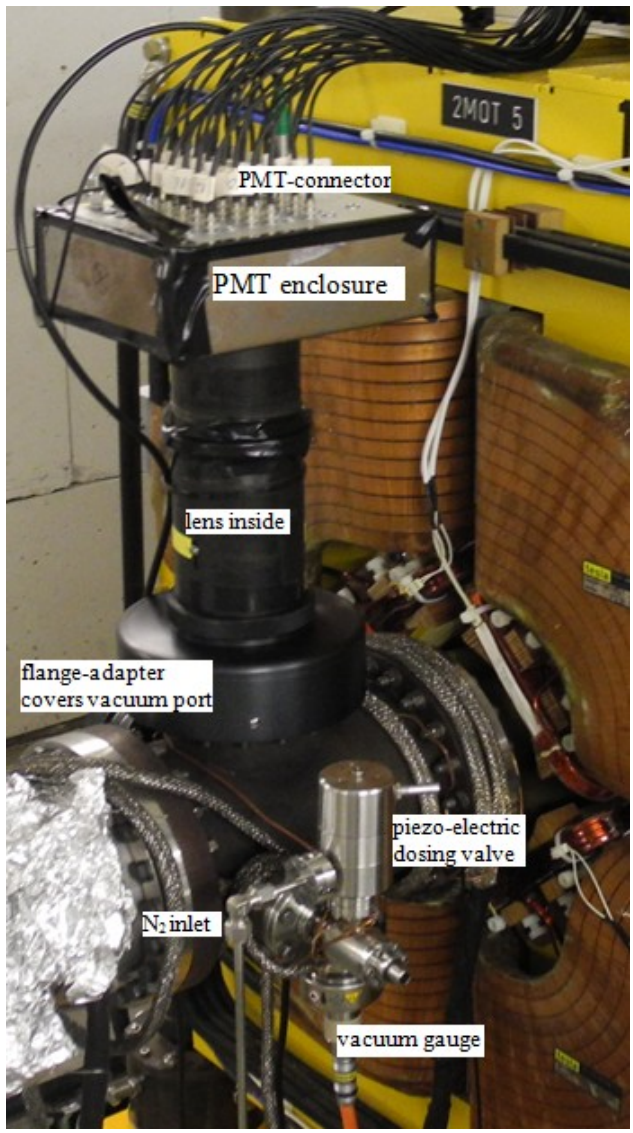

Figure 1: SPM installation in COSY. Shown is the vacuum chamber with the horizontal vacuum port for light extraction and the vacuum ports for N_2 injection and vacuum measurement.

A housing made of steel seals the electric connections and the backside of the PMT against incoming light and electromagnetic fields. All elements of the lens tube are blackened inside to reduce light reflection. The joints are sealed by tape to avoid light from outside of the chamber.

#k.reimers@fz-juelich.de

ISBN 978-3-95450-119-9

BEAM SPOT MEASUREMENT USING A PHOSPHOR SCREEN FOR CARBON-ION THERAPY AT NIRS

K. Mizushima#, E. Takeshita, T. Furukawa, T. Shirai, K. Katagiri, Y. Hara, K. Noda,
National Institute of Radiological Sciences, Chiba, Japan

Abstract

A two-dimensional beam imaging system with a terbium-doped gadolinium oxysulfide (Gd2O2S:Tb) phosphor screen and high-speed charge coupled device (CCD) camera has been used to measure the beam spot for scanned carbon-ion therapy. The system can take the image of the beam spot with the frequency of 50 Hz. Using this system, the time stability of the unscanned-beam spot size and position was verified in the isocenter. This system was also used to check a beam alignment by observing a shadow, which appears on the beam spot image, of the steel sphere located on the reference axis.

INTRODUCTION

In charged particle cancer therapy with pencil beam scanning, the time stability of the beam position and size is important factor to provide the prescribed dose distribution. The large fluctuations of them are capable of increasing damage to normal tissues in the vicinity of the tumor and producing a hot or cold dose region in the target volume. To verify their stability at the isocenter in the treatment room, National Institute of Radiological Sciences (NIRS) [1] in Japan developed a two-dimensional (2D) beam imaging system.

NIRS has performed the three-dimensional scanning irradiation with a carbon-ion pencil beam [2] since May 2011. The carbon-ion beam is provided from the Heavy Ion Medical Accelerator in Chiba (HIMAC) synchrotron using the RF-knockout slow extraction method [3]. The beam energy is changed from 430 MeV/u to 140 MeV/u stepwise by the multiple-energy synchrotron operation [4], and small changes of the beam range are controlled by inserting the PMMA plates with various thicknesses. In the HIMAC synchrotron, the flattop is extended in order to extract the beam for a long time. The beam size variation due to emittance growth, therefore, should be cared during a long extraction period. The beam position drift is also cared although the beam position is controlled with the feedback system integrated into the control system of the scanning magnet power supply.

The 2D beam imaging system developed at NIRS can obtain the 2D beam profiles with the frequency of 50 Hz and observe the stability of the beam position and size at the isocenter in the treatment room. This system consists of a phosphor screen and high-speed charge coupled device (CCD) camera. This system construction is identical to that of the beam monitor system installed in the high-energy beam transport line at HIMAC [5]. The 2D beam imaging system also functions as a beam alignment adjustment system by setting a steel sphere on the reference axis. The beam alignment can be checked by observing a shadow of the steel sphere on the beam spot image.

Using the 2D beam imaging system, the fluctuations of the unscanned-beam spot position and size were observed in the isocenter to verify the time stability of the delivered beam for scanning irradiation. On the other hand, the misalignment of the beam has been routinely checked for quality assurance. In this paper, we describe the 2D beam imaging system and the measurement results using it.

2D BEAM IMAGING SYSTEM

System Configuration

A schematic drawing of the 2D beam imaging system is shown in Fig. 1. A terbium-doped gadolinium oxysulfide (Gd2O2S:Tb) phosphor screen is mounted at an entrance surface of the beam inside the dark box. The light radiated from the phosphor screen is carried to the high-speed 8-bit CCD camera (Type XG-H035M, KEYENCE, Japan), for protecting the camera from the radiation damage, via a mirror placed at a 45 degree to the beam direction. The typical observed image of the beam spot is shown in Fig. 2. The spatial resolution in this system is about 0.2 mm/pixels.

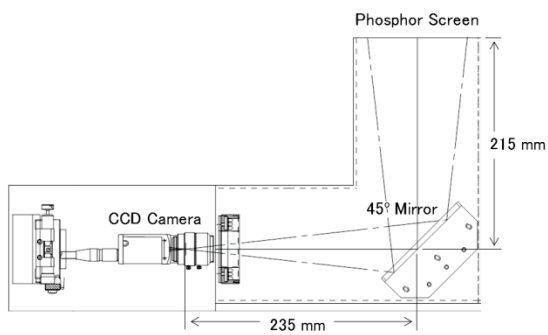

Figure 1: Schematic drawing of the 2D beam imaging system.

Figure 2: Typical image of the beam spot measured by the 2D beam imaging system.

#mizshima@nirs.go.jp

ISBN 978-3-95450-119-9

DESIGN OF A HIGH-PRECISION FAST WIRE SCANNER FOR THE SPS AT CERN

R. Veness, N. Chritin, B. Dehning, J. Emery, J. Herranz Alvarez, M. Koujili, S. Samuelsson, J.L. Sirvent, CERN, Geneva, Switzerland

Abstract

Studies are going on of a new wire scanner concept. All moving parts are inside the beam vacuum and it is specified for use in all the machines across the CERN accelerator complex. Key components have been developed and tested. Work is now focussing on the installation of a prototype for test in the Super Proton Synchrotron (SPS) accelerator.

This article presents the specification of the device and constraints on the design for integration in the different accelerators at CERN. The design issues of the mechanical components are discussed and optimisation work shown. Finally, the prototype design, integrating the several components into the vacuum tank is presented.

INTRODUCTION

Wire scanners are installed in the LHC and all circular machines in the injector chain as a means to measure the transverse beam profile and hence emittance. The motivation for the development of a new scanner design has been described in a previous article [1], along with the concept with the rotor of the motor and wire position measurement system inside the beam vacuum [see Figure 1]. Development of key components, in particular the motor and control system, are well advanced [2]. Work is now focussing on the integration of all the required components with the aim of producing a scanner capable of 20 ms^{-1} scanning speed combined with 2 µm position precision.

A number of mechanical components require careful optimisation. These include the motor housing, shaft, bearings, fork and wire. In addition, the design concept includes an in-vacuum optical position encoder in order to reach the required precision. Development of these components is described in the following sections.

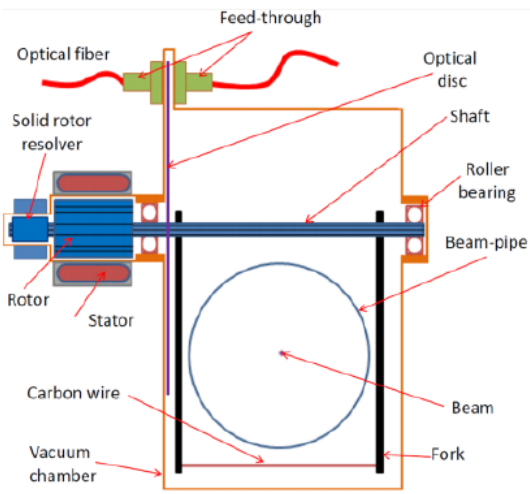

Figure 1: Fast Wire Scanner concept.

INTEGRATION CONSTRAINTS

Wire scanners are currently installed in the PS, Booster, SPS and LHC at CERN. It would greatly simplify operation and maintenance if the same basic design could be implemented for all of these machines. To this end, the main constraints in terms of machine physics, operation and environment have been analysed for each machine. These are summarised in Table 1.

Table 1: Summary of Integration Constraints from the CERN Accelerator Complex

Machine	Scan aperture (mm)	RF Screen	Bakeout	Space Constraint
PS Booster	146x70	N	N	Axial, Transverse
PS	146x70	N	N	Axial
SPS	152x83	Y	N	-
LHC	65x65	Y	Y	Transverse

The scan aperture is the horizontal and vertical space that must be cleared by the wire. RF screens are required in some machines to minimise impedance and RF heating effects. Integration of new scanners into existing machines must take into account machine geometries and equipment. Axial space constraints occur in machines with a tight lattice whereas transverse constraints are seen with parallel equipment on the beamline (eg, the cryogenic distribution line in the LHC). It can be seen from table 1 that each of the machines brings constraints to the design. A solution has been adopted where the main components can be integrated into designs for the PS, SPS and LHC. Each machine will require a different fork geometry and a different flange interface, but other main components and principles will be common. The layout of the Booster with 4 rings in very close proximity mean that it has not yet been possible to integrate the design into this machine.

Combining these constraints leads to a design with aperture range up to 152 by 152, with the option to include RF screen and to be bakeable to 200°C in order to activate a low emission yield getter coating used in the LHC vacuum system.

DESIGN OF COMPONENTS

Motor Housing

The motor housing has the function of separating the rotor in-vacuum and stator on the atmospheric side of the

ISBN 978-3-95450-119-9

HIGH DYNAMIC RANGE BEAM IMAGING WITH TWO SIMULTANEOUSLY SAMPLING CCDS

P. Evtushenko#, D. Douglas, JLab, Newport News, USA

Abstract

Transverse beam profile measurement with sufficiently high dynamic range (HDR) is a key diagnostic to measure the beam halo, understand its sources and evolution. In this contribution we describe our initial experience with the HDR imaging of the electron beam at the JLab FEL. Contrary to HDR measurements made with wire scanners in counting mode, which provide only two or three 1D projections of transverse beam distribution, imaging allows to measure the distribution itself. That is especially important for non-equilibrium beams in the LINACs. The measurements were made by means of simultaneous imaging with two CCD sensors with different exposure time. Two images are combined then numerically in to one HDR image. The system works as an online tool providing HDR images at 4 Hz. An optically polished YAG:Ce crystal with thickness of 100 μm was used for the measurements. When tested with a laser beam, images with a dynamic range (DR) of about 10^5 were obtained. With the electron beam the DR was somewhat smaller due to the limitations in the time structure of the tune-up beam macro pulse.

MOTIVATION

High current CW SRF LINACs with average current of several mA have been used to provide electron beam for high average brightness, high power IR FELs [1]. It is proposed that LINACs with similar average current and beam energy in the range 0.6 – 1.2 GeV can be used as the drivers for next generation of high average brightness light sources operated in X-ray wavelength range in seeded FEL configuration [2-5]. The existing pulsed FELs, operating now in the soft and hard X-ray wavelength ranges, utilize average currents many orders of magnitude less than the above-mentioned mA. At the same time, operation of the IR/UV-Upgrade at Jefferson Lab with average current of up to 9 mA has provided an experience base with high-current LINAC operation [1]. The primary operational difference between such high current LINACs and storage rings, even with a few hundred mA of average current, is that LINAC beams have neither the time nor the mechanism to come to equilibrium, in contrast to storage ring beams, which are essentially Gaussian. This has significant operational impact. When a LINAC is setup, by establishing the longitudinal and transverse match, a tune-up beam with small average current is used. Such an accelerator setup is based most frequently on measured mean and RMS parameters such as beam size, bunch length, and energy spread. When going from tune-up mode to higher duty cycle and CW operation, it is frequently found that the "best" RMS-data-based setup must be changed to allow for high current operation to eliminate beam losses. Even when this modification is successful, it is time-consuming process involving some trial and error. It is frequently unclear what the sources of the problem are, and which adjustments to the low-density parts of the phase space distribution were effective in improving performance. This is highly undesirable for any user facility where high availability is required. Also of significance is that the resulting setup does not necessarily provide the best beam brightness and is a compromise between acceptable brightness and acceptably low beam losses.

Contributing to this problem is the fact that the measurements used for machine setup are typically based on methods with a DR of 10^3 or even less. It is not surprising that the relevant (from the high current operation and beam loss point of view) low-intensity and large-amplitude parts of the phase space are simply not visible during machine tuning.

Therefore, we think that the proper solution to the aforementioned tune-up problem is to base the tuning on the measurements with much larger, than routinely used now, DR, such that the very low intensity and large amplitude parts of phase space distribution are taken in to account from the very beginning. We are presently developing such diagnostics at the JLab FEL. The ultimate goal is to be able to measure both the transverse and longitudinal phase space with a DR of about 10^6. Measurements of both phase spaces can be based on the HDR transverse beam profile measurements, which is the first step in our program. One of the techniques we are developing is the HDR beam imaging. Here we present our technique and first results of transverse beam profile measurements with extended DR and its application to emittance and Twiss parameters measurements.

EXPERIMENTAL SETUP

Operation of the JLab FEL relies very heavily on the transverse beam profile measurements made in many places around the machine. Even with a relatively compact footprint the IR and UV recirculators beamlines have 62 viewers and synchrotron light monitors in total. This has allowed us to accumulate a lot of experimental experience with transverse beam profile measurements. From this experience we know the intensity of the beam image on the CCD matrix from OTR or YAG:Ce viewer with the typical beam size and with the amount of beam charge in the tune-up macro pulse. It also agrees well with calculations. Thus one can tell that, for the measurements with the OTR and DR of 10^6 an additional gain in the range between 10 and 100 would be needed, and the measurements with YAG:Ce may not need additional

*Work supported by US DOE office of Basic Energy Sciences under the early career program; DOE award number FWP#JLAB-BES11-05
Pavel.Evtushenko@jlab.org

ISBN 978-3-95450-119-9

RESIDUAL GAS IONIZATION PROFILE MONITORS IN J-PARC SLOW-EXTRACTION BEAM LINE

Y. Sato#, K. Agari, E. Hirose, M. Ieiri, Y. Katoh, M. Minakawa, R. Muto, M. Naruki, S. Sawada, Y. Shirakabe, Y. Suzuki, H. Takahashi, M. Takasaki, K. H. Tanaka, A. Toyoda, H. Watanabe, and Y. Yamanoi, KEK/IPNS, Tsukuba, Ibaraki 305-0801, Japan
H. Noumi, RCNP, Osaka, Japan

Abstract

Residual gas ionization profile monitors (RGIPMs) for slowly extracted proton beams at Japan Proton Accelerator Facility Complex (J-PARC) have been developed to monitor transverse profiles of intense proton beams up to 50 GeV-15 μA. To minimize beam loss and residual dose on the beam line devices, the RGIPMs working around 1 Pa vacuum pressure have been developed. The present manuscript reports the working principles, fabrications, installations, and operations of the RGIPMs in detail.

INTRODUCTION

Hadron Experimental Facility at J-PARC is a multi-purpose facility for particle and nuclear physics, using intense secondary beams [1]. Primary proton beams accelerated up to 30 GeV in the Main Ring are continuously extracted for 2 seconds in every 6 seconds, and transported to Hadron Experimental Facility through the slow-extraction beam line. The maximum beam power is designated to be 50 GeV-15 μA (750 kW in total power). Since the beam loss on the transport beam line must be minimized to keep residual activation of beam line devices as low as possible, non-interceptive type of beam monitor is desirable.

Residual gas ionization profile monitors (RGIPMs) are widely used in many accelerator rings [2][3]. Electrons or ions produced by proton beams passing through residual gas, whose pressure is normally 10^{-6} Pa or less, are guided to a micro-channel plate (MCP) with electrostatic and /or magnetic fields applied between gap electrodes. The signals amplified in a MCP by typically a factor of 10^4 are observed as transverse profile distributions. The conventional RGIPM with MCPs is an acceptable choice, but they have some issues as follows;

1. More than ten monitors required in a transport beam line enhance purchasing cost due to MCPs.
2. MCPs do not have sufficient hardness against severe radiation around the production target.

The present RGIPMs have been developed to overcome above issues [4]. Since the vacuum pressure in the slow-extraction beam line is about 1 Pa, the signal is sufficiently large enough without MCP. The amount of charge measured by the RGIPM can be estimated as follows,

$$Q = N_p \frac{dE}{dx} \rho_{air} \frac{P_{air}}{P_{stp}} \frac{1.602\times10^{-19}}{N_I} L, \qquad (1)$$

where Q is measured charge in coulomb per unit length, dE/dx is an energy loss per unit length when 30 GeV protons are passing through air, N_p is a number of protons, ρ_{air} is density of residual gas, P_{air} is pressure of residual gas in a beam pipe, P_{stp} is a standard temperature pressure, N_I is mean energy to produce an electron-ion pair in normal air, L is length of electrode in beam direction. When N_p is 10^{13}, dE/dx is 2 MeV/(g/cm^2), ρ_{air} is 1.2×10^{-3} g/cm^3, P_{air} is 1 Pa, N_I is 38 eV/pair, and L is 8 cm, the equation (1) gives 8 nC, that is sufficient amount for charge integration circuits without amplification.

Operation of RGIPM in 1 Pa pressure arises a different issue. The mean free path of the electrons drifting in 1 Pa pressure (λ_e) is estimated to be about 30 mm, assuming that typical elastic cross section of electrons on nitrogen and oxygen molecules is 10^{-15} cm^2 [5]. Since typical gap length between electrodes in the present RGIPMs is 10 cm or more, observed profile distributions would become considerably broader than the actual size of beam when electrons are guided with a uniform electric field between the electrodes.

To reduce broadening due to diffusion, a uniform magnetic field can be applied parallel to the electric field in the present RGIPMs. Motion of the electrons drifting in a uniform magnetic field is limited in a Larmor radius (r_e). According to a standard transportation theory [6] under a magnetic field, the diffusion coefficient of drifting electrons with an electrostatic field (D) is given by,

$$D = \frac{\lambda_e^2}{2\tau}, \qquad (2)$$

where τ is mean collision time, dependent on mean velocity of electrons. When a magnetic field is applied parallel to the electric field, the diffusion coefficient of electrons across a magnetic field ($D_\perp$) is given by,

$$D_\perp = \frac{r_e^2}{2\tau}, \qquad (3)$$

When the applied magnetic field is set to be 420 gauss and the Larmor radius of electron is 0.25 mm, the diffusion coefficient given by the equation (3) is reduced by factor of $(\lambda_e/r_e)^2 = (30/0.25)^2 = 14400$. A naive evaluation of broadning due to diffusion of electrons with a kinematic energy T_e is estimated as follows,

#yoshinori.sato@kek.jp

ISBN 978-3-95450-119-9

BUNCH-COMPRESSOR TRANSVERSE PROFILE MONITORS OF THE SwissFEL INJECTOR TEST FACILITY

Gian Luca Orlandi*, Masamitsu Aiba, Simona Bettoni, Bolko Beutner, Helge Brands, Rasmus Ischebeck, Eduard Prat, Peter Peier, Thomas Schietinger, Volker Schlott, Vincent Thominet
Paul Scherrer Institut, 5232 Villigen PSI, Switzerland
Christopher Gerth, DESY Hamburg, Germany

Abstract

The 250 MeV SwissFEL Injector Test Facility (SITF) is the test bed of the future 5.8 GeV SwissFEL linac that will drive a coherent FEL light source in the wavelength range 7-0.7 and 0.7-0.1 nm. Aim of the SITF is to demonstrate the technical feasibility of producing and measuring 10 or 200 pC electron bunches with normalized emittance down to 0.25 mm.mrad. A further goal is to demonstrate that the electron beam quality is preserved in the acceleration process, in the X-Band linearizer and the magnetic compression from about 10 ps down to 200 fs. The SITF movable magnetic bunch-compressor is equipped with several CCD/CMOS cameras for monitoring the beam transverse profile and determining the beam energy spread: a YAG:Ce screen and an OTR screen camera at the mid-point of the bunch compressor and a SR camera imaging in the visible the Synchrotron Radiation emitted by the electron beam crossing the third dipole. Results on the commissioning of such instrumentations, in particular in the low charge limit, and measurements of the beam energy spread vs. the compression factor will be presented.

INTRODUCTION

The SwissFEL project aims at the construction of a 5.8 GeV electron linac driving a coherent FEL light source in the wavelength regions 7-0.7 and 0.7-0.1 nm. The relative compact size of the facility (the SwissFEL total length is about 700 m, linac+undulators+experimental area) being a constraint for the linac energy performance, high brilliance features are imposed to the electron source by the lasing condition. Projected emittance 0.65/0.25 mm.mrad and longitudinal length of 25/2 fs (RMS) at the undulator are indeed the design parameters of the 200/10 pC electron bunches of the SwissFEL [1]. In the two different charge operation modes of the SwissFEL, sequences of two electron bunches separated in time by 28 ns will be produced at a repetition rate of 100 Hz by a photocathode gun and accelerated by S-band Travelling Wave (TW) accelerating structures (injector section) up to 330 MeV and, finally, by a C-band TW linac up to the final energy of 5.8 GeV. Thanks to a magnetic switchyard and a further accelerating section (up to 3.4 GeV), two different undulator lines will be simultaneously electron-supplied at 100 Hz: the hard X-ray undulator line (ARAMIS) and the soft X-ray undulator line (ATHOS). The electron beam, produced at the cathode of the RF gun by a Ti:Sa laser with a flat-top longitudinal profile (3.6/10 ps FWHM), will reach the undulator after a two-stage longitudinal compression by means of two magnetic chicanes. The magnetic compression scheme foresees an energy chirping of the electron beam, achieved in the S-band injector, and a longitudinal phase space linearization performed by a couple of X-band cavities upstream the first magnetic chicane.

The preparatory phase of the future SwissFEL is carried out at the 250 MeV SwissFEL Injector Test Facility (SITF). This is composed of, see Fig. 1: a Copper photo-cathode and a Standing-Wave (SW) S-band 2.5-cell RF gun accelerating a 10/200 pC electron bunch up to 7.1 MeV/c at a repetition rate of 10 Hz; four S-band TW RF structures accelerating the beam up to a maximum final energy of 250 MeV; a compression section composed of a X-band cavity (under installation) and a magnetic chicane; finally, downstream a SW S-band 5-cell Transverse Deflecting Cavity (TDC), a FODO section and an energy spectrometer where both the transverse and the longitudinal phase spaces of the electron beam are experimentally characterized. Goal of the experimental activity so far performed at the SITF is to check the reliability of the key components of the future accelerating machine, to optimize the procedures to experimentally characterize the electron beam parameters, to demonstrate the feasibility of an electron source with the required high brilliance quality and, finally, to show that the high quality features of the electron beam are preserved by the X-band linearizing scheme of magnetic compression. The campaign of measurements carried out so far at SITF established and consolidated several measurement techniques of the beam projected and slice emittance measurements for both the charge operation modes and of the longitudinal phase space, for instance. The outcome of this experimental work [2, 3] confirmed that the extremely high beam quality constraints required by the SwissFEL design can be achieved. The bunch compressor is one of the key components of the future SwissFEL whose main diagnostics have been recently commissioned or is under commissioning as in the following described.

BUNCH-COMPRESSOR DIAGNOSTICS

The vacuum chamber of the magnetic bunch compressor (BC) is a flexible structure composed of two arms and a central part whose rigid components are joined together

* gianluca.orlandi@psi.ch

ISBN 978-3-95450-119-9

TURN-BY-TURN OBSERVATION OF THE INJECTED BEAM PROFILE AT THE AUSTRALIAN SYNCHROTRON STORAGE RING

M.J. Boland, Australian Synchrotron, Clayton, Victoria 3168, Australia
T. Mitsuhashi, KEK, Ibaraki, Japan
K.P. Wootton, The University of Melbourne, Victoria 3010, Australia

Abstract

A fast gated intensified CCD (ICCD) camera was used to observe the beam profile turn-by-turn in the visible light region. Using the visible light from the optical diagnostic beamline on the storage ring at the Australian Synchrotron an optical telescope was constructed to focus an image on the ICCD. The event driven timing system was then used to synchronise the camera with the injected beam. To overcome the problem of dynamic range between the amount of charge in an injected bunch and the stored beam, the beam was dumped by slowly phase flipping the RF by 180 degrees between each one 1 Hz injection cycle. The injection process was verified to be stable enough so that measurements of the different turns could be captured on successive injections and did not need to be captured in single shot. The beam was seen to come in relatively cleanly in a tight beam but would then rapidly decohere due to the strong non-linear fields needed to run the storage ring at high chromaticity. It would take thousands of turns for the beam to damp down again and recohere into a tight beam spot again. This measurement technique will be used to tune the storage ring injection process.

MOTIVATION

Observation of the beam profile can give extra information that is not available using other position diagnostics which are only sensitive to the centroid of the beam, such as BPMs, DCCT or striplines. Turn-by-turn beam profiles of the beam in the Australian synchrotron storage ring can be captured using the visible light Optical Diagnostic Beamline which is equipped with an ICCD [1].

In May of 2012, the Australian Synchrotron changed its user beam mode from decay mode to top-up injection. Since the x-ray beamline shutter are open when the top-up beam is injected into the storage ring it has become more important to optimise the injection process. Two areas that can be improved in the system are the injection kicker bump and the sextupole settings. By observing the beam profile and motion during injection it is planned to improve the injection efficiency and the beam stability during injection.

Turn-by-turn measurements of the transverse beam position can be made using electron BPMs [2], however these measure only the bunch centroid. Using a synchrotron light monitor, the transverse electron beam distribution can be measured. Employing the ICCD camera, we are able to gate acquisition fast enough to measure single bunches on single turns. Hence, events on a highly reproducible cycle – like injection – can be accurately measured.

Of particular interest is both closing the injection bump [3], as well as minimising the effect of sextupoles within the injection bump [4].

EXPERIMENTAL SETUP

The optical diagnostic beamline (ODB) of the Australian Synchrotron [5, 6] was used to image the visible light from the injected electron beam. To accommodate this imaging apparatus, the lens in the optical chicane [5] was removed. Instead, the principal focusing optic was positioned on the optical table, as described elsewhere in these proceedings [7]. We form a real image of the electron beam photon source at the ICCD camera.

The imaging system of the ICCD camera [1] can be triggered down to a shutter gate of 200 ps, sufficient to capture a single bunch of 23 ps which are spaced by 2 ns in the storage ring. Acquisition using the ICCD was triggered using the programmable accelerator timing system [8] Event Receivers which are synchronised to the accelerator RF system. The event-driven timing system was used to synchronise the camera with the injected beam and change the delay to monitor a different bunch or a different turn on a 1 Hz cycle. The reproducibility of the data was checked from one injection to the next to confirm that data taken on different turns during different injection events can be combined in a single data set.

The storage ring can be injected to a maximum of 200 mA with an injection rate of $\approx$ 1 mA per shot at a 1 Hz injection rate. To overcome the problem of sufficient dynamic range of the ICCD to observe both the an injected bunch and the stored beam, the stored beam was dumped by slowly phase flipping the storage ring RF phase by 180 degrees at the end of each 1 Hz injection cycle. In this way the storage ring was empty of charge during each injection and the ICCD could be set to maximum sensitivity to observe the low current injection shot. In order to record the sequence of images of the beam each turn, the gated ICCD camera was triggered by delay times equal to a multiple of the revolution period. The timing system can be set in unit of clock cycles which simplifies this process. The Event Receivers have a clock frequency of $\approx$125 MHz, so 90 clock cycles equals one revolution cycle of $\approx$1.38 MHz.

ISBN 978-3-95450-119-9

LATEST RESULTS FROM THE 4.8 GHz LHC SCHOTTKY SYSTEMS

M. Favier, O. R. Jones, CERN, Geneva, Switzerland

Abstract

This paper will present the latest results from the LHC 4.8GHz travelling wave schottky system, summarising measurements performed with both lead ions and protons during the 2011 and 2012 LHC runs. It will also describe attempts to improve the system architecture in order to make it more immune to the strong coherent lines observed with proton bunches even at these very high frequencies.

INTRODUCTION

Since 2010, the transverse LHC schottky systems have been undergoing commissioning. These sensitive detectors, designed by FNAL and installed in the LHC, are based on a slotted wave-guide structure resonating at 4.8GHz. They allow for a non-invasive observation of the tune, chromaticity, momentum spread and emittance [1, 2]. The theoretical performance of the system and its first results with proton beams has been described in previous publications [3, 4]. This article will present the measurements performed with lead ions during the 2011 LHC heavy ion run and make a comparison to protons measurements taken in 2012. It will also discuss methods of optimising the hardware in order to reduce the effects of the strong coherent lines still observed with protons bunches even at this high frequency.

SCHOTTKY SPECTRA WITH PROTONS AND LEAD IONS

The 2011 LHC heavy ion run gave the opportunity to compare the performance of these schottky devices when operating with lead ions and protons. These measurements were performed throughout the LHC cycle from injection, up the energy ramp, into collision and throughout the stable beams period (i.e. during physics data taking). As described in [3] an RF gate is used to allow acquisition of single bunches while maintaining a good signal to noise level. In these measurements the gate was typically set to 50ns to make sure that all the signal from a single bunch was captured with the current 50ns spacing used for protons physics. Figures 1 and 2 show the typical evolution of the schottky signals along the LHC cycle for ions and protons respectively. It can be seen that with ions the transverse schottky sidebands are clearly visible in the spectra at injection, up the ramp and during the entire stable beams period. This allows for a continual measurement of both tune and chromaticity throughout the entire fill. For protons, however, the transverse schottky sidebands disappear during the ramp and only re-appear several tens of minutes into the stable beams period. The reason for this is linked to the controlled longitudinal blow-up performed on the beam during the ramp to maintain a constant bunch length. It is then thought that the bunches continue to oscillate longitudinally for quite some time after this longitudinal blow-up is switched off at top energy, before quietening down when the transverse sidebands once again appear.

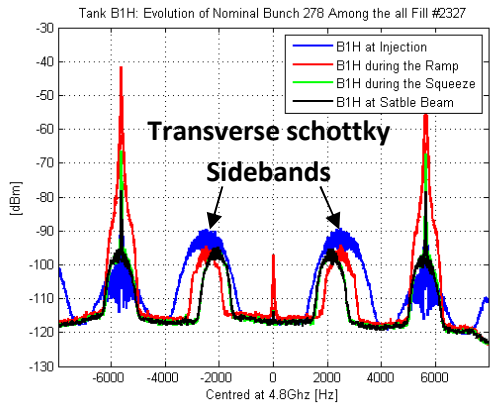

Figure 1: Evolution of the schottky signal for a nominal Pb^{82+} bunch ($9x10^9$ charges) along fill #2327.

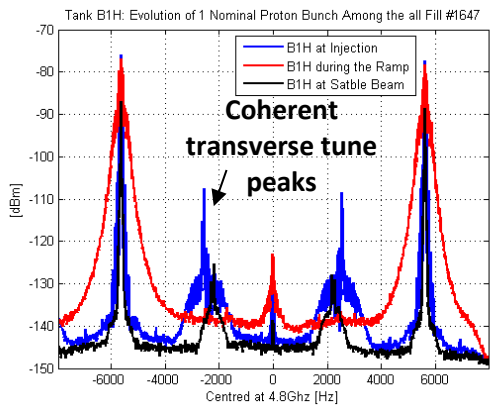

Figure 2: Evolution of the schottky signal for nominal proton bunch ($1.2x10^{11}$ charges) along fill #1647. In red the schottky spectra during the ramp during which the transverse schottky sidebands are no longer visible.

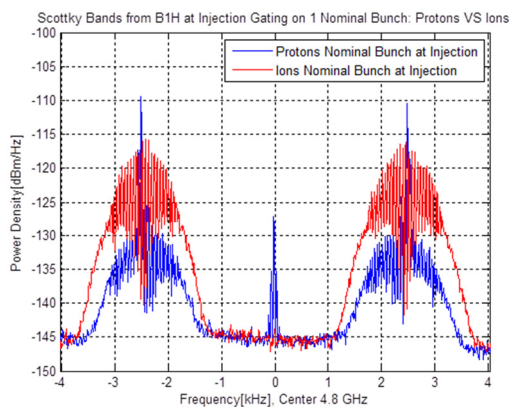

Figure 3: Schottky signal comparison at injection between a nominal ion bunch (red) and a nominal proton bunch (blue).

ISBN 978-3-95450-119-9

BETATRON TUNE MEASUREMENT AND AUTOMATIC CORRECTION SYSTEMS AT NEWSUBARU STORAGE RING

S. Hashimoto#, Y. Hamada, S. Miyamoto, NewSUBARU, Hyogo, Japan

Abstract

At the NewSUBARU electron storage ring, two different kinds of systems for betatron tunes have been developed: a high-precision tune monitor and a real-time measurement and automatic correction system. The high-precision tune monitor has the resolution of 0.0002 and uses frequency analysis methods such as SRSA, zoom FFT, in addition to usual FFT. Fluctuations of tune due to a slight difference of filling pattern in the top-up operation and tune shifts due to the decrease of stored current in the decay operation can be observed with this monitor. The tune monitoring and automatic-correcting system has been developed to compensate tune shifts during the energy ramp from 1.0 to 1.5 GeV. This system can measure and correct betatron tunes every 0.5 sec to keep tunes to the optimal values. The system also has a tune survey function that can automatically measure the beam lifetime in a tune diagram to find the optimal operating point experimentally.

INTRODUCTION

The NewSUBARU synchrotron radiation facility [1,2] of University of Hyogo [3] is located in the SPring-8 site and has a 1.5 GeV electron storage ring. Synchrotron radiation in the soft X-ray regime is applied to industrial purposes such as EUV Lithography, LIGA, the development of new materials, and the generation of gamma ray by Compton scattering. Electron beams are injected from 1.0 GeV Linac of SPring-8. The ring operates in the top-up mode at 1.0 GeV and the decay mode at 1.5 GeV. The main parameters of the ring are shown in Table 1.

Table 1: Main Parameters of the NewSUBARU Ring

Beam energy	1.0 – 1.5 GeV
Circumference	118.7 m
RF frequency	499.955 MHz
Stored Current	500 mA (max.)
Harmonic Number	198
Synchrotron Frequency	6 kHz
Betatron Tune	6.28 (H) / 2.22 (V)
Operation mode in user time	220 mA Top-up @1.0GeV 350 mA Decay @1.5GeV

One of the problems on machine operation is a betatron tune shift during user time. Tune shifts were observed in the following cases: (1) current dependence in the decay mode operation, (2) dependence on a slight difference of filling pattern in the top-up operation, (3) during energy ramping from 1.0 to 1.5 GeV. In our ring a stripe-line kicker shakes electron beams vertically to enlarge the Touschek lifetime. Thus horizontal and vertical tunes can be usually observed even during user time.

In this paper we introduce two different kinds of systems concerning betatron tunes, the one is for precise measurement and the other is for real-time tune correction.

#hashi@lasti.u-hyogo.ac.jp

BETATRON TUNE MONITOR

To measure betatron tunes with a high resolution we developed a precise tune monitor. Although the update rate is relatively slow, the monitor has the resolution of 0.0002 and can measure a slight change of tune or its fine structure.

Hardware

Signals from four electrodes of a Beam Position Monitor are analyzed using a BPM signal processing circuit (bergoz LRBPM). The output signals representing horizontal and vertical beam positions are digitized by a digital oscilloscope (NI PXI-5102) in a PXI chassis. The digitizer has 15MHz bandwidth and 20MS/s sampling speed. The PXI system was connected to a PC through Ethernet. The digitized waveform data in time domain, whose typical number of samples per channel is 25600, was transferred to the PC. The application software developed by National Instruments (NI) LabVIEW performs frequency analysis from the position data. The PC runs as a virtual machine on a host machine using VMware workstation.

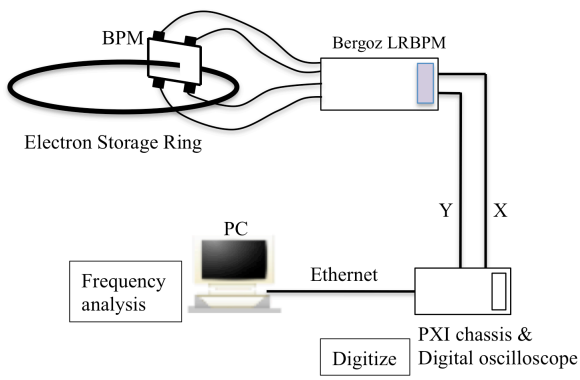

Figure 1: Layout of the precise tune monitor.

Frequency Analysis

The advantage of performing frequency analysis at the PC is that resources of high-performance PC can be used for the frequency analysis requiring a huge amount of

ISBN 978-3-95450-119-9

DEVELOPMENT AND FIRST TESTS OF A HIGH SENSITIVITY CHARGE MONITOR FOR SwissFEL*

S. Artinian, J. Bergoz, F. Stulle, Bergoz Instrumentation, Saint-Genis-Pouilly, France
V. Schlott, P. Pollet, Paul Scherrer Institut, Villigen, Switzerland

Abstract

The compact X-ray free electron laser SwissFEL, which is presently under development at the Paul Scherrer Institut (PSI) in Villigen, Switzerland, will operate at comparably low charges, allowing the compression of the electron bunches to a few femto-seconds (nominal 200 pC mode) and even towards the atto-second range (short bunch 10 pC mode). A high precision charge measurement turns out to be a challenge, especially in the presence of dark currents, which may occur from high gradient RF gun and accelerating structure operation. In response to this challenge, a higher sensitivity charge transformer and new beam charge monitor electronics were developed in collaboration between Bergoz Instrumentation and PSI. The Turbo-ICT captures sub-pC bunch charge thanks to a new magnetic alloy exhibiting very low core loss. Transmission over a carrier using narrow-band cable television technique preserves the signal integrity from the Turbo-ICT to the BCM-RF. Electro-magnetic and RF interferences are strongly attenuated; the dark current signal is suppressed. First beam test results, which have been performed at the SwissFEL Test Injector Facility (STIF), are presented in this contribution.

SwissFEL AND THE SwissFEL TEST INJECTOR FACILITY

SwissFEL is a compact free electron laser user facility presently under design at the Paul Scherrer Institut in Villigen, Switzerland [1, 2]. The project comprises two FEL beam lines, which will be realized in two phases. The three hard X-ray ARAMIS end stations (phase 1) will provide highly brilliant SASE radiation from 1 to 7 Ångström while the soft X-ray ATHOS beam lines (phase 2) will range from 7 to 70 Ångström [3]. SwissFEL will be operated at 100 Hz repetition rate with two bunches per RF pulse at a bunch distance of 28 ns. Bunch distribution towards the two FEL beam lines will be accomplished at electron energies of 2.1 GeV by fast kickers in a switchyard. The nominal operation at low bunch charges between 10 and 200 pC provides excellent transverse emittances and allows the utilization of compact (in-vacuum) undulators providing full hard X-ray photon flux at comparably low electron energies of 5.8 GeV. Full compression of the low charge electron bunches will lead to ultra-short pulses of < 20 fs (rms at 200 pC) and < 2 fs (rms at 10 pC) in the nominal SwissFEL operation modes and even to towards the atto-second range in a specific short bunch mode of operation. A status of the SwissFEL facility and simulations of its accelerator and FEL performance have recently been summarized in [4].

Most of the design aspects for the SwissFEL accelerator sub-systems as well as the experimental verification of the initial electron beam parameters are presently examined at the 250 MeV SwissFEL Test Injector Facility (STIF) (Fig. 1) [5, 6]. An extensive experimental program is dedicated towards the generation and measurement of the low charge, low emittance electron beam. In this context, prototypes of beam instrumentation specifically designed for the low charge operation modes are being designed and tested – such as cavity beam position monitors [7], transverse profile monitors [8], bunch compressor diagnostics [9] as well as the beam charge monitors presented in this paper.

First operational experience at STIF and preliminary results from (mainly longitudinal) sensitivity studies of electron beam parameters [10] indicate that the tightest tolerances for SwissFEL are driven by the peak current stability, which is mainly related to the longitudinal stability of the RF system (mainly in the injector) and the stability of the bunch charge. In this respect, a reliable and high precision bunch charge measurement with an anticipated resolution of 1% at the low charge (10 pC) operation mode, especially in the presence of dark current from the high brightness RF gun and/or the high gradient accelerating structures, turns out to be an important pre-requisite for stable and reproducible SwissFEL user operation. The design of a prototype bunch charge monitor, the so called Turbo-ICT, and the related BCM-RF electronics as well as first test measurements at the STIF are presented in the following.

TURBO-ICT & BCM-RF PRINCIPLE

The Turbo-ICT sensor and the BCM-RF electronics receiver perform bunch charge measurements with low noise and high accuracy. The Turbo-ICT combines an Integrating Current Transformer [11] of a new kind and front-end electronics in one assembly. The original ICT developed for LEP in 1989 was redesigned to measure bunch charges as low as 10 pC with 1% resolution. Several techniques were used to maximize the signal taken from the beam and minimize the noise from various sources: beam dark current, electronics noise, RF and other electromagnetic interferences.

To maximize the amplitude of signal taken from the beam, the ICT integration time is reduced by a factor of 25 compared to the classical ICT making its amplitude 25

* The work was done within a Paul Scherrer Institut / Bergoz Instrumentation collaboration under a June 2010 MoU.

ISBN 978-3-95450-119-9

BEAM SIZE MONITOR FOR TPS

Chien-Kuang Kuan, Tse-Chuan Tseng, I Ching. Sheng, Shen-Yaw Perng, June-Rong Chen
National Synchrotron Radiation Research Center, Hsinchu, Taiwan

Abstract

Third-generation light source TPS under construction in NSRRC has two diagnostic beamlines in the storage ring. Visible SR interferometers and X-ray pinhole cameras are widely used to measure the transverse beam profile in synchrotron light sources. In phase I we shall adopt both methods for application as beam-size monitor. The visible SR interferometer uses a double slit to obtain a one-dimensional interference pattern along the horizontal or vertical axis. A simple X-ray pinhole camera is designed to measure the size, emittance and energy spread of the electron beam. In this paper we present the design and calculation of these two beam-size monitors for TPS.

INSTRODUCTIONS

Taiwan Photon Source (TPS) is under construction at National Synchrotron Radiation Research Center (NSRRC). The electron beam stored in the storage ring of circumference 518 m has energy 3 GeV and current 500 mA. In phase I we shall have two diagnostic beamlines, using radiation from a bending magnet: one is a dedicated diagnostic beamline; the other is constructed together with the bending beamline. The rms beam sizes at these places are theoretically 40 μm in the horizontal plane and 16.5 μm in the vertical plane for 1 % coupling. We adopt two methods to measure the beam size -- a visible SR interferometer and an X-ray pinhole camera.

Both methods of measuring the beam size are simple, cheap and reliable, and can measure the vertical beam size of 16.5 μm. The visible SR interferometer [1,2] has better resolution than the X-ray pinhole camera [3], but is constrained by the maximum opening angle between the slits. The X-ray pinhole camera is an imaging system. There are many effects on the point spread function (PSF) in the imaging system, including diffraction and pinhole dimension. The deconvolution of the PSF determines the smallest image size measurable with the imaging system. We use the X-ray pinhole camera to measure the beam size, emittance and energy spread of the electron beam.

If the coupling is down to 0.1%, the rms beam size is theoretically 5.2 μm in the vertical plane. It is difficult to measure accurately a beam size in this range with these two methods; it is possible, but must be done carefully: there are too many constraints and errors induced by the optical components. In this paper we present the design, calculation and smallest resolution of the beam size for these two beam size monitors for TPS.

VISIBLE SR INTERFEROMETER

Figure 1 shows the layout of the visible SR interferometer. This interferometer is based on an investigation of the spatial coherence of SR. An interferogram in the CCD is shown in fig. 2; fitting the interferogram yields visibility γ from Eq. (1):

$$\text{Visibility } V = \frac{I_{\max} - I_{\min}}{I_{\max} + I_{\min}} = \frac{2\sqrt{I_1 I_2}}{I_1 + I_2}|\gamma| \tag{1}$$

The beam size σ_{beam} comes from the relation [1],

$$\sigma_{beam} = \frac{\lambda \cdot R}{\pi \cdot S} \cdot \sqrt{\frac{1}{2} \cdot \ln\left(\frac{1}{\gamma}\right)} \tag{2}$$

in which λ is the wavelength of the observation, R is the distance from the light source to the double slit, and S is the slit separation.

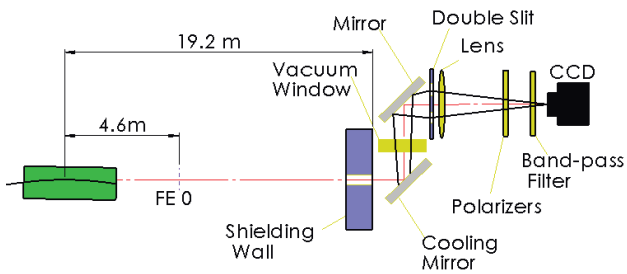

Figure 1: Layout of the visible SR interferometer.

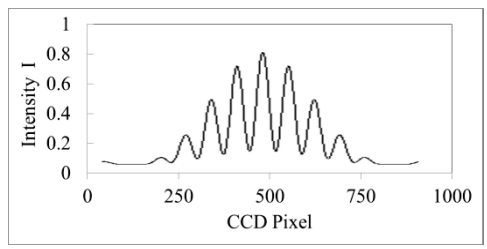

Figure 2: Interferogram in the CCD.

The parameters used are wavelength λ = 500 nm, distance R = 20 m, and maximum possible visibility γ = 0.97. With these values inserted into Eq. (2), the possible resolution of the beam size depends on the slit separation S as shown in fig. 3. Using S = 70 mm and visibility γ = 0.97, the beam size is about 5 μm. The opening angle between the slits, 70/20 = 3.5 mrad, is constrained by the bending chamber; the minimum gap in the bending chamber of the TPS case is 3.8 mrad. The main error of the visible SR interferometer arises from the distortion of the mirror by the radiation power. We use a cooling mirror made of Be to diminish the mirror distortion. With visibility γ=0.97, the background of noise in the CCD

ISBN 978-3-95450-119-9

BEAM INSTRUMENTATION GLOBAL NETWORK [BIGNET]: A COMMON WEB PORTAL FOR BEAM INSTRUMENTALISTS

J-J. Gras, CERN, Geneva, Switzerland

Abstract

This document will present an initiative launched during the International Particle Accelerator Conference (IPAC11) to define and produce a common web portal for Beam Instrumentation, with the aim of allowing any beam instrumentalist to easily and efficiently:

- find the laboratories with machines using beams of similar characteristics (particle type, total beam intensity, bunch intensity, frequency, energy)
- find the person who is working there on the beam observable concerned (i.e. beam position, loss, intensity, transverse or longitudinal profile, tune) and how to contact him/her
- create discussion forums with the right audience on hot beam instrumentation topics or issues
- advertise topical events and workshop
- provide links towards documents describing system designs and performance assessments...

This document will cover the status and prospects of the project with the aim to invite and welcome new laboratories to join the adventure.

INTRODUCTION

On regular occasions over the past years, user requirements have put increasing demands on the CERN accelerator complex beam instrumentation.

These requests are most of the time easy to summarize as “improve the performance” of a given instrument and “quantify precisely the uncertainty of its measurements”.

Implementation on the other hand often turns out to be a difficult and challenging task and it was quickly realized during this process that there was no easy way to share issues, questions and progress with people probably facing similar kinds of problems in other laboratories.

The opportunity of the 2nd International Particle Accelerator Conference (IPAC11) was therefore taken to discuss the subject with beam instrumentation colleagues from other institutes and it was agreed that something useful could be done in this domain. That is how BIGNet (for Beam Instrumentation Global Network) started.

INITIAL OBJECTIVES AND PLANS

The aim of the project was to build ‘something’ that would allow any beam instrumentalist to:

- Easily find the laboratories with accelerators producing beams with similar characteristics (particle type, total beam intensity, bunch intensity, energy…)
- Easily find the experts working at these institutes on the different beam observables (i.e. beam position, loss, intensity, transverse or longitudinal profile, tune…) and how to contact them.
- Launch (or participate in) discussion forums with the right people
- Advertise events such as workshops on specific instrumentation technologies and beam instrumentation related conferences.
- Provide links towards documents describing system designs and performance assessments
- Find job offers in the field...

The obvious solution was to develop a web site providing all the relevant features to host and maintain this data (i.e. accelerator and beam parameters, expert lists…), a calendar and discussion forums.

Each participating laboratory would nominate a local administrator to maintain the information (i.e. machine and beam parameters, instrument and expert lists, local events…) related to their laboratory.

Once this was in place, any beam instrumentation expert could then use the site content and create or participate to discussions

The plan was to develop and assess a prototype of this web site during 2012 in collaboration with some volunteer local administrators in other laboratories and to propose it to a wider audience during IBIC2012. That is where we stand today.

CURRENT STATUS OF BIGNET

The current implementation of the BIGNet web site (see https://espace.cern.ch/info-bi-portal/default.aspx) is based on the SharePoint [1] infrastructure available at CERN. This option was taken for the following reasons:

- The SharePoint infrastructure is extremely flexible and embeds all the functionalities to handle discussions, alerts, access rights etc.
- It allows the export of data into standard formats such as Excel tables, which would make migration to another platform possible if eventually required.
- It is widely used at CERN so an efficient support from the CERN-IT department can be relied upon.

This choice allowed the rapid development of a prototype web site. Its current entry page is shown in Fig. 1. Despite the good flexibility and functionality of this architecture, the look and feel can in some cases remain clumsy. If this is felt to be too penalizing for the final implementation other options could be considered, but as it is this web site already allows assessment of the usefulness of such a tool and permits the type of services and interfaces it should provide to be defined.

The following chapters will give details on the content and functionalities of the main subpages of this site.

ISBN 978-3-95450-119-9

BPM ELECTRODE AND HIGH POWER FEEDTHROUGH – SPECIAL TOPICS IN WIDEBAND FEEDTHROUGH

Makoto Tobiyama#
KEK Accelerator Laboratory, 1-1 Oho, Tsukuba 305-0801, Japan

Abstract

Since most of the beam in accelerator runs in the vacuum chamber consists of metal, it is needed to have 'feedthrough' to get or to put the RF signal from or to beam. For example, we can get the beam signal by using button-type electrode which have electrical isolation material to seal the vacuum. Now, many types of vacuum feedthrough with coaxial structure are available commercially. Nevertheless, it is meaningful to understand the design principle of the feedthrough needed for the beam instrumentation, especially for short bunch length, high beam current machine. I will show the design method of the feedthrough such as BPM electrodes or high power feedthroughs using 3D EM-codes such as HFSS or GdfidL based on several examples developed for SuperKEKB accelerators.

INTRODUCTION

In particle accelerators, so many wideband feedthroughs are used to monitor the electromagnetic signal and to excite or damp the beam. Figure 1 shows examples of the feedthroughs used in KEKB rings. Though it is easy to purchase good feedthroughs commercially in the market, understanding the characteristics of the feedthrough is still very important.

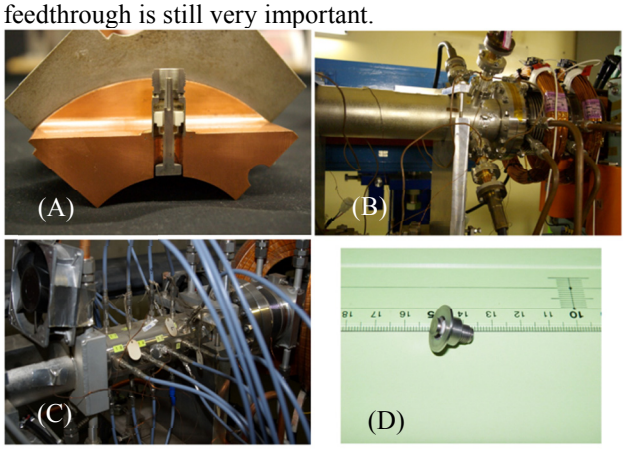

Figure 1: Feedthroughs used in KEKB rings: (A) Cut-model of N-type button electrode for LER. (B) High power feedthrough for the transverse kicker. (C) Bunch position detection chamber for bunch-by-bunch feedback. (D) SMA-type button electrode.

In this tutorial, we at first briefly review the transmission line theory which is needed to understand the specification of the feedthrough. Next, we show the example of the two widely used simulation tools to design the feedthrough: one is the frequency domain method to optimize the S-Parameters, and the other is time domain method to calculate the beam induced signal such as wake filed or the output signal of the electrode. Finally, several examples of the button electrodes and feedthroughs used KEKB and SuperKEKB accelerators are shown.

#makoto.tobiyama@kek.jp

REVIEW OF THE TRANSMISSION THERORY

There are many good textbooks such as reference [1, 2] to introduce the microwave theory and techniques, we here only show several definitions used afterwards.

Frequency Domain View

Figure 2 shows a trans-mission line with characteristic impedance of Z_0 with a termination Z_r and a resulting SWR for wavelength λ.

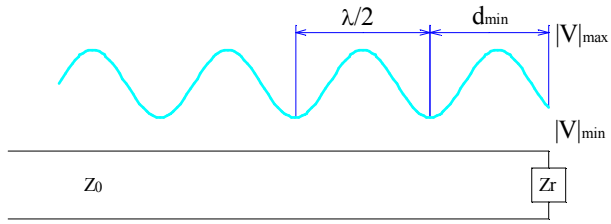

Figure 2: Transmission line with a termination.

The Standing Wave Ratio (SWR) S can be written using V_{max} and V_{min} or reflection constant ρ as

$$S = \frac{|V|_{max}}{|V|_{min}} = \frac{1+|\rho|}{1-|\rho|}$$

and the load impedance can be estimated as

$$z_r = \frac{Z_r}{Z_0} = \frac{1+\rho}{1-\rho} = \frac{1-jS\tan\beta d_{min}}{S-j\tan\beta d_{min}}$$

where $\beta = \omega\sqrt{LC}$ in the case of loss less transmission line.

In a linear two port network shown in Fig. 3, we can define the S-Parameters as follows:

$$\begin{pmatrix} \mathbf{b_1} \\ \mathbf{b_2} \end{pmatrix} = \begin{pmatrix} S_{11} & S_{12} \\ S_{21} & S_{22} \end{pmatrix} \begin{pmatrix} \mathbf{a_1} \\ \mathbf{a_2} \end{pmatrix}.$$

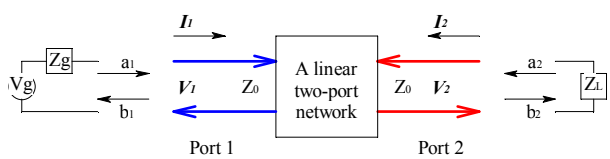

Figure 3: A linter two-port network.

ISBN 978-3-95450-119-9

BIGGER, BRIGHTER AND MORE POWERFUL

H. Schmickler [CERN, Geneva, Switzerland]

Abstract

The community of high energy physics has several proposals for more powerful accelerator projects. This presentation reviews all current projects with center of mass energies above 10 GeV in the field of hadron accelerators, lepton colliders and lepton-hadron colliders. Special emphasis is given on the new needs for beam instrumentation.

CONTRIBUTION NOT RECEIVED

ISBN 978-3-95450-119-9

FEMTOSECOND RESOLUTION BUNCH PROFILE DIAGNOSTICS

B. Schmidt [DESY, Hamburg, Germany]

Abstract

The generation of ultrashort x-ray pulses in the femtosecond (fs) regime in FELs requires electron bunches with lengths significantly below 1 ps with a strong tendency to aim for the 1 fs scale. This greatly challenges the present beam diagnostic methods. In this paper, we will present an overview of the existing and proposed techniques of bunch profile diagnostics including transverse deflecting cavities, electro optic methods, frequency domain techniques as well as more complex approaches like "optical replica synthesizers" (ORS).

CONTRIBUTION NOT RECEIVED

ISBN 978-3-95450-119-9

ELECTRON STORAGE RING AS A SINGLE SHOT LINAC BEAM MONITOR*

Y. Shoji#, K. Takeda, University of Hyogo, Ako 678-1205, Japan
Y. Minagawa, Y. Takemura, S. Suzuki, T. Asaka, JASRI, Sayo 679-5198, Japan

Abstract

The SPring-8 linac has been used as an injector to the electron storage ring, NewSUBARU. There exists a shot-to-shot fluctuation in the injection efficiency during top-up operation. In order to understand the source of the fluctuation, we have developed single shot diagnostics of the injected beam using the visible light beam line of the ring. The techniques utilized the phase rotation of betatron or synchrotron oscillation in the ring. The time-resolving visible light monitor in the ring, a streak camera or ICCD gated camera, records the profiles of the injected linac beam over multiple revolutions. The time profile recorded at the point of injection reveals the bunch structure in the 1 ns macro pulse, which contains three linac bunches. The time profile at after 1/4 of the synchrotron oscillation period gives the energy profile of a pulse. The bunch-by-bunch spatial profiles over consecutive several revolutions after the injection can be used to reconstruct the transverse emittance of each bunch.

INTRODUCTION

The electron storage ring NewSUBARU [1] has used the SPring-8 linac [2] as an injector for top-up operation since 1998. However, fine parameter tuning is required for stable injection because of the small ring acceptance. For that process, single shot linac beam monitors were necessary to measure beam parameters with the injection efficiency. Although the feedback control of steering magnets using BPMs along the transport line [3] improved the stability, the injection efficiency still fluctuates due to the injected linac beam. We have developed single shot diagnostics utilizing the phase rotation in the ring, providing an opportunity to understand fluctuations in the injection efficiency.

We used the time resolving visible light profile monitors of the electron storage ring. The time profile at the instance of the injection, recorded by a streak camera, gives the bunch structure in a pulse. The time profile after 1/4 of the synchrotron oscillation period gives the energy profile. The dual sweep streak camera can also be used to record the spatial profile of several turns. The fast sweep separated linac bunches in a macro pulse and the slow sweep separated profiles from different turn numbers. The betatron oscillation in the ring produced a phase rotation allowing the reconstruction of the beam emittance. Here the beam emittance means not only the area but the ellipse in the transverse phase space.

The stability of the linac beam was evaluated from the shot-to-shot variation. We could also see differences of beam parameters in the bunches of the same macro pulse.

The measurements detailed here required dedicated time at the facility because the stored beam should not exist in the ring. This meant that storage of the injected beam was not necessary. The ring parameters, such as the beta functions, betatron tunes, etc. could be fully optimized for the measurement. This also means that a booster synchrotron of any facility can be used as a monitor if it has a light extraction port.

In addition to the two aforementioned monitors, we will discuss the possibility of using an ICCD gated camera, capable of recording several spatial profiles, allowing analysis of the H/V coupling of the injected beam.

PARAMETERS OF DAILY OPERATION

Averaged Beam Parameters

Figure 1 shows the layout of the SPring-8 linac, the booster synchrotron, and NewSUBARU storage ring. Table 1 shows the main parameters for the linac.

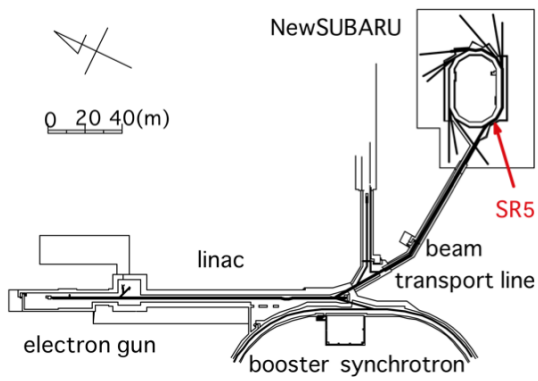

Figure 1: Layout of the 1 GeV SPring-8 linac, the booster synchrotron, and the NewSUBARU storage ring.

Table 1: Main Parameters of the Linac

Electron energy	1 GeV
Rf frequency	2856 MHz
Common pulse rate	1 Hz
Common pulse width	1 ns
FWHM Bunch length; front/middle	10 ps / 14ps
Full energy spread; front / middle	0.4% / 0.6%
Transverse emittance (FWHM^2)	100 π nmrad.

*Work supported by "comprehensive support program for the promotion of accelerator science and technology" by KEK.
shoji@lasti.u-hyogo.ac.jp

ISBN 978-3-95450-119-9

DESIGN AND EXPECTED PERFORMANCE OF THE NEW SLS BEAM SIZE MONITOR*

N. Milas, M. Rohrer, A. Saa Hernandez, V. Schlott, A. Streun , PSI, Villigen, Switzerland
A. Andersson, J. Breunlin, MaxLab, Lund, Sweden

Abstract

The vertical emittance minimization campaign at SLS, realized in the context of the TIARA WP6, has already achieved the world's smallest vertical beam size of 3.6 μm, corresponding to a vertical emittance of 0.9 pm, in a synchrotron light source. The minimum value reached for the vertical emittance is only about five times larger than the quantum limit of 0.2 pm. However, the resolution limit of the present SLS emittance monitor has also been reached during this campaign, thus, to further continue the emittance minimization program the construction of an improved second monitor is necessary. In this paper we present the design and studies on the performance of this new monitor based on the image formation method using vertically polarized synchrotron radiation in the visible and UV spectral ranges. This new monitor includes an additional feature, providing the possibility of performing full interferometric measurement by the use of a set of vertical obstacles that can be driven on the light path. Simulations results are used to investigate the possible sources of errors and their effects on imaging and the determination of the beam height. We also present the expected performance, in terms of emittance accuracy and precision, and discuss possible limitations of this new monitor design.

MOTIVATION

The main objective of the TIARA (Test Infrastructure and Accelerator Research Area) work package 6 [1, 2] is the achievement and control of ultra-low vertical emittances. This is of large interest for present and future storage ring based light sources in order to utilize small period / gap undulators, which provide higher photon energies, and for the design of damping rings for future linear colliders to obtain their desired high luminosities. In this context, a vertical emittance tuning and optimization program has been launched at the Swiss Light Source (SLS) at Paul Scherrer Institut (PSI) in Villigen, Switzerland [3]. The main activities include (a) the suppression of betatron coupling and vertical dispersion by beam-assisted realignment of the storage ring magnets and the subsequent application of correction schemes using skew quadrupoles, (b) the measurement of small vertical beam sizes by means of a high resolution beam profile monitor and (c) the determination of intra beam scattering contributions to the emittance.

SLS Vertical Emittance Minimization

In case of ideal flat storage ring lattices, extremely low vertical equilibrium emittances can be obtained, which are only limited by the direct recoil of the emitted photons [4]. For SLS this so called quantum limit of the vertical emittance is at 0.2 pmrad. In reality, however, magnet errors and alignment tolerances (typically in the order of few tens of μms) as well as beam position measurement errors lead to betatron coupling and vertical dispersion causing a subsequent emittance growth to several pmrad or even tens of pmrad. Thus, as a first step towards emittance minimization, a beam-assisted re-alignment of the SLS storage ring magnets (lattice) was carried out in April 2011, leading to a substantial reduction of the rms vertical corrector kick from initially ~ 130 μrad to ~ 50 μrad. On the wa to a systematic vertical dispersion correction, the BPM roll errors were determined and regarded as “fake” vertical dispersion contributions, when the model-based dispersive skew quadrupole correction was applied. As a result, the spurious vertical dispersion could be reduced by using the 12 dispersive skew quadrupoles to < 1.3 mm rms. In a final step, a SVD model-based betatron coupling correction was performed with the 24 non-dispersive skew quadrupoles, which reduced the coupling part of the orbit response matrix by almost a factor of 2.5. Several iterations of this procedure including a final random optimization lead to a vertical beam height of 3.6 ± 0.6 μm and a corresponding vertical emittance of 0.9 ± 0.4 pmrad [5]. Figure 1 shows this final “random walk” optimization of the SLS vertical beam height, measured with the existing π-polarization monitor [6], which reached its resolution limit during this emittance minimization campaign.

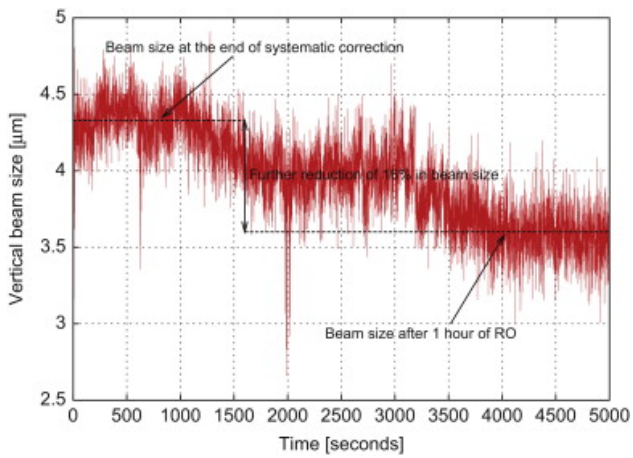

Figure 1: Random optimization of the SLS vertical beam height. The resolution limit of the existing π-polarization monitor has been reached at 3.6 ± 0.6 μm.

*The presented work has received funding from the European Commission under FP-7-INFRASTRUCTURES-2010-1/INFRA-2010-2.2.11 project TIARA (CNI-PP). Grant agreement no. 261905.

ISBN 978-3-95450-119-9

MEASUREMENT OF NANOMETER ELECTRON BEAM SIZES WITH LASER INTERFERENCE USING IPBSM

Jacqueline Yan, Sachio Komamiya, Masahiro Oroku, Taikan Suehara, Yohei Yamaguchi, Takashi Yamanaka, University of Tokyo, Tokyo, Japan
Yoshio Kamiya, ICEPP, University of Tokyo, Tokyo, Japan
Sakae Araki, Toshiyuki Okugi, Toshiaki Tauchi, Nobuhiro Terunuma, Junji Urakawa, KEK, Ibaraki, Japan

Abstract

An e- beam size monitor, called the "Shintake Monitor" (or "IPBSM"), is installed at ATF2's virtual interaction point ("IP"). It plays a crucial role in achieving ATF2's Goal 1 of focusing the vertical e- beam size (σ_y*) down to a design value of 37 nm, using an ingenious technique of colliding the e- beam against a target of laser interference fringes. σ_y* is derived from the modulation depth of the resulting Compton signal photons measured by a downstream γ detector. IPBSM is the only existing device capable of measuring σy* as small as 20 nm with better than 10% resolution, and can accommodate a wide range of σ_y* up to a few μm by switching between laser crossing angles θ = 174° , 30°, and 2° - 8° according to beam tuning status.

The effects of several major hardware upgrades have been confirmed during beam time, such as through suppressed signal jitters, improved resolution and stable measurements of σ_y* down to about 150 nm by Feb 2012. The aims of the extensive 2012 summer reform implemented upon the laser optics are higher reliability and reproducibility in alignment. Our goal for the autumn 2012 run is to stably measure σ_y* < 50 nm. This paper describes the system's design, role in beam tuning, and various efforts to further improve its performance.

INTRODUCTION

The International Linear Collider (ILC) holds great potential for detection and detailed research of new physics beyond the Standard Model. Clean e-e+ collisions enable observations of the most fundamental processes free of synchrotron radiation loss. However ILC faces stringent demands for luminosity, expressed here as:

$$L = \frac{n_b N^2 f_{rep}}{4\pi \sigma_x^* \sigma_y^*} H_D \qquad (1)$$

n_b : no.of bunches, N : bunch population,
f_{rep} : repetition rate, H_D: disruption parameter.

It is apparent from the Gaussian beam cross section in the denominator that beam focusing is crucial for achieving high luminosity. The design IP beam sizes for ILC are (σ^*_x, σ^*_y) = (640, 5.7) nm[1]. At the Accelerator Test Facility 2 (ATF2), a FFS test facility for ILC located in KEK, "Goal 1" is to to verify the "Local Chromaticity Correction" scheme by demonstrating focusing of σ_y* to 37 nm, the design size energy-scaled down from ILC[2]. "Goal 2" is to nm precision beam trajectory stabilization under such a small σ_y*. IPBSM, installed at ATF2's virtual IP, is the only existing device capable of measuring σ_y* as small as 20 nm. Its outcomes are indispensible for Goal 1, and thus for realization of ILC.

Figure 1: Location of Shintake Monitor in the ATF(2) beamline [3,7].

Measurement Scheme of IPBSM

Figure 2 shows the schematic layout of IPBSM, which consists of laser optics, a γ detector, and DAQ electronics[5]. The pulsed laser beam is split into two paths by a half mirror, then made to cross to form interference fringes at their focal points matched to IP. The phase between the paths, controlled by a piezoelectric stage, is scanned relative to the e- beam traversing the fringes perpendicularly. A downstream γ detector measures the modulation depth (M) of the resulting Compton scattered photon signal at each phase. M is large for focused beams, and small for dispersed beams (Fig. 3).

Laser fringe intensity is expressed using intensity of magnetic field (***B***), averaged over time as:

$$\overline{B_x^2 + B_y^2} = B^2(1 + \cos\theta \cos 2k_y y) \qquad (2)$$

x and y are coordinates perpendicular to e- beam. k_y = ksin(θ/2) (θ:laser crossing angle, λ:laser wavelength) is wave number component normal to fringes. Assuming Gaussian distribution, N, number of Compton photons, is related to beam centre y_0 and σ_y* as[4].

$$N \propto \int_{-\infty}^{\infty} \frac{1}{\sqrt{2\pi}\sigma_y} \exp\left(-\frac{(y-y_0)^2}{2\sigma_y^2}\right) \overline{(B_x^2 + B_y^2)} dy \qquad (3)$$

$$\Rightarrow N = \frac{N_0}{2}\left\{1 + \cos(2k_y y_0)\cos\theta \exp\left(-2(k_y\sigma_y)^2\right)\right\}$$

M, interpreted as ratio of amplitude to average, is calculated in Eq. (4) from N_+ and N_- , max. and min., respectively, of signal intensity. Figure 3 relates M and σ_y*, calculated as in Eq. (5). Here, measurable range is determined by the laser fringe pitch "d" (Table 1)[5, 7].

ISBN 978-3-95450-119-9

DIRECT OBSERVATION OF THE DUST-TRAPPING PHENOMENON

Y. Tanimoto, High Energy Accelerator Research Organization (KEK), Tsukuba, Japan

Abstract

Dust trapping is a phenomenon known to cause a sudden decrease in beam lifetime at electron storage rings. It has been one of the most serious operational problems at the Photon Factory Advanced Ring (PF-AR) since the 1980s, and many efforts have been made to resolve it. In a recent experimental study on dust trapping, video cameras fortuitously captured the culprit, recording a luminous micro-particle trapped in the electron beam, just as if a shooting star were traveling in the beam tube. In successive research, supersensitive cameras repeatedly observed trapped dust particles, and revealed that they behaved differently under different conditions. This article summarizes the experimental results, as well as some theories about dust trapping that are consistent with the observations.

INTRODUCTION

Stored beams in circular accelerators are susceptible to lasting interaction with particles of opposite polarity. In electron or antiproton storage rings, the beam captures positively charged ions or dust particles. The latter phenomenon is called dust trapping, and a hypothesis that explains the observations was proposed in the early 1980s [1-3].

Dust trapping often causes operational problems because it can severely disturb stored beams; it leads to a sudden decrease in the electron beam lifetime and to a sudden increase in the antiproton beam emittance. In this article, we mainly discuss the phenomenon in electron storage rings.

During dust trapping, gamma-ray bursts are often detected at the extension of the beam orbit as a result of bremsstrahlung scatterings between the electron beam and the trapped dust particle [4-6]. This can also cause operational problems to users of synchrotron radiation (SR) and high-energy physics when it occurs upstream of the beam line and detectors [7-9]. In experimental research on dust trapping, however, detection of such gamma rays has provided indirect evidence of the interaction between beam and dust.

In order to clarify the mechanism behind this phenomenon, dust-trapping theories consistent with observations have been developed, considering dynamic and thermal conditions for trapped dust particles [2, 10-16]. These theories explain how the dust can remain trapped for a long time in spite of the interaction with high-intensity stored beams. The main theories will be briefly reviewed in Chapter 2.

From an operational point of view, it is important to locate the dust sources and then to take effective measures to suppress the dust trapping. Some known dust sources will also be reviewed in Chapter 2.

At KEK PF-AR (formerly called "TRISTAN AR"), dust trapping occurred more frequently following the major reconstruction in 2001. Our long-term investigation on the phenomenon suggested that distributed ion pumps (DIPs) produced dust particles, so we installed more than 60 sputter ion pumps to replace the DIPs [17]. However, switching all the DIPs off suppressed the occurrence by only 50%, suggesting that there were other dust sources at PF-AR. Further investigation indicated that electric discharges at some in-vacuum undulators or a feedback kicker were causing dust trapping, so we surface-conditioned these discharge-prone devices by storing 25% higher beam current than usual. As a result, the occurrence of dust trapping was suppressed by 70% compared to that before taking the countermeasures [18].

In addition, we started an experimental study at PF-AR which was primarily designed to intentionally replicate dust trapping by simulating the above two conditions for dust production. In one experiment, we fortuitously observed a trapped dust particle with video cameras [19], and found it effective to conduct the dust-trapping research by direct observation [20]. Important results of the experimental demonstrations and the dust-trapping observations will be presented with some video snapshots in Chapter 3.

DUST-TRAPPING PHENOMENON IN STORAGE RINGS

Previous Reports on Dust Trapping

In the early 1980s, the dust-trapping phenomenon started to be reported around the world. The CERN Antiproton Accumulator (AA) suffered from unexpected sudden increases in beam emittance, and the phenomenon was so mysterious that they nicknamed it "AA-ghost" [3]. They concluded later that the phenomenon was related to dust particles stirred up by vibration of stochastic cooling shutters [21].

Also in the 1980s, some second-generation light sources such as PF-ring [22, 23] and NSLS [2] experienced the problem that the beam lifetime suddenly dropped and the stored beam decayed faster. At PF-ring, they found that the phenomenon occurred less frequently when the DIPs were switched off [22].

Until around 2000, dust problems were often reported at electron storage rings for light sources and for high-energy physics such as TRISTAN AR [5], DCI and SuperACO [6], CESR [13], HERA, DORIS and PETRA [24-26], ESRF [27], KEKB [9], PEP-II [8], and BEPC [28].

Experimental studies on dust trapping have been carried out at several accelerators. In the early 1990s, Marin observed bremsstrahlung bursts at SuperACO and DCI [6], and revealed that trapped dust moved

ISBN 978-3-95450-119-9

DIAGNOSTICS UPDATE OF THE TAIWAN PHOTON SOURCE

C. H. Kuo, K. H. Hu, P. C. Chiu, C. Y. Liao, C. Y. Wu, Y. S. Cheng, S.Y. Hsu, Jenny Chen, K. T. Hsu

NSRRC, Hsinchu 30076, Taiwan

Abstract

Taiwan Photon Source (TPS) is a 3 GeV synchrotron light source which is being construction at campus of NSRRC. Various diagnostics are in implementation and will deploy to satisfy stringent requirements of TPS for commissioning, top-up injection, and operation. These diagnostics include destructive monitors, beam intensity observation, trajectory and beam positions measurement, synchrotron radiation monitors, beam loss monitors, orbit and bunch-by-bunch feedbacks, filling pattern and miscellaneous devices. Current status will summarize in this report.

INTRODUCTION

The TPS is a latest generation of synchrotron light source featuring high brightness with extremely low emittance [1]. Civil construction and installation will be finished in 2013. Machine commissioning is scheduled in 2014. The accelerator system consists of a 150 MeV S-band linac, linac to booster transfer line (LTB), 0.15–3 GeV booster synchrotron, booster to storage ring transfer line (BTS), and 3 GeV storage ring. The diagnostics will help TPS to achieve its design goals. Major diagnostics related parameters for the booster synchrotron and the storage ring are summarized in Table 1. Beam size and divergence angle is summary in Table 2.

Diagnostics for the TPS accelerator system were summary in reference [2]. Diagnostics of linear accelerator and transfer lines will help to generate and delivery high quality electron beam to booster and storage ring. Booster diagnostics will provide beam parameters include orbit, working tunes, circulating current, filling pattern, beam size, bunch length, emittance, and derived parameters. The diagnostics are designed to provide a complete characterization stored beam in the storage ring, including averaged beam current, fill pattern, beam lifetime, closed orbit, working tunes, chromaticity, beam size, beam loss pattern, beam density distribution, emittance, bunch length, and etc. To utilize the benefits of the high brightness and small beam sizes of TPS sources, photon beams must be extreme stable both in position and angle to the level of better than 10% of beam sizes and divergence. Table 2 provides the electron beam sizes and angular divergences for the selected TPS sources. The most stringent beam measurement and stability requirement will be for the vertical position at the 7 m straight for ID source (σ_y = 5.11 μm); this will require special consideration for measuring both electron and photon beams.

Table 1: Major Parameters of the Booster Synchrotron and the Storage Ring

	Booster Synchrotron	Storage Ring
Circumference (m)	496.8	518.4
Energy (GeV)	150 MeV – 3 GeV	3.0
Natural emittance (nm-rad)	10.32 @ 3 GeV	1.6
Revolution period (ns)	1656	1729.2
Revolution frequency (kHz)	603.865	578.30
Radiofrequency (MHz)	499.654	499.654
Harmonic number	828	864
SR loss/turn, dipole (MeV)	0.586 @ 3 GeV	0.85269
Betatron tune ν_x/ν_y	14.369/9.405	26.18 /13.28
Synchrotron tune νs	-	0.00611
Momentum compaction (α_1, α_2)	-	2.4×10^{-4}, 2.1×10^{-3}
Natural energy spread	9.553×10^{-4}	8.86×10^{-4}
Damping partition $J_x/J_y/J_s$	1.82/1.00/1.18	0.9977/1.0/ 2.0023
Damping time $\tau_x/\tau_y/\tau_s$ (ms)	9.34/ 16.96 / 14.32	12.20/ 12.17 / 6.08
Natural chromaticity ξ_x/ξ_y	-16.86/-13.29	-75 / -26
Dipole bending radius ρ (m)	17.1887	8.40338
Repetition rate (Hz)	3	-

Table 2: The Electron Beam Sizes and Divergence

Source point	σ_x (μm)	$\sigma_{x'}$ (μrad)	σ_y (μm)	$\sigma_{y'}$ (μrad)
12 m straight center	165.10	12.49	9.85	1.63
7 m straight center	120.81	17.26	5.11	3.14
Dipole (1° source point)	39.73	76.11	15.81	1.11

BEAM INTENSITY MONITORING

The TPS 150 MeV linac system was contracted to the RI Research Instruments GmbH [3]. The schedule for delivery and commissioning is in early of 2011 at test site. The linac will move to the TPS building in late 2012 after TPS building available. Beam instrumentation comprises five YAG:Ce screen monitors for beam position and profile observation, two fast current transformers (FCT) to monitor the distribution of charge and one integrating current transformer (ICT) for monitoring total bunch train charge. Wall current monitors (WCM), which is formed by equally spaced broadband ceramic resistors, mounted on a flexible circuit board and wrapped around a short ceramic break, will give information on beam charge as well as longitudinal profiles of electron bunches. All of mentioned diagnostics were provided by the vendor except the profile measurement data acquisition and analysis [4].

ISBN 978-3-95450-119-9

MODERNIZED OF THE BOOSTER SYNCHROTRON DIAGNOSTICS IN THE TAIWAN LIGHT SOURCE

C. H. Kuo, K. H. Hu, P. C. Chiu, C. Y. Liao, C. Y. Wu, Y. S. Cheng, S.Y. Hsu, Jenny Chen, K. T. Hsu, NSRRC, Hsinchu 30076, Taiwan

Abstract

Taiwan Light Source (TLS) is a 1.5 GeV synchrotron based light source which was dedicated 20 years ago. After several major and minor upgrades, the TLS now operated in top-up mode since late 2004. A new 3 GeV Taiwan Photon Source (TPS) is in construction to provide more x-ray users. To provide a test bed for the diagnostic devices in booster synchrotron for the TPS project, the diagnostics of the TLS booster synchrotron is revised recently. It can also provide up-to-date diagnostics for the TLS booster to help to achieve a better operation of the injector for the TLS storage ring. Efforts of these upgrades and modifications are summary in this report.

INTRODUCTION

The TLS booster synchrotron was delivered in 1992 [1]. Some diagnostics of the TLS booster revised in recently by borrow components for the TPS project before its commissioning in 2014. Two goals of these revised efforts, the first goal is as test bed for the TPS project to do hardware, software, and application development. The second goal is to provide better understanding its characteristics of the TLS booster synchrotron. The major parameters of the TLS booster synchrotron are summarized in Table 1. This study focus on BPM electronics, tune monitor, synchrotron radiation monitor, and perform some preliminary test to check functionality and performance.

Table 1: Major design parameters of the TLS booster synchrotron relate to diagnostics.

Parameters	Value
Energy	1.5 GeV (operated at 1.3 GeV before 1999)
Circumference	72 m
Periodicity	12
Energy spread	5×10^{-4}
Momentum compaction factor	0.058
RF frequency	499.654 MHz
Harmonic number	120
Tune	$\nu_x \sim 4.4$, $\nu_y \sim 2.43$
Chromaticity	$\xi_x \sim -6.5$, $\xi_y \sim -2.8$
Betatron function (max)	$\beta_x \sim 11.9$ m, $\beta_y \sim 11$ m
Repetition rate	10 Hz

BPM ELECTRONICS

Beam position monitor (BPM) in the TLS booster synchrotron was mounted 45 degrees on the chamber at between the dipole and the quadrupoles. The lattice of the booster synchrotron is FODO type with periods of 12. There are 23 BPMs used around the synchrotron, because one location is used as a photon port. The BPM location on the booster is shown in Fig. 1. Past efforts to measure closed orbit and turn-by-turn position of in the TLS booster synchrotron during ramping from 50 MeV to 1.3 GeV are summarized in references [2, 3, 4]. Energy ramping of the TLS storage ring from 1.3 GeV to 1.5 GeV was done in 1995 to enhance x-ray emission. The booster synchrotron was raised from 1.3 GeV to 1.5 GeV in 1999 to provide full energy injection for the storage ring.

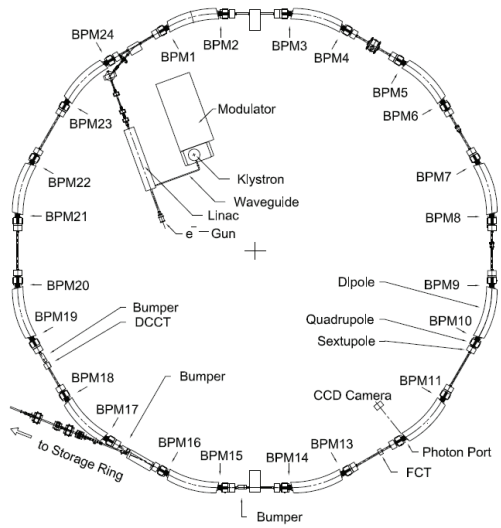

Figure 1: BPM layout of the TLS booster synchrotron.

The BPM cabling and electronics were completely modified during shutdown in August, 2012. BPM electronics borrow from the TPS project. These BPM electronics will available before TPS commissioning in 2014. The four buttons of each BPM were connected to a Libera Brilliance+ [5] BPM module directly. The BPM electronics provide turn-by-turn data for x, y, and sum signals. Further processing include spectral analysis, decimated raw data to reduce amount of data, data averaging, etc. are easy to do by various software applications after data readout from BPM electronic.

Validation checking and preliminary measurement are in proceeding since the accelerator startup from shutdown in the early September. The preliminary measured orbit is shown in Fig. 2. The extraction is disabled, so, the beam can survive almost full booster cycle (100 msec).

ISBN 978-3-95450-119-9

THE CALIBRATION FACTOR DETERMINED AND ANALYSIS FOR HLS BUNCH CURRENT MEASUREMENT SYSTEM*

Y.L. Yang#, T.J. Ma, B.G. Sun, P. Lu, J.G. Wang, J.Y. Zou, C.C. Cheng
NSRL&SNST, USTC, Hefei 230029, P. R. China

Abstract

For bunch current measurement system, button electrode or strip-line electrode can be selected as its signal pickup, peak value or integral of signal from pickup can be used to indicate the related bunch current value. To obtain the absolute value of bunch current, the calibration factor should be determined with the help of DCCT. So, the calibration factor is a key parameter for bunch current measurement system. At HLS, the stretch effect of bunch length was observed when bunch current decay over time and this will affect the performance of bunch current detection for different pickups and calculate methods, which mean the calibration factor will be much different. In this paper, theoretical analysis and experimental validation results are performed to find out an acceptable solution about pickup and signal processing method for bunch current measurement system at HLS. The results show that, the best performance can obtained by adopting strip-line pickup.

INTRODUCTION

Bunch current measurement is necessary elements for most accelerators, especially for synchrotron radiation light source. A lot of various types of measurement systems are developed by now [1-4]. Current transformers, pickup-electrodes and wall current monitors are most widespread among devices for bunch current measurement.

Hefei Light Source (HLS) is a synchrotron light source, many button pickups and strip-line pickups have been mounted on the vacuum pipe for the measurement of electron beam position called as BPM. Typically, a BPM have four electrodes to calculate both vertical and horizontal beam position. Additionally, the sum signal from the four electrodes carry the bunch charge information and its change rate is less than 0.005 when beam position alternated within 4mm [5]. So the sum signal can be used to calculate the bunch current.

HLS storage ring operates in 800MeV with 204.016MHz RF and 45 bunches, the bunch separated from each other only 5 ns, and the bunch length is about 300ps. So, two type of four-electrode pickup can be selected as the pickup of HLS bunch current measurement system [6]: button electrode and strip-line electrode. Peak value or integral of bunch signal from pickup can be used to calculate the related bunch current value. To obtain the absolute value of bunch current, the calibration factor should be determined with the help of DCCT. At HLS, the stretch effect of bunch length was observed [7] when bunch current decay over time and this will affect the performance of bunch current detection for different pickups and calculate methods, which mean the calibration factor will be much different. So, theoretical analysis and experimental validation results are performed to find out an ideal solution for bunch current measurement at HLS.

*Work supported by National Natural Science Project (11105141) and Chinese Universities Scientific Fund.
#ylyang@ustc.edu.cn

BUNCH CURRENT CALCULATE

The electrons in a bunch from storage ring are usually expressed with a Gaussian distribution. When the total charge in bunch is Q_0 and bunch length is σ_τ, formula 1 show the expression of a bunch in time domain.

$$I_b(t) = \frac{Q_0}{\sqrt{2\pi}\sigma_\tau}\exp(-\frac{t^2}{2\sigma_\tau^2}) \tag{1}$$

For button pickup, the sum signal of four electrodes can be expressed as follow:

$$\begin{aligned} V_\Sigma(t) &= k\frac{dI_b(t)}{dt} \\ &= -k\frac{Q_0}{\sqrt{2\pi}\sigma_\tau^2}\exp(-\frac{t^2}{2\sigma_\tau^2}) \end{aligned} \tag{2}$$

k is the scale factor of electronics. The chart was shown in Figure 1(a) [8].

Peak value and integral value of each bunch sum signal carry bunch charge information, which can be obtained from formula 2:

$$V_{peak} = K_P\frac{Q_0}{\sigma_\tau^{\,2}} \propto \frac{Q_0}{\sigma_\tau^{\,2}} \tag{3}$$

$$V_{integral} = \int_{t_1}^{0} V_\Sigma(t)dt = K_I\frac{Q_0}{\sigma_\tau} \propto \frac{Q_0}{\sigma_\tau} \tag{4}$$

Where K_p is the calibration factor for using peak value of sum signal and K_I is the calibration factor for using integral of sum signal. The above equation shows the strong influence of the bunch length σ_τ, both on V_{peak} and $V_{integral}$.

Alike, for strip-line electrode, the chart was shown in Figure 1(b) and the sum signal expression is:

$$V_\Sigma(t) = \frac{\varphi Z}{4\pi}\left[I_b(t) - I_b\left(t - \frac{2l}{c}\right)\right] \tag{5}$$

ISBN 978-3-95450-119-9

PULSED ELECTRON BEAM CURRENT AND FLUX MONITOR FOR THE RACE-TRACK MICROTRON

B.J. Patil, Department of Physics, Abasaheb Garware College, Karve Road, Pune, India
Shahzad Akhter, N.S. Shinde, V.N. Bhoraskar, S.D. Dhole*,
Department of Physics, University of Pune, Ganeshkhind, Pune, India

Abstract

In electron irradiation experiments on the materials, a true current of the electron beam is to be known to calculate the electron fluence received by the sample. Therefore, a pulsed electron beam current and flux monitor alongwith electronic system for an electron accelerator called Race-Track Microtron has been designed and developed. The sensing device used was a ferrite core having suitable number of turns of copper wire wound around it, through which the electron beam was passed without loss in the intensity. With an appropriate developed electronic circuit, the instantaneous value of the induced voltage was measured which in turn provides value of the electron beam pulsed current. The total charge passed through the ferrite core per unit time was therefore recorded and an integrated value of the total charge in a given period could be derived. This system can be used to measure the electron flux in the range from 10^8 electron/cm^2 to 10^{16} electron/cm^2. Moreover, this system has been used successfully in a few electron irradiation experiments where the knowledge of the electron fluence received by the sample is required.

INTRODUCTION

Charged particle accelerators deliver particle beams either in the pulse or continuous mode. In case of continuous beam current, combination of Faraday cup and current meter can serve the purpose of flux measurement. However, in case of pulsed electron beam, analog meters are not sensitive to the small beam pulse width which may vary from nanoseconds to microseconds. In such cases, integration of the charge collected over a known period is required to obtain particle fluence received by the target.

The Microtron, an electron accelerator of the University of Pune is operated in a pulse mode with pulse width 2 μs and pulsating rate variable in the range 50 *pps* to 200 *pps*. The energy range can be set in two ranges 0.5 to 1 MeV and 6 to 8 MeV. For many applications, samples are exposed with electrons and fluence level (e$^-$/cm^2) is required to be known with accuracy around 1%. In this laboratory, for irradiation experiments, a Faraday cup is being used to measure electron fluence received by the sample. In this method, a conducting plate made of graphite or aluminum is placed in the beam path and the charge collected is measured by a current integrator. The thickness of the plate is kept much more than the range of the electrons. However, all the incident electron do not flow to the integrator because a fraction of the incident electron are lost due to backscattering. Secondary emitted electrons also reduce the charge reaching the current integrator. Due to this problem, it was difficult to estimate fluence level by measuring the charge received by the sample. To avoid this problem an induction type current transformer[1, 2, 3] and pulse integrator have been designed and fabricated to measure pulsed electron beam current and hence fluence received by a sample.

* sanjay@physics.unipune.ac.in

DESIGN PRINCIPLE OF INDUCTION MONITOR

The measurement of pulse current using ferrite core is based on the principle of current transformer[2]. If ideal transformer conditions are assumed i.e. unity coupling without core losses and winding reactances much greater than respective primary and secondary resistances, the ratio of primary and secondary current inversely proportional to the turns ratio

$$\frac{i_p}{i_s} = \frac{N_s}{N_p} \tag{1}$$

Where i_p= primary current, i_s = secondary current, N_s = number of secondary turns, N_p= number of primary turns

In many cases, while the monitoring of primary current requires a voltage output from the secondary, the secondary current passes through load resistance R$_L$

$$V_s = i_p . \frac{N_p}{N_s} R_L \tag{2}$$

Considering N_s=50, N_p=1, then i_p=$i_s \times 50$

$$V_s = i_s R_L \therefore i_s = \frac{i_p}{50} \tag{3}$$

$$V_s = i_p \tag{4}$$

Relation 3 gives the magnitude of voltage V_s directly proportional to the primary beam current.

DESIGN PRINCIPLE OF THE CURRENT TRANSFORMER

The current monitor consists of a ferrite core type T45HP3 having OD 46 mm, ID 28.6 mm and width 13

ISBN 978-3-95450-119-9

BPM SELECTION FOR BEAM CURRENT MONITORING IN SSRF*

Zhichu Chen†, Yongbin Leng‡, Yingbing Yan, SSRF, SINAP, Shanghai, China

Abstract

Although New Parametric Current Transformers (NPCT), commonly called Direct Current Current Transformer (DCCT), is the general solution of beam current monitor, Beam Position Monitor (BPM) sum signals may still surpass it in some aspects such as the faster data rate and higher resolution in low current situations. Nevertheless, an additional monitor should be harmless. Meanwhile, the DCCTs in the storage ring of Shanghai Synchrotron Radiation Facility (SSRF) have been suffering from various noise and the signals from the BPMs could be an aid to provide the beam current more accurately. There're 140 BPMs in the storage ring in SSRF but not all of them are suitable for this particular usage. This article focuses on the methods used here to dynamicly choose the BPMs that meet the criteria.

INTRODUCTION

Beam current is one of the fundamental parameters to be measured in any particle accelerators and its direct current (DC) component is especially important in synchrotrons and storage rings. Thus, DCCT is almost the most widely used DC monitor in modern light sources around the world for its fine resolution less than 1 μA r.m.s. [1] and long-term stability.

An NPCT175 from Bergoz Instrumentation have been positioned on the storage ring as the beam current monitor and another one in addition as its backup since the beginning of the commisioning in SSRF [2, 3]. Both of them have been suffering from various noise from time to time [4]:

- power line noise,
- narrow band noise which is strongly related to the beam current,
- random square wave noise from nowhere.

Figure 1 shows a typical performance of the DCCT without any noise mentioned above and the BPM sum signal. The quasi-constant resolution of DCCT reading is less than 2 μA in all circumstances and that can be regarded as the limitation of the electronics. The situation of the BPM is a little more complex. The resolution of a single BPM is better than the DCCT's for a really low current (weaker than 10 mA) but gets worse as the beam current rises. Averaging the whole BPM system, on the other hand, can improve the performance significantly. The resolution of the BPM system is better than that of the DCCT when the current is weaker than 60 mA and it seems still under control even the current is stronger. It all seems that the BPM alternative is especially suitable for the low current mode. It is not unreasonable to assume that some BPM may act worse than the others and the new BPM set will work even better. The purpose of our beam experiment is to find an algorithm to dynamicly maintain such a list in which each BPM is relatively stable.

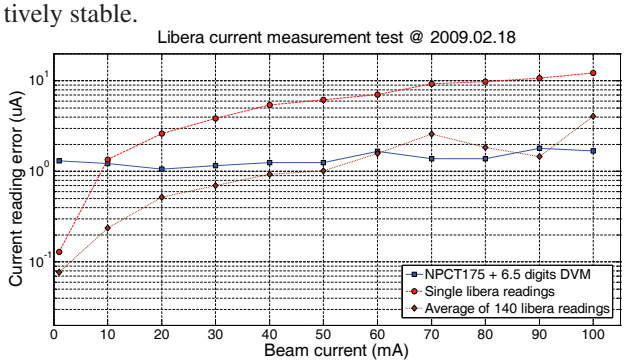

Figure 1: A performance evaluation of DCCT and BPM sum signal as the beam current monitor.

There're 140 BPMs on the storage ring [2] and some of the probes can be considered stable enough to accomplish the task of been current monitors. Using the BPM sum signal to relatively measure the DC beam current has already been a handful means during the commisioning of SSRF [2]. This idea is being urged by all the benefits it can offer: faster data rate, dead time free and sensitive even in low current situations. Hence, a performance evaluation is needed to pick out the qualified BPMs.

PRINCIPLES

The sum signal on the pick-ups of a BPM does not position insensitive. For such a resolution requirement, the nonlinearity problem must be taken into account. There're positions that the transverse motion of the beam is fierce and the BPMs at these locations are less desirable. Some BPMs might suffer from some kind of local noise like the DCCT does, or just encounter some machining, installation, even connection problems. So the algorithm we need will only choose good BPMs at good positions.

Some algorithms have been tried and compared, but it turns out that the one inspired by the theory of Principal Component Analysis (PCA) is better than others. One example is that we used to rate the BPMs by the r.m.s. of the difference the each BPM "waveform." The noisy or unstable BPMs could be picked out without problem. The one smooth but wrongly decayed or slowing drifting can get away. But PCA can be helpful to list all of them.

Overview of PCA

PCA is a useful mathematical technique for finding patterns in data of high dimension which has been introduced to the particle accelerator physics [5]. Only a statistical analysis of the BPM data matrix is needed to study the

* Work supported by National Natural Science Foundation of China (No. 11075198)

† chenzhichu@sinap.ac.cn

‡ Corresponding author, leng@sinap.ac.cn

ISBN 978-3-95450-119-9

APPLICATION OF SINGLE CRYSTAL DIAMONDS (scCVD) AS BEAM CONDITIONS MONITORS AT LHC

E. Castro, DESY, Zeuthen, Germany on behalf of the DESY and BRM CMS group.

Abstract

The properties of single-crystal diamonds (scCVD): radiation hardness, low leakage current with negligible temperature dependence and fast signal response, make them attractive to be used as robust particle counters in areas of high radiation dose. The Beam Conditions and Radiation Monitoring system (BRM) of the CMS experiment includes the monitor BCM1F (Fast Beam Conditions Monitor) consisting of 8 scCVD sensors. BCM1F monitors the flux of particles from beam induced backgrounds and from collisions. It protects the inner CMS detectors from high background and delivers feedback on the beam conditions to the LHC.

Since the LHC start up in September 2008, BCM1F has revealed to be a valuable tool in the daily operation of the CMS experiment and the LHC. It was successfully used to keep the background level low, to identify vacuum leaks via the enhanced rate of halo particles from interactions of beam particles with residual gas atoms in the beam-pipe, and to perform an on-line luminosity measurement. In order to cope in future with higher bunch density and luminosity an upgrade of the BCM1F front-end-electronics and data acquisition is foreseen.

Due to the positive experience with the CMS BCM1F, the LHC was equipped with currently 6 BCM1F modules at several positions along the ring where beam losses will be analysed. The modules deliver information about hit rate and arrival time distributions projected on the time of an orbit, allowing to count halo particles originating from each bunch. A characterisation of both BCM1F systems using data collected during the LHC operation is presented.

INTRODUCTION

The CMS experiment contains several systems within BRM to measure independently the dose at several positions inside and near the detector, and the flux of ionising particles [1]. Three systems use diamond sensors. Two systems, using polycrystalline sensors [2], integrate the sensor current over microsecond time intervalls and may induce beam aborts when the current reaches preset limits.

The 8 BCM1F modules are particle counters to monitor the flux of particles with a time resolution of nanoseconds [3]. They consist of scCVD sensors, fast and radiation hard front-end ASICs and and a laser driven analog signal transmission. The back-end electronics containing fast ADCs, discriminators, scaler and TDCs and the data acquisition are operated independently from the CMS data acquisition.

To monitor the particle flux along the LHC 6 more modules, forming the BCM1F4LHC system, are installed at several IPs, as shown in Figure 1. The back-end electronics of BCM1F4LHC is similar to the one of BCM1F and located near the LHC control room.

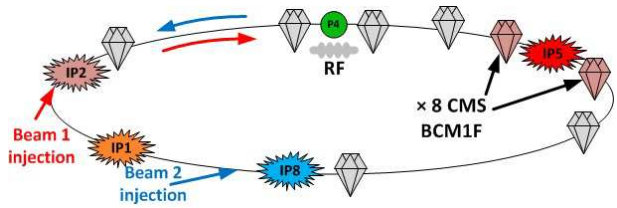

Figure 1: Location of BCM1F modules along the LHC ring.

SINGLE CRYSTAL CVD DIAMOND SENSORS

The charge collections efficiency of scCVD sensors is nearly 100% and signals of sensors with a thickness of about 500μm are sufficiently large to count MIPs. They are operated as solid state ionisation chambers by applying high voltage to thin metal plates on both sides of the sensor to generate an electric field in the bulk. Signals are created due the drift of both electrons and holes with high mobility.

The scCVD sensors used in BCM1F have an area of $5\times5\text{mm}^2$ and a thickness of 500μm. They have been manufactured by Element Six Ltd. as a result of the collaboration with the CERN RD42 project. A first application of an scCVD diamond sensor in a collider experiment was described in Ref. [4].

THE CMS BCM1F

The BCM1F consists of 2 planes of 4 modules each located at 1.8m on either side of the IP at a distance of 4.5cm from the beam pipe. Each module contains a scCVD sensor, radiation hard front-end electronics and optical transmission of the signal, as shown in Figure 2. The peaking time of the front-end ASIC is about 25 ns and the time resolution about 2 ns. The distance between the sensors and the IP is optimal for the separation of incoming and outgoing particles and corresponds to a time-of-flight of $\sim$6 ns for relativistic particles.

THE BCM1F4LHC BLM SYSTEM

Six scCVD diamonds were installed in the LHC tunnel near the beam-pipe to monitor the beam halo and analyse beam losses. They are positioned next to collimators to be sensitive to losses originating from protons hitting the walls of the collimators, and next to ionisation profile monitors

ISBN 978-3-95450-119-9

SYSTEM ARCHITECTURE FOR MEASURING AND MONITORING BEAM LOSSES IN THE INJECTOR COMPLEX AT CERN

C. Zamantzas, M. Alsdorf, B. Dehning, S. Jackson, M. Kwiatkowski, W. Vigano,
CERN, Geneva, Switzerland

Abstract

The strategy for beam setup and machine protection of the accelerators at the European Organisation for Nuclear Research (CERN) is mainly based on its Beam Loss Monitoring (BLM) systems. For their upgrade to higher beam energies and intensities, a new BLM system is under development with the aim of providing faster measurement updates with higher dynamic range and the ability to accept more types of detectors as input compared to its predecessors. In this paper, the architecture of the complete system is explored giving an insight to the design choices made to provide a highly reconfigurable system that is able to fulfil the different requirements of each accelerator using reprogrammable devices.

INTRODUCTION

During the upgrade of each injector line at the European Organisation for Nuclear Research (CERN), an up-to-date Beam Loss Monitoring (BLM) system will be included for the monitoring of the beam losses and machine protection. That is, apart from the high reliability and availability expectations from the system, the architecture chosen should provide a generic, highly configurable and high-performing system.

The acquisition part should provide the ability to accept several detector types as input. In the majority of the cases, it is foreseen to use ionisation chambers similar to those developed for the LHC. Nevertheless, several other types, e.g. secondary emission monitors, diamonds and Cherenkov detectors, will need to be used also in some locations to cover particular cases. For the transport of the signal between the detector and the front-end coaxial double shielded cables are employed and wherever possible all cables pass through enclosed cable trays. That is, make use of any possible means for noise reduction.

The digitisation of the detector current output will use a new design concept and is currently under implementation. The input channel circuit should be able to measure a current input from 10 pA to 200 mA. That is, a dynamic range of 10^{11}.

Further, the processing part of the system will combine the information gathered by each channel and keep several moving integration windows between 2 μs and 1.2 s. The calculated values for each channel will be checked continuously against predefined threshold values both at the hardware and software level, as well as will be forwarded in the control room and databases for online observation and later analysis. The BLM system, through its direct connection to the beam interlock system, will have the ability to either block all upcoming injections, when the machine protection thresholds get exceeded, or selectively block specific upcoming injections, by tracking losses for each individual beam cycle destination separately.

The system is making use of reprogrammable devices, i.e. Field Programmable Gate Arrays (FPGA), to allow flexibility and target all injectors' requirements. A block diagram of the architecture of the system can be seen in Fig. 2.

ACQUISITION ELECTRONICS

The acquisition electronics are comprised by the digitiser modules, the control module and the crate that provides the hosting and interconnections.

Acquisition Crate (BLEAC)

The acquisition crate (BLEAC) can support up to eight 6U sized acquisition modules. It is based on a custom designed backplane that provide connection for 64 input channels and to each inserted module the needed connection to the power supply voltages and control signals.

The crate's backplane provides in addition support for direct injection of a remotely adjustable reference current either via a dedicated input or via an internal current source. To achieve this each channel's input pass through a relay contact. This option will be used in the future firstly for an automatic calibration procedure and secondly for a channel connection check. That is, the system will be able to guarantee the full dynamic range and maximum linear response possible of each channel, as well as check regularly the complete channel's connection and its ability to trigger the beam interlock.

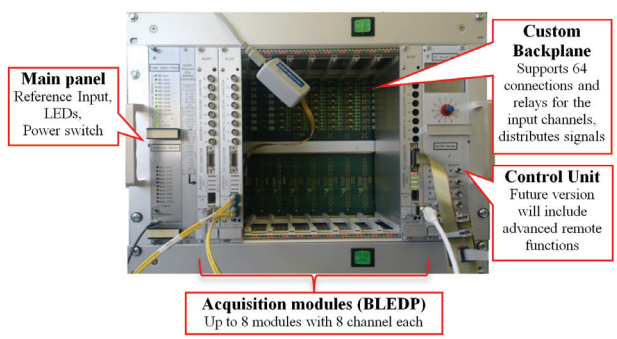

Figure 1: Picture of the BLEAC acquisition crate.

ISBN 978-3-95450-119-9

OPTICAL-FIBER BEAM LOSS MONITOR FOR THE KEK PHOTON FACTORY

T. Obina# and Y. Yano, KEK, Tsukuba, Ibaraki 305-0801 Japan

Abstract

A beam loss monitor using optical fibers has been developed to determine the loss point of an injected beam at the Photon Factory (PF) 2.5-GeV electron storage ring. Large-core optical fibers were installed along the vacuum chamber of the storage ring that cover the entire storage ring continuously. Two injection systems: kicker magnets and a pulsed sextupole magnet, are used for routine operation at the PF. In this paper, details of the loss monitor system and the difference in beam loss when using the two injection system are reported.

INTRODUCTION

In the KEK Photon Factory (PF) 2.5-GeV storage ring, an electron bunch is injected directly from a linear accelerator (linac) that is shared by KEKB-HER, -LER and PF-AR [1]. The three rings (PF, KEKB-HER, -LER) share the linac pulse-by-pulse at a maximum rate of 50 Hz. Because ambient temperature affects the stability of a large water cooling plant, we sometimes need to adjust the injection parameters—such as injection energy or injection angle to the storage ring. A beam loss monitor with high position and time resolution is strongly desired for this kind of tuning procedure for the PF-Ring.

Many kinds of loss monitor have been proposed and used in many different facilities [2]. For example, a loss monitor with a PIN diode can detect very small losses, but is easy to saturate with background X-rays or lost electrons during injection. Another problem is that a large number of detectors is required to cover the entire ring. A pulse-counter type detector is suitable for average loss detection, but the time resolution is no better than 1 revolution time (624 ns) in the PF-Ring. The other candidate is an ionization chamber constructed using coaxial cable applying a high voltage. We did not select this type of detector due to the limited space in our ring, and they are relatively heavy and an obstacle to maintenance work.

The use of a beam loss monitor using optical fibers is common in many linear accelerators or FEL facilities[3-6]. In the KEK linac, loss detection using optical fibers has been developed—starting from an arc sensor for the accelerating tube—since before 2007 [7]. Optical fibers are suitable for our purpose because of the ease of covering the entire ring with them, they have better time and position resolution than other methods, and they are cost effective. On the other hand, they have disadvantages, such as needing an external trigger, their difficulty in detecting CW loss, they provide small coverage in the plane perpendicular to the beam, and there is difficulty in the calibration of absolute beam loss.

#takashi.obina@kek.jp

In this study, first we tested the fiber beam loss monitor in a location where the normalized horizontal aperture is small, then we installed a total 10 fibers to cover the circumference of the entire ring circumference.

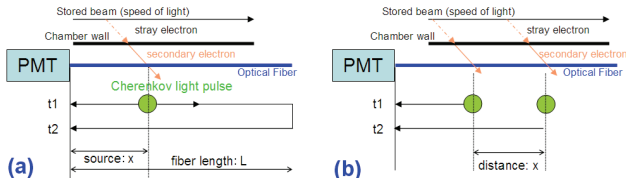

Figure 1: Schematic drawing of detection principle for: one loss point (a), and two loss points (b). In both cases, the loss is coming from a single bunch.

PRINCIPLES OF LOSS DETECTION

Electrons that are not captured in the storage ring hit the vacuum chamber wall and produce secondary electrons outside the vacuum chamber. Secondary electrons that run through quartz fiber generate Cherenkov light provided the energy of the electrons is high enough. As shown in Fig. 1, a photomultiplier tube (PMT) is used for the detection of a light pulse. There are three candidates for the PMT layout: one PMT at the upstream end, one PMT at the downstream end, and a PMT at both ends of the fiber. We opted to use one PMT on the upstream side because of its better time resolution than the downstream end, and the small reflection produced by the opposite side of a fiber can determine the exact location of the light pulse.

With one loss point, as shown in Fig. 1(a), the source position is determined by measuring the arrival time of the direct light (t_1 in the figure) and the reflected light (t_2), using simple arithmetic $x=L-(t_2-t_1)*v_{fiber}/2$, where v_{fiber} is the speed of light propagation in a glass medium, which is equal to $^2/_3$ the speed of light in a vacuum (v_c).

Figure 1(b) shows a case where two light pulses are produced by a single passage of a bunch. The time difference between two direct pulses becomes longer because the direction of the electron bunch and the light pulse are opposite. It is useful to introduce an "effective" propagation time for the calculation of two direct pulses: $v_{eff} = 2/5 * v_c$ (equivalent to 8.3 ns/m).

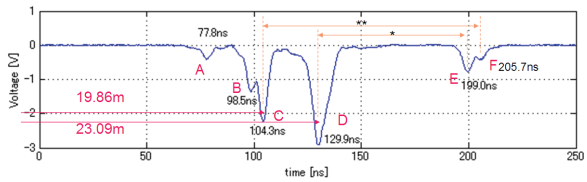

Figure 2: Determination of loss location.

ISBN 978-3-95450-119-9

SSRF BPM SYSTEM OPTIMIZATION AND UPGRADE*

Y.B. Yan#, Y.B. Leng, L.Y. Yu, W.M. Zhou
SINAP, Shanghai, P.R. China

Abstract

The beam position monitor (BPM) system at SSRF was fully equipped with Libera Electrons. It have operated steadily for nearly five years. During the summer shutdown of 2012, more than 50 Libera Electrons were upgraded to Libera Brilliance, which are used mainly for fast obit feedback system. The software version of the whole system is upgraded from 1.42 to 2.07. Meanwhile, some other hardware and software optimizations were carried out. After this upgrade, the stability and performance have been significantly improved. This paper will introduce the details of the optimization and upgrade.

OVERVIEW

Shanghai Synchrotron Radiation Facility (SSRF) is a third generation light source, which located at the Zhangjiang Hi-Tech Park, Shanghai, P.R. China. Its small emittance requires a high resolution Beam Position Monitor (BPM) system, in order to achieve beam stability at the micron level. The same BPM system can also been used to measure the turn-by-turn beam position for various machine studies.

SSRF BPM system was fully equipped with Libera Electrons, which are produced by Instrumentation Technologies [1]. A total of 181 units (3 units for the LINAC, 8 units for the transfer lines, 30 units for the booster and 140 units for the storage ring) were used for BPM signal processing and orbit feedback system. It have operated steadily for nearly five years. During the summer shutdown of 2012 more than 50 Libera Electrons were upgraded to Libera Brilliances, which are used mainly for the fast obit feedback system. The software version of the whole system is also upgraded. This paper will introduce the details of the upgrade.

HARDWARE UPGRADE

The Libera Brilliance features the high precision position measurement of the electron beam in the circular accelerator. Digital signal processing inside the Libera units support programmable bandwidth and can facilitate all the required position measurements: pulsed, first turns, turn-by-turn and regular closed orbit.

The upgrade from Libera Electron to Libera Brilliance represents an economical way of getting a brand new instrument. The hardware difference between them is mainly on the analog board. Libera Brilliance uses a new analogue board with 16-bit ADCs (instead of 12-bit), as shown in Fig. 1. The beam current dependence performance (linearity) and the read-out performance are improved drastically. It's easy to achieve sub-micron resolution in the turn-by-turn data and some tens of nanometres in the FA (Fast Application) data.

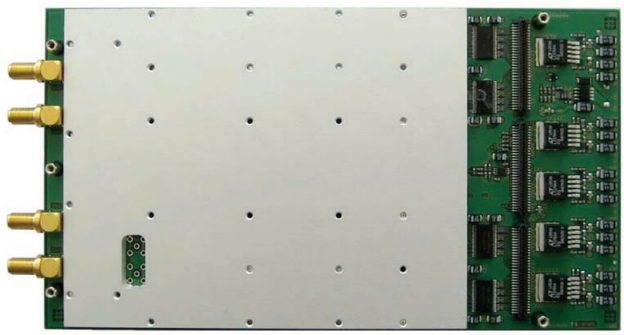

Figure 1: The analog board of Libera Brilliance.

SOFTWARE UPGRADE

The old software releases of our BPM system (Libera Electron) is 1.42. For the software upgrade, there are mainly two reasons.

- Libera Brilliance and Libera Electron share the same software releases and CSPI (Control System Program Interface), which can simplify the management and configuration.
- Some existing problems can be solved via the software upgrade, such as event overflow, phase lock failed occasionally, etc.

Actually, there are several releases from 1.42 to 2.07. During the process, the existing bugs were fixed, the platform was updated, and a lot of new functionalities were added. Some major changes are list below:

- Updated health daemon keeps the fan rotation speed above 4100 rpms. This was done to avoid transistor overload at lower rpms.
- OS was upgraded to armel platform (EABI). Notable improvements to the Linux platform (from Debian arm to Debian armel).
- Post-mortem can be triggered from three different sources: external trigger, interlock or post-mortem specific settings (X, Y positions, ADC overflow).
- The average of the sum signal between two triggers was calculated on sum data @ FA data rate.
- Spike removal was implemented in the FPGA (for FA/SA data) and in the SBC (turn-by-turn data) to eliminate glitches due to the switching. This functionality is configured with several parameters (average window length, apply window length, offsets).
- Table of BCD correction offsets was introduced in order to improve Beam Current Dependence (BCD) performance. Depending on the level of the current,

*Work supported by Chinese Academy of Science and National Natural Science Foundation of China (No. 11075198 and 11105211)
#yanyingbing@sinap.ac.cn

ISBN 978-3-95450-119-9

AN DBPM CALIBRATION METHOD IMPLEMENTED ON FPGA *

X.D. Sun#, Y.B. Leng†, SINAP, CAS,Shanghai, CHINA

Abstract

An calibration method on the four channels of DBPM is discussed. Using interpolation, the method is implemented on FPGA, which can handle the data on-line. The calibration algorithm is mono-channel dependent and is intended to solve the beam current dependence problem and increase resolution. Orientations of the method are presented. Basic design diagrams of the pipelined FPGA modules are listed and comparisons are made before and after the calibration.

INTRODUCTION

Due to the gain inconsistency across different channels of DBPM and the gain nonlinearity of the mono channel , problems of beam current dependence occur, which blurs beam position measurement.

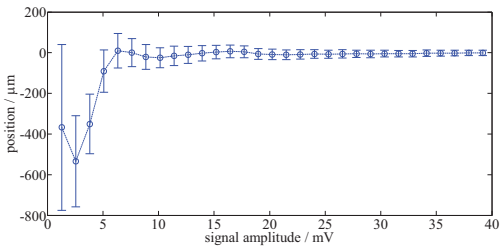

Figure 1: The beam current position dependence problem of the DBPM .

When Beam stays at the same position with increasing intensity, the same demodulated position output is expected but in practice not. The demodulated position output tend to be stable as beam current intensity increases as show in figure1. This is resulted from the fact that the channel give different gain to signal with the same frequency band but varying intensity, which we call signal channel nonlinearity and another aspect that four channels give different gain to the same signal.

The across channel inconsistency is caused by hardware inconsistency on the front end, which means that the four channel outputs differ with the same inputs, as shown in figure 2. whilst the mono channel nonlinearity refers to the fact that the gain of a channel to inputs with different intensity and deviates from a linear gain. The two aspects are shown together in figure3.

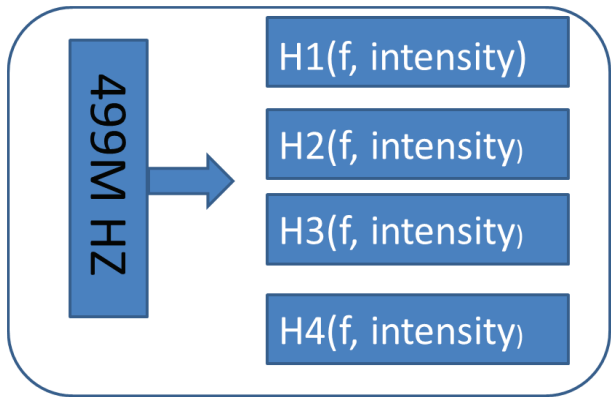

Figure 2: The four channel gain inconsistency of DBPM.

Different calibration methods have been proposed and implemented as a solution on respective instrument [2][4][5]. Libera EBPM use a Quasi-crossbar switch to randomly connect inputs to different channels thus in average remedy the inconsistency [2][3]. The SNS use the wave reflection to do calibration on the s plane analysis [5].

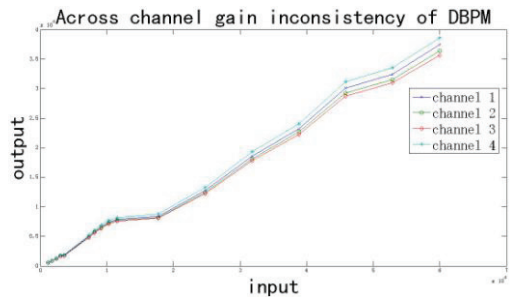

Figure 3: Across channel gain inconsistency of DBPM.

We have put forward a new approach based on DDC algorithm and attest its validity using Matlab on PC offline [4]. In this article, the calibration method using piece-wise linear interpolation is realized it on our self-developed DBPM using FPGA, thus the calibration is implemented on line directly after TBT data.

The advantage of our tactic is that it can remedy the inconsistency across different channels and the mono channel inconsistency together.

The basic idea of our method is that it try to align the four channel inconsistency to a single reference.

*Work supported by National Nature Science Fundation of China 11075198, #sunxudong@sinap.ac.cn, † leng@sinap.ac.cn

ISBN 978-3-95450-119-9

BEAM POSTION MONITOR FOR ENERGY RECOVERY LINAC*

I. Pinayev#, BNL, Upton, NY 11973, USA

Abstract

The energy recovery linacs have co-propagating beams inside the same vacuum vessel. These beams can have different trajectories, which should be distinguished by beam position monitors (BPM). In this paper we present a concept of a BPM utilizing the phase information for calculation individual position of each of the two beams (accelerating and decelerating). The practical realizations are presented and achievable accuracy is estimated.

INTRODUCTION

Most commonly used method for BPM is based on the evaluation of the signals induced on the pick-up electrodes (PUEs) by a circulating beam. Beam position is calculated from the signal amplitudes using delta over sum [1]. For the vertical plane BPM with two PUEs the equation is

$$y = k\frac{U_{up}-U_{down}}{U_{up}+U_{down}} \quad (1)$$

where U_{up} and U_{down} are the amplitudes, k is a scaling factor, which is determined by geometry. For a symmetrical system and beam in the center both signals have equal amplitudes and the corresponding position readback is zero.

With two (or more) beams circulating inside the vacuum chamber we need to separate the signals and process them individually. For the colliders with beams moving in the opposite directions this task is solved by utilizing the striplines, which have directional properties. The signals appear on the different ports and conventional processing units can be utilized.

This technique is not suitable for energy recovery linacs (ERL) where two or more beams co-propagate through a vacuum system and each beam has its own trajectory.

PROPOSED METHOD

For ERL with two co-propagating beams the time delay between accelerated and decelerated bunches is fixed by design and it becomes possible to employ the phase of the PUE signal to extract information on the position of each bunch. If bunches, separated by a flyby time Δt_{12}, have different positions then each PUE sees different longitudinal "center of gravity" (see Fig. 1) and there is a phase shift between two signals. For a processing unit, utilizing signal processing at frequency ω, and small displacements of the first and the second bunches δ_1 and δ_2 ($S\delta_1, S\delta_2 \ll 1$, where $S=1/k$ is a sensitivity coefficient) we can write the linearized equations:

*Work supported by Brookhaven Science Associates under Contract No. DE-AC02-98CH10886 with the U.S. DoE
#pinayev@bnl.gov

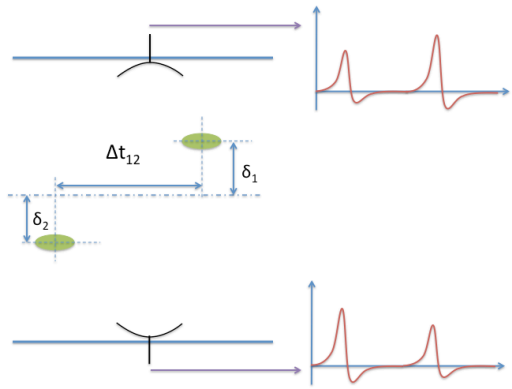

Figure 1: Signals induced on the pick-up electrodes by two bunches with different coordinates. Because of bunches' displacements the amplitudes of the induced voltages differ.

$$\begin{aligned} U_{up} &= U_1(1+S\delta_1)\sin\omega(t+\Delta t_{12}/2) + \\ &\quad U_2(1+S\delta_2)\sin\omega(t-\Delta t_{12}/2) \\ U_{down} &= U_1(1-S\delta_1)\sin\omega(t+\Delta t_{12}/2) + \\ &\quad U_2(1-S\delta_2)\sin\omega(t-\Delta t_{12}/2) \end{aligned} \quad (2)$$

When both bunches have equal charges (a valid assumption for ERL) then we re-write Eq. 2 as

$$\begin{aligned} U_{up} &= U_0\cos\tfrac{\omega\Delta t_{12}}{2}\left(2+S(\delta_1+\delta_2)\right)\sin\omega t + \\ &\quad U_0 S\sin\tfrac{\omega\Delta t_{12}}{2}(\delta_1-\delta_2)\cos\omega t \\ U_{down} &= U_0\cos\tfrac{\omega\Delta t_{12}}{2}\left(2-S(\delta_1+\delta_2)\right)\sin\omega t - \\ &\quad U_0 S\sin\tfrac{\omega\Delta t_{12}}{2}(\delta_1-\delta_2)\cos\omega t \end{aligned} \quad (3)$$

Neglecting second order terms we can estimate amplitudes ($A=\sqrt{U_{sin}^2+U_{cos}^2}$) of the signals induced on PUE

$$\begin{aligned} A_{up} &\approx 2U_0\left(1+S\tfrac{\delta_1+\delta_2}{2}\right)\cos\tfrac{\omega\Delta t_{12}}{2} \\ A_{down} &\approx 2U_0\left(1-S\tfrac{\delta_1+\delta_2}{2}\right)\cos\tfrac{\omega\Delta t_{12}}{2} \end{aligned} \quad (4)$$

Substitution of the found amplitudes into the Eq. 1 gives

$$\hat{y} = k\frac{S(\delta_1+\delta_2)}{2} = \frac{(\delta_1+\delta_2)}{2} \quad (5)$$

That means that using information on the amplitude we measuring the average position of the beam. Now we will consider the phases of the signals. Using the same assumptions we will find

ISBN 978-3-95450-119-9

HOM CHOICE STUDY WITH TEST ELECTRONICS FOR USE AS BEAM POSITION DIAGNOSTICS IN 3.9 GHZ ACCELERATING CAVITIES IN FLASH§

Nicoleta Baboi#, Bastian Lorbeer, DESY, Hamburg, Germany
Pei Zhang, DESY, Hamburg, Germany; UMAN, Manchester, UK
Nathan Eddy, Brian Fellenz, Manfred Wendt, Fermilab, Batavia, USA

Abstract

Higher Order Modes (HOM) excited by the beam in the 3.9 GHz accelerating cavities in FLASH can be used for beam position diagnostics, as in a cavity beam position monitor. Previous studies of the modal choices within the complicated spectrum have revealed several options: cavity modes with strong coupling to the beam, and therefore with the potential for better position resolution, but which are propagating within all 4 cavities, and modes localized in the cavities or the beam pipes, which can give localized position information, but which provide worse resolution. For a better characterization of these options, a set of test electronics has been built, which can down-convert various frequencies between about 4 and 9 GHz to 70 MHz. The performance of various 20 MHz bands has been estimated. The best resolution of 20 μm was found for some propagating modes. Based on this study one band at ca. 5 GHz was chosen for high resolution position monitoring and a band at ca. 9 GHz for localized monitoring.

INTRODUCTION

Higher Order Mode Beam Position Monitors (HOM-BPM) are devices that can be used to center the beam in accelerating cavities [1,2]. Since their principle relies on monitoring beam excited dipole modes, which are the main transverse component of the potentially damaging wakefields [3], they can help improve the quality of the charged particle beam. Moreover, they can be calibrated in terms of beam offsets, resembling a classical BPM.

HOM-BPMs have been built for the TESLA 1.3 GHz cavities at FLASH [1,4] and are routinely used for centering the beam. We are planning to build similar monitors for the 3.9 GHz cavities [5] in the same facility, often referred to as third harmonic cavities. The implementation is however much more complicated than in TESLA cavities for various reasons, briefly reviewed in the next section. Extensive studies have been made with the aim of defining the specifications of the HOMBPMs. The studies started with transmission measurements in each of the 4 cavities before and after installation in the cryo-module [6]. They continued with the dependencies of dipole modes on the transverse beam position, which had as result the identification of several regions in the HOM spectrum suitable for beam position monitoring [6,7]. The studies culminated with the examination of the potential of each region with a set of test electronics [8], which makes the subject of this paper. As a result, the specifications for the final electronics have been defined.

§Work supported in part by the European Commission under the FP7 Research Infrastructures grant agreement No.227579
#nicoleta.baboi@desy.de

FLASH

FLASH [4] is a Free Electron Laser facility generating short laser-like pulses with a wavelength between about 4 and 45 nm. It is also a test facility for the European X-ray FEL and the International Linear Collider. The first part of the linac is shown in Fig. 1. The photo-electric gun generates electron bunch trains with an energy of 5 MeV. These are accelerated by the first cryo-module, ACC1, containing 8 TESLA cavities. The subsequent cryo-module ACC39 is used to linearize the energy spread along the bunch generated by the non-linear accelerating field in ACC1 [9].

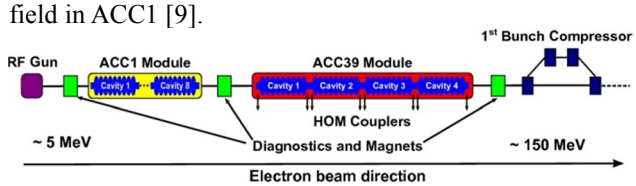

Figure 1: Schematics of the FLASH injector section.

The Third Harmonic Cavities

Four 3rd harmonics cavities are installed in the ACC39 cryo-module (Fig. 2). They are denoted with C1 to C4, in the beam direction. There are 9-cells per cavity. Each cavity is equipped with an input coupler and 2 HOM couplers, placed in the connecting beam-pipes, to extract energy from the beam excited HOMs and thus reduce their effect on the beam quality.

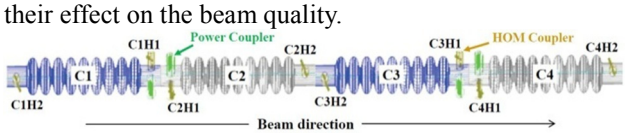

Figure 2: The four cavities in the ACC39 cryo-module. C2H1 means cavity 2, HOM-coupler 1.

The cavity design is inherited from the TESLA cavity. Figure 3 shows a picture of a 3.9 GHz cavity compared to a TESLA cavity. The main difference is the beam pipe diameter, which is larger than one third of the beam pipe in the TESLA cavity. This enables all HOMs to propagate along the module and therefore be damped by the couplers of all cavities.

ISBN 978-3-95450-119-9

TPS BPM ELECTRONICS PERFORMANCE MEASUREMENT AND STATISTICS

P. C. Chiu, K. H. Hu, C. H. Kuo, K. T. Hsu
NSRRC, Hsinchu 30076, Taiwan

Abstract

The BPM electronics Libera Brilliance+ are developed for Taiwan Photon Source (TPS) which is a 3 GeV synchrotron light source constructed at NSRRC. This BPM electronics can accommodate four BPM modules with integrated FPGA-based hardware. The BPM was contracted in the 2nd quarter of 2011; I-Tech award the contract to provide BPM electronics for the TPS project. The first prototype had been delivered in August 2011 and performed the preliminary test to verify fundamental specifications; the rest units had been delivered respectively in December 2011 and June 2012. The acceptance test for all units had been completed during June to August of 2012. Performance of each unit are individually tested and measured. Statistics data will be summarized in this report.

INTRODUCTION

The TPS is a state-of-the-art synchrotron radiation facility featuring ultra-high photon brightness with extremely low emittance [1]. Civil constructions are expected to be finished in early 2013. Machine commissioning is scheduled in 2014. The TPS accelerator complex consists of a 150 MeV S-band linac, linac to booster transfer line (LTB), 0.15–3 GeV booster synchrotron, booster to storage ring transfer line (BTS), and 3 GeV storage ring. The storage ring has 24 DBA lattices cells with 6-fold symmetry configuration. This synchrotron machine requires beam position stability less than 1/10 beam size therefore the position measurement system is also required to achieve one hundred or even tens of nanometer resolution. TPS has decided to adopt Libera Brilliance+ [2] electronics for the position measurement. The new instrumentation has the satisfactory performance and diagnostic functionalities as well as provides interface for fast orbit feedback application [3]. The vast tests including current dependency, filling pattern dependency, temperature dependency, latency estimation, long-terrn and short-term stability have been done and summarized in this report. Statistics data will be summarized.

BPM SPEC AND FUNCTIONALITES

The TPS storage ring is divided into 24 cells and there are 7 BPMs per cell; the booster ring has six cells where each cell is equipped with 10 BPMs. The number of BPM modules installed in the BPM platform might vary due to various install consideration and future expansion. Therefore, the BPM platform is designed to accommodate maximum 4 BPM modules. The TPS acquire 76 BPM platforms in MicroTCA based form factor and 228 BPM processors modules for storage ring and booster synchrotron application exclude the spares or the extra BPM due to the later design change.

The conceptual functional block diagram of the BPM is shown in Fig. 1. It will be embedded with EPICS interface for control, monitor and configuration. The timing AMC module would provide functionalities of synchronization, trigger, interlock and post-mortem. The BPM platform should also accommodate the FPGA module for fast feedback application for the future expansion.

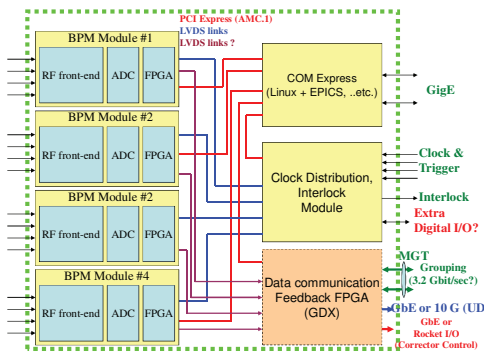

Figure 1: BPM platform functional block diagram.

The major specifications that the system must be fulfilled are also listed in Table 1.

Table 1: TPS BPM Performance Requirements

Parameters	Beam Charge/Current Range	Spec. (in rms)	Measured (in rms)
Single pass sensitivity and resolution	100 pC	< 1 mm	0.2 mm
Turn-by-turn resolution	0.5 mA	< 1 mm	0.15 mm
	10 mA	< 100 um	10 um
	500 mA	~ 1 um	1um
Resolution (10 Hz update rate)	0.5~10 mA	< 1000 nm	80 nm
	100~500 mA (14 dB range)	< 100 nm	20 nm
Resolution (10 KHz update rate)	100~500 mA	< 200 nm	100 nm
Beam current dependence	100~500 mA	< 1000 nm	200 nm
Filling pattern dependence	100~500 mA	< 1000 nm	200 nm
Temperature dependence		<1000 nm/°C	~ 100 nm/°C

ISBN 978-3-95450-119-9

DEVELOPMENT OF THE BEAM POSITION MONITORS FOR THE SPIRAL2 LINAC

M. Ben Abdillah, P. Ausset, J. Lesrel, P. Blache, P. Dambre, G. Belot, E. Marius
Institut de Physique Nucléaire d'Orsay, France

Abstract

The SPIRAL 2 facility will deliver stable heavy ion beams and deuteron beams at very high intensity, producing and accelerating light and heavy rare ion beams. The driver will accelerate between 0.15mA and 5 mA deuteron beam up to 20 MeV/u and also q/A=1/3 heavy ions up to 14.5 MeV/u.

The accurate tuning of the Linac is essential for the operation of SPIRAL2 and requires from the Beam Position Monitor (BPM) system the measurements of the beam transverse position, the phase of the beam with respect to the radiofrequency voltage and the beam energy.

This paper addresses all aspects of the design, realization, and calibration of these BPM, while emphasizing the determination of the beam position and shape. The measurements on the BPM are carried out on a test bench in the laboratory: the position mapping with a resolution of 50 µm is performed and the sensitivity to the beam displacement is about 1.36dB/mm at the centre of the BPM. The characterization of the beam shape is performed by means of a special test bench configuration.

An overview of the electronics under realization for the BPM of the SPIRAL2 Linac is given.

OVERVIEW

SPIRAL2 represents a major advance for research on exotic nuclei. It will provide better insight into the table of nuclides, thereby fostering the discovery of new properties of matter.

SPIRAL 2 Linac is installed in Caen, France. It is composed of 2 types of cryomodules A and B respectively for low (β= 0.04) and high (β=0.2) energy sections. Each of these cryomodules contains respectively one or two resonators superconducting radiofrequency cavities.According to beam dynamics calculations, all the cavities operate at 88.0525MHz.

A doublet of magnetic quadrupoles takes place between the cryomodules for the transverse horizontal and vertical focusing of the beam.

Measurement of the particle beam position in accelerators is an essential part of beam diagnostics, and the Beam Position Monitors (BPMs) provide the basic diagnostics tool for commissioning and operation of accelerators. One of the primary applications of the BPMs is the stabilization of the particle beam positions through feedback.

In order to save room, BPM will be inserted in the vacuum pipe inside the quadrupoles which will be buried at their turn in the quadrupole magnet.

Different beams are accelerated by SPIRAL2; Table 1 shows the main characteristics of some of these beams at the start and at the end of the linac.

Table 1: Beam Characteristics

	Linac start	Linac End
Beam relative velocity β	0.04	0.2
Beam energy (MeV)	1.46	40

The specifications of the required BPM resolution for beam position feedback in SPIRAL2 linac are listed in Table 2.

Table 2: BPM Specifications

Beam position resolution	50 um
Beam position range	±20 mm
Beam shape resolution	20%

This paper addresses the design, realization and calibration of these BPMs; it also shows the design adopted for the realization of the BPMs acquisition cards.

BPM DESIGN

SPIRAL2 BPMs have four electrodes mounted directly within the focusing magnets as shown in Figure 1 (A zoom of the BPM portion is shown on the right) . A BPM has four electrodes that couple to the beam through the image charge produced by the beam [1].

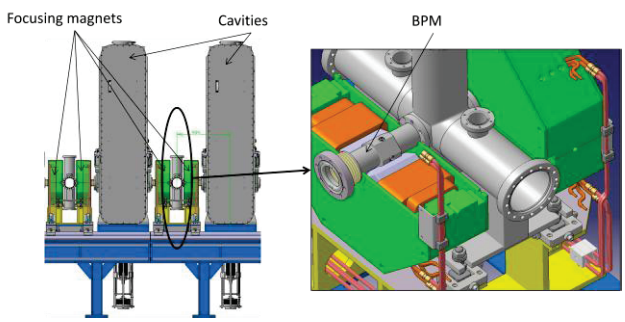

Figure 1: BPM position inside the linac.

The influence of the electrode dimensions on the signal level and harmonic content for different beams was calculated using the method described by Schulte [2]. The BPM electrodes are considered as capacitors that are

ISBN 978-3-95450-119-9

FIRST TESTS OF A LOW CHARGE MTCA-BASED ELECTRONICS FOR BUTTON AND STRIP-LINE BPM AT FLASH

B. Lorbeer*, N. Baboi, F. Schmidt-Föhre, Deutsches Elektronen-Synchrotron†, Hamburg, Germany

Abstract

Current FEL based light sources foresee operation with very short electron bunches. These can be obtained with charges of 100pC and lower. The typical charge range for FLASH, DESY, Hamburg spans a range from 100pC up to 1nC. The electronics currently installed at button and strip-line BPMs have been designed for best performance at higher charges and have reached their limits. Currently, for low charges a new type of electronics is being developed to overcome these limitations. These electronics are conforming with the MTCA.4 for physics standard [1]. The next generation of FLASH BPM electronics is suitable for measurements of button and strip-line BPMs. Furthermore, the first measurement results taken with beam at FLASH, DESY are presented here.

INTRODUCTION

Free-electron-laser (FEL) user facilities like FLASH at DESY and LCLS at SLAC have been established as very useful sources in the VUV and X-Ray regime. Apart from the laser-like features of these sources, the short light pulses produced by these machines are very attractive for users. Recently it turned out that the typical pulse length of about 100fs can be shortened substantially. The operation of these FEL facilities have demonstrated that beam charges smaller than 100pC allow the generation of very short electron bunches resulting in FEL pulse lengths in the few fs regime [2, 3]. Since existing electronics for button and strip-line beam position monitors (BPM) of FLASH have been designed for a charge of about 1 nC, they show insufficient resolution for machine operation below 300pC. Therefore, a new type of button and strip-line electronics is under development. The dynamic range has been extended to lower charges to match the increasing need for low charge operation. At FLASH the Micro Telecommunication Computing Architecture (MTCA) for physics standard will replace the old Versa Module Eurocard (VME) based electronics of the old BPM system. The standard introduces a new environment for the analog front-end and digitizer electronics. The specifications for the new FLASH BPM electronics match with the ones from European XFEL [4]. The requirement for single-bunch resolution is 50μm in an aperture of +/- 3mm of center with a beam line diameter of 40mm [5]. In this paper the first prototype BPM electronic system based on the MTCA.4 standard is introduced. The analog electronics are described in detail. The first measurements with single-bunch operation are presented.

* bastian.lorbeer@desy.de
† DESY

OVERVIEW

The MTCA-based button and strip-line BPM system is schematically shown in Fig. 1.

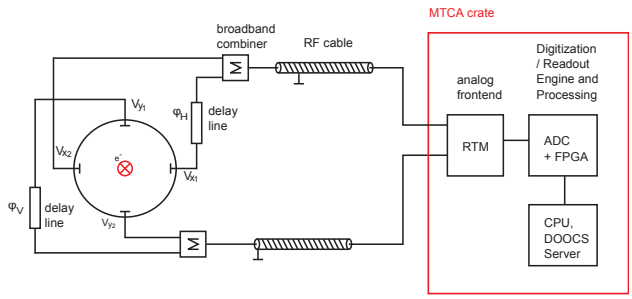

Figure 1: BPM conceptual system setup. One signal of each plane from the BPM is combined with the other after a delay of ca. 100ns. The combined signals are then transported over a long RF cable from the tunnel to the electronic racks.

It follows the well-known Delay Multiplex Single Path Technology (DMSPT), originally developed in 1986 for the HERA accelerator at DESY[6]. The pick-ups of the button and strip-line BPMs are oriented in the vertical and horizontal plane in the beam line. The strip-line monitor under test is the main type of standard BPM currently in operation at FLASH. The beam line diameter is 34mm and the strip-line length is 200mm. The button monitor used here is a prototype button BPM for the E-XFEL. It is an improved HERA type button pick-up design to match the needs in linear machines such as FLASH, and the E-XFEL. The button diameter is 16mm and the beam line diameter is 34mm. It has been installed and studied in the last year at FLASH [7]. The signals V_{x_1} and V_{x_2} in the horizontal, and V_{y_1} and V_{y_2} in the vertical plane are concatenated with the help of a broadband radio frequency (RF) combiner. This is done by inserting a delay of 100ns for V_{x_1} and V_{y_1} with respect to the other signal in each plane. Finally the signals are travelling on a 80 m long 3/8" RF-cable from a patch panel in the tunnel to a patch panel at an electronic rack outside the tunnel. This method has a superior common mode electromagnetic interference (EMI) rejection compared to a single RF cable connection for both signals in each plane. Typical signals from a button and a strip-line monitor are shown in Fig. 2. A zoom of the signals is shown in Fig 3.

The rise-time of both signals is in the order of a few hundred picoseconds. Though the signal shape for both types of BPM is entirely different, the front-end can measure both types of waveforms. With a beam charge of 100pC and a centered beam the signal strength is $180\mathrm{mV_{peak}}$ for the strip-line and $270\mathrm{mV_{peak}}$ for the button BPM. The

ISBN 978-3-95450-119-9

DESIGN OF RF FRONT END FOR CAVITY BEAM POSITION MONITOR BASED ON ICS*

B.P. Wang#, Y.B. Leng†, L.Y. Yu, W. M. Zhou, R.X.Yuan, Z.C. Chen,

SSRF, SINAP, Shanghai, China.

Abstract

RF front end has the significant impact on the performance of cavity beam position monitor (CBPM) which is indispensable beam instrumentation component in free electron laser (FEL) or linear collider facility. With many new advances in data converter and radio technology, complex RF front end design has been greatly simplified. Now a based digital intermediate frequency (IF) receiver architecture RF front end for CBPM has been designed by using surface mount components on print circuit board (PCB). The front end contains analog-digital converter used to digitize the IF signals. The whole system would be integrated to a digital board developed by our lab to produce the dedicated signal processor for CBPM. There is a Xilinx Vertex-5 FPGA device on the digital board and relevant signal processing algorithm has been implemented on it using VHDL. The details about design would be introduced blow.

INTRODUTION

CBPM is a key beam instrumentation component only which could reach sub micron or nano resolution in all beam position measure solutions[1][7][8][10]. So it was seen as a necessary solution to measure beam position in the long undulator section of shanghai soft X ray FEL facility[2] which is on the way. Nowadays, CBPM signal processing system is on the stage of development and some preliminary system hardware frame has been completed, and relevant offline signal algorithms also have been verified and implemented in Matlab[4]. The whole system hardware frame contains RF front end accomplished by using microwave connectors and high speed ADC board integrated digital signal processing chip-FPGA on which the online algorithm was implemented. It also makes pulse-by-pulse position measurement come true. Some bench test results have been acquired. But in the aspect of system integration and cost, the current system did not behave well. So taking all the elements into account we decided to develop the new RF front end by using surface mounted components on the PCB. Also the RF front end, including the RF signal conditioning module and ADC module, by using high speed connectors, was integrated into a digital board which consists of Vetex 5 FPGA chip and ARM signal board computer[3]. So the dedicated and high integration level signal processor for CBPM may replace the previous system as results of cost saving.

* Work supported by National Natural Science Fundation of China (11075198)

wbplll@sinap.ac.cn † lengyongbin@sinap.ac.cn

LAYOUT DESIGN

The RF front end topology used a single stage three channels digital IF receiver architecture[9] which contains three sections: an RF signal conditioning module, a based phase locked loop (PLL) LO and ADC module. Figure 1 shows the schematic of RF front end.

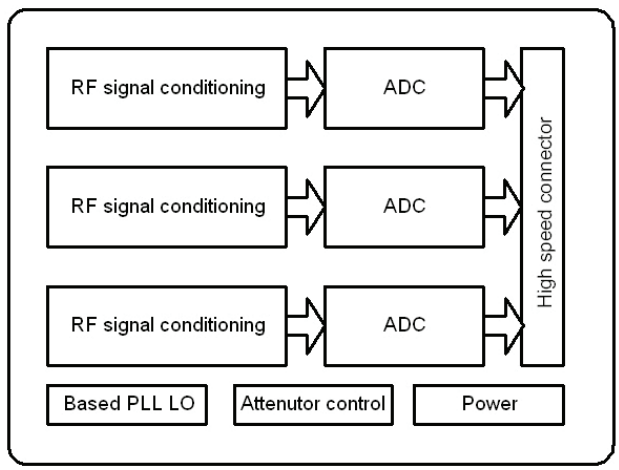

Figure 1: Schematic of RF front end.

In the signal conditioning module, the output signal of CBPM must enter into band pass filter to eliminate interference from other resonant mode. But surface mounted band pass filter was not chose in our design since its characteristic of stop band attenuation could not meet CBPM requirement of high quality factor [4]. So a connector of resonant cavity BPF was also needed prior to the board level RF front end.

RF CONDITIONING

The function of RF signal conditioning module is to downconverted RF signals to IF signals which could be digitized by some high precision ADC. Details about signal conditioning module were shown in Figure 2.

Considering the protection of amplifier against high power surges, we chose a limiter prior to the amplifier as its maximum input power is about 11dBm. And then RF signals were first amplified by low noise amplifier (LNA) of 16dB gain. A digital attenuator was used to adjust the signal intensity and make the RF channels compatible to high Q and low Q cavity. A mixer converted the RF signals down to 20MHz IF signals. A 22MHz cutoff low

ISBN 978-3-95450-119-9

PERFORMANCE OF A DOWNCONVERTER TEST-ELECTRONICS WITH MTCA-BASED DIGITIZERS FOR BEAM POSITION MONITORING IN 3.9GHz ACCELERATING CAVITIES

T. Wamsat*, N. Baboi, B. Lorbeer, Deutsches Elektronen-Synchrotron DESY, Hamburg, Germany
P. Zhang, The University of Manchester, Manchester, U.K.

Abstract

Beam-excited higher order modes (HOM) in 3.9GHz accelerating cavities are planned to be used for beam position monitoring at the European XFEL. The selected HOMs are located around 5460MHz, with a bandwidth of 100MHz and 9060MHz, with a bandwidth of 50MHz. A downconverter electronics, built for tests at FLASH, converts the HOMs to an intermediate frequency of 70MHz. The MTCA (Micro Telecommunications Computing Architecture) standard will be used for the XFEL. Thus it is important to have a performance study of the downconverter test-electronics using the MTCA digitizer card SIS8300. In the digitizer the IF frequency of 70MHz is undersampled with a clock frequency of 108MS/s. The paper presents the performance of the digitizer together with the test-electronics. A comparison with a 216MS/s VME (Versa Module Eurocard) digitizer is made.

INTRODUCTION

The ACC39 module in FLASH, DESY [1] contains four third harmonic cavities operating at 3.9GHz as shown in Fig. 1. An electron bunch passing through these cavities generates wakefields, which can be decomposed into higher order modes (HOM). These HOMs, available from existing coupler, can be used to determine transverse beam positions in the cavities [2] [3].

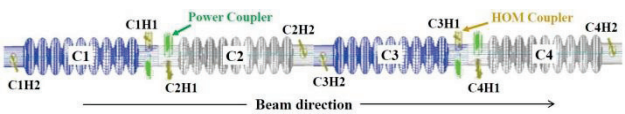

Figure 1: Schematic of the four cavities within ACC39.

In 3.9GHz cavities HOMs around 5460MHz and 9060MHz are used to determine the beam position [4].

Measurement Setup

The HOM signals are downconverted to an intermediate frequency (IF) of 70MHz which is then digitized. Figure 2 shows the schematic block diagram of the downconverter, built by FNAL [4].

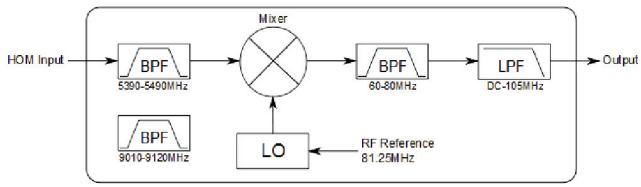

Figure 2: Schematics of the downconverter analog box.

A bandpass filter (BPF) with an appropriate frequency band filters the HOM signal and then it is connected to a mixer. A local oscillator (LO) which uses a 81.25MHz reference from the master oscillator of FLASH generates the required LO frequency. The IF signal is then filtered with a 20MHz bandpass filter. After a proper amplification, the IF is further filtered by a lowpass filter (LPF) to reduce the noise. To switch the analog box to another frequency, the bandpass filter was swapped and the frequency of the LO was changed accordingly to ensure an IF of 70MHz.
The analog electronics is shown in Fig. 3.

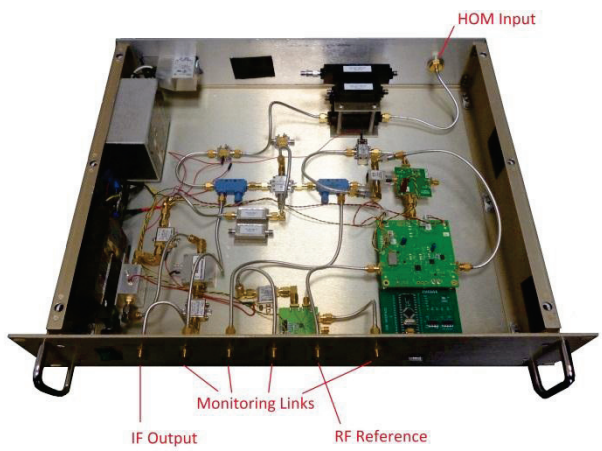

Figure 3: Downconverter analog box.

The downconverted HOM signal was digitized by the VME and also by the MTCA. The former used a sampling rate? of 216 MHz, and the second 108MHz. The setup used to make a comparison between the VME and MTCA is shown in Fig. 4.

*thomas.wamsat@desy.de

ISBN 978-3-95450-119-9

DESIGN OF CAVITY BPM PICKUPS FOR SWISSFEL

Fabio Marcellini, Boris Keil, Martin Rohrer, Markus Stadler, Jerome Stettler, Daniel Marco Treyer,
PSI, Villigen, Switzerland
Dirk Lipka, Dirk Noelle, Maike Pelzer, Silke Vilcins, DESY, Hamburg, Germany

Abstract

SwissFEL is a 0.1nm hard X-ray Free Electron Laser being built at PSI. A photocathode gun, S-band injector and C-band linac provide 2 bunches at 28ns spacing, 10-200pC charge range, 100Hz repetition rate, and 5.8GeV maximum energy. A fast distribution kicker will provide one bunch each to one hard X-ray and one soft X-ray undulator line. For linac and undulators, first prototypes of dual-resonator cavity BPM pickups have been designed and one undulator prototype has been fabricated. The pickups were optimized for low charge and short bunch spacing in the linac. Design considerations, simulation and first test results will be reported.

INTRODUCTION

SwissFEL [1] requires three different BPM pickup types, due to the different beam pipe apertures along the machine: 38mm in the injector, 16mm in the linac, and 8mm in the undulators. The desired BPM RMS noise and drift is <1 μm for the undulators, <5 μm for the linac, and <10 μm for the injector, for a charge range from 10-200pC. For the SwissFEL undulators, we will use dual-resonator cavity BPMs due to their good achievable drift and noise level even at low charge.

At the SwissFEL injector test facility (SITF) that is operational since 2010, resonant striplines are used as "working-horse" BPMs, achieving 7 μm RMS noise down to charges of 5pC [2], while a test section at the end of the machine is used for cavity BPM tests.

For the final SwissFEL machine, we plan to use cavity BPMs in the accelerator, including injector and linac. This will allow to have a homogeneous BPM system and to be able to use the latest electronics generation for the whole machine, based on our developments for the E-XFEL BPM system [3].

Both the RF and mechanical designs of the present SwissFEL cavity pickup prototypes were largely inspired by devices developed in Japan for the XFEL/Spring-8 [4] and at DESY for the E-XFEL [5]. In particular, we plan to use the 3.3GHz working frequency of the E-XFEL undulator BPMs also for SwissFEL injector and linac pickups. This choice allows us to adapt our E-XFEL cavity BPM electronics to SwissFEL linac and injector BPM requirements with relatively small effort, thus maximizing the synergies of the E-XFEL BPM collaboration between PSI and DESY on this subject and minimizing costs and man power.

For the present SwissFEL BPM pickup prototypes, we adapted the loaded quality factor (Q) and sensitivity to the lower bunch charge range (10-200pC) and bunch spacing (28ns) of SwissFEL, since the E-XFEL BPM pickups were designed for 100-1000pC and 222ns bunch spacing.

As shown in Fig. 1, each pickup consists of two cavities having a folded shape to limit their transverse dimensions and get a more compact device. The working modes are TM_{110} (dipole) for the so called position cavity and TM_{010} (monopole) for the reference cavity. When the beam crosses the two cavity gaps it induces signals proportional to the product of charge and position offset in the position cavity, and to the charge only in the reference cavity. The beam position is then obtained by dividing the two signal amplitudes, which are available at the outside by means of properly designed couplers. In particular, the position cavity has four rectangular waveguides that couple to the dipole mode while rejecting the monopole mode that would otherwise limit the resolution of the electronics.

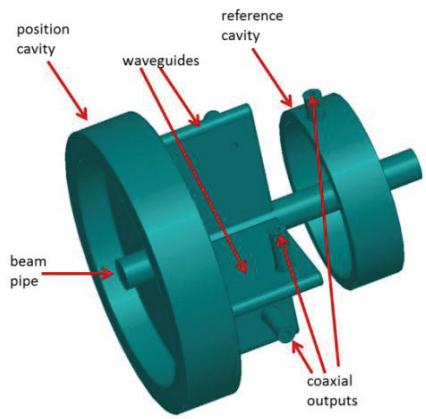

Figure 1: Cavity BPM pickup schematic view (shown: vacuum).

The waveguides are connected to the cavity volume through slots placed 90° apart from each other on one cavity side wall. Each waveguide has a transition to a coaxial line which ends with a standard type-N connector output. In the reference cavity the signal is coupled out by means of a coaxial line where the inner conductor passes through the cavity (predominantly magnetic coupling). The position and the reference cavities must have a sufficiently large distance to each other to avoid crosstalk. This distance needs to be increased with increasing diameter of the beam pipe.

In the following sections, the undulator and linac pickup design as well as lab measurements of the RF characteristics of the first undulator pickup prototypes are presented. The design of the injector BPM has not yet started.

UNDULATOR CAVITY BPM

Design and Simulation Results

The design of the SwissFEL BPM system is based on the E-XFEL cavity BPMs where the pickup is developed by DESY and the electronics by PSI. Since SwissFEL

ISBN 978-3-95450-119-9

SIGNAL TRANSMISSION CHARACTERISTICS IN STRIPLINE-TYPE BEAM POSITION MONITOR

T. Suwada*, KEK, Tsukuba, Ibaraki 305-0801, Japan

Abstract

A new stripline-type beam position monitor (BPM) system is under development at the KEK electron/positron injector linac in order to measure transverse beam positions with a high precision less than 10 μm towards the Super KEKB-factory (SKEKB) [1] at KEK. The new stripline-type BPMs with a large aperture compared with previously designed BPMs have been designed for the installation in the positron capture section. In this report, the basic design for the fabrication of the prototype BPM, the theoretical analysis, and the experimental investigation on the signal transmission characteristics and its performance are in detail described on the base of a coupled-mode analysis in uniform transmission lines.

INTRODUCTION

A stripline-type BPM is a well-known beam diagnostics device to measure transverse beam positions in a plane perpendicular to the beam axis. There are many excellent review articles on this subject (see, for example, [2, 3]). In general, a stripline-type BPM has four stripline electrodes which are mounted on the inner surface of a circular pipe with $\pi/2$ rotational symmetry. The upstream port of the stripline electrode is a signal pickup and the downstream port may be short- (or 50-Ω-) terminated to the pipe ground or left open.

When a charged-particle beam passes through the BPM, a characteristic signal with bipolar shape is induced on all the stripline electrodes due to electromagnetic coupling between the electrodes and the beam. The induced signals are fed into a detection electronics through vacuum-feedthrough pickups, and the signal intensities are measured by the detection electronics. The transverse beam positions can be obtained by calculating a weighted average of the four signal intensities based on algebraic calculations. This is a basic principle on measuring transverse beam positions with a stripline-type BPM.

The signal intensity induced on each stripline electrode can be generally analyzed based on a so-called wall-current model [2], in which the wall current is a mirror current induced on the stripline electrode. Based on this model, the signal intensity may be proportional to the intensity of the wall current, that is, the beam charges, and also proportional to the angular width of the stripline electrode. Such the analysis may be fundamentally based on an electrostatic model taking into account only electrostatic coupling between the stripline electrodes and the beam.

In conventional stripline-type BPMs, there are some varieties in spatial configuration and mechanical structure of the stripline electrodes which are mounted on the inner surface of the BPM. The stripline electrode with a finite angular width viewed from the beam may be mounted with a certain gap between the electrode and the inner surface of the pipe. In such a mechanical configuration, not electrostatic coupling but electromagnetic coupling may dynamically arise between the electrodes and also between the electrodes and the beam, and thus, the signal intensities may change to some extent from the wall-current model.

From another point of view on a signal-gain calibration in a stripline-type BPM, it is important to analyze the electromagnetic coupling strengths between the stripline electrodes. An excellent calibration procedure has been implemented to stripline-type BPMs by Medvedko *et al.* of SLAC [4]. In this calibration procedure, an on-board calibrator embedded in the detection electronics sends its calibration signal to one of the electrodes. When the calibration signal is fed into the electrode, similar bipolar signals are induced on the other electrodes due to electromagnetic coupling. The induced signal goes back to the corresponding channel in the detection electronics in which the signal intensity is precisely measured. Thus, in such a calibration procedure, not only the signal gains in the detection electronics but also the transmission losses in entire transmission lines including the stripline electrodes themselves can be calibrated with high precision. Thus, this new calibration procedure make use of electromagnetic coupling between the stripline electrodes of the BPM.

Although electromagnetic coupling between the stripline electrodes is an important physical phenomena in the stripline-type BPM, only a few analyses have been performed to investigate the signal transmission characteristics taking into account electromagnetic coupling between the electrodes. A new analysis on the signal transmission characteristics with electromagnetic coupling between the electrodes are presented in this article. The new analysis exploits a similar method developed in microstripline circuits with electromagnetic coupling. Based on the new analysis, the signal transmission characteristics in the stripline-type BPM is systematically investigated in frequency domain along with experimental verification.

STRIPLINE-TYPE BEAM POSITION MONITOR

A new stripline-type BPM with a large aperture is shown in Fig. 1. This BPM is under development for the new positron beam line so as to reduce the beam losses in the positron transmission as small as possible. The mechanical structure of the BPM is a conventional stripline-type

* tsuyoshi.suwada@kek.jp

ISBN 978-3-95450-119-9

DEVELOPMENT OF NEW BPM ELECTRONICS FOR THE SWISS LIGHT SOURCE

W. Koprek, R. Baldinger, R. Ditter, B. Keil, G. Marinkovic, M. Roggli, M. Stadler, PSI, Villigen, Switzerland

Abstract

PSI is currently developing new BPM electronics for the Swiss Light Source (SLS). Although the present "DBPM1" system that was designed 12 years ago still allows to achieve excellent beam stability and uptime, the development of a new system is motivated by long-term maintenance, improved performance in line with increasing user requirements, and new features and functionality provided by latest electronics technology. The new system is based on a generic modular BPM electronics platform developed by PSI that will also be used for linac based Free Electron Lasers (FEL) like European XFEL and SwissFEL. The hardware and firmware architecture of the present prototypes as well as first test results will be presented.

PRESENT SLS BPM SYSTEM

The Swiss Light Source is operational since eleven years and delivers high brightness photon beams to experimental stations. One of the most important properties of the machine is high stability and reproducibility of the electron orbit at the location of the radiation source points. The high stability is maintained by a fast global orbit feedback (FOFB) [1]. The feedback consists of 72 BPMs and 72 corrector magnets grouped in 12 sections as presented in Fig. 1.

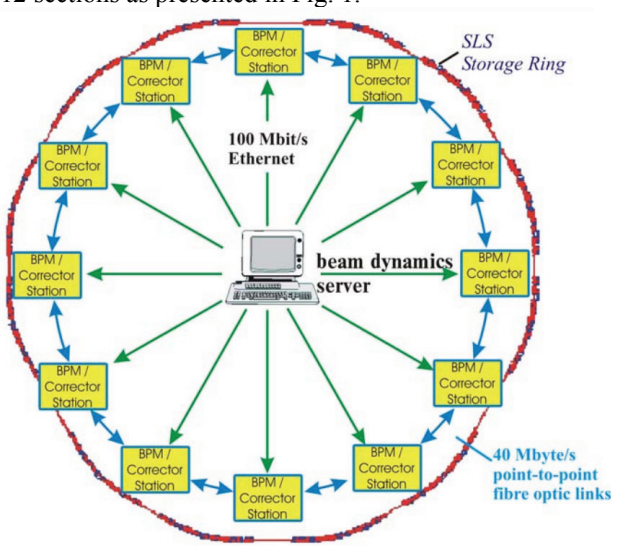

Figure 1: Overview of SLS global orbit feedback.

Each section typically contains six BPMs. The horizontal and vertical position of the six BPMs is calculated in a single DSP board and the data is exchanged with adjacent sections through fibre optic links. This structure allows, on the same DSP board, calculation of the current set values for six vertical and six horizontal dipole corrector magnets from 18 beam position readings, with an update rate of 4 kHz.

BPM UPGRADE DEVELOPMENTS

The planned upgrade of BPM system is motivated by long-term maintenance, improved performance and future user requirements. By using the latest FPGA, ADC and RF technology, the resolution and latency of the new BPM system can be improved significantly. In contrast to the present system where the 500MHz signals from the button pickup electrodes are mixed to a 36MHz IF that is sampled by 12-bit ADCs at 31MSPS, the new electronics will (under-)sample the 500MHz pickup signals directly. The system will be based on a generic modular electronics framework developed at PSI [2]. While the present BPM digitizer boards just provide button pickup signal amplitudes and the FOFB DSP boards are used to calculate a calibrated beam position and related data like RMS values, the new BPM electronics will take over this functionality and provide calibrated position data to the control system and to a new global fast feedback network via multi-gigabit fiber optic links.

General Layout

Figure 2 shows the different modules of the present prototype electronics for the new SLS BPM system. The 500MHz signals of the button pickup electrodes are received by an RF front-end (RFFE) that performs amplification and filtering (no mixers). The RFFE is connected to four 16-bit ADCs of a mezzanine, where two mezzanines are plugged onto one FPGA carrier board (GPAC = Generic PSI ADC Carrier).

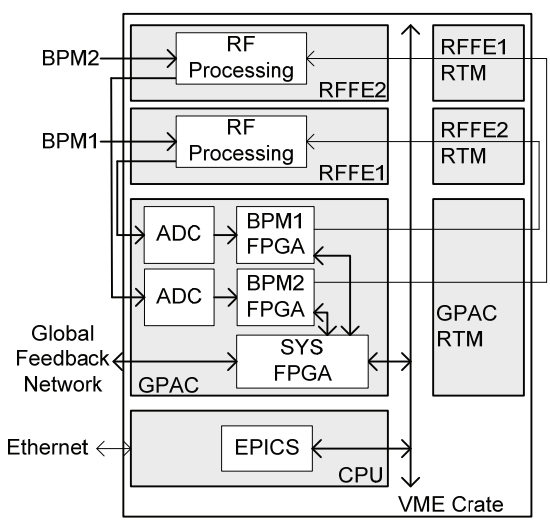

Figure 2: Block diagram of the new SLS BPM system.

ISBN 978-3-95450-119-9

BEAM TEST RESULTS OF UNDULATOR CAVITY BPM ELECTRONICS FOR THE EUROPEAN XFEL

M. Stadler*, R. Baldinger, R. Ditter, B. Keil, R. Kramert, G. Marinkovic, M. Roggli,
PSI, Villigen, Switzerland
D. Lipka, D. Nölle, M. Pelzer, S. Vilcins-Czvitkovits, DESY, Hamburg, Germany

Abstract

The European X-ray Free Electron Laser (E-XFEL) will use dual-resonator cavity BPMs (CBPMs) between the SASE undulators and in the beam transfer lines to measure and stabilize the beam trajectory. The BPM electronics is developed by PSI, while the pickup mechanics is developed by DESY. BPM electronics beam tests with three adjacent pickups have been performed at the SwissFEL injector test facility (SITF) at PSI. The system architecture and algorithms, achieved performance and noise correlation measurements of the present electronics prototypes will be presented.

INTRODUCTION

The European XFEL (E-XFEL) [1] has a superconducting 17.5GeV main linac that will provide trains of up to 2700 bunches, with 0.1-1nC bunch charge range, 600μs train length, ≥222ns bunch spacing, and 10Hz train repetition rate. A kicker/septum scheme can distribute fractions of the bunch train to two main SASE undulator lines followed by "secondary undulators" for spontaneous or FEL radiation. The E-XFEL will provide SASE radiation down to below 0.1nm wavelength and supports arbitrary bunch patterns within a bunch train, with bunch spacing of n*111ns, where n is an integer >1.

The E-XFEL is presently under construction in Hamburg, with first injector beam scheduled for 2014 and first main linac beam and SASE for 2015.

The cavity BPM electronic system is being developed at PSI [2,3]. For preliminary performance measurements an array of 3 E-XFEL cavity BPMs have been installed at the SwissFEL injector test facility [4].

CAVITY PICKUP

The 3.3 GHz cavity pickups were designed at DESY [5]. They have the parameters given in Table 1.

Table 1: Undulator cavity BPM pickup parameters (10mm beam pipe aperture)

	position cavity (TM110 mode)	reference cavity (TM010 mode)
Resonant frequency	3300 MHz	3300 MHz
Sensitivity	2.8 mV/nC/μm	42 V/nC
Cavity loaded-Q	70	70

*markus.stadler@psi.ch

BPM ELECTRONICS

The present BPM electronics prototype consists of:

- The RF front-end electronics (RFFE): One I/Q downconverter and LO synthesizer for reference, x- and y-position signal channel, and an ADC sampling clock synthesizer. Active local temperature stabilizers are employed for drift reduction.
- 6-channel, 16-bit 160MS/s analog-to-digital converters for all RFFE I and Q baseband differential output signals.
- Digital signal processing hardware ("GPAC" board) for signal processing and interfacing to control, feedback, timing and machine protection systems.

RF Frontend

The simplified block diagram of the RFFE electronics used is shown in Fig. 1. The basic principle of the BPM electronic and cavity design is based upon ref. [6].

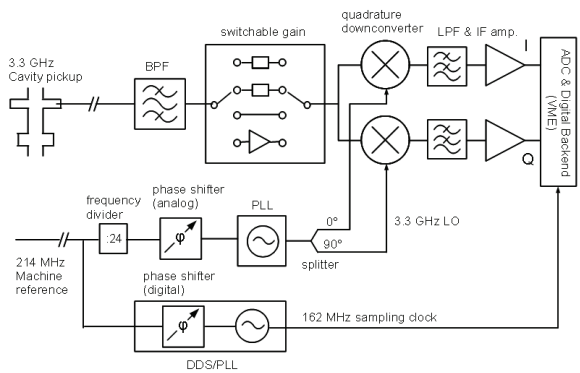

Figure 1: Simplified downconverter block diagram (one channel).

An input bandpass filter selects the cavity signal components around 3.3GHz. The filter is followed by a switchable gain section. The gain is selected depending on the actual bunch charge (4 charge ranges).

The quadrature downconverter operates with an LO frequency of approximately 3.3GHz. This frequency is equal for all three channels (reference-, x- and y-channel).

A reference signal (214 MHz at the SwissFEL injector test facility, 216.66 MHz at EXFEL) is provided from the machine reference system. This signal is divided by 24 with a divider common to all LO PLLs on the RFFE.

The ADC is clocked by a signal also generated on the RFFE. Its phase is controllable in 0.5° steps around the

ISBN 978-3-95450-119-9

IMPLEMENTATION OF AN FPGA BASED SYSTEM SURVEY AND DIAGNOSTIC READER WITH THE AIM TO INCREASE SYSTEM DEPENDABILITY

Marcel Alsdorf, Bernd Dehning, Maciej Kwiatkowski, William Vigano, Christos Zamantzas
CERN, Geneva, Switzerland

Abstract

The operation and machine protection of accelerators practically rely on their underlying instrumentation systems and a failure of any of those systems could pose a significant impact on the overall reliability and availability. In order to improve the detection and in some cases the prevention of failures, a survey mechanism could be integrated to the system that collects crucial information about the current system status through a number of acquisition modules.

The implementation and integration of such a method is presented with the aim to standardize the implementation, where the acquisition modules share a common build and are connected through a standardized interface to a survey reader. The reader collects regularly data and controls the readout intervals. The information collected from these modules is used locally in the FPGA device to identify critical system failures and results in an immediate failsafe reaction with the data also transmitted and stored in external databases for offline analysis.

INTRODUCTION

The basic functionality of the System Survey and Diagnostic Reader is to readout diagnostic data from external chips and sensors connected to an FPGA, process them and finally log them in a database or directly use them on-chip to monitor the system status.

The general goal is, to utilize such a reader on the beam-loss monitoring (BLM) electronics for the CERN injector complex. This system consists of three FPGAs mounted on three different PCBs, where each of them is connected to different kinds of external diagnostic chips and sensors. For a detailed overview on this particular system see TUPA09 [1].

To realize this goal, a design is needed, that is suitable for many different environments. In this case such an environment would be primarily defined by the number and types of different diagnostic interfaces and by the means of processing and forwarding those informations to an external logging database.

In the following sections the fundamental concepts, the design and the implementation of this System Survey and Diagnostic Reader will be presented, that is independent from the types of external diagnostic interfaces used and from its surrounding environment.

GENERAL CONCEPT

The key to any new hardware or software design or the enhancement of a given one is to evaluate the performance of it with regards to the quality characteristics defined in ISO 25010 [2]. Through this method, the usefulness of a design can be evaluated and weak points can be revealed and reinforced accordingly.

One approach to achieve this goal is to carefully divide the underlying problem into multiple smaller and easily solvable problems. In a software environment this is an old and well know approach called Divide-and-Conquer. In a hardware environment it is fairly unused. Due to typically long development times in hardware design, designers are often times discouraged to invest even more time in the generalization and optimisation of their design according to those quality characteristics. In term it is often overlooked, that in most cases it is sufficient to invest this additional time only once and to profit from it thereafter in upcoming design challenges.

In the here presented System Survey and Diagnostic Reader the approach is taken to logically divide the hardware design into two abstraction levels. The fundamental architecture of the design builds the lower level. This architecture defines the structure of design components, the general behaviour of them and their way of communicating with each other. The upper level on the other hand is defined by the functional model of the design. On this abstraction level those before mentioned components are seen as sub-functions, that can be combined to build more complex functions and consequently entire digital systems.

In the following two sections the fundamental architecture and the functional model for the System Survey and Diagnostic Reader are presented and analysed with respect to their improvements in design quality. As fundamental architecture a modular structure is used called Common Modular Interconnect (CMI).

COMMON MODULAR INTERCONNECT

In a typical digital architecture functional modules are specifically build with respect to their surrounding environment. This approach leads to various problems. Firstly, they depend on the timing behaviour of their surrounding modules. If there are modules, that take a given amount of time to complete their task, they introduce a high delay in this area of the design. Consequently, neighbouring modules have to be adapted to ensure proper timing. This condition in turn limits those neighbouring modules to work

ISBN 978-3-95450-119-9

DEVELOPMENT OF A BEAM LOSS MEASUREMENT SYSTEM WITH GIGABIT ETHERNET READOUT AT CERN

M. Kwiatkowski, M. Alsdorf, E. Angelogiannopoulos, B. Dehning,
S. Jackson, W. Vigano, C. Zamantzas, CERN, Geneva, Switzerland

Abstract

The aim of the BLM Dual Polarity module under development at the European Organisation for Nuclear Research (CERN) is to measure and digitise with high precision the current produced by several types of beam loss detectors. In its default configuration, it is expected to provide data to the processing electronics through two point-to-point connections with bidirectional multi-gigabit optical links. For the development phases as well as later serving as a standalone measurement system, its reconfigurable FPGA device is exploited to provide a soft-core CPU with a custom made server. This server, running on the CPU, will expose through the Gigabit Ethernet connection and the TCP/IP protocol different types of data in the network. In this paper the development of the system and of the communication protocol is explored as well as the accompanying client application that is realised with the purpose of commanding, collecting storing and viewing the different types of data.

INTRODUCTION

During the upgrade of each injector line at the European Organisation for Nuclear Research (CERN), an up-to-date Beam Loss Monitoring (BLM) system will be included for the monitoring of the beam losses and machine protection. For this reason, a new BLM system is under design [1].

The BLM Dual Polarity (BLEDP) module is the first stage of that system with the purpose to collect and digitise the current output from the detector. The acquisition crate will be able to host up to eight of these modules. The BLEDP module should be able to digitise input current from eight input channels each having a wide range from 10 pA up to 200 mA.

To accomplice this, the range is split into two partially overlapping sub-ranges and for each of them a different circuit and measurement method is used. The current from 100 μA up to 200 mA will be measured directly by the ADC as a voltage drop on the input resistor. It is so called Direct Analogue to Digital Conversion (DADC) method. The current in the lower range from 10 pA to 10 mA will be measured by making use of a low noise Fully Differential Frequency Converter (FDFC). More about the analogue front-ends used in both of the measurement methods can be found in [2].

The BLEDP module is equipped with a Cyclone 4GX150 FPGA device which is responsible for processing the FDFC data [3] and controlling the analogue circuitries. In the standalone version of the module, an Ethernet server is implemented in addition in the FPGA. To achieve this, the Nios-II soft-core processor which is running under control of a μC/OS-II real-time operating system is realised in the FPGA device. In this configuration, each of the modules in the acquisition crate have a separate link to the network. The measurement data collected is send to a dedicated supervision application which is used for online view as well as offline data storage and analysis. This paper focuses on the Ethernet implementation in the FPGA and it describes briefly the client application developed.

DATA TRANSMISSION

The data frame, shown in Fig. 1, was designed to satisfy both of the measurement methods which are automatically selected by the BLEDP module. That selection of the measurement method depends on the input current. In addition, the protocol must be capable of transmitting acquisition data from a single or multiple channels. The channel number or multi-channel transmission is requested by a command send by connected client. The measurement method and the channel information are attached as a header to the data sample which is acquired every 2 μs and transmitted to the client. That is, each BLEDP frame will be 32 bits wide in total and it will consist of the header and the measurement data. The data rate per channel is therefore around 16 Mbit/s. The size of the data depend on the measurement method. The FDFC mode requires a 20 bit data field, whereas the DADC mode requires only a 16 bit. At the time of the writing, the DADC mode as well as the automated measurement method switching is not yet fully supported by the BLEDP firmware. Therefore, the size of the data field in this mode could be changed in the final specification. The data frames of the BLEDP are encapsulated in TCP/IP frames. The TCP protocol was selected due to its high reliability and automatic data reordering at the receiver side. However, it is expected to be also necessary to transmit data frames encapsulated into UDP format for the case of multichannel and raw data transmissions.

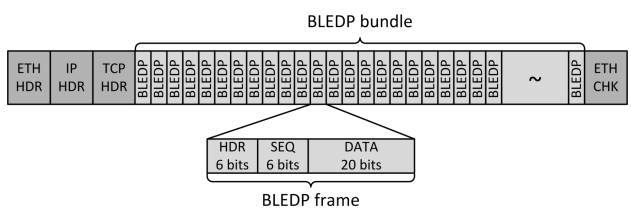

Figure 1: Structure of the BLM Data Frame transmitted over an Ethernet packet.

ISBN 978-3-95450-119-9

A REAL-TIME FPGA BASED ALGORITHM FOR THE COMBINATION OF BEAM LOSS ACQUISITION METHODS USED FOR MEASUREMENT DYNAMIC RANGE EXPANSION

M. Kwiatkowski, C. Zamantzas, M. Alsdorf, B. Dehning, W. Vigano,
CERN, Geneva, Switzerland

Abstract

The aim of the Beam Loss Monitoring Dual Polarity (BLEDP) module under development at the European Organisation for Nuclear Research (CERN) is to measure and digitise with high precision the current produced by several types of beam loss detectors.

The BLEDP module consists of eight analogue channels each with a fully differential integrator and an accompanying 16 bit ADC at the output of each analogue integrator. The on-board FPGA device controls the integral periods, instructs the ADC devices to perform measurements at the end of each period and collects the measurements. In the next stage it combines the number of charge and discharge cycles accounted in the last interval together with the cycle fractions observed using the ADC samples to produce a digitised high precision value of the charges collected.

This paper describes briefly the principle of the fully differential integrator and focuses on the algorithm employed to process the digital data.

INTRODUCTION

The LHC Injectors Upgrade project was launched at CERN to provide higher intensity beam for the LHC, which will allow to increase further its luminosity. A new Beam Loss Monitoring (BLM) system is under design [1] for the monitoring of the beam losses and the machine protection.

The BLM Dual Polarity (BLEDP) module is the first stage of that system. The acquisition crate will be able to host up to 8 BLEDP modules each having 8 analogue inputs to attach various types of detectors. The BLEDP module should be able to digitise input current in the wide range from 10 pA up to 200 mA.

In specific, the range is split into two partially overlapping sub-ranges and for each of them a different measurement method is used. The current from 100 μA up to 200 mA should be measured directly by the ADC as a voltage drop on the input resistor. The current in the lower range from 10 pA to 10 mA is measured by making use of a low noise differential integrator. The BLEDP module is equipped with a Cyclone IV GX FPGA which is responsible for processing of the integrator output combined with the ADC samples to reach higher accuracy. The digitised result will be transmitted via the fibre optic link into the processing part of the system.

In the stand-alone version of the system, the data is send via a Gigabit Ethernet link into a dedicated JAVA supervision application which is used for on-line view of the measurements as well as offline data storage and analysis. More information about this version of the system and the methods employed can be found in [2].

MEASUREMENT METHODS

The analogue front-end of the BLEDP module can measure input current in a wide dynamic range. To achieve this, the input current in the lower range is measured by a Fully Differential Frequency Converter (FDFC) circuit and in the higher range by a direct Analogue to Digital Conversion (DADC) circuit. In the DADC method the ADC converter is attached to the input resistor on which the voltage drop is measured. In the FDFC method the ADC is attached to the differential output of the integrator.

The analogue switch, that selects which of the two circuits is active at any given time, is controlled by the FPGA device. A module operating in the FPGA is monitoring the data stream and depending on the measurements it receives selects the most suitable measurement method for the next period.

This paper focuses on the FDFC method which require processing of both the ADC samples and the comparator pulse stream. A simplified schematic of the FDFC analogue front-end is shown in Fig. 1.

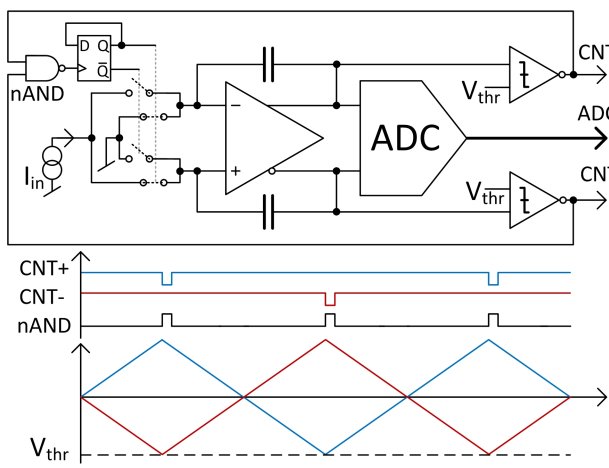

Figure 1: Fully Differential Frequency Converter.

The input current is directed by the analogue switches to the positive or negative branch of the differential integrator. The current arriving is charging the capacitor of

ISBN 978-3-95450-119-9

SIGNAL EQUALIZER FOR SPS ECLOUD/TMCI INSTABILITY FEEDBACK CONTROL SYSTEM*

K. Pollock†, J. Dusatko, J.D. Fox, C. Rivetta, D. Van Winkle, SLAC, Menlo Park, USA
R. Secondo, CERN, Geneva, Switzerland

Abstract

The 4 GS/sec Ecloud/TMCI instability control system in development for the CERN SPS requires 1.5 GHz of processing bandwidth for the beam pickups and signal digitizer. An exponentially tapered stripline pickup has sufficient bandwidth, but has a phase response that distorts the beam signal in the time domain. We report on results from the design and implementation of an equalizer for the front end signal processing with correction for the pickup and cable responses. Using a model of the transfer functions for the pickups and the cabling, we determine a desired frequency response for the equalizer. Design for the circuitry and component value fitting is discussed as well as board construction and reduction of parasitic impedances. Finally, we show results from the measurement of an assembled equalizer, and compare them with simulations.

DEFINITION OF THE PROBLEM

Electron clouds and transverse mode coupling induce intra-bunch instabilities for high intensity beams in circular accelerators [1]. A feedback instability control system is in development to sample the vertical displacement of the bunch at 4 GS/sec such that the transverse head-tail modes can be detected and the necessary correction signal applied [2].

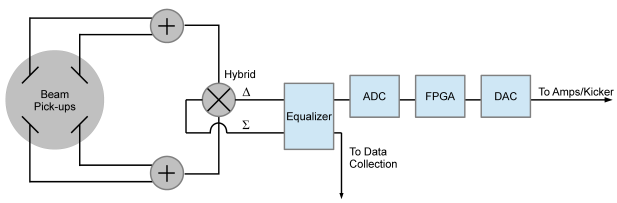

Figure 1: Instability control system diagram.

In order to measure the higher order transverse modes we need a pick-up with a bandwidth of up to 1.5 GHz. Exponentially tapered stripline couplers have sufficient bandwidth and flat frequency response at high frequencies, however, the phase response of the pick-ups distorts the beam signal [3]. Also, the long cables between the beam tunnel and signal processing introduce further distortion of the beam signal. The combination of these responses results in the deviation from the Gaussian as seen in Figure 2, and equalization is needed to recover original signal. An accurate time domain picture of the bunch is critical because this information will be used to apply a specific correction signal centered on the bunch.

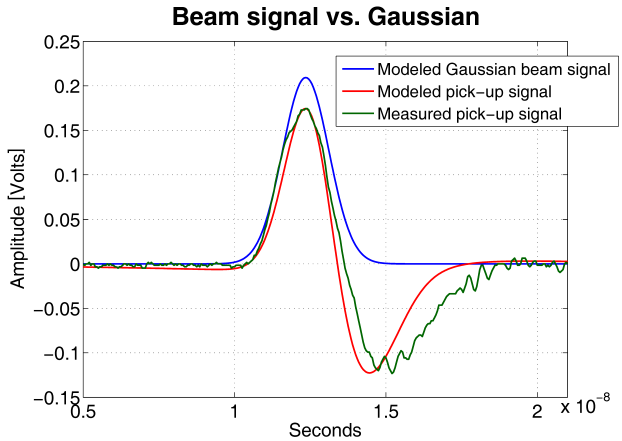

Figure 2: The beam shape is expected to be close to Gaussian, however the pick-up and cabling cause distortion in the time domain. Shown above is the modeled pick-up signal (red) and a measured signal (green).

The responses of the pick-up and cabling have been modeled and measured for the system at the SPS [4]. The transfer function of the pickup is modeled as

$$H_p(s) = \frac{s}{s+\frac{ca}{2L}} * (1 - e^{-(a+\frac{-2Ls}{c})})$$

where L is the pick-up length and equals 0.375 m, a is the coefficient that describes the exponential taper and equals 2.48, and c is the speed of light. This is plotted in Figure 3.

The cable transfer function is represented by

$$H_c(s) = e^{\frac{1}{2}(-a_0(1+j)0.707\sqrt{\frac{s}{\pi}}-a_1\frac{s}{2\pi})}$$

The coefficients a_0 and a_1 are the measured cable coefficients. For the current cables $a_0 = 1.05\times10^{-4}$ and $a_1 = 3.5\times10^{-10}$. The transfer function magnitude and phase are plotted in Figure 4.

The equalization can be done with either software or hardware. A digital signal processing approach is attractive because any desired transfer function can be used and it can be changed easily, however, for our system this approach becomes too computationally intensive. For a software implementation the processing cost increases by n^2 whereas with a hardware equalizer circuit it is possible to do n channel parallel processing. Also, the cabling and pick-ups are unlikely to change often. For these reasons, an analog equalizer circuit has been designed.

* Work supported by the US-DOE under Contract DE-AC02-76SF00515 and US-DOE LARP program
† kmpollock@stanford.edu

ISBN 978-3-95450-119-9

FAST ORBIT FEEDBACK CALCULATION IMPLEMENTATION FOR TPS

P. Leban, A.Bardorfer, Instrumentation Technologies, Solkan, Slovenia
K.T.Hsu, C.H.Kuo, NSRRC, Hsinchu, Taiwan

Abstract

Fast orbit feedback (FOFB) application is planned for the Taiwan Photon Source (TPS) at storage ring commissioning. Part of the application is transferred to the beam position electronics which implements global orbit position data concentration, its processing and actuating the magnet power supply controllers via optical links. The beam position electronics (Libera Brilliance+) includes gigabit data exchange (GDX) modules with Virtex6 field programmable gate array. The feedback calculation algorithm is based on the SVD – the PI controller will be applied in the modal space for individual eigenmodes. The calculation will be distributed to all GDX modules to reduce overall latency. Each GDX module will calculate either 4 vertical or 4 horizontal magnet corrections.

This article presents details about the FOFB topology and implementation in the GDX module.

SYSTEM OVERVIEW

The TPS storage ring will use a 24-cell DBA lattice and will have 24 straight sections for insertion devices, six of them 12 m-long and 18 of them 7 m-long. It will be a combined-function magnets lattice structure with 10 nm rad emittance and will be located in the inner tunnel of the TPS storage ring [1].

The Libera Brilliance+ instrument is a beam position processor instrument used in the TPS. It provides wide and narrow bandwidth data paths with excellent measurement and stability capabilities [2]. The fast orbit feedback capability (FOFB) is provided by an extension module – the Gigabit Data Exchange (GDX) module. The GDX module is tightly connected with its neighbour BPM and TIM modules and receives fast position data streams over Low-voltage Differential Signalling (LVDS) links to ensure low latency [3].

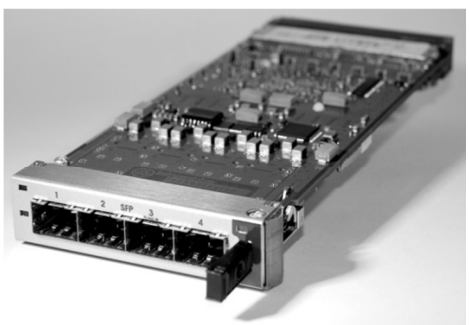

Figure 1: The Gigabit Data eXchange module.

The module contains Virtex6 field programmable gate array (FPGA) with TPS custom-made FOFB application. There is also 1 GB of DDR3 available as a circular buffer for the fast data.

CONTROL TOPOLOGY

The Libera Brilliance+ instruments are daisy-chained with fibre optic or copper cables to form a single group of 168 BPMs installed in 48 chassis (see Figure 2). Each instrument runs the EPICS IOC and communicates over GbE network interface to the Control System. The FOFB application runs in the FPGA in the GDX modules. FOFB related parameters are controlled by Libera BASE, running in the Libera Brilliance+.

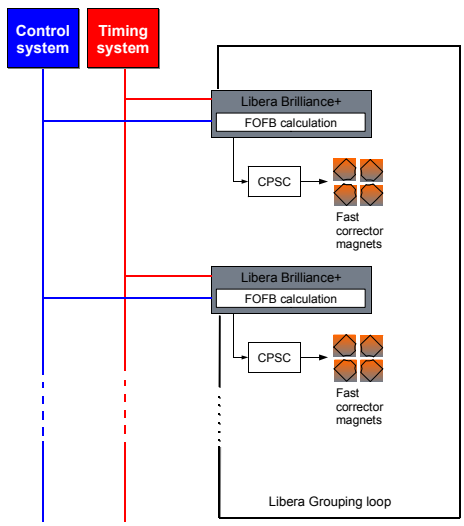

Figure 2: Global control topology.

There are 8 fast corrector magnets located in each of the cells: 4 for the horizontal and 4 for the vertical direction. Fast corrector magnets are controlled by a Corrector Power Supply Controller (CPSC) device which features 2 optical inputs (SFPs) and 8 analogue outputs (20 bit) [4]. Each cell contains 2 Libera Brilliance+ instruments with 3 or 4 BPM modules and 1 GDX module. One Libera Brilliance+ calculates and outputs the data for one set of the fast corrector magnets only (either horizontal or vertical). See Figure 2 for more details.

ISBN 978-3-95450-119-9

INVERSE RESPONSE MATRIX COMPUTATION FOR THE STORAGE RING SLOW ORBIT FEEDBACK CONTROL: SYNTHESIZED TOPOLOGICAL INVERSE COMPUTATION

J. M. Lee#, J. Y. Huang*, C. Kim, Accelerator Division, Pohang Accelerator Laboratory, POSTECH, 790-784, Korea

Abstract

For the storage ring orbit feedback control, the inversed SVD (Singular Value Decomposition) method is normally working under stabilized orbit situation, but less effective at relatively large orbit fluctuation. To overcome such numerical drawback, we investigated the alternative feedback control based on the solution tracking algorithm. Using our novel STIC (Synthesized Topological Inverse Computation), we simulated the formation of residual tune orbit under the closed orbit dynamics response matrix, measurable relationship between BPM-data readout and corrector-MPS setting. By placing empirical evidence of beam based alignment measurement, we achieved remarkable numerical fidelity on our STIC feedback algorithm, especially ascribing the topological importance of inverse response matrix computation. We demonstrated the STIC-inherent triggering behaviour and adaptive pattern-notched feedback stability.

INTRODUCTION

Practically useful for SOFB (slow orbit feedback) with assistance of FOFB (fast orbit feedback), the inversed SVD manipulation [1] is not fully acceptable because a type of consecutive instability noise irreversibly accumulates in the beam trajectory deviation. On the other hand, a novel numerical algorithm – emerging from a topological math approach – can lead to numerical self-consistency and solution tracking, dramatically suppressing ill-posed instability problems associated with numerical truncation residuals. This approach, known as a singularity regularization method, makes it feasible to compute a feature-invariant inverse matrix and system-matched de-noising filter. For deep investigation of the closed orbit feedback control, we applied our novel recipe of inverse computation, namely STIC(Synthesized Topological Inverse Computation) [2]. Fundamentally, this Orbit-STIC feedback is similar to the numerical computation of the inner origin function ascribing a type of complex systems. In our other study [2], we described the singularity inhibitor algorithm with essential topological nature engaged in the symplectic transformation (e.g. S-matrix, satisfying A_3=SA_1 with S^2=-I). Because this inverse math algorithm deals with the phase-component feature, commonly required is the complete phase-space relationship, e.g. the horizontal and vertical coupling term in the closed orbit response matrix. Even though LOCO (linear optics closed orbit) configurations are so complicated, entire physics of beam dynamics feature can be extracted from the measured response matrix. In this study, we introduced the PLS-II response matrix, even not so much matured since upgrading commission year 2012. [3] Proper matrix refinement can be made both numerically and empirically, according to our self-consistent manner of filtering out the uncertainty of measurement errors escaping from beam dynamics constraints. We are deeply investigating our advanced feedback algorithm, Orbit-STIC, practically in collaboration with world-wide accelerator community.

jaymin@postech.ac.kr
* huang@postech.ac.kr

NUMERICAL PROCEDURES

As depicted in Fig. 1, the closed orbit feedback algorithm can be expressed with the following equations:

$$\Delta \boldsymbol{x}_{BPM} = \Delta \boldsymbol{x}_i - \Delta \boldsymbol{x}_o = \mathbf{R}\,(\Delta \boldsymbol{g}_i - \Delta \boldsymbol{g}_o) \quad (1)$$

$$\overline{\Delta \boldsymbol{g}} = \Delta \boldsymbol{g}_o + (\Delta \boldsymbol{g}_i - \mathbf{R}^{-1}\,\widetilde{\Delta \boldsymbol{x}_i}) \quad (2)$$

$$\overline{\Delta \boldsymbol{x}} = \mathbf{R}\,\Delta \boldsymbol{g}_o = \mathbf{R}\,\mathbf{R}^{-1}\,\Delta \boldsymbol{x}_0 \quad (3)$$

$$\overline{\Delta \boldsymbol{g}} = \mathbf{R}^{-1}\,\overline{\Delta \boldsymbol{x}} + (\mathbf{I} - \mathbf{R}^{-1}\mathbf{R})\,\mathbf{R}^{-1}\,\widetilde{\Delta \boldsymbol{x}_i} \quad (4)$$

$$\overline{\Delta \mathbf{g}_s} = \boldsymbol{\gamma}\mathbf{U}_s^{(0)}\,\overline{\Delta \boldsymbol{x}} + \mathbf{U}_s^{(\gamma)}\,\widetilde{\Delta \boldsymbol{x}_i} \quad (5)$$

$$\mathbf{U}_{\mathbf{stic}}^{(\gamma)} = [\mathbf{R}_{\mathbf{stic}}^{-1}\mathbf{R}]_r^{-1}\left(\mathbf{I} - \boldsymbol{\gamma}\,\mathbf{R}_{\mathbf{stic}}^{-1}\mathbf{R}\right)\mathbf{R}_{\mathbf{stic}}^{-1} \quad (6)$$

$$\mathbf{U}_{\mathbf{svd}}^{(\gamma)} = \left(\mathbf{I} - \boldsymbol{\gamma}\,\mathbf{R}_{\mathbf{svd}}^{-1}\mathbf{R}\right)\mathbf{R}_{\mathbf{svd}}^{-1} \quad (7)$$

$$\begin{aligned}\overline{\Delta \mathbf{g}_{\mathbf{svd}}} &= \boldsymbol{\alpha}\,\mathbf{U}_{\mathbf{svd}}^{(0)}\,\Delta \boldsymbol{x}_p + \mathbf{U}_{\mathbf{svd}}^{(\alpha)}\,\Delta \boldsymbol{x}_p \\ &= \left((\mathbf{1}+\boldsymbol{\alpha})\mathbf{I} - \boldsymbol{\alpha}\,\mathbf{R}_{\mathbf{svd}}^{-1}\mathbf{R}\right)\mathbf{R}_{\mathbf{svd}}^{-1}\,\Delta \boldsymbol{x}_p \end{aligned} \quad (8)$$

Eqs (1)-(4), include the basic recursive formula for the feedback control. Eqs (5)-(7), are the modified formalism based on Eq(4). This is efficient and convenient way of stabilizing the iteration process. For the STIC feedback in Fig. 2, as $\boldsymbol{\gamma} \to \mathbf{1}$, it is proper to get the stabilized BPM-solution (Δxo). In contrast, for the SVD method, as $\boldsymbol{\alpha} \to \mathbf{1}$, the feedback speed is retarded and eventually extinguished. (Refer to Table 1.) Typically, when the particular orbit solution is given as Δx_p, the corrector-MPS setting is simply computed according to Eq (8). Two

ISBN 978-3-95450-119-9

DIGITAL LONGITUDINAL BUNCH-BY-BUNCH FEEDBACK SYSTEM FOR THE HLS II

W.B. Li, Z.R. Zhou, B. G. Sun#, F. F. Wu, P. Lu, Y. L. Yang, W. Xu, J.Y. Zou,
School of Nuclear Science and Technology & National Synchrotron Radiation Laboratory,
University of Science and Technology of China, Hefei, 230029, China

Abstract

In order to suppress the longitudinal coupled bunch instabilities, a digital longitudinal bunch-by-bunch feedback system will be developed in the upgrade project of Hefei Light Source (HLS II). The longitudinal feedback system consists of a pickup BPM, a front-end/back-end signal processor unit to detect the phase errors of all electron bunches, an iGp signal processor to calculate correction signals of those bunches, two RF power amplifiers, and a longitudinal kicker to supply proper correction energy kicks to individual bunches. A new waveguide overloaded cavity longitudinal feedback kicker has been designed with broadband and high shunt impedance. In this paper, we describe an overview of the new longitudinal feedback system.

INTRODUCTION

In the synchrotron light source, a storage ring of electron beam with many bunches is necessary to meet the demand for the high brightness. The electromagnetic field created by these bunches can interact with the surrounding metallic structures generating 'wake fields', which act back on the trailing bunches producing growth of the oscillations. If the growth is stronger than the damping, the longitudinal coupled bunch instabilities occur and the oscillation becomes unstable. In addition, the higher order modes (HOM's) of RF cavities in the storage ring can also cause the longitudinal coupled bunch instabilities.

During the operation of Hefei Light Source (HLS), the longitudinal coupled bunch instabilities were observed, but there were no effective measures to suppress these longitudinal instabilities. It was one of the main limitations of beam intensity. To overcome this obstacle, a brand new digital longitudinal bunch-by-bunch feedback system whose main design parameters are listed in Table 1 will be installed in the storage ring during the upgrade project of Hefei Light Source (HLS II), and the beam intensity will increase to more than 300 mA. This paper describes an overview of the longitudinal feedback (LFB) system and mainly introduces the development of the longitudinal kicker.

LONGITUDINAL FEEDBACK SYSTEM

The digital longitudinal feedback system for the HLS II consists of a beam position monitor (BPM), a front-end/back-end signal processor, an integrated Gigasample processor (iGp12-45F), two RF power amplifiers and a longitudinal feedback kicker [1]. The functional block diagram of the system is shown in Figure 1.

Table 1: Main design parameters of the LFB system

Parameters	Value	Unit
beam energy	800	MeV
RF frequency	204	MHz
revolution frequency	4.53	MHz
harmonic number	45	
number of FIR taps	32	
central frequency of kicker	969	MHz
bandwidth of kicker	102	MHz
shunt impedance of kicker	2083	Ω

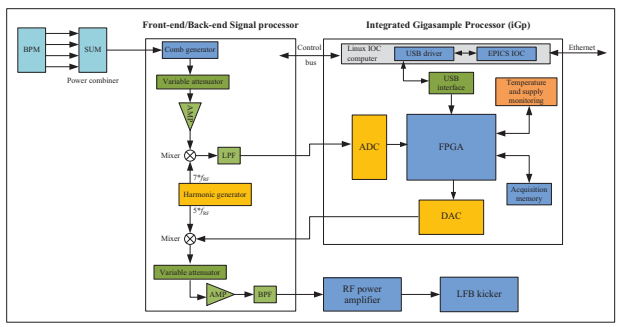

Figure 1: Functional block diagram of the longitudinal feedback system.

The signals from the BPM pickups are combined and then transferred to a 2-cyle comb filter to produce a coherent tone burst at seventh harmonic of the RF frequency. The phase error detection is performed by the double balanced mixer where the signal from the comb generator is compared with one 1428 MHz ($=7\times f_{RF}$) signal coming from a harmonic generator. After being sent to a low pass filter (LPF) to reduce the noise, the detected phase error signals are fed to the digital signal processing subsystem (iGp12-45F processor) which consists of a high-speed 12-bit analog-to-digital converter (ADC), a field programmable gate array (FPGA), and a high-speed 12-bit DAC, all driven by the RF frequency clock. The detected phase error signals can be sampled and digitized by the ADC. The feedback correction output signals are calculated by programmable 32-taps finite impulse response (FIR) filter algorithm at

ISBN 978-3-95450-119-9

FPGA BASED FAST ORBIT FEEDBACK SYSTEM FOR THE AUSTRALIAN SYNCHROTRON

Y-R. E. Tan, T. Cornall, S. A. Griffiths, S. Murphy, E. Vettoor,
Australian Synchrotron, Clayton, Australia

Abstract

An initial design for a Fast Global Orbit Feedback System based on FPGAs has been proposed for the Australian Synchrotron Light Source (ASLS). The design uses a central processor (Xilinx Virtex 6) for all the computations and fast optical connections to distribute the computed data to corrector magnet power supplies. The network topology consists of two fibre optic rings. The first ring is used by the Libera Electron's to aggregate the beam position data at 10 kHz using Instrumentation Technologies' Grouping algorithm. The second ring is used to transmit the computed data. The cycle frequency of the feedback is 10 kHz with a targeted total latency of under 400 us. We shall give an overview of the design goals and discuss the merits of the current implementation. We shall also present the measured bandwidth of the stainless steel vacuum chamber and test results from initial prototyping work.

INTRODUCTION

The ASLS is a 3 GeV light source open to users since 2007. Although not implemented at the start, the plan was to implement the fast global orbit feedback system at a later stage when the need arose. The beam stability requirement is that the RMS of the beam motion be < 10% of one sigma of the transverse beamsize, σ.

The RMS of the beam motion is different depending on the location around the ring and ranges between 0.6 µm up to 3.5 µm. To identify the frequencies that contribute to the overall motion, Figure 1 shows the integrated spectrum of the beam motion collected during regular operations from the storage ring BPM electronics, Instrumentation Technologies' Libera Electron (Libera), at a sampling rate of 10 kHz. The largest contributor to the beam motion is at the mains frequency at 50 Hz and its harmonics with mechanical vibrations contributing to the noise below 100 Hz. The recent improvements to the beamlines have meant that some are now seeing the effects of the 50 Hz beam motion.

To improve the beam stability a fast global orbit feedback system was proposed. Fortunately there are many existing solutions to learn from; CLS [1], Elettra [2], SLS [3], Soleil [4], SPEAR III [5], TLS [6] and NSLS II [7]. One requirement desired for the design was to have a single centralised processing station. The number of BPMs in the feedback (98 in total) was sufficiently small to make this possible. This has the potential to reduce hardware costs and simplify the design of the system where synchronisation of multiple processing stations is not needed.

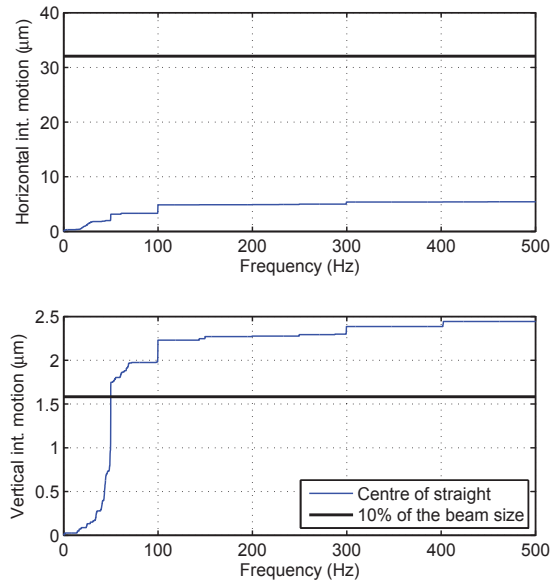

Figure 1: Integrated spectrum of the beam motion at ID5 (IVU). The vertical beamsize is based on the model with the current emittance coupling value of 1%.

The proposed layout of feedback system is shown in Figure 2 where the outer fibre optic ring is used to aggregate the position data from all the BPMs and the inner ring is used to distribute the corrections to the corrector power supply units (PSUs). A 1000 Base-T GbE connection links the outer ring with the inner ring through the central processor.

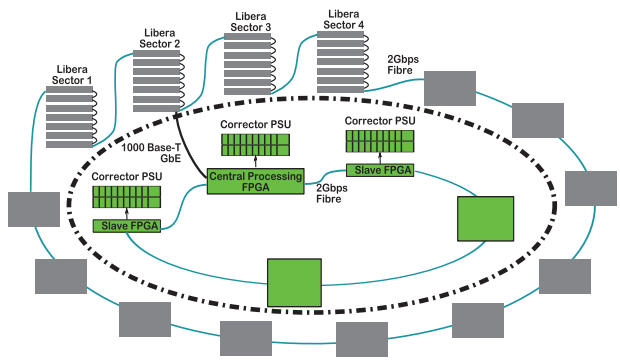

Figure 2: Proposed layout of the feedback system forming two fibre optic rings (2 Gbps). The FPGAs send corrections to the corrector PSUs via serial lines. The PSU, Liberas and FPGAs have network connections to the control system.

ISBN 978-3-95450-119-9

ULTRA-SHORT ELECTRON BUNCH AND X-RAY TEMPORAL DIAGNOSTICS WITH AN X-BAND TRANSVERSE DEFLECTING CAVITY*

P. Krejcik†, Y. Ding, J. Frisch, Z. Huang, H. Loos, J. W. Wang, M-H. Wang,
SLAC, Menlo Park, CA, USA
C. Behrens, DESY, Hamburg, Germany
P. J. Emma, LBNL, Berkeley, CA, USA

Abstract

The technique of streaking an electron bunch with a RF deflecting cavity to measure its bunch length is being applied in a new way at the Linac Coherent Light Source with the goal of measuring the femtosecond temporal profile of the FEL photon beam. A powerful X-band deflecting cavity is being installed downstream of the FEL undulator and the streaked electron beam will be observed at an energy spectrometer screen at the beam dump. The single-shot measurements will reveal which time slices of the streaked beam have contributed to the FEL process by virtue of their greater energy loss and energy spread relative to the non-lasing portions of the electron bunch. Since the diagnostic is located downstream of the undulator it can be operated continuously without interrupting the beam to the users. The resolution of the new X-band system will be compared to the existing S-band RF deflecting diagnostic systems at SLAC and consideration is given to the required RF phase stability tolerances required for acceptable beam jitter on the monitor. Simulation studies show that about 1 fs (rms) time resolution is achievable in the LCLS over a wide range of FEL wavelengths and pulse lengths.

INTRODUCTION

X-ray Free Electron Lasers such as the Linac Coherent Light Source (LCLS) can produce very short pulses of a few femtoseconds (10^{-15}s) duration [1]. This makes them a powerful tool for observing ultrafast phenomena, such as molecular dynamics. The challenge for the accelerator community is to measure this pulse duration at the fs level. An even greater challenge is to measure both the photon pulse duration and the electron bunch since the emission process does not result in a one to one correspondence.

The transverse deflecting cavity (TCAV) is now a well established diagnostic instrument at FEL linacs to measure the temporal profile and slice properties of the electron beam [2]. In this new application the instrument is installed downstream of the undulator where it streaks the spent electron beam and is observed on a profile monitor screen located at the beam dump [3]. This gives a unique opportunity to observe the FEL process in the time-resolved energy profile of the beam without interrupting beam to the users.

*This work was supported by Department of Energy Contract No. DE-AC0276SF00515
† Corresponding author email pkr@slac.stanford.edu

EXISTING TCAV SYSTEM AT SLAC

Two transverse deflecting cavities are currently in use on the LCLS accelerator and operate at the S-band, 2856 MHz. A short 40 cm section is located in the injector and a longer 2.44 m long structure is located in the main linac, downstream of the second bunch compressor. Both of these structures were actually designed and built in the 1960's [4]. The principle of operation is shown in Figure 1, where a bunch at 0° phase crossing of the rf appears streaked on a downstream screen.

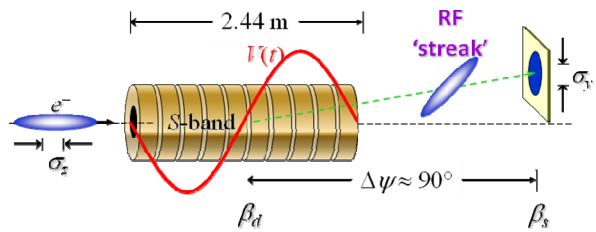

Figure 1: Principle of operation of the TCAV.

The size of the streaked beam σ_y is related to the bunch length σ_z by

$$\sigma_y^2 = \sigma_{y0}^2 + \beta_d \beta_s \sigma_z^2 \left(\frac{k_{RF} e V_0}{E_s} \sin \Delta\psi \cos\phi \right)^2 \quad (1)$$

where σ_{y0} is the unstreaked transverse beam size, β_d and β_s are the beta functions at the deflector and screen, k_{RF} the wave number, V_0 the rf amplitude, E_s the beam energy $\Delta\psi$ the betatron phase advance from deflector to screen and ϕ the phase of the rf.

TCAV Operated with an Energy Spectrometer

The utility of the TCAV diagnostic is further enhanced if the beam is observed on an energy spectrometer screen where the energy dispersion is in the plane perpendicular to the rf deflection. The screen measurement reveals the time-resolved energy and energy spread. The example shown in Figure 2 is from the straight-ahead energy spectrometer screen where the LCLS injector beam is bent in the horizontal plane onto a beam dump. The beam is streaked in the vertical plane so that the curvature of the on-crest rf acceleration of the beam is observed, as well as the "slice" energy spread of the beam. The latter quantity is particularly important for determining the performance of the FEL.

ISBN 978-3-95450-119-9

DIAGNOSTICS BEAMLINE OPTIMISATION AND IMAGE PROCESSING FOR SUB-PS STREAK CAMERA BUNCH LENGTH MEASUREMENT

C.A. Thomas*, I. Martin, G. Rehm, Diamond Light Source, Oxfordshire, UK

Abstract

For the low-alpha beam mode at Diamond, standard theory predicts rms bunch lengths as small as 0.6 ps with a momentum compaction factor set to $\alpha = 0.8 \cdot 10^{-6}$. In order to be able to reliably measure such a short bunch, we have been optimising the optical design of the visible diagnostics beamline, and we have implemented image processing to take into account the point spread function of the streak camera. The optical design has reduced a large chirp of 15 ps to less than 2 ps over the 400-550 nm bandwidth. It has also permitted the transport of almost all the available power, increasing the power by a factor 30, yet maintaining the possibility to focus the beam down to less than 20 µm into the streak camera for the best static streak camera point spread function. The implemented de-convolution technique extends the performance of the streak camera to bunch length measurements of less than the 1 ps PSF of the streak camera. In this paper we present these two essential features required to measure sub-ps bunches with a streak camera.

INTRODUCTION

For the low-alpha beam mode at Diamond, rms bunch lengths based on synchrotron frequency measurement are calculated to be as small as 0.6 ps. In special user low alpha beam mode the bunch length is set to be of the order of 2.5 ps. Measuring such small bunch lengths reliably can be quite challenging. For such a measurement we use a streak camera[1] (SC), for which the resolution as defined using the Rayleigh criterion and specified by the manufacturer is 2 ps (measured using narrowband pulses with a few photons per pulse). The corresponding rms resolution is then 0.75 ps. This should allow the SC to be able to measure bunch lengths 2 ps or less. However, control of the bandwidth and the power of the photon pulse is fundamental: too much power will induce Coulomb explosion of the electron bunch in the streak tube, and thus measurement of a longer bunch. Too little power will render the measurement dependant on the jitter of the many pulses needed to form an image.

In addition to this, one needs to take into account the possible chirping of the pulse going through various lengths of glass. To reach the photocathode of the SC, a pulse passes through at least the 4.3 mm of quartz on the entry of the SC tube. In our case there is also 6.3 mm of fused silica from a vacuum-air separation window. But the beam needs to be transported and focussed onto the photocathode, and the use of lenses will cause any broadband pulse to be chirped, potentially becoming longer than the electron bunch length that generated it. This is what we called the dynamic point spread function of the SC [1]. It is measurable with the time resolved spectrum of the pulse which shows the length and centroid of the pulse as function of the spectrum. With the original refractive focussing optics a non-linear chirp of 15 ps over 150 nm bandwidth with a maximum gradient of 140 fs/nm was measured. This chirp induces a dynamic point spread function rms width of approximately 6.5 ps. Re-designing the focussing optics using mirrors reduced this chirp to less than 2 ps for the same 150 nm bandwidth, with a maximum gradient 30 fs/nm [2]. Control of the power and bandwidth of the pulse is a first step, but with bunch lengths equal or less than the static PSF width, a very accurate knowledge of the PSF is absolutely necessary to allow the deconvolution and so recover the original bunch profile.

In this paper, we present which conditions are necessary for the measurement of ps bunch lengths. We first present the optical design of the Diagnostics beamline which allows the focussing of an un-chirped pulse with almost all the available power from the bending magnet synchrotron radiation onto the SC photocathode. Then we briefly introduce the Lucy-Richardson image deconvolution technique applied to the SC images. Finally, before some concluding remarks we show measurement of ps bunch lengths after the optimisation and deconvolution technique presented previously has been applied.

OPTICAL DESIGN

The improvement of the performance of the SC goes in two steps. The first one is the re-design of the front focusing optics (FO), replacing the achromatic Nikkor lens by an assembly of mirrors (Fig. 1). The second one is a re-design of the beam transport from the source to the SC with the aim to transport the maximum available power. The new design collimates the beam and reduces its transverse size at the same time, in order to transport the geometrical beam through the 30x50 mm aperture of the chicane in the radiation shield wall. A layout of the design is shown in Fig. 3.

Streak Camera Reflective Front Optics

The main objective of replacing the reflective FO of the SC by a refractive FO is to suppress the chirp induced by the refraction index of the objective lens in the broad spectrum synchrotron radiation pulse. This way all the UV-visible power spectrum can be used for bunch length mea-

* cyrille.thomas@diamond.ac.uk
[1] Optronis GmbH

ISBN 978-3-95450-119-9

FIRST OPERATION OF THE ELECTRO OPTICAL SAMPLING DIAGNOSTICS OF THE FERMI@ELETTRA FEL

M. Veronese*, A. Abrami, E. Allaria, M. Bossi, M.B. Danailov, M. Ferianis,
L. Fröhlich, S. Grulja, M. Predonzani, F. Rossi, G. Scalamera, C. Spezzani, M. Tudor, M. Trovò
Sincrotrone Trieste S.C.p.A., Trieste, Italy

Abstract

The FERMI@Elettra seeded FEL has demanding specifications in terms of longitudinal properties of the electron beam. Several diagnostics are installed along the linac. At the entrance of the FEL1 undulator chain an electro optical sampling (EOS) station based on the spatial encoding scheme is installed. The EOS provides both time jitter and longitudinal profile measurements in a non-destructive way. The layout of this system is described and the first operational measurement results obtained are reported. The paper includes also the capability of this diagnostics to perform the temporal coarse alignment of the seed laser to the electron beam. Finally a discussion on the future developments foreseen for this system is given.

INTRODUCTION

FERMI@Elettra is a seeded FEL operating in the spectral range from VUV to soft x-rays. It is based on a SLAC/BLN/UCLA type RF-gun and a normal conducting LINAC, currently operated at 1.2 GeV, but designed to reach 1.5 GeV. The longitudinal compression is provided by two magnetic chicanes BC1 and BC2 (respectively at 300 MeV and 600 MeV). The FEL has two undulator chains, namely FEL1 and FEL2. The first, FEL1, is a single cascade HGHG seed system designed to provide hundreds of microjoule per pulse in the wavelength range from 100 to 20 nm. The second, FEL2, is a double cascade seeded system designed to reach 4 nm as the shortest wavelength. A deep knowledge of the longitudinal parameters such as: longitudinal charge distribution, time of arrival jitter, slice energy spread and slice emittance is needed. For this reason FERMI@Elettra has been equipped with several longitudinal diagnostics to provide the necessary information for the commissioning and operation of the accelerator. They are: the Cherenkov low energy profile measurement with a femtosecond streak Camera, the Coherent Bunch Length Monitors (CBLM), the Bunch Arrival Monitors (BAM), the RF-deflecting cavities at low energy (LERFD) and at high energy (HERFDs) and finally the Electro Optical sampling stations (EOS). In this paper we present the layout and the first operational results from the EOS installed at the entrance of the FEL1 chain of FERMI. The Electro Optical Sampling provides single shot non-destructive longitudinal profile and time jitter measurements. For this reason it is installed just before the modulator undulator. In this position the EOS system provides also the coarse temporal alignment of the seed laser to the electron beam. In general an electro optical sampling diagnostics, makes use of the very large transient electric coulomb field of ultra-relativistic electron bunches to map their longitudinal profile. The electric field induces a variation in the crystal structure of an electro optic crystal. The refractive index variation is detected by optical polarization analysis. Since this effect is very fast, it reproduces the longitudinal distribution of the electron bunch with high fidelity. An ultrafast laser with pulse duration on the scale of 100 fs is an optimal probe. Several single shot schemes have been introduced and have been shown to be very effective (e.g. [1, 2]). For the FERMI FEL1 EOS we have chosen the spatial encoding scheme [3, 4]. This scheme is capable of providing high resolution measurements with the energy per pulse delivered by a compact, commercial, fiber laser oscillator.

For ultra-relativistic electrons the electric coulomb field has a large transverse component. For a single electron the electric field distance b from electron bunch in the plane (x,y) orthogonal the propagation direction (z) is [5]:

$$E_{y=b} = \frac{e}{4\pi\epsilon_0}\frac{\gamma b}{(b^2+\gamma^2 z^2)^{3/2}} \quad (1)$$

For an electron bunch with N_e electrons, the longitudinal distribution normalized to the maximum current, $\rho(z)$, can be approximated for the FERMI case to a rectangular distribution that is conveniently modeled by the difference of two Heaviside functions: $\rho(z) = H(z+FW\cdot/2) - H(z-FW\cdot/2)$. Then the total field along the axis is then:

$$E_{beam} = \int \rho(z-z')E_{0,b,z'}dz' \quad (2)$$

From Eq. 1 above , it is clear that the minimum distance between electron beam and EO crystal is a critical parameter and its proper selection depends on several factors. Very small distances are desirable, but this would induce wake-fields on the electron beam. Trajectory fluctuations may cause the e-beam to hit the EO crystal, possibly damaging it and producing ionizing radiation dose on the downstream undulators. Finally, in the EOS area, the seed laser travels collinearly to the electron beam, focusing from its entrance point upstream the EOS to reach it minimum width at the center of the modulator downstream the EOS. The seed laser has a high energy per pulse (up to tens of microjoules at a wavelength of 260 nm) that could potentially damage the crystal in case of an accidental impact. In practice, we should set the distance b at minimum to 5 mm. For a 500

* marco.veronese@elettra.trieste.it

ISBN 978-3-95450-119-9

STATUS OF THE LCLS EXPERIMENT TIMING SYSTEM*

J. Frisch, C. Bostedt, R. Coffee, A. Fry, N. Hartmann, J. May, D. Nicholson, S. Schorb, S. Smith,
SLAC, Menlo Park, CA 94309, USA

Abstract

X-ray / optical laser pump - probe experiments are used for a significant fraction of the scientific work performed at LCLS[1]. The experimental laser systems are locked to the timing of the electron beam through a combination of RF and optical fiber based systems. The remaining ~100 femtosecond RMS jitter of the X-rays relative to the optical laser is measured shot-to-shot by both a RF timing detector, and by direct X-ray to optical cross-correlation, and the result is used to correct the experiment timing to 10s of femtoseconds. We present the present status of the system and plans for future upgrades.

SYSTEM OVERVIEW

The experiment timing system locks the RF reference for the experimental laser (typically used as a pump in pump / probe measurement) to the average beam time from the accelerator. The timing system also measures the shot-to-shot electron beam time relative to the RF reference and provides this data to the experiment for offline jitter correction. In addition, where practical a direct X-ray to laser cross correlator is used to measure the relative beam times for offline correction. A simplified block diagram of the system is shown in Figure 1.

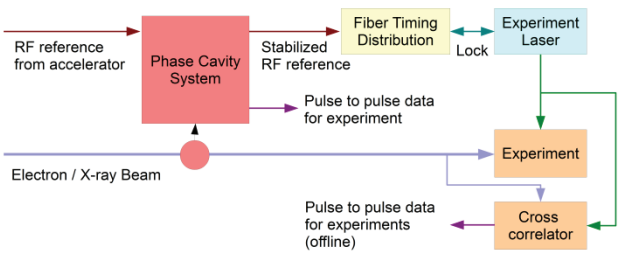

Figure 1: System Overview.

ACCELERATOR TIMING

The LCLS operates at a repetition rate of 120Hz, typical for room temperature accelerators. Since the RF fields completely decay between pulses there is significant pulse-to-pulse timing jitter that cannot be corrected with feedback; for LCLS this is on the order of 100fs RMS. Experiments which require better timing resolution rely on measuring the beam time on each pulse and correcting the data offline.

RF SYSTEMS FOR TIMING

RF systems provide a convenient method for providing timing synchronization. The timing noise of an RF system is given approximately as: $\Delta T = \frac{\sqrt{BW \cdot P_{n(1Hz)}/P}}{\omega}$. Where P is the RF power, BW the system bandwidth $P_{n(1Hz)}$ is the noise power in a 1 Hz bandwidth, ω the RF frequency in rad/sec and ΔT the RMS timing jitter. Most RF systems can operate near (a few dB) the thermal noise limit $\sim 4 \times 10^{-21} W/Hz^{1/2}$ with transmission powers of a few millwatts.

For fiber systems the receiver noise is typically $\sim 10^{-11} W/Hz^{1/2}$optical (limited by the noise in the pre-amplifier)[2]. Since the detector output voltage typically scales linearly with optical power, the phase sensitivity varies inversely with optical power (rather than inverse square root for RF systems).

Oscillators have phase noise that increases with decreasing frequency since they are measured relative to an absolute clock. Most high quality commercial oscillators are based on quartz resonators, however there exist some lower phase noise (but more expensive) oscillators based on microwave sapphire resonators.

A comparison of the phase noise of RF systems is given in Figures 2 and 3. Figure 2 shows the phase noise density in femtoseconds /Hz$^{1/2}$, Figure 3 shows the phase noise integrated down from 10KHz (a typical feedback bandwidth) in femtoseconds. Phase noise for 2 fiber system is also shown, representing examples of simple and high performance fiber systems.

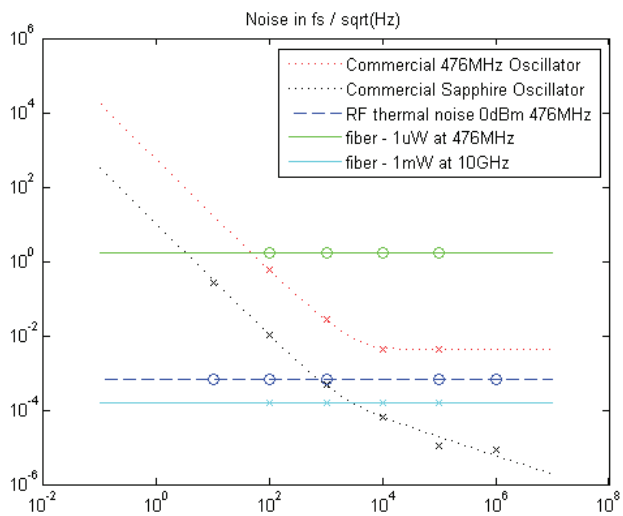

Figure 2: Phase noise in fs/Hz$^{1/2}$ for various RF and fiber systems.

* Work Supported by DOE Contract DE-AC02-76SF00515

ISBN 978-3-95450-119-9

STREAK CAMERA MEASUREMENTS AT ALBA: BUNCH LENGTH AND ENERGY MATCHING

U. Iriso and F. Fernández, CELLS, Cerdanyola, Spain

Abstract

This report describes the electron beam longitudinal studies performed at ALBA Storage Ring using the streak camera. We first show the usual studies involving precise bunch length measurements and related beam parameters like energy spread. Next, the studies to match the injected beam in energy and phase are reported and compared with simulations.

INTRODUCTION

Since the beginning of the ALBA Storage Ring commissioning in March 2011, a beam diagnostics beamline (BL34) is operational. It uses the visible part of the synchrotron radiation and is mainly devoted for longitudinal beam studies using the Streak Camera (SC), an Optronis SC-10 model, with synchroscan frequency working at 250 MHz to distinguish the beam bunches spaced by 2 ns.

The SC converts the incoming photons into electrons, which are swept to transpose its longitudinal (time) structure into a transverse footprint. The sweeps are performed by a fast and a slow unit. We always use the fast sweep in the "synchroscan mode", which sweeps continuously a sinusoidal field of 250 MHz at different amplitudes, allowing sweep speeds of 15, 25 and 50 ps/mm. The slow unit provides sweep speeds from 660 ps to 5 ms/mm, triggered usually at 50 Hz and synchronized with both the storage ring (SR) revolution frequency and the injection repetition rate (3 Hz). The working principles of SC are thoroughly explained in Ref. [1].

Table 1: ALBA Storage Ring Main Parameters

Parameter	Value
energy, E [GeV]	3.0
hor emittance, ϵ_x [nm-rad]	4.6
revolution time, T [ns]	896
harmonic number, h	448
rf freq., f_{rf} [MHz]	499.6
dipole field, B [T]	1.42
synchrotron freq., f_s[kHz]	6.5
rf voltage (max), V[MV]	3.6

In this report, we first describe the SC characterization and its sweep speed calibration. Next, the bunch length measurements of the stored beam are reported including the energy spread measurements. Finally, we show measurements of the injected beam, including booster bunch length and longitudinal damping time. Table 1 lists the ALBA Storage Ring (SR) parameters relevant for these studies.

EXPERIMENTAL SET-UP

The light used at BL34 is extracted from the first bending after the injection section. At 8.5 m from the source, we locate an in-vacuum mirror (VMIR) whose purpose is to reflect only the visible part of the synchrotron radiation spectrum. We do so by moving up the mirror (to about 2 mrad), and so avoiding the x-ray part of the spectrum circulating in the orbit plane – see Fig. 1. The light is then directed perpendicular towards the other side of the shielding wall, already in atmospheric pressure. At this point (and at 9 m from the source), we locate a 4m lens in order to focalize the light into the experimental set-up. Next, 6 conventional mirrors direct the light through the shielding wall performing a vertical chicane to prevent radiation outside the SR tunnel. Finally, the light arrives to the experimental setup in BL34. The light optical path and optical elements are shown in Fig. 2, and more details are explained in Ref. [2].

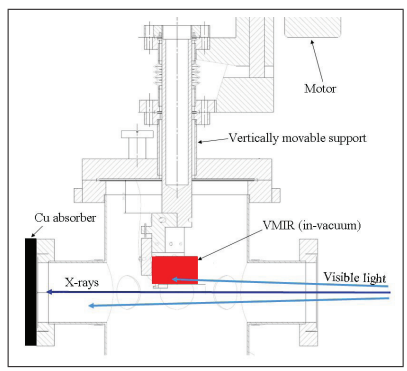

Figure 1: Sketch of the in-vacuum mirror (VMIR) and holder. The mirror is kept up around 2 mrad to avoid the x-ray part of the synchrotron radiation. The mirror is equipped with 3 thermocouples (not shown in the sketch) to prevent damages induced by possible overheating.

STREAK CAMERA CHARACTERIZATION

The "synchroscan sweep" is a sinusoidal electric field of 250MHz whose amplitude is varied to allow three different deflection speeds: 15, 25, and 50 ps/mm. The sweep is synchronized with the machine rf system working at 500 MHz. In order to crosscheck the linearity of these sweeps, we compared the bunch phase wrt sweep phase controlled by the SC. While the non-linearity is negligible for the 15 and 25 ps/mm speeds, this is not the case for the slowest vertical sweep: 50ps/mm (see Fig. 3). The total range swept with this speed corresponds to 990ps, which for the 250 MHz

ISBN 978-3-95450-119-9

MIDDLE-INFRARED PRISM SPECTROMETER FOR SINGLE-SHOT BUNCH LENGTH DIAGNOSTICS AT THE LCLS*

T. Maxwell†, Y. Ding, A.S. Fisher, J. Frisch, H. Loos
SLAC National Accelerator Laboratory, Menlo Park, CA 94025, USA
C. Behrens, Deutsches Elektronen-Synchrotron, Hamburg, Germany

Abstract

Modern high-brightness accelerators such as laser plasma wakefield and free-electron lasers continue the drive to ever-shorter bunches. At low-charge (< 20 pC), bunches as short as 10 fs are reported at the Linac Coherent Light Source (LCLS) [1]. Advanced time-resolved diagnostics approaching the fs-level have been proposed requiring the support of rf-deflectors [2–4], modern laser systems, or other complex systems. Though suffering from a loss of phase information, spectral diagnostics remain appealing by comparison as compact, low-cost systems suitable for deployment in beam dynamics studies and operations instrumentation. Progress in mid-IR imaging and detection of the corresponding micrometer-range power spectrum has led to the continuing development of a single-shot, 1.2 - 40 micrometer prism spectrometer for ultra-short bunch length monitoring. In this paper we report further analysis and experimental progress on the spectrometer installation at LCLS [5].

INTRODUCTION

In low-charge mode, the LCLS FEL linac produces 13.6 GeV electron bunches with lengths on the order of a few micrometers and transverse spot size of ~50 μm [1] for delivery to the undulator hall to generate x-ray FEL pulses of comparable duration. Diagnosis of the longitudinal distribution at the undulator entrance is desired for FEL optimization studies and presents a unique challenge to the resolution of existing diagnostics, reaching into the 1-fs scale. Time-domain measurements of the LCLS beam by use of an x-band transverse deflecting-mode cavity are already being pursued [2–4]. Alternative frequency-domain diagnostics have advantages of economy, requiring only standalone optics capable of recording the spectrum of coherent beam radiation (CxR).

Under a change in trajectory or medium, the beam will radiate. In the 1-D line-charge approximation and neglecting other transverse effects, the radiation emitted will have a power spectrum that's given by

$$I(k) \propto I_e(k)\left[N + N(N-1)\left|f(k)\right|^2\right] \qquad (1)$$

where $I_e(k)$ is the power spectrum for an individual electron in the given process, N is the number of electrons, the "form factor" $f(k)$ is the Fourier transform of unit-normalized longitudinal charge distribution $\rho(z)$, and the wavenumber is defined as $k \equiv 1/\lambda$ (the spatial frequency).

The second term in the bracketed sum of Eq. (1) represents the CxR, having an additional factor N enhancement over the incoherent radiation over wavelengths corresponding to a large form factor. With a measurement of the beam spectrum in the region where the coherent spectrum falls off, one can then in principle deduce the bunch length. As a rule of thumb for the coherent cut-off wavelength, we consider a bunch with unit-normalized Gaussian distribution of rms length σ_z. In this case the corresponding form factor-squared $|f(k)|^2$ is also a Gaussian of frequency-independent peak amplitude that falls to 50% at the cut-offs

$$k_{50\%} = \frac{\sqrt{\ln 2}}{2\pi\sigma_z} \approx \frac{0.133}{\sigma_z} \Rightarrow \lambda_{50\%} \approx 7.55\sigma_z \qquad (2)$$

Prior LCLS studies on low-charge operation suggest bunch length scaling linearly with charge at a constant peak current [1]. For $Q = 10 - 200$ pC, we have $\sigma_z = 0.5$ - 50 μm for typical bunch compression. This yields coherent enhancement down to $\lambda = 3.5$ - 40 μm (up to $k = 2900$-250 cm^{-1}).

As the distribution of the LCLS beam can vary from shot-to-shot, traditional scanning THz interferometry methods are avoided in favor of a single-shot mid-IR spectrometer inspired by that demonstrated in [6]. Here we provide an update on a one-stage, Single-Shot THz Prism Spectrometer (SSTPS) installation designed to cover this spectral range [5], favoring compactness and simplicity.

SYSTEM OVERVIEW

Current LCLS relative bunch length monitors utilize the coherent edge radiation (CER) emitted at the exit of upstream bending magnets [7]. For the present application in the straight section of the LCLS beam transport hall, coherent transition radiation (CTR) from the beam impinging on an inserted foil [8] was chosen. Referring to the overview for the SSTPS system in Fig. 1, light from the foil (A) will be collected and focused onto the spectrometer slit (F). Light at the slit is collimated through a custom KRS-5 mid-IR prism to provide dispersion (H) before being focused onto a linear pyroelectric detector array (J). All-reflective imaging optics are used to avoid unwanted chromatic abberations. The system is considered in two parts: the light collection optics (A-F) and the spectrometer proper (F-J).

* Work supported in part by US Department of Energy contract number DE-AC02-76SF00515.

† tmaxwell@slac.stanford.edu

ISBN 978-3-95450-119-9

BEAM INSTRUMENTATION FOR THE COSY ELECTRON COOLER

E. Bekhtenev, V. Bocharov, M. Bryzgunov, A. Bubley, A. Denisov, G. Karpov,
V. Panasyuk, V. Parkhomchuk, V. Reva , BINP SB RAS, Novosibirsk, Russia
V. Kamerdzhiev, L. Mao, K. Reimers, FZ-Jülich, Germany
J. Dietrich, TU-Dortmund and HIM Mainz, Germany

Abstract

The report deals with beam instrumentation of the electron cooler for COSY storage ring. The electron cooler is an electrostatic accelerator designed for beam energy up to 2 MeV and electron current up to 3 A in energy recovery mode. The electron beam is immersed in longitudinal magnetic field so the electron motion is strongly magnetized. The control electrode in the electron gun is composed of four electrically isolated sectors. Applying AC voltage to one sector allows tracing of motion of that particular part of the beam. The electron beam shape is registered with the combination of 4-sector electron gun and the BPMs. This method allows observing both dipole and quadruple (galloping) modes of electron beam oscillation. Compass probe for measuring and tuning the direction of magnetic field in the cooling section is described. A monitor based on a few small Faraday cups for measuring the electron beam profiles is presented.

INTRODUCTION

The 2 MeV electron cooler for COSY was built at BINP [1]. The design energy and good performance of the subsystems were demonstrated during electron beam commissioning in Novosibirsk. Further conditioning with electron beam is required to achieve electron currents above 200 mA at high energy. It will be done after the installation in COSY.

The electron beam is transported to and from the cooling section by two transport lines (see Fig. 1). This is due to the requirement of the HV system being installed outside the accelerator radiation shielding.

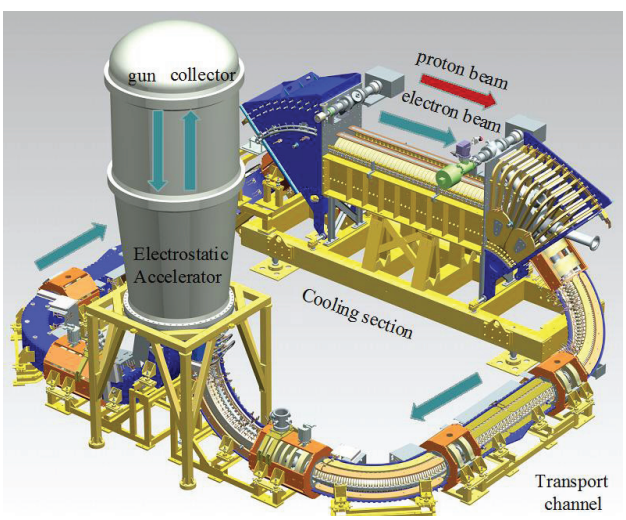

Figure 1: Layout of the 2 MeV electron cooler.

Lossless beam transport is essential for operation in the energy recovery mode. Beam position measurement and correction are necessary for beam loss minimization and accurate beam alignment in the cooling section. The design of the cooler includes numerous beam diagnostic systems. 12 beam position monitors (BPMs) provide position information in the electron transport lines and in the cooling section. The electron gun and its high voltage power supplies were designed having beam diagnostics in mind. Only electron gun features directly related to beam diagnostics are discussed in this paper. A Faraday cup array is used to measure the profile of the electron beam at low average current. Periodic verification of the magnetic field straightness in the cooling section is required to ensure best possible cooling.

ELECTRON GUN

Beam position measurements require modulation of the electron current. This is done by applying AC voltage at 3 MHz and up to 10 V to the gun control electrode (see Fig. 2). Furthermore, the control electrode of the electron gun is composed of four electrically isolated sectors [2]. Applying AC voltage to one sector at a time allows the use of BPMs for tracing the corresponding part of the electron beam. Comparing the positions of each sectors from BPM to BPM or the sector positions in a single BPM at different currents in the corrector coils it is possible to analyze the optics in the transport line.

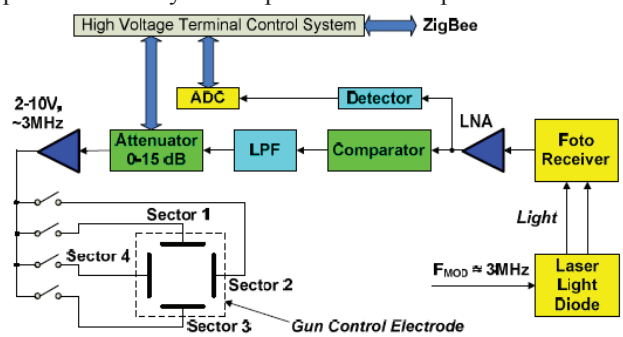

Figure 2: Diagram of the gun modulation electronics.

The modulation electronics is mainly located inside the HV vessel at potential of up to 2 MV. Modulation signal is transmitted to high voltage part by means of light [3]. Laser diode ADL-66505TL mounted on a viewport outside the HV vessel is used as optical transmitter. Its optical output power is stabilized at the level of 20 mW. Silicon PIN photodiode BPW34 located at 0.3 m distance from the laser diode is used as optical receiver. Combination of a low noise amplifier (LNA) and a comparator allows to have stable modulation voltage at

ISBN 978-3-95450-119-9

ELECTRON CLOUD DENSITY MEASUREMENTS USING RESONANT TE WAVES AT CESRTA*

J.P. Sikora†, M.G. Billing, D.O. Duggins, Y. Li, D.L. Rubin,
R.M. Schwartz, K.G. Sonnad, CLASSE, Ithaca, New York, USA
S. De Santis, LBNL, Berkeley, California, USA

Abstract

The Cornell Electron Storage Ring has been reconfigured as a test accelerator (CESRTA) with beam energies ranging from 2 GeV to 5 GeV of either positrons or electrons. Research at CESRTA includes the study of the growth, decay and mitigation of electron clouds in the storage ring. Electron Cloud (EC) densities can be measured by resonantly exciting the beam-pipe with microwaves where standing waves are established between discontinuities. The EC density that is within the standing waves will change the beam-pipe's resonant frequency. When the EC density is not uniform, it is especially important to know the standing wave pattern in order to know exactly where the EC density is being sampled by the microwaves. We present our current understanding of this technique in the context of new test sections of beam-pipe installed in August 2012. This includes bench measurements of standing waves in the beam-pipe, simulations of this geometry and recent EC density measurements with beam.

INTRODUCTION

In August 2012, four sections of test beam-pipe were assembled and installed in the CESRTA storage ring. Each chamber is instrumented with a Time Resolved Retarding Field Analyzer (TR-RFA) to evaluate the mitigation properties of the different geometries and surface coatings. The TR-RFA detects the flux of cloud electrons into the beam-pipe wall [1].

There are two different cross sections of round beam-pipe, one smooth and the other with triangular grooves on the top and bottom inside surfaces as shown in Fig. 1. With these two cross sections, one pair has been made with a surface of bare aluminum. The other pair have a coating of Titanium Nitride (TiN) on the inner surface. The chambers are assembled together and when installed, each chamber will be centered in one of four chicane dipole magnets.

Having established the basic technique for the resonant TE wave measurement of EC density [2, 3, 4, 5], we investigated the possibility of using this technique to make independent EC density measurements on each of the four test chambers. Each resonance has its own characteristic standing wave pattern and the TE Wave measurements are localized to the region of the standing wave. So the choice of the resonances used in a measurement determines where the cloud is sampled along the length of the beam-pipe.

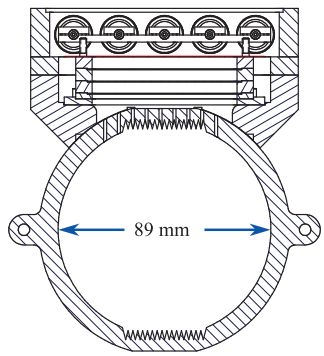

Figure 1: A cross section of grooved beam-pipe is shown above with a Time Resolved RFA assembly on the upper surface.

BENCH MEASUREMENTS

A bead pull is a common technique for measuring the fields in resonant cavities [6]. If a small dielectric bead is positioned in a cavity, there will be a shift in its resonant frequency that is proportional to E^2 of the standing wave at the location of the bead.

Previous bench measurements had been made using various combinations of grooved and smooth sections of beam-pipe. These measurements showed that the first two resonances were mostly confined to a grooved section if it is between smooth sections of beam-pipe [4]. This is due to the fact that the cutoff frequency of the grooved pipe is lower than that of the smooth pipe. This result influenced the decision to alternate grooved and smooth beam-pipe when assembling the actual vacuum chambers.

Bead Pull of the Assembly

Before it was installed in the storage ring, a bead pull measurement was made on the four chamber assembly (Fig. 2). For the measurement, short sections of smooth beam-pipe were added to the ends of the assembly and the flanges at the far ends had aluminum plates covering the openings in order to produce reflections. A 0.3 cm^3 nylon bead was positioned inside the beam-pipe using a thin mono-filament fishing line. At each position along the length of the beam-pipe, the frequency shift was measured by recording the peak response on a spectrum analyzer.

The electrodes of three Beam Position Monitor (BPM) flanges in the assembly were used to couple microwaves in

* This work is supported by the US National Science Foundation PHY-0734867, PHY-1002467 and the US Department of Energy DE-FC02-08ER41538, DE-SC0006505.

† jps13@cornell.edu

ISBN 978-3-95450-119-9

GATLING GUN TEST STAND INSTRUMENTATON*

D. Gassner #, I. Ben-Zvi, J. Brutus, C. Liu, M. Minty, A. Pikin, O. Rahman,
E. Riehn, J. Skaritka, E. Wang
Brookhaven National Laboratory, Upton, NY 11973, USA

Abstract

To reach the design eRHIC luminosity, 50mA of polarized electron current is needed. This is more than what the present state-of-the-art polarized electron cathode can deliver. A high average polarized current injector based on the Gatling gun [1] principle is being designed. This technique will employ multiple cathodes and combine their multiple bunched beams along the same axis. A proof-of-principle test bench will be constructed that includes the 220 keV Gatling gun, beam combiner, diagnostics station, and collector. The challenges for the instrumentation systems and the beam diagnostics that will measure current, profile, position, and halo will be described.

INTRODUCTION

A future electron-ion collider called eRHIC [2] is being designed at Brookhaven National Laboratory. It will utilize a polarized electron source based on an electron gun with multiple photocathodes arranged in circular configuration similar to a traditional Gatling gun. It is driven by IR lasers with circular polarization [3]. The electron bunches from individual cathodes will be funneled to a common beam-line axis by a fast combiner with a rotating magnetic field [4]. A test setup is being designed for testing the primary components of this high average polarized current pre-injector. The electron beam parameters [5] are listed in Table 1. The performance of the innovative electron gun and combiner designs will be determined by the resulting electron beam characteristics that will be measured by the diagnostic systems. Due to the challenges presented by commissioning a variety of innovative subsystems at the same facility, a phased approach will be employed. The phase one proof of principle plans include using 2 of the 20 gallium arsenide photocathodes to generate the first beams at low rep-rates (~1Hz). The diagnostics plan for this project is presently in the preliminary design stage. The present schedule for this Laboratory Directed Research and Development (LDRD) project is to demonstrate the Gatling gun for use as a practical source for an Energy Recovery Linac by 2015. Existing state-of-the-art guns can produce average current of several hundred uA. Groups at JLAB and Mainz have achieved average current of several mA but with rather poor lifetime [6]. By extrapolating past experience with future expectations we hope to achieve 149-hour cathode lifetime [7].

Table 1: Gatling Gun Electron Beam Parameters

Electron Parameters	
Electron Beam Energy	220 keV
Charge per Bunch	0.1 – 3.5 nC
Electron Beam Current	2 mA/cathode
RMS Norm Emittance	17 mm-mrad
Bunch Repetition Rates	1 Hz – 14 MHz
Energy Spread (full)	22 keV
Energy Spread (97%)	8 keV
FWHM Bunch Length	1.5 ns
Trans beam size at YAG	15 mm round

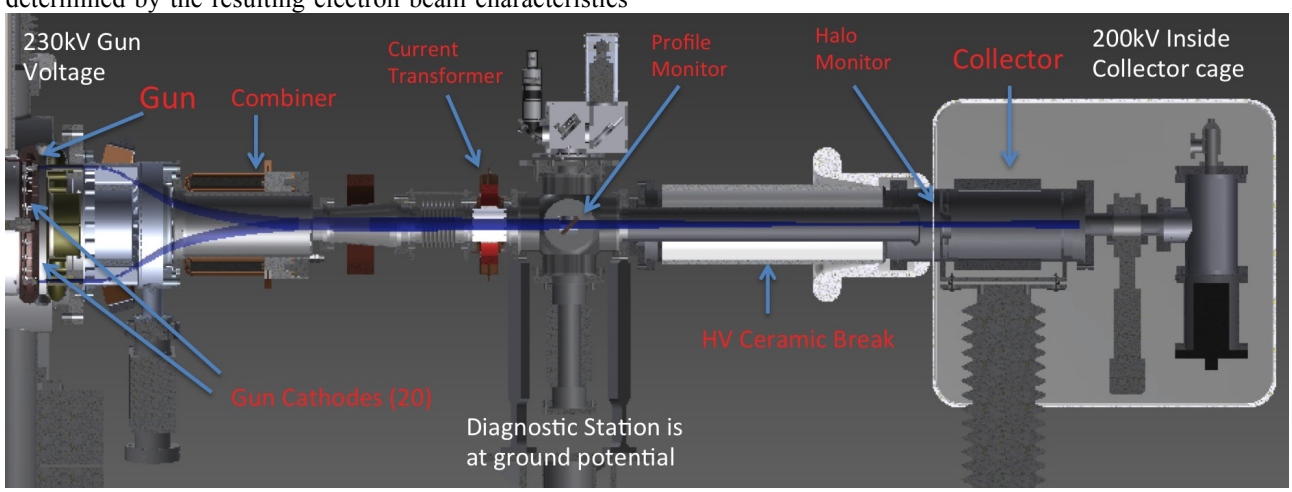

Figure 1: Gatling Gun test stand cut-away side view. Some of the transport magnets and BPM are not shown.

*Work supported by the auspices of the US Department of Energy
#gassner@bnl.gov

ISBN 978-3-95450-119-9

ABORT DIAGNOSTICS AND ANALYSIS DURING KEKB OPERATION

H. Ikeda*, J. W. Flanagan, T. Furuya, M. Tobiyama, KEK, Tsukuba, Japan
M. Tanaka, MELCO SC,Tsukuba, Japan

Abstract

KEKB has stopped since June 2010 for upgrading the luminosity 40 times, i.e. SuperKEKB. During the operation of 11 years, a pair of controlled beam abort systems worked more than 10000 times to protect the hardware components of KEKB accelerator and the detector against the high intensity beams of high and low energy rings (HER and LER, respectively). Optimization of the abort trigger was necessary to balance efficient operation with the safety of the hardware. Therefore, we analyzed one-by-one all of the aborts, and continually adjusted the abort system. The diagnostic system was based on a high-sampling-rate data logger that recorded beam currents, RF signals and beam loss monitor signals. The beam oscillation signals, vacuum pressure and detector dose rate were also examined. This paper describes the typical abort causes, optimizations of abort levels, and abort statistics over approximately eight years after having arrived at high current operation.

INTRODUCTION

KEKB was an energy asymmetric electron positron collider dedicated to B meson physics. An electron ring of 8 GeV (HER) and a positron ring of 3.5 GeV (LER) were installed in a tunnel. The maximum achieved currents of the electron and positron rings were 1.35 A and 2.0 A respectively so far. When a large beam loss is expected, the beam should be quickly dumped in order to avoid the damage to the accelerator and the Belle detector components due to high current beams. A controlled beam abort system was installed for this purpose [1]. The system triggered more than 10000 aborts during the KEKB operation for eleven years. Optimization of the condition to issue the abort trigger was necessary to compromise between efficient operation and safety of the hardware. Therefore, we analyzed all of the aborts one by one, and continually adjusted the abort system.

SETUP OF ABORT MONITOR

The diagnostic system was based on a high-sampling-rate data logger that recorded beam currents, RF signals, signals from beam loss monitors and the Belle detector at the moment of the beam abort. In addition to the data stored in the data loggers, beam oscillation, vacuum pressure, the earthquake sensor and the dose rate of the Belle detector were also examined to analyze the beam abort.

Loss monitor signals of whole rings were collected at four local control rooms (LCRs), and were sent to the data loggers distributed in five LCRs where both loss monitor signals and RF cavity signals were obtained.

The signal flow of the data loggers is shown in Fig. 1. Logged data were beam current measured by a direct-current-current transformer (DCCT) [2], a part of loss monitor signals from PIN photo-diodes (PD) and ion chambers (ICs), signals from the RF cavities, i.e. cavity voltages and output of klystrons, the beam phase signal showing the deviation of the synchronous phase, the injection trigger timing and the Belle PD signal. Most PDs were fixed on the movable masks of each ring, and determined the ring in which the beam loss occurred. On the other hand, ICs were installed in the whole tunnel and covered the wide range in space, but could not distinguish the ring. These signals were useful to diagnose the cause of the beam abort since they had a strong correlation with the beam condition. The recorded data were sent to the KEKB central control room (CCR) via the KEK internal network then monitored by operators. The information was ready for inspection within a few minutes after the abort. The beam oscillation signals were obtained from the beam oscillation recorder (BOR) [3]. The signals were also ready within a few minutes after the abort. The BOR recorded the bunch-by-bunch beam position over 4000 turns immediately before the beam abort so as to detect vertical and horizontal beam oscillations.

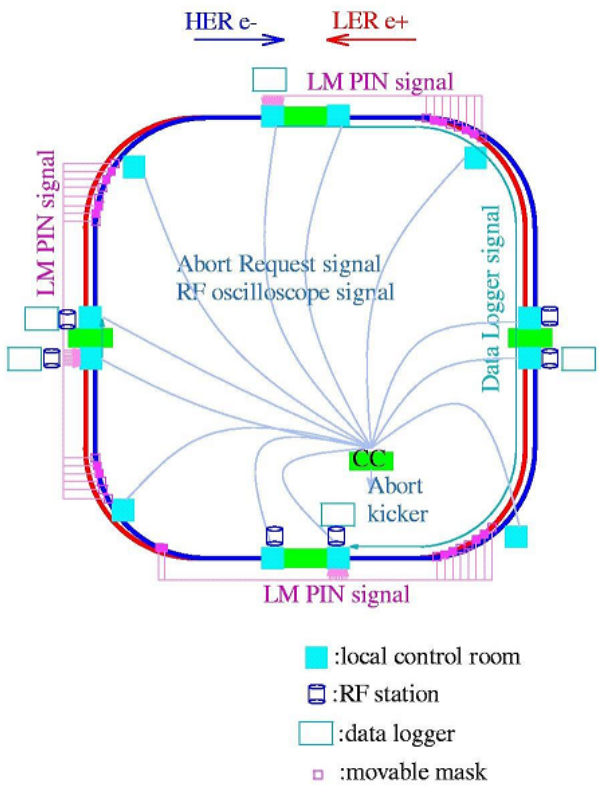

Figure 1: A signal flow of data loggers.

ISBN 978-3-95450-119-9

EXTREME LIGHT INFRASTRUCTURE (ELI BEAMLINES) – RESEARCH AND TECHNOLOGY WITH NEW ULTRA-SHORT PULSE INTENSE LASER DRIVEN SOURCES OF ENERGETIC PHOTONS AND CHARGED PARTICLES

L. Pribyl, L. Juha, G. Korn, T. Levato, D. Margarone, B. Rus, S. Sebban, S. Ter-Avetisyan,
ELI-Beamlines, Institute of Physics, Prague, Academy of Sciences Czech Republic.

Abstract

We are giving an overview on the development of the "Extreme Light Infrastructure (ELI) Beamlines facility", which will be a high-energy, repetition-rate laser pillar of the ELI project, [1]. It will be an international facility for both academic and applied research, slated to provide user capability from the beginning of 2016. The main purpose of the facility is the generation and applications of laser driven high-brightness X-ray sources and accelerated particles (electrons, protons and ions).

The laser system will be delivering pulses with length ranging between 10 and 150 fs and will provide high-energy Petawatt and 10-PW peak powers.

The short photon wavelength (20 eV-1 MeV) laser driven sources are either based on direct interaction of the laser beam with a gaseous or solid target or will first accelerate electrons which then will interact with laser produced wigglers or directly injected into undulators. The main planned short pulse laser driven x-ray and charged particles sources and their parameters are presented together with basic requirements on the relevant beam detectors.

LASER SOURCES

ELI experimental area is divided into six experimental halls E1 to E6 (see Fig. 1), where a wide range of secondary x-ray or charged particle sources driven by a set of laser sources is located. The developed state-of-the-art laser sources are divided into four systems L1 to L4, each providing a specific range of pulse energies, lengths and repetition rates.

The laser system L1 involves two high-repetition-rate kHz beamlines employing the technique of Petawatt Field Synthesizer (PFS). Upon compression using chirped mirrors, each of the kHz beamlines will provide about 200 mJ, 20 fs pulses.

The 10-Hz repetition rate L2 system providing PW-class pulses (10 and 20 J) will consist of diode-pumped multislab lasers pumping a large Ti:sapphire broadband amplifier and also an OPCPA chain.

The L3 system exploits the technology of multislab Nd:glass operating at near room temperature and running at10 Hz repetition rate. The system will provide about 30 J in ~20 fs pulses at 10 Hz, corresponding to approximately 1.5 PW peak power. Additionally to the main 1.5 PW pulses the system will provide inherently jitter-free synchronized auxiliary pulses with peak power of ~50 TW.

The designed laser system finally involves a 10-PW beamline in the L4 section. The system is designed to exploit the technology of mixed Nd:glass capable to deliver CPA pulses with bandwidth >13 nm, which are

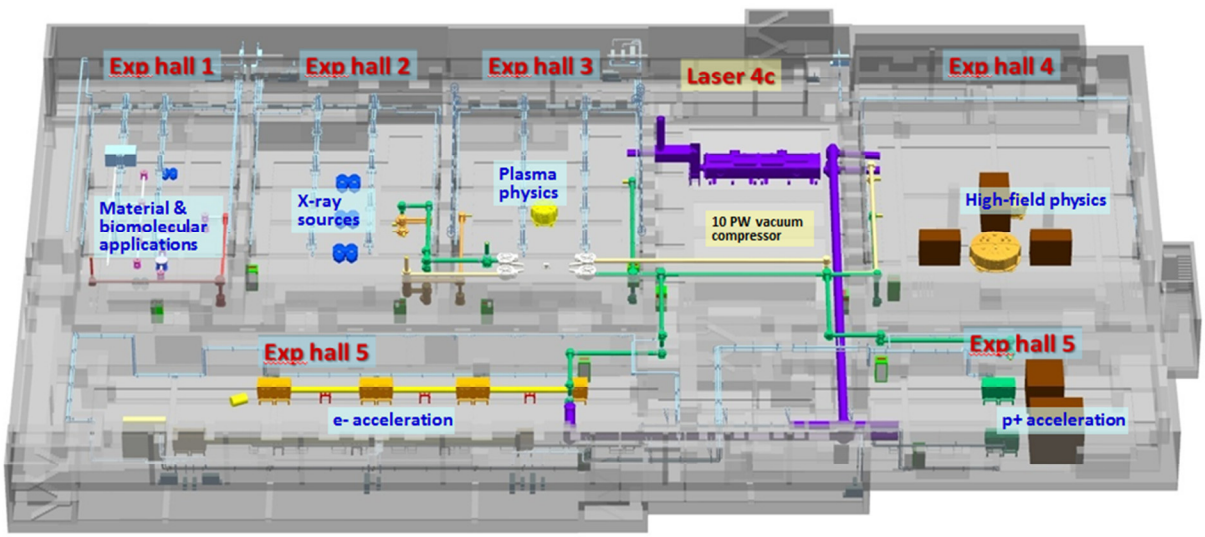

Figure 1: Overview axonometric layout of the basement floor of the ELI-Beamlines laser building showing the experimental halls E1 to E6. The halls will be equipped progressively with vacuum chambers, experimental instrumentation and beam delivery units, according to the project implementation plan. The overall footprint dimensions of the basement floor are about 110 x 65 m^2.

ISBN 978-3-95450-119-9

BEAM DIAGNOSTICS OF CENTRAL JAPAN SYNCHROTRON RADIATION RESEARCH FACULTY ACCELERATOR COMPLEX

M. Hosaka, N. Yamamoto, K. Takami, T. Takano, A. Mano, E. Nakamura,
H. Moriomoto,Y. Takashima, Synchrotron Radiation Reserch Center, Nagoya University, Furo-cho, Chikusa-ku, Nagoya, Aichi 464-8603, Japan
M. Katoh, UVSOR Facility, Institute for Molecular Science, 38 Nishigo-Naka, Myodaiji-cho, Okazaki, Aichi 444-8585, Japan
Y. Hori, High Energy Accelerator Research Organization, KEK, 1-1 Oho, Tsukuba, Ibaraki 305- 0801, Japan
S. Sasaki, JASRI/SPring-8, 1-1-1, Kouto, Sayo-cho, Sayo-gun, Hyogo 679-5198, Japan
S. Koda, Saga Light Source, 8-7 Yayoigaoka, Tosu, Saga, 841-0005, Japan
A. Murata, K. Nakayama Toshiba Corp., 8 Shinsugita, Isogoko-ku, Yokohama, 235-8523, Japan

Abstract

A new synchrotron radiation facility, Central Japan synchrotron radiation research facility (tentative name) has been built in Aichi area, Japan. Principal diagnostics system for the accelerator complex has been installed and data have been obtained on beam profile, beam position, current and betatron tunes. Using the diagnostics system, the accelerator complex has been successfully commissioned.

INTRODUCTION

Central Japan synchrotron radiation research facility (tentative name) is constructed in collaboration between Nagoya University, Aichi prefectural government, Aichi Science & Technology Foundation (ASTF), industries and other universities in Aichi area. The main aim of the facility is to provide synchrotron radiation for researches and industries.

Basic design of the accelerators including beam diagnostics system was done by Nagoya University and mechanical design of the accelerator components was done by Toshiba Corporation and Nagoya University. Construction and installation of the accelerator components was done by Toshiba Corporation.

Construction of the facility started in 2010 and finished in Apr. 2012. Commissioning of the accelerator complex started in Mar. 2012. At each stage of the commissioning, the beam diagnostics system played an essential role. In this paper, the beam diagnostics system and the data taken with the system during the commissioning is described.

OVERVIEW OF ACCELERTOR COMPLEX

The Central Japan Synchrotron Radiation Research Facility's accelerator complex consists of a 50 MeV linac, a 1.2 GeV booster synchrotron and a 1.2 GeV storage ring. As shown in Fig. 1, main accelerator components are installed in a shielding wall.

Table 1: Parameters of Accelerator Complex

Storage ring	
Electron energy	1.2 GeV
Circumference	72 m
RF frequency	499.654 MHz
Beam current	> 300 mA
Natural emittnace	53 nm-rad
Betatron tune	(4.72, 3.23)
Normal bend	1.4 T, 39 deg.
Superbned	5 T, 12 deg.
Booster synchrotron	
Electron energy	50 MeV - 1.2 GeV
Circumference	48 m
RF frequency	499.654 MHz
Natural emittnace	220 nm-rad
Repetition rate	1 Hz
Injection linac	
Electron energy	50 MeV
RF frequency	2,856 MHz
Repetition rate	1 Hz
Gun Pulse length	0.56, 0.70, 1.05 nsec

A short bunch (< 1 nsec) electron beam generated by a thermionic electron gun is accelerated by the linac to 50 MeV. Injection of the electron beam bunch to the booster synchrotron is made on axially using a kicker magnet. The booster synchrotron is designed to be compact and therefore the mechanical aperture is small. For example, the gap height of the bending duct is only 16 mm.

The accelerated electron beam to 1.2 GeV is extracted by a kicker magnet and injected into the storage ring using 4 kicker magnets. The storage ring has a special feature that hard X-ray SR can be produced from 4 superconductive bending magnets (super-bend). The injector works at 1 Hz. The circumference of the storage ring is 72 m and frequency of the acceleration cavity is 499.654 MHz. The control system of the accelerators is based on EPICS. Parameters of the accelerator complex are shown in Table 1. A detailed description of the accelerators can be found in [1].

ISBN 978-3-95450-119-9

THE FIRST EXPERIENCE WITH LHC BEAM GAS IONIZATION MONITOR

Mariusz Sapinski, William Andreazza, Bernd Dehning, Ana Guerrero,
Marcin Patecki, Reine Versteegen, CERN, Geneva, Switzerland

Abstract

The Beam Gas Ionization Monitors (BGI) are used to measure beam emittance on LHC. This paper describes the detectors and their operation and discusses the issues met during the commissioning. It also discusses the various calibration procedures used to correct for non-uniformity of Multi-Channel plates and to correct the beam size for effects affecting the electron trajectory after ionization.

INTRODUCTION

The Beam Gas Ionization monitors (BGI), often called Ionization Profile Monitors (IPM) on LHC are configured to measure electrons produced in ionization of Neon gas, injected into LHC vacuum chamber. The pressure of injected gas reaches 10^{-8} mbar. The beam passes between two ceramic electrodes with difference of potentials of 4 kV, over a distance of 85 mm. This potential brings the electrons to Multi-Channel Plate (MCP, from Photonis), where the signal is amplified. A phosphor screen is located 2 mm behind the MCP. It is deposited on a right-angle prism, which is the only optical element inside the vacuum. In order to minimize the transverse spread of the electrons, external magnetic field of 0.2 T, directed along electric field lines, is applied. Light produced by the phosphor screen is directed through a vacuum window to an optical system and a CID intensified camera (Thermo-Scientific CID8712D1M-XD4). A schematics of the LHC BGI and a picture of the outside flange are shown in Fig. 1.

The image is amplified in tunnel electronics, which also allows to control the gate of the camera and gain of the internal camera intensifier. A cable of about 150 meter length connects the tunnel electronics with a frame-grabber, which is a BTV card installed in a VME crate in the underground gallery. There is no access to the gallery during machine run.

Server programs are running on the crate CPU, controlling the HV and processing the image. The beam profiles are fitted with gaussian assuming linear contribution from the background.

MCP USAGE

During the 2011 run the HV on the MCPs was kept on for most of the time. As a result a local decrease of gain, mainly in the typical beam position, were visible. This non-homogenity of the MCP response affects the beam profile reconstruction.

Therefore, it was decided to exchange the MCPs during the winter technical stop. Due to technical difficulties the operation has been performed on beam one BGIs only (two out of four installed on LHC). The exchange has not been done in a clean room, what could affect the durability of the new equipment. A picture of an MCP in its holder is shown in Figure 2.

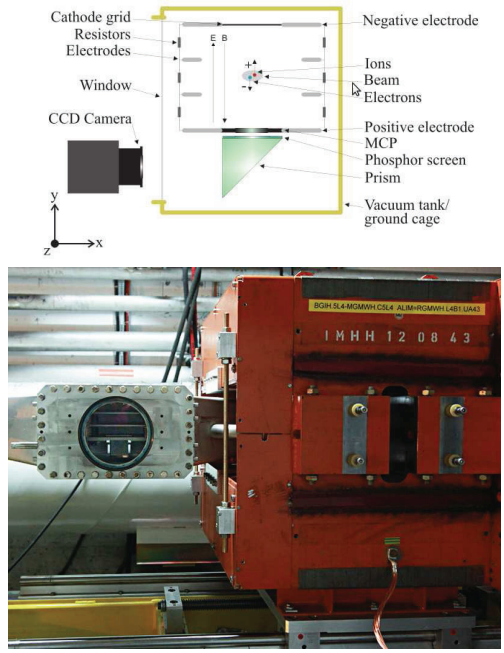

Figure 1: Up: a schematics of LHC BGI (from [1]). Bottom: a photo of the LHC BGI (flange with optical port) in the tunnel, with magnet displaced.

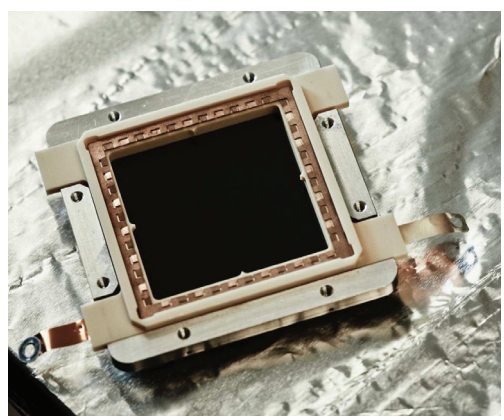

Figure 2: Multi-channel plate in its holder.

The newly installed MCPs had a much higher gain but, at the same time, were more sensitive to the signals produced by high-intensity beams. One of them got broken during a scrubbing run in March 2012, when a large electron cloud

ISBN 978-3-95450-119-9

DEVELOPMENT OF TURN-BY-TURN DIAGNOSTIC SYSTEM USING UNDULATOR RADIATION

M. Masaki #, A. Mochihashi, H. Ohkuma, S. Takano and K. Tamura
Japan Synchrotron Radiation Research Institute (JASRI/SPring-8), Hyogo, Japan

Abstract

At the diagnostic beamline II (BL05SS) [1] of the SPring-8 storage ring, a turn-by-turn beam diagnostic system using undulator radiation has been developed to observe fast phenomena such as stored beam oscillations during the top-up injections, blowups of beam size and energy spread coming from the instabilities of a high current single bunch and so on. The fast diagnostic system observes a spatial profile of undulator radiation on a selected harmonic number. Especially, The profile widths of the higher harmonics than the 10th-order are sensitive to variation of the energy spread. The principle and experimental setup of the turn-by-turn diagnostic system, and examples of beam observations are reported.

MAIN INSTRUMENTS OF BL05SS

BL05SS is a diagnostic beamline with an insertion device (ID05) which magnet array is of planar Halbach type with the 51 periods of 76 mm long. The maximum deflection parameter K is 5.8. Elaborate tuning of the magnetic field leads to the fundamental random phase error of 1.6 degree (r.m.s.) at the maximum K so that we can clearly distinguish individual higher order harmonics of the undulator radiation [2]. This is essential for the beam diagnostics, especially, energy spread measurement. To shape the radiation, a 4-jaw slit is installed in the frontend section at a distance of about 25 m from the source point. A double crystal monochromator using Si (111) is placed in the optics hutch at a distance of about 70 m from the source. The undulator radiation on a harmonic number selected by the monochromator goes into the experimental hutch where the turn-by-turn beam diagnostic system is installed at a distance of about 90 m from the source point (Fig. 1).

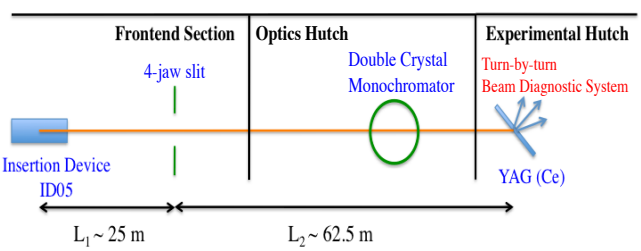

Figure 1: Turn-by-turn beam diagnostic system and the related main instruments of BL05SS

masaki@spring8.or.jp

EXPERIMENTAL SETUP OF THE TURN-BY-TURN BEAM DIAGNOSTIC SYSTEM

The turn-by-turn beam diagnostic system is intended to observe fast motions of electron beam using spatial profiles of the monochromatic undulator radiation. This system consists of a fast fluorescence screen, imaging optics and a fast CCD camera with an image intensifier (Fig. 2). The fast fluorescence screen placed in vacuum is YAG (Ce) crystal with 0.1 mm thick and its decay time is several tens of nano seconds. An X-ray profile of undulator radiation with photon energy of about 10 keV is converted into a visible light profile on the YAG (Ce) screen. Converted center wavelength is 550 nm and its bandwidth is about 100 nm (FWHM). The imaging optics transforms the 2D-profile on the YAG (Ce) screen to two line profiles projected in the horizontal and vertical directions. Visible light is split into two light paths by a half mirror and one-dimensional focusing optics using cylindrical lenses is implemented in each light path. In the path-1, the strong vertical focusing makes a horizontal-projected line profile. The horizontal strong focusing in the path-2 makes a vertical-projected line profile. These two projected line profiles are simultaneously imaged on a photoelectric surface of the image intensifier (HAMAMATSU: C9548-02MP47). The material of the photoelectric surface is GaAsP. The image intensifier embeds dual micro channel plates (MCPs) and P47 phosphor screen with short decay time. The minimum width and the maximum repetition rate of the MCP gate are 10 ns and 210 kHz, respectively. The fast CCD camera (Roper Scientific: ProEM 512B) captures the intensified images of the two line profiles. The pixel number and size are 512(X)*512(Y) and 16 μm, respectively. This CCD camera has a special function referred to as the kinetics readout mode, which is very useful for the turn-by-turn measurements of the spatial profiles. By illuminating only a small portion of the CCD sensor, a series of sub-flames can be captured and vertically shifted in microseconds vastly increasing the time resolution. The fastest shift rate is 0.45 μs/pixel in each sub-frame. The sub-frame is triggered independently by an external signal synchronizing with the beam revolution signal or its frequency-dividing signal. The imaging optics and the camera position are adjusted to locate the illuminating area in a lower part of the CCD sensor. The smaller vertical size of the sub-frame enables profile measurements with higher repetition rate, which requires vertically strong focusing of the light on the narrow sub-frame.

ISBN 978-3-95450-119-9

METHODS TO REDUCE THE SYSTEM ERROR FOR HIGH POWER MSSW EMITTANCE METER

S. X. Peng*, P. N. Lu, H. T. Ren, J. Zhao, Y.Xu, Z.Y.Guo, Z. X. Yuan and J. Chen
State Key Laboratory of Nuclear Physics and Technology & Institute of Heavy Ion Physics, Peking University, Beijing 100871, China.

Abstract

Recently a new Multi-Slit Single-Wire (MSSW) type high power beam emittance meter named as HIBEMU-5 has developed in Peking University (PKU). Compared to previous MSSW devices, HIBEMU-5 greatly reduced the system error from 16.4% to 3.7% by specific designs to solve the incomplete short-slit sampling and fixed slit-wire distance. The problems of previous PKU devices are analyzed in part one. In part two, we describe the specific updating methods to solve its short-slit disadvantage by re-designing a longer-slit board with sufficient cooling, detail the mechanical scheme of changing the slit-wire distance for different beam divergence. The commissioning results given at part three prove that this new long slits design is successful to complete the beam sampling without being distorted by high power H^+ beam. And the movable wire cup is able to locate the best measurement position for different beam focusing.

INTRODUCTION

Multi-Slit Single-Wire (MSSW) method is popular in emittance measurement for high power beams[1]. The slits are used to sample the beam and the wire that locates some distance downstream the beam is used to obtain the beam divergence angle. To ensure the measurement accuracy, the length of slits should be longer than the beam diameter so that the sampling is complete and the thickness of slits board should be as thin as possible to avoid its collimation effect. As a measurement device, it should have the universal ability to deal with different kinds of beam no matter it's divergence is larger (low energy heavy ion beam) or smaller(high energy light ion beam).

At Peking University (PKU) we have developed 4 MSSW emittance meters[2][3][4]. Their processing technic and electronic equipments have been upgraded one by one. But they have two common demerits. First, a 0.3 mm thick molybdenum board with 25 or 35 slits is attached at the bottom of the water cooled Faraday cup to sample the beam and the slit board exposes to the whole beam all the time during the measurement period. Very thin slit board prevents cooling directly and the heat absorbed from the beam hit can only be taken away through Faraday cup. To avoid heat distortion, the length of slits is shortened to 5 mm. But 5 mm is much shorter than the size of the beam diameter in most cases. And this leads to incomplete sampling. As shown in Fig. 1, the incomplete sampling brings a system error of about 8.7% for a ϕ 50mm typical Gaussian distributed beam[5].

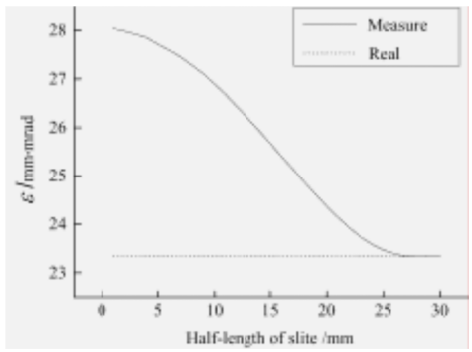

Figure 1: Emittance simulation with different slit length[5].

The second demerit is the fixed length L between slit and wire. This limits the universality of MSSW emittance meters. For an emmitance device whose slits interval is d, the beamlet will start to overlap at a distance of D.

$$D \approx d/2\sqrt{\varepsilon/\beta}$$

Here ε is beam emittance and β is Twiss parameter. For different beam focusing D is different. $L=D$ is the best condition, or L is slightly less than D is also tolerable for this emmitance measurement unit. If $L<<D$, too less data can be collected in the whole scanning; If $L>D$, data overlaps between adjunct slits, as shown in Fig.2. Both improper conditions can generate an error up to 5%.

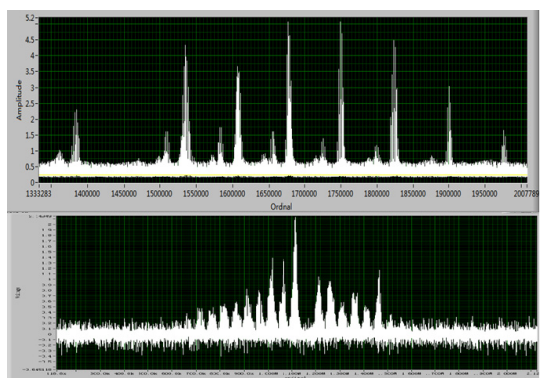

Figure 2: (up)situations of $L<<D$ with too less data collected, (down) conditions of $L>D$ with data overlap.

*Correspondence author.
Electronic mail: sxpeng@pku.edu.cn

ISBN 978-3-95450-119-9

TRANSVERSE-ACCEPTANCE MEASUREMENT SYSTEM FOR JAEA AVF CYCLOTRON

Hirotsugu Kashiwagi#, Nobumasa Miyawaki, Satoshi Kurashima, Susumu Okumura,
Takasaki Advanced Radiation Research Institute, Japan Atomic Energy Agency
1233 Watanuki-machi, Takasaki, Gunma, 370-1292, Japan

Abstract

We are developing an acceptance measurement system to evaluate the matching of the emittance of an injection beam to the acceptance of the AVF cyclotron. The system is composed of a phase-space collimator in the low energy section and beam intensity monitors which are installed just after the phase space collimator and in the high energy section. The phase-space collimator, which consists of two pairs of movable slits, is used to inject beams with very small-emittance into the cyclotron by defining position and divergence angle of the beam from an ion source. The acceptance is measured as the phase space distribution of the ratio of the beam intensity at the high energy section to that at the phase space collimator. In the preliminary test, only a part of distribution for the acceptance was measured because the injection-beam emittance from an ion source did not cover the whole acceptance. A steering magnet has been added to expand measurable area by scanning the injection beam in synchronization with the acceptance measurement. The result of a test experiment showed the emittance of the injection beam was able to be enlarged more than ten times. It was confirmed that this technique was valid as the method of increasing the injection emittance for measuring the whole of the acceptance.

INTRODUCTION

The JAEA AVF cyclotron in TIARA (Takasaki Ion accelerators for Advanced Radiation Application) produces various kinds of ion beams from 10 MeV H^+ to 490 MeV $^{192}Os^{30+}$ for research in biotechnology and materials sciences. The ion species and/or energy of the beam are changed frequently (223 times a year in 2011 [1]). Since the operating parameters of the cyclotron vary according to the kind of beam, the parameters need to be optimized for each beam to be accelerated and be delivered to the target port with minimum beam loss.

Regarding the optimization of the beam injection to the cyclotron, it is required for the beam emittance to be matched to the acceptance of the cyclotron. A part of the injected beam outside the acceptance is lost in the cyclotron. The condition of the injection in longitudinal direction is determined mainly by the voltage and phase of a buncher. The optimization procedure has been established [2]. As for the condition of the injection in the transverse direction, parameters of the magnets in the low energy beam transport line are fine-tuned manually by monitoring the accelerated beam current. However, it is not easy to assess optimum condition because various parameters are mutually related and the acceptance is not precisely known.

We are developing a transverse acceptance measurement system to evaluate the state of the beam injection. The system will help to optimize the injection condition in the transverse direction.

This paper shows the outline of the measurement system and a preliminary measurement test. In addition the enlargement of the effective emittance of the injection beam for expansion of the measurable area that is currently under developing is described.

SYSTEM FOR TRANSEVERSE-ACCEPTANCE MEASUREMENT

The system for transverse acceptance measurement is shown schematically in Fig. 1. The main components of the system are the phase-space collimator in the low energy beam transport line and the intensity monitors in the high energy section. One of the monitors is selected depending on the position where the acceptance is measured. To measure the acceptance for accelerating and transporting the beam to the deflector entrance in the cyclotron, for example, a current monitor inside the cyclotron is used, while in the case of acceptance to the outside of the cyclotron a Faraday cup in the high energy beam transport line is used.

Measurement of the acceptance is made by injecting every portion in the whole phase-space, which should be large enough to cover the acceptance. The acceptance can be estimated from the sum of the portions of the beam which passes through the system.

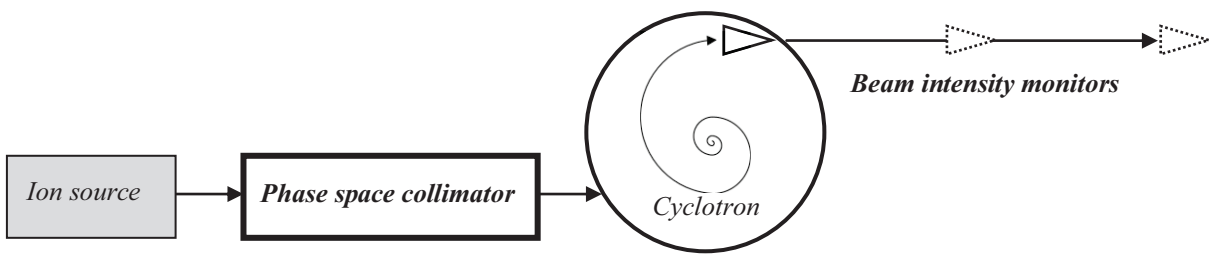

Figure 1: The system for transverse acceptance measurement.

#kashiwagi.hirotsugu@jaea.go.jp

ISBN 978-3-95450-119-9

NUMERICAL ANALYSIS ON THE GAIN-REDUCTION CHARACTERISTICS OF MULTI-WIRE PROPORTIONAL CHAMBERS

Ken Katagiri, Takuji Furukawa, and Koji Noda,
Dept. of Accelerator and Medical Physics, National Institute of Radiological Sciences, Chiba, Japan

Abstract

In order to investigate the gain-reduction characteristics of the multi-wire proportional chamber (MWPC) for different geometric parameters, we performed numerical simulations using a numerical code. The numerical code was developed using a two-dimensional drift-diffusion model to evaluate the gas gain taking into account the reduction effect caused by the space charge effect of the moving positive ions. We investigated the gain-reduction rate for several parameters of the anode-anode distance when beam intensity was increased. We found that the gain reduction could be improved by decreasing the anode-anode distance, owing to the sharing of the initial-ion pairs among the anode wires. From these results, we discuss a desirable distance between the anode wires to improve the gain reduction.

INTRODUCTION

Several tens of MWPCs have been installed in the beam transport line at HIMAC (Heavy Ion Medical Accelerator in Chiba) to diagnose the beam profiles [1]. Also in the scanning irradiation system, which was started to be operated for the cancer treatment in 2011, the MWPCs are used to evaluate the beam position and to construct 2-D fluence maps [2]. In normal operation for treatments, the MWPCs are operated in the current mode and irradiated by high-rate incident particles of $\sim 10^8 - 10^9$ particles per second (pps). Under such a beam condition, gain reduction of the output signal is observed. The gain reduction is due to the distorted electric field, which originates from the space charge of the accumulated ions. If the gain reduction is large, the measured beam profiles may differ from the actual profiles. Therefore, modification of the MWPCs to suppress the gain reduction is an important issue.

In the treatment operation at HIMAC, the irradiation period of ~1 s is much longer than that required by ions to travel from the anodes to the cathodes. Therefore, the gain reduction process cannot be explained only by the remaining ions around the anodes, and it is expected to be transient during the beam irradiation. Information on the relations between the gas-gain variation and the ion-density distribution is necessary for modification of the MWPC parameters, such as anode radius and distance between electrodes. For those reasons, we developed a 2-D simulation code to evaluate the gas gain taking into account the gain-reduction effect [3].

Using the numerical code, we performed analyses on the dynamics of ions/electrons in a helium-filled MWPC to improve the gain reduction. In this paper, we report the simulation results of the gas gain for several parameters of the anode-anode distance. Also we discuss the transient dynamics of the ions, which leads to the variation of the output signal.

SIMULATION METHOD

The 2-dimentional drift-diffusion model was employed to analyse the dynamics of the ions and electrons. In order to simplify the analysis, electrons (e^-) and positive ions (He^+) were only taken into account. The two advection-diffusion equations and the Poisson equation were coupled and solved numerically. The pressure and the temperature inside the MWPC were assumed to be 10^5 Pa and 300 K, respectively. Figure 1(a) – (c) show schematic diagrams of the MWPC in a discrete space. Three types of MWPC with different anode-anode distance were considered for comparison. The 6×6 mm region of the MWPC were discretized by rectangular grids. The anode-anode distance d was altered by changing the number of the anode wires in 6-mm region: 1 wire for $d = 6$ mm (Fig. 1(a)), 2 wires for $d = 3$ mm (Fig. 1(b)), and 3 wires for $d = 2$ mm (Fig. 1(c)). The periodic boundary condition was applied to the boundaries at $x = -3$ mm and 3 mm. The outlet boundary condition was applied to the surface of the two cathodes at $y = -3$ mm and 3 mm, and to the surface of the anodes. Incident projectiles were injected with constant rate of $I = 5 \times 10^8$ pps from $t = 0$. The beam profile formed by all the projectiles was determined to be a Gaussian distribution of $2\sigma = 3.0$ mm, as shown Fig. 1(d). The beam profile along the z-axis was assumed to be homogeneous in the depth direction of 3 mm. The number of the ion-pairs was determined by W-value and energy deposition of 350-MeV/u projectiles in 1-atm He gas [3].

RESULTS AND DISCUSSION

Conditions for Comparisons of the Gain-reduction Characteristics

Figure 2 shows the calculation results of the gas gain without the gain reduction. In order to calculate the no-reduction regime, the space-charge effect was excluded by considering the low rate beams. In order to compare the gain-reduction characteristics, the applied voltages of three types of MWPC need to be determined to obtain same gas gain in the no-reduction regime. For that reason, the applied voltages were determined to obtain the gas gain of $M = 30$: $V = 847$ V for $d = 2$ mm, $V = 751$ V for $d = 3$ mm, $V = 674$ V for $d = 6$ mm.

ISBN 978-3-95450-119-9

THE ATF2 MULTI-OTR SYSTEM: STUDIES AND DESIGN IMPROVEMENTS*

J. Alabau-Gonzalvo, C. Blanch Gutierrez, A. Faus-Golfe, J.J. Garcia-Garrigos, J. Resta-Lopez
IFIC (CSIC-UV), Valencia, Spain
J. Cruz, D. McCormick, G. White, M. Woodley, SLAC, Menlo Park, California, USA

Abstract

A multi-Optical Transition Radiation (mOTR) system made of four stations has been installed in the extraction line of ATF2 and has been fully operational since September 2011. The system is being used routinely for beam size and emittance measurements as well as for coupling correction and energy spread measurements. In this paper we present the current design and a OTR monitor future upgrade to avoid the wakefields when a simultaneous measurement is made. Finally we report the measurements made in ATF2 during 2011-2012.

INTRODUCTION

ATF2 is an extension of the Damping Ring (DR) of ATF built at KEK (Japan) [1, 2]. ATF2 is a prototype of a Final Focus System (FFS) for a Future Linear Collider such as the International Linear Collider (ILC) or the Compact Linear Collider (CLIC). The first of the ATF2 goals is to generate a vertical beam size of 37 nm at the Interaction Point (IP). The second ATF2 goal it to achieve nanometer-level beam stabilization at the IP in order to be able to demonstrate the capabilitiy of this optics design to reliably deliver high luminosities at future high-energy linear colliders. A mOTR system was installed in the ATF2 extraction line (EXT line) during autumn 2010. This system consists of four OTR monitors [3], and is currently being used for beam size measurement and emittance reconstruction during the ATF2 operation. The mOTR system was installed near an existing wire scanner system (WS) [4] in order to compare the performance of both systems. The WS needs a high number of pulses to make a measurement, resulting in an overestimation of the size due to the beam position and intensity jitter. Moreover, it can take several minutes to complete a single set of beam size measurements. On the other hand, the OTRs are capable of single-shot measurements of the beam ellipse at the beam repetition rate (1.56 Hz). This permits reconstructing the emittance with high statistics and making correlated measurements such as studying the emittance preservation during the extraction from the ATF DR. The minimum beam size that the OTR system can measure is about 2 μm (the 2-lobe distribution of the OTR light starts to become a dominant factor at this scale, whereupon a different measurement scheme would be required). The measurement resolution of this system is typically a few-percent. Figure 1 shows the layout of the mOTR system in the diagnostics section of the EXT line, highlighting the WS location for comparison.

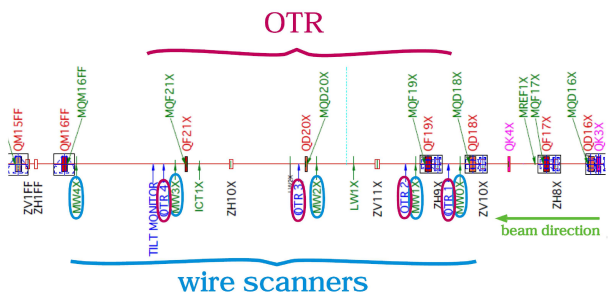

Figure 1: Layout of the ATF2 diagnostics section of the EXT line where the WS and the Multi-OTR system are located, the beam going from right to left.

CURRENT DESIGN AND FUTURE UPGRADES

The 4 OTRs are based on the design of a previous one labeled as OTR1X [5], placed near one of the WSs in order to compare them and to demonstrate the ability to measure the small beam sizes likely to be found after a linear collider DR. Some of the issues presented in the old design were improved in the new one: the footprint was lowered from 55 cm to less than 30 cm, the target actuator was placed on the top, thus reducing the interference problems with the supporting structure, the lens darkening and the camera damage due to radiation was solved by using a 90 degree mirror and a lead protection shield, the targets were changed using two made of 2 μm aluminum and two targets made of 3 to 5 μm kapton with 0.12 μm aluminum coating.

Figure 2 shows a general overview of the new OTR design and Figure 3 shows it as it is installed in ATF2 EXT line. The yellow scotch covers the main body and the side window to protect from light coming in from outside. Below it, the vertical and horizontal stepper motors are shown. From the body, in the upper-left direction is the target actuator and in the upper-right direction the optical elements. The lead shielding for preventing CCD camera damage can be seen on the left of the OTR. At the left and right sides of the body there are a couple of bellows that allows some horizontal and vertical displacement of the whole OTR system.

* Work supported by: FPA2010-21456-C02-01 and by Department of Energy Contract DE-AC02-76SF00515

ISBN 978-3-95450-119-9

INJECTED BEAM PROFILE MEASUREMENT DURING TOP-UP OPERATION

M.J. Boland, Australian Synchrotron, Clayton, Victoria, Australia
T. Mitsuhashi, KEK, Ibaraki, Japan
K.P. Wootton, The University of Melbourne, Victoria, Australia

Abstract

A coronagraph-like apparatus was constructed on the optical diagnostic beamline on the storage ring to observe the injected beam during top-up operations. An image was created on an intensified CCD (ICCD) that can be gated on a single bunch or on a bunch train for a stronger signal. The bright central stored beam was obscured so the comparatively faint injected beam could be observed. The injected beam comes in at a large enough offset so that it was clearly visible above any diffraction or beam halo signals. The beam profile measured was in good agreement with the observations made of the injected beam only using a telescope apparatus. The measurements were made during user beam in top-up operation mode and can be used to optimise the injection process.

CORONAGRAPH APPARATUS

The beam current injected into the Australian Synchrotron storage ring is ≈1 mA per shot in multi-bunch mode and ≈0.05 mA per shot in single-bunch mode. This is a relatively small current compared with the 200 mA of stored beam. In order to measure the beam profile of the injected beam in the presence of the stored beam and requires an apparatus with a dynamic range of more than four orders of magnitude. However, the stored beam can be masked so that an ICCD camera on the optical diagnostic beamline is sensitive enough to capture a single bunch injection. A coronagraph apparatus used to measure beam halos [1] was adapted to masked the stored beam and used to observe the injected beam during user mode top-up operation. The mask needed to be wide enough to obscure the stored beam size plus the residual oscillations caused by the injection kickers but narrow enough to observe the injected beam. During the first few turns the beam at the optical diagnostic beamline (ODB) source point reaches a horizontal amplitude of between -5 and 2 mm (see Fig. 4 and Ref. [2]) so a vertical mask was used which allows the injected beam to observed on either side of the mask.

EXPERIMENTAL SETUP

The ODB at the Australian Synchrotron [3, 4] was used to image the visible light from the injected electron beam. To accommodate this imaging apparatus, the lens in the optical chicane [3] was removed. Instead, the principal focusing optic was positioned on the optical table, as highlighted in Figure 1 below. A real image of the electron beam photon source was formed close to the ICCD camera [5]. The

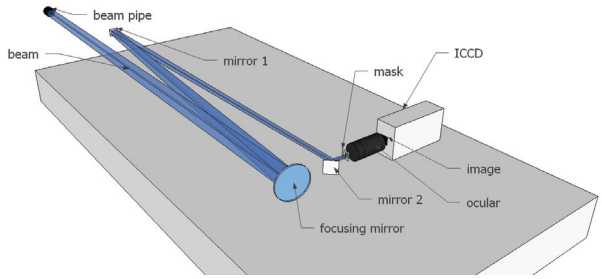

Figure 1: Optical table configuration for the ICCD coronagraph measurement.

mask was then cut to stop the stored beam (shown in Fig. 2) but allow the injected beam to be observed on either side of the mask. Fig. 3 shows the first five turns with only the stored beam and no injected beam. The mask was made large enough to obscure this beam motion due to the kicker imbalance.

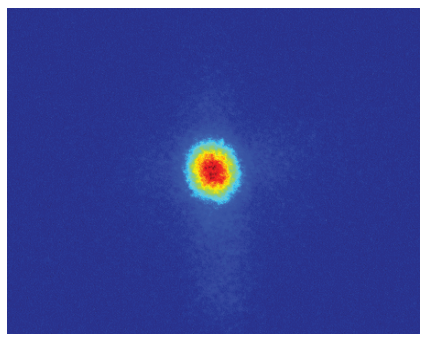

Figure 2: One turn of stored beam with a 5 mA single bunch in the ring.

Figures 2, 3 and 4 show that in principle if the stored beam including the kicker imbalanced induced motion, is masked out, the injected beam can be observed during top-up injection on turns 1 and 3.

RESULTS

The best image captured can be seen in Fig. 5 where turns 1 and 3 of the injected beam can be seen to the left and right of the masked stored beam. Turn 2 is also masked since the horizontal phase advance places the injected beam almost on top of the stored beam, as can be seen in the image with only the injected beam in Fig. 4. Turn 1 is quite washed out in Fig. 5 since the ICCD gain had to be reduced

ISBN 978-3-95450-119-9

DEVELOPMENT OF A BEAM PROFILE MONITOR USING NITROGEN-MOLECULAR JET FOR INTENSE BEAMS *

Y. Hashimoto#, Y. Hori, T. Morimoto, S. Muto, T. Toyama, K. Yoshimura, KEK/J-PARC, Japan
T. Fujisawa, T. Murakami, K. Noda, NIRS, Japan
D. Ohsawa, Kyoto University, Japan

Abstract

A non-destructive beam profile monitor using a sheeted jet beam of nitrogen molecule as a target has been developed for intense proton beams. The pressure of the sheeted target was 5e-4 Pa at the beam collision point. For beam core region, light emitted from nitrogen excite-deexcite process by proton beam collision is measured by a high sensitive camera with a radiation resistant image intensifier. For beam tail region, ionized electrons are used for detecting. Design study of such a hybrid type detector is discussed mainly in this paper.

INTRODUCTION

By using molecular jet as a thin planer target for beam profile measurement, the collision point with the proton beam is able to determine clearly. In addition two-dimensional beam profile can be obtained. Mainly two physical processes of ionization and excitation (and deexcitation) in the collision can be considered for beam profile detection.

Detecting method of using electron or ion produced by ionization due to proton beam collision is ordinal [2]. In this method detecting efficiency is higher and measurement can be done in short time as within a bunch length of 100ns. If confinement for electron or ion collection is possible, this method has advantage than light detection. On this method an electron or an ion is entered into multiplication device like a micro channel plate (MCP). Because yield of electron or ion is extremely high in case of high intensity proton beam, the gain of multiplication easily becomes lower due to hitting damage, so the gain should be calibrated as accurate as possible. This is additional problem to the electron or ion detection.

In measuring beam profile of high intensity beam, beam tail's signal is important as well as beam core's. Because beam tail has an effect on limiting on performances of the accelerator such as beam loss and some beam instability.

In former design [1], only beam core's signal detection with deexcitation light of nitrogen molecule was considered for fast detection as within a bunch separation time. If precise beam tail measurement is able at the same detecting point, it has advantageous characteristics for accelerator operation and beam physics.

Considering above points of view, we are now studying design on hybrid method of electron and photon detection for simultaneous profile measuring of beam core and tail using molecular-jet beam.

*Work supported by Grant-in-Aid for Scientific Research
#yoshinori.hashimoto@kek.jp

HYBRID TYPE DETECTION

Our monitor employs a sheeted nitrogen molecular target. In collision on the target with proton beam, reaction of ionization and excitation occurs on the nitrogen molecules. These phenomena produce the ionized pair of electron and nitrogen-molecule ion, and photon respectively. It is an effective method that using the deexcitation light in the part of beam core having rich proton density, and on the other, using ionized nitrogen molecule in the part of beam tail having poor proton density. At the former part, accurate collection of ionized electron or ion is rather difficult because of strong induced electro-magnetic field by dense proton beam, so the light detection has an advantage as free from such a violate field. On the contrary, at the latter part, a light detection becomes difficult because of poor photon yield. In this part beam field's effect also be reduced by distance from beam center, so a method using the produced electron or ion is advantageous than the light detection. Besides collecting efficiency at a detector is almost full in case of using electron, it is about 10% in case of using photon in which solid angle of a first optical element limits the detection yield.

Number of produced pair of electron and ion on ionization is larger than produced photon number on deexcitation at the same energy of incident proton beam. Production energies of electron with ion and photon of visible light region are 35 eV and 3.6 keV respectively [3].

Concerning these detection methods, we have already demonstrated. The light detection method was verified with low energy ion beams [1], and ion detection type monitor has been already realized in the medical ion synchrotron of the HIMAC [2].

DETECTION EQUIPMENT DESIGN

Horizontal and vertical cross-sectional views of colliding region of the jet beam with the proton beam are presented in Fig. 2 and Fig. 3 respectively. The jet beam of nitrogen molecule is formed as a sheeted target at the collision point.

Nitrogen Molecular Jet Beam

Expected dimensions of the target are as follows: thickness of 1-3 mm, width of 50-100, and length of 100-200 mm (in duration time of 140-280 μs). The jet runs with a terminated velocity by jet process of about 730 m/s after skimmer. The target thickness is determined by width of final slit located exit of the jet generator. Due to the thickness yields an error on measured beam size, it is

ISBN 978-3-95450-119-9

DIAMOND MIRRORS FOR THE SUPERKEKB SYNCHROTRON RADIATION MONITOR

J.W. Flanagan, M. Arinaga, H. Fukuma, H. Ikeda, KEK, Tsukuba, Japan

Abstract

The SuperKEKB accelerator, a 40x luminosity upgrade to the KEKB accelerator, will be a high-current, low-emittance double ring collider[1]. The beryllium primary extraction mirrors used for the synchrotron radiation monitors at KEKB suffered from heat distortion due to incident synchrotron radiation, leading to systematic changes in magnification with beam current and necessitating continuous monitoring and compensation of such distortions in order to correctly measure the beam sizes[2]. The heat loads on the extraction mirrors will be higher at SuperKEKB, with heat-induced magnification changes up to 40% expected if the same mirrors were used as at KEKB. We are working on a design based on mirrors made of quasi-monocrystalline diamond, which has much higher heat conductance and a lower thermal expansion coefficient than beryllium. With such mirrors it is targeted to reduce the beam current-dependent magnification effects to the level of a few percent at SuperKEKB. The design of the mirror and its heat sink/holder will be presented, along with numerical simulations of the expected heat-induced mirror surface deformations will be presented.

INTRODUCTION

The synchrotron radiation monitors at SuperKEKB will use source bends in the same locations as at KEKB, which are the 5 mrad "weak bends" heading into the Fuji (LER) and Oho (HER) straight sections. The source bend parameters are shown in Table 1. The source bend for the LER will be replaced with one with a longer core and larger bending radius (a re-used LER regular arc bend magnet) in order to reduce the SR power intensity. Despite the reduced bending radius, the increase in beam energy and beam current means that the incident angular power density will be higher (72 W/mrad) than that of the KEKB LER (48 W/mrad). The source bend will remain the same at the HER, and the effect of the increased current of the beam is almost cancelled out by the reduced beam energy, so that the angular power density is only a little bit higher than at KEKB.

It is planned to move the chambers a bit further downstream from the source bends than they were at KEKB, which will help reduce the SR power intensity hitting the primary extraction mirrors. However, the heat deformation of the KEKB mirrors was already a very significant problem, requiring complicated measures to measure and compensate for the distortion in real time in order to correct the beam-current dependence on the measured beam size. For this reason, we are pursuing the design of mirrors made of diamond, which has a higher heat conductivity and lower thermal expansion coefficient than beryllium. The design of the mirror will be described in the next section.

Table 1: SR Source bend parameters

Parameter	KEKB		SuperKEKB	
	LER	HER	LER	HER
Energy (GeV)	3.5	8	4	7
Current (A)	2	1.4	3.6	2.6
Bending radius (m)	85.7	580	177.4	580
SR Power (W/mrad)	48	136	72	149

DESIGN

The design of the mirror is based on CVD diamond, made by Cornes Technology (formerly Seki Technotron) and EDP Corporation. For best thermal conductivity, the idea mirror material would be a pure monoctystalline diamond, rather than a polycrystalline one. The monocrystalline diamond also gives good surface smoothness after polishing, with an Ra from 2-10 nm expected. For optical reflectivity, a metallic surface is needed.

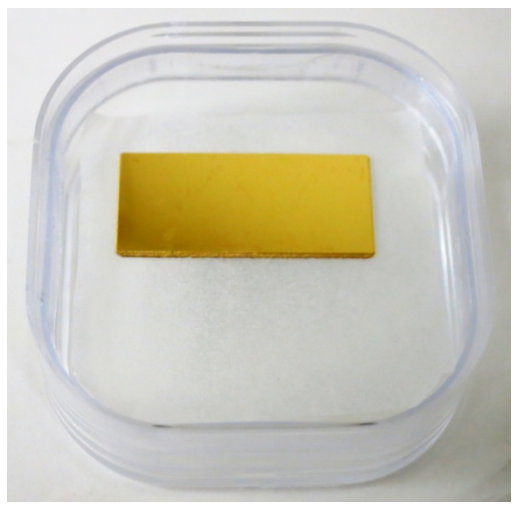

Figure 1: 10 mm x 20 mm x 0.65 mm prototype diamond mirror, consisting of two 10 mm x 10 mm monocrystals, with 3 μm Au reflective coating.

ISBN 978-3-95450-119-9

INTRA UNDULATOR SCREEN DIAGNOSTICS FOR THE FERMI@Elettra FEL

M. Veronese*, A. Abrami, E. Allaria, M. Bossi, A. Bucconi M. De Marco, L. Frölich, M. Ferianis, L. Giannessi, S. Grulja, R. Sauro, C. Spezzani, M. Tudor Sincrotrone Trieste, Trieste, Italy
T. Borden, Facility for Rare Isotope Beams, Michigan State University, East Lansing, MI, USA
F. Cianciosi, ESRF, Grenoble, France

Abstract

The FERMI@Elettra seeded FEL poses demanding requirements in terms of intra undulator diagnostics due to the short wavelength of its FEL radiation and to the coexistence of the electron and photon FEL beams. An advanced multi-beam screen system has equipped both FEL1 and FEL2. The system has been designed for transverse size and profile measurement on both the electron beam and the FEL radiation. Challenging design constrains are present: COTR suppression, seed laser suppression, FEL wavelength range and minimization of the ionizing radiation delivered to the undulators. This paper describes the novel design and the obtained performance with the FERMI intra undulator screen system (IU-FEL).

INTRODUCTION

FERMI@Elettra is a seeded FEL operating in the spectral range from VUV to soft x-rays [1]. It is based on a SLAC/BLN/UCLA type RF-gun, a normal conducting LINAC, currently operated at 1.2 GeV (up to 1.5 GeV). Longitudinal compression is provided by two magnetic chicanes BC1 and BC2 (respectively at 300 MeV and 600 MeV). The FEL has two undulator chains, namely FEL1 and FEL2. The first, FEL1, is a single cascade HGHG seed system designed to provide hundreds of microjoule per pulse in the range from 100 to 20 nm. The second, FEL2, is a double cascade seeded system designed to reach 4nm at the shortest wavelength. On both chains, in between the undulators several devices are installed: phase shifter, cavity BPM, a quadrupole and the intra undulator screen (IU-FEL). The IU-FEL screen is a multipurpose screen designed to provide transverse beam size measurements of the electron beam, the seed laser beam and the FEL beam. At present, seven stations are installed on the first FEL1 line and eight on the FEL2 line. The initial design of the system was performed in collaboration with Argonne National Laboratory. The setup presented in this paper has been deeply upgraded based on specific operational experience. Similar intra undulator diagnostics have been developed and tested at sFLASH at DESY [2].

GENERAL LAYOUT

The FEL1 and FEL2 chains are depicted in Figure 1. The FEL1 chain starts with the modulator where interaction with the seed laser occurs. The modulator is followed by the dispersive section that converts the energy modulation in current modulation (bunching). The first IU-FEL station is installed downstream the dispersive section before the first radiator. This station is used, in conjunction with a standard multi-screen upstream the modulator, to perform a transverse alignment of the seed laser with the electron beam in order to guarantee the spatial overlap of the two beams in the modulator. This means that the IU-FEL screen should have the capability to image the electron beam and the seed laser at the same time. The other six IU-FEL stations are installed at each break in between the radiators. They provide imaging of both the electron beam and of the FEL electron beam with high resolution. The seed laser beam has a waist in the modulator, from there on the beam size increases due to its natural divergence. Moreover the vacuum chamber of the undulators has a vertical aperture of only 7 mm. This means that already after the second radiator the seed laser transverse profile is dominated by the reflection and diffraction from the vacuum chamber. In FEL2 the first cascade consisting of the modulator, the first dispersive section and the first two radiators, basically replicates the FEL1 chain. Downstream, the delay line is installed. It is a magnetic chicane that is used to delay the electron bunch with respect to the FEL radiation from the first stage. Zero delay would mean seeding with the FEL radiation emitted by the first stage on the same portion of the electron beam used for the first which has corrupted electron beam properties (emittance and energy spread). The delay line allows to seed on a fresh portion of the electron beam with unperturbed properties (fresh bunch technique). Downstream the delay line, a second modulator is installed and then a the second dispersive section. From there the radiators of the second stage will amplify the bunching by the second dispersive section after the seeding process which now has also a shorter wavelength. The final

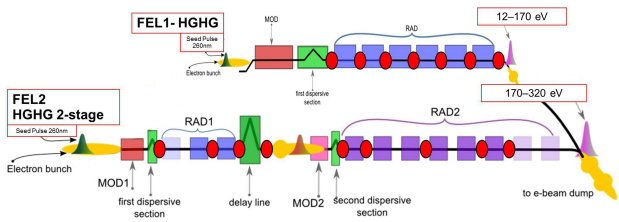

Figure 1: FERMI FEL1 and FEL layout. The IU-FEL station are marked as red dots.

* marco.veronese@elettra.trieste.it

ISBN 978-3-95450-119-9

MEASUREMENT OF THE FREQUENCY SPECTRUM ON THE BEAM PROFILE CONTROLLED BY RF KICKER

Y. Yamamoto, Ritsumeikan University SR Center, Kusatsu, Shiga, Japan

Abstract

The frequency spectrum on the beam profile was measured at the compact superconducting storage ring of Ritsumeikan University. The radiation detector was used an avalanche photodiode module with a high frequency response of 1 GHz for the visible ray. Signals from the detector were transferred to a spectrum analyzer. The beam profile was magnified strongly by a conventional profile monitor system. We scanned the beam profile in vertical direction by shifting the detector. The distribution of peak intensity as a function of the position on beam profile was obtained.

INTRODUCTION

The world smallest electron storage ring AURORA with a super conducting magnet was developed by Sumitomo Heavy Industries [1]. Ritsumeikan University installed this storage ring in 1996. Since then, the SR center was utilized for synchrotron radiation researches [2]. There are 14 beamlines (XAFS, PES, Imaging and LIGA) and 2 beam-monitor-lines operated in the center. The number of registered users in last year was 405 in total, in which number of outside users was 149.

AURORA is the weak focusing type with the simplest lattice composed of a single bending magnet, which produces an exactly axial symmetric magnetic field with little error magnetic field. The vertical beam size was measured to use the SR-interferometer by Mitsuhashi et al in 1997 [3-4]. The result of the size to be 10.5 μm showed ability of the SR-interferometer. At the user operation, we controlled the vertical beam size to keep 130 μm by RFKO to extend beam lifetime [5-6]. We tried to measure the frequency spectrum on the beam profile to monitor any instability by RFKO.

Table 1 lists the parameters of the injector and the ring. Figure 1 shows the storage ring and beamlines in the experimental hall.

EXPERIMENTAL SETUP

Measurement system which was composed by the radiation detector (APDM: avalanche photodiode module, C5658 HAMAMATSU), spectrum analyzer (U3200 ADVANTEST) and PC was constructed behind the beam extraction port BL-9 and BL-16 at the atmosphere [7]. A thick beryllium flat mirror was set to reflect the primary ray by 90° to extract the visible component in the vacuum chamber. This visible ray through the optical glass window to divide the vacuum and atmosphere was reflected again by an aluminium mirror, and introduced into the measurement system.

y-yama@st.ritsumei.ac.jp

Table 1: Parameters of the Injector and Storage Ring

Injector parameters	
Energy	150 MeV
Repetition	3 Hz
Peak current	1 mA
Pulse width	2 μs

Storage ring parameters	
Energy	575 MeV
Stored current	300 mA
Circumference	3.14 m
Radius of curvature	0.5 m
Field strength	3.8 T
RF frequency	190.86 MHz
Number of cavities	1
Harmonic number	2
Critical energy of radiation	844 eV
Vertical beam size(σ)	0.0105 mm
Vertical beam size: user operation (σ)	0.13 mm
Horizontal beam size(σ)	1.1 mm
Beam lifetime	300 min

Figure 1: Photograph showing the storage ring and beamlines in the experimental hall.

The stored beam profile was magnified strongly by the conventional profile monitor using objective lens and magnifying lens. The radiation detector was scanned with using the micrometer on the beam profile in vertical direction. For the operating condition of the kicker for RFKO, the center of frequency was 57.6 MHz in agreement with vertical betatron frequency ($f_{\beta y}$), deviation of frequency modulation 200 kHz, sweep frequency 1, 3 or 10 kHz. Stored beam current was about 200 mA at every measurement.

ISBN 978-3-95450-119-9

FLYING WIRE BEAM PROFILE MONITORS AT THE J-PARC MR

S. Igarashi#, D. Arakawa, Y. Hashimoto, M. Tejima, T. Toyama, KEK, Ibaraki, Japan
K. Hanamura, MELCO SC, Ibaraki, Japan

Abstract

Transverse beam profiles have been measured using flying wire monitors at the main ring of the Japan Proton Accelerator Research Complex. We use carbon fibers of 7 μm in diameter and the scan speed of 10 m/s. The wire is attached with an aluminum flame of 140 mm of the rotation radius and rotated with a DC servomotor. A potentiometer is attached to the wire flame and the angle readout is used for the feedback of the servomotor and the wire position measurement. The secondary particles from the beam-wire scattering are measured with a scintillation counter. Beam profiles are reconstructed by making the scatter plot of the scintillator signal and wire position. We have successfully measured both horizontal and vertical beam profiles of up to 1.2×10^{13} protons per bunch. The monitors have been proven to be useful for the beam commissioning.

INTRODUCTION

The main ring (MR) of the Japan Proton Accelerator Research Complex (J-PARC) is a high intensity proton accelerator and delivers the protons for the nuclear and elementary particle physics, such as the neutrino oscillation experiment (T2K). The injection energy is 3 GeV and the extraction energy is 30 GeV. For the user run we have achieved the beam power of 200 kW with 8 bunches of 1.3×10^{13} protons per bunch (ppb). Two bunches of protons are injected in MR from the rapid cycling synchrotron (RCS) through the beam transport line (3-50BT). Two bunches are injected four times in one cycle to fill 8 out of 9 rf buckets in 120 ms. The acceleration starts after the fourth injection.

The beam loss minimization and localization at the collimator are necessary to minimize residual radiation activities in MR and required for the maintenance of the accelerator components. The typical beam loss is 1% during the injection period and 0.7% at the beginning of the acceleration. It is important to understand the beam loss mechanism for further beam power increase.

The transverse beam profile is one of important beam parameters to measure for understanding of the beam loss mechanism. We have installed ion profile monitors (IPM) [1] and flying wire in MR. IPM uses phenomena that the proton beam ionizes the residual gas. Multi-ribbon profile monitors [2] have been installed at five places in 3-50BT and one in MR. They are being used to measure the injection beam profiles.

FLYING WIRE MONITOR

A flying wire monitor uses a carbon fiber of 7 μm in diameter as a target. It is to be scanned across the beam with the maximum speed of 10 m/s. The wire is attached with an aluminum flame of 140 mm of the rotation radius and rotated with a DC servomotor. A potentiometer is attached to the wire flame and the angle readout is used for the feedback of the servomotor and the wire position measurement. The secondary particles from the beam-wire scattering are detected with a scintillator (Fig.1). The beam profile is then reconstructed from the scintillator response and the wire position measurement. If the wire scanning disturbs the beam, the profile measurement is not precise. The minimum target material and fast wire scanning are necessary. Flying wire monitors have been used in several proton accelerators. It was also developed in KEK-PS [3] and modified for J-PARC MR [4].

The wire flame is rotated from -150°, which is the standby position, to +150° and comes back to the standby position. The movement is done in 0.2 s. The wire scanning takes about 5 ms for a typical size of the beam. The scintillator signals and the potentiometer output signals for the wire position are digitized with a digitizer RTD720A with a 20 ns sampling for a 20 ms time range. The 1 M sample data are averaged over 10 k sample to make arrays of 100. The data of the potentiometer signal is calculated to make wire position data. Scattered plots are made for the scintillator data as a function of the wire position to make beam profiles.

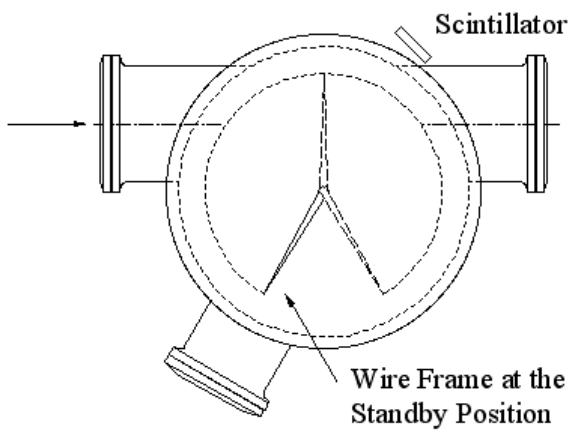

Figure 1: The flying wire monitor.

Both horizontal and vertical flying wire monitors were installed in the straight section of the beam injection and collimation systems in 2008 (Fig.2). Because they were originally at the downstream of the collimator, the beam background affected the profile measurement. They were moved to the upstream of the beam injection and collimation systems in 2010 to avoid the beam background. The background was then suppressed and the profile measurement of the high intensity beam became

#susumu.igarashi@kek.jp

ISBN 978-3-95450-119-9

USE OF GAFCHROMIC FILMS TO MEASURE THE TRANSVERSE INTENSITY DISTRIBUTION OF A LARGE-AREA ION BEAM

Y. Yuri, T. Ishizaka, T. Yuyama, I. Ishibori, S. Okumura, and A. Kitamura (Ogawa),
Takasaki Advanced Radiation Research Institute, Japan Atomic Energy Agency, Japan
T. Yamaki and S. Sawada, Quantum Beam Science Directorate, Japan Atomic Energy Agency, Japan

Abstract

A technique of forming a large-area uniform ion beam by multipole magnets is developed at the TIARA cyclotron facility of Japan Atomic Energy Agency. The quality of the uniform ion beam is described by the cross-sectional area and uniformity. A technique has, therefore, been developed to measure the two-dimensional transverse intensity distribution of the ion beam using Gafchromic radiochromic films, which are widely used for dose distribution evaluation in radiation therapy. The coloring response of Gafchromic films irradiated with ion beams is investigated as a change in the optical density of the film. It has been found that the optical density increases linearly with the ion-beam fluence and that, thus, the relative transverse intensity distribution of ion beams can be measured using the film at practical fluence ranges for materials and biological research. Furthermore, it is confirmed, by evaluating the microscopic pore area-density distribution in a track-etched polymer film, that the uniform intensity distribution of the multipole-focused beam is realized microscopically, too.

INTRODUCTION

A research and development (R&D) study is in progress on formation and irradiation of a large-area uniform beam using multipole magnets at the ion accelerator facility, TIARA, of Japan Atomic Energy Agency (JAEA) [1]. It is necessary to evaluate the quality of the uniform beam both precisely and handily. As a possible technique, we have, thus, employed Gafchromic radiochromic films (Ashland Inc.) [2] for the evaluation of the cross-sectional area and uniformity of the large-area uniform ion beams. The film, whose color turns blue due to radiation exposure, was originally produced for dose evaluation in X-ray or gamma-ray radiotherapy, but can be also applied to the intensity distribution measurement for different kinds of beams. The use of the film is suitable for the present purpose since the film has various characteristics such as high spatial resolution, large area, relatively low-dose range, and easy handling.

Therefore, ion-beam irradiation experiments for the film calibration were performed at the TIARA azimuthally-varying-field (AVF) cyclotron [3] to investigate the coloring response. For precise and handy evaluation, general-purpose scanners were employed to analyze a change in the optical density of irradiated films, instead of using a dedicated two-dimensional spectrophotometer.

Furthermore, the beam intensity distribution determined by the Gafchromic film was compared with the microscopic area-density distribution of track-etched pores in a polyethylene terephthalate (PET) film [4].

CALIBRATION OF GAFCHROMIC FILMS

Procedure

Two types of Gafchromic films have been chosen for the present study [2]: One is HD-810, whose active layer (6.5 μm thick) is behind a 0.75-μm-thick surface layer and coated on a 97-μm-thick polyester substrate. The other is EBT2, whose active layer (30 μm thick) is put between 80-μm and 175-μm polyester layers. According to the manufacturer [2], the available photon dose ranges of the films are 10~400 Gy and 0.01~10 Gy, respectively.

The following procedure was taken for film calibration: First of all, the films were irradiated uniformly with 10-MeV ^{1}H and 520-MeV ^{40}Ar beams from the AVF cyclotron in TIARA. The beam current was measured by a Faraday cup near the target. The irradiation time was controlled by an electrostatic beam deflector from 10^{-3} to 10^{1} s, depending on the fluence, intensity of the beam and the film type. Then, the irradiated film was read by general-purpose scanners to digitize into a TIFF image with 16-bit RGB color intensity values. Two different kinds of flat-bed scanners were employed for film reading: Canon LiDE50 (reflection type) and Epson ES-10000G (reflection/transmission type). The irradiated films were scanned in more than one day after irradiation to prevent the color variation right after irradiation. Finally, the optical density d_X was determined for each X of RGB color values by the equation: $d_X = \log_{10}\left(2^{16} - 1/X\right)$.

Results

Figure 1 shows the fluence response of HD-810 films irradiated with 10-MeV H beams and scanned by LiDE50. The optical densities of all three color intensities increase linearly with the particle fluence at a low fluence and then are saturated at a high fluence. The optical density obtained from the red color component is the largest in the linear-response region. On the other hand, the blue component is the least sensitive. This reflects the fact that the absorption of the irradiated film is the highest in the wavelength between 650 and 700 nm [2]. Thus, the fluence of 10-MeV H beams can be measured from 1×10^{9} to 2×10^{11} cm^{-2} with a moderate S/N ratio by choosing an appropriate color component of HD-810. When the films were scanned by ES-10000G with a transmission mode, the optical densities were slightly

ISBN 978-3-95450-119-9

DESIGN OF THE BEAM PROFILE MONITORS FOR THE SXFEL FACILITY

L.Y.Yu, J.Chen, W.M.Zhou, K.R.Ye, Y.B.Leng
SINAP, Jiading, Shanghai 201800, P.R.China

Abstract

The Shanghai X-ray Free Electron Laser Facility will begin construction at next year. The linac electron beam energy is 0.84 GeV. Over 50 beam profile monitors with OTR and YaG screen will be installed along the linac and undulators. The profile monitor system design is a challenging task, since the system has to measure transverse electron beam sizes from millimeter down to 40μm scale with a 20μm resolution and 50μm repeat positioning accuracy. This paper describes the design of the mechanical detector, the integrated step-servo motor controlling system, the beam imaging system, as well as the software system.

INTRODUCTION

SXFEL proposal was approved in February 2011 by China government, the construction is expected to start at the SSRF campus in early 2012. This test facility, based on an 840MeV electron linac, aims at generating 8.8nm FEL radiation with two-stage cascaded HGHG scheme[1]. Figure 1 shows the layout of the SXFEL linac.

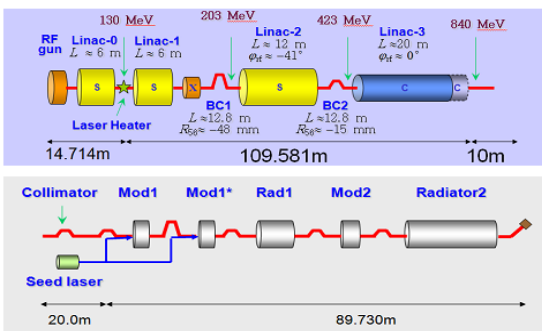

Figure 1: Layout of the SXFEL accelerator & undulator.

SXFEL injector have 3 beam diagnostic stations, require 6 beam profile monitors designed by Tsinghua University, linac part requires about 31 beam profile monitors or so, undulator part require 21 beam profile monitors.

Table 1 list the physical specification of the beam profile monitors[2].

We are going to use Yag/OTR screens and wire canners as the beam profile monitors originally. Considering the cost, reliability and we have not any experiences on wire scanners, so we decide to improve the design of Yag/OTR profile monitor to satisfy the specification. In addition the system has to be robust, remote controlled and easy to maintain, we adopt a new type integrated step servo motor to redesign the mechanical detector and select a high resolution CCD, the whole profile system is more compact.

Table 1: Specification of the beam profile monitors

Parameter	Linac	Undulator
Quantity	31	21
Monitor length	210mm	150mm
Repeat positioning accuracy	50 μm	
Resolution	20 μm	
Charge range	0.02~1nC	
RMS beam length	0.015~4 ps	
Measuring range	15*15/5*5 mm^2	

MECHANICAL DETECTOR

The beam profile monitor will be a main diagnostic tool during the commissioning of SXFEL experiments. It has three position screens for test. One is the calibration screen, The beam profile monitor is not only used to measure the electron beam transverse shape and size, but also to synchronize the seeding laser and electron beam on spatial domain and temporal domain respectively. So all beam profile monitor is designed as shown as Figure2 with four stages pneumatics screen monitor. One screen which material is YAG:Ce crystal plate is used at the initial commissioning and at low beam charge situation, another screen which material is made from 100nm aluminium deposited on a polished silicon wafer[3], generating optical transition radiation(OTR) when Electron hits on it, is used to measure beam energy spread and beam emittance respectively, because the OTR represents a linear radiation source while YAG screen has the saturation problem. The last screen is calibration screen where holes array radius is 1mm and spacing is 5mm. It is used for calibrate the optical relay and CCD image acquisition system. The light of beam can be extracted from both viewport, at the undulator location, the energy of seeding laser is very huge to damage the CCD camera, so the beam image can be obtained from backside viewport. The camera is located below beam pipe 1.1 meter through planar - mirror optical relay to reduce the radiation damage. The viewport flange can be replaced conveniently with crystal viewport flange

ISBN 978-3-95450-119-9

STORAGE RING TUNE MEASUREMENTS USING HIGH-SPEED METAL-SEMICONDUCTOR-METAL PHOTODETECTOR

S. Dawson, D.J. Peake, R.P. Rassool, The University of Melbourne, Melbourne, Australia
R.J. Steinhagen, CERN, Geneva, Switzerland
M.J. Boland, Australian Synchrotron, Clayton, Australia

Abstract

In any storage ring, the measurement and control of betatron tunes is an integral part of optimising the stability and lifetime of the stored particle beam. This contribution presents a novel relative beam position measurement system relying on a direct synchrotron-light detection using fibre-coupled, high-speed Metal-Semiconductor-Metal (MSM) Photodetectors (PD) in a custom-made balanced RF biasing circuit.

The system will be described along with its first results measuring the tunes for the storage ring at the Australian Synchrotron. The results are compared to the existing electro-magnetic BPM-based tune measurements taken.

INTRODUCTION

The Australian Synchrotron storage ring is a 3.0 GeV electron ring with a circumference of 216 m, situated in Melbourne, Australia [1]. Its nominal characteristics are summarised in Table 1.

Table 1: Nominal Characteristics of the Australian Synchrotron Storage Ring

Characteristic	Value	Unit
Energy	3.0	GeV
Circumference	216	m
Revolution Frequency	1.388	MHz
Betatron Tunes	(13.291,5.220)	(Q_x, Q_y)
	(403.9, 305.4)	kHz
Chromaticity	(3.5, 13)	(ξ_x, ξ_y)

Tune diagnostics systems, typically integrated into the beam position monitoring (BPM) or transverse feedback subsystems, are essential for any synchrotron and are used to control the actual tune working point to prevent the onset of instabilities that can occur if the fractional tune approaches low-order resonances of the accelerator lattice.

The majority of tune measurement systems require excitation of the otherwise stable beam, and measure the resulting beam motion over time. The digitised position data is typically transformed into the frequency domain, where any beam movement corresponding to the tune will show up as a spectral peak. For most systems, a small amount of excitation is required to separate the tune signal from the measurement noise, therefore tune measurements often cannot be performed during user time.

This contribution describes a high-bandwidth, low-noise BPM utilising visible synchrotron radiation that has been successfully tested at the Australian Synchrotron light source. The aim of this system is to utilise the high bandwidth of the system to allow for tune measurements of stable beam.

EXPERIMENTAL SETUP

The synchrotron-light based beam position monitor system (SL-BPM) described in this paper is built on the original Fill Pattern Monitor (FPM), which is based on a single high-speed Metal-Semiconductor-Metal Photodetector (MSM-PD) to measure the electron beam density in real time [2].

Both systems use the synchrotron light that is emitted by the electron passing through one of the main bending magnets, separated from the X-rays using a vertical mirror above the beam axis, focused through a lens, and then guided into an optical hutch where it is split to be used by either system. The visible part of the synchrotron radiation was chosen since the system can be implemented using standard optical components such as mirrors and lenses that also allow for rapid changes in the experimental set-up, and to anticipate a possible future use of the system in the Large Hadron Collider (LHC) that produces synchrotron light with the peak power being in the visible range.

For the nominal SL-BPM system, the light is focussed onto a set of length-matched optical fibres that are grouped to a diamond-type structure as illustrated in Figure 1, and each being individually fibre-coupled to its own MSM-PD.

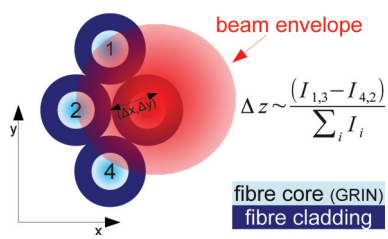

Figure 1: Fibre diamond geometry in relation to the projected synchrotron-light beam spot size.

The SL-BPM uses the same MSM-PDs as the earlier FPM [2, 3], that are robust, very low-noise, cost-effective and with a typical rise-time of 30 ps being ideally suited for high bandwidth measurements. Besides the given model,

ISBN 978-3-95450-119-9

SPECTRUM OF MULTI-BUNCH POSITION MODEL AND PARAMETER ACQUISITION ALGORITHM*

Yong Yang, Yongbin Leng#, Bao Peng Wang, SSRF, Shanghai, China

Abstract

Based on the spectrum of turn-by-turn model for the storage ring, spectrum of multi-bunch position model was derived through some assumptions. Spectrum of excited electron beam position was analysed in Shanghai Synchrotron Radiation Facility (SSRF) and Genetic Algorithm was used to obtain the model parameters when fitting multi-curve data. Results show that, after 100 times iteration, all the correlation of fitted data and original data can be up to 95%, and the model can accurate estimate a bimodal split of the spectrum curve.

INTRODUCTION

The emergence of the third generation of the light source, marks the synchrotron radiation light is developing to the direction of high-energy and high luminance. Stable high flow intensity and bunch instability is the focus of concern in the beam diagnostic study. A spectrum curve of bunch position with bimodal split was found in SSRF when the storage ring ran at multi-bunch mode. Establishing an appropriate bunch position spectrum model is necessary for further study of bunch instability and other parameters of the ring accelerator storage ring.

Model parameters acquisition method is the first problem to be solved after modeling. The genetic algorithm (GA) is an optimization method put forward by American professor HOLLAND in 1975, which simulates biological evolution in the natural selection mechanism according to the theory of biological evolution and genetic variation principle. Compared with other optimization methods, GA has the advantage of global parallel search, not easy to fall into local optimum, and has no special requirements to the optimize function itself, neither continuous nor differentiable [1]. Therefore, the genetic algorithm is especially suitable to solve the optimal solution of complex nonlinear and multidimensional space.

Multi-bunch Spectrum model

Spectrum Function of Single Bunch Mode

To accurately determine tune value of the accelerator, a suitable spectrum model of bunch position has been established for storage ring running at single bunch mode in the previous. And the relationship between tune value and beam current was found.

Literature [2] shows that the spectrum function of the bunch position in single bunch mode can be expressed as:

$$f(x)=\begin{cases}\dfrac{a-d}{\sqrt{1+b^2\left(\dfrac{2c-x}{c}-\dfrac{c}{2c-x}\right)^2}}+d,(x<c)\\ \dfrac{a-d}{\sqrt{1+b^2\left(\dfrac{x}{c}-\dfrac{c}{x}\right)^2}}+d,(x\geq c)\end{cases}\quad(1)$$

Wherein a is the curve peak; b represents the curve width, the characterization of the quality factor Q of the vacuum chamber; c is the frequency value at the peak of the curve in the observed range; d is the offset for noise.

When the spectral curve within the observation range is expanded to the entire band, the formula (1) should be translational as a whole, i.e., replace x with x-f. So the spectrum function is:

$$f(x)=\begin{cases}\dfrac{a-d}{\sqrt{1+b^2\left(\dfrac{2c-x+f}{c}-\dfrac{c}{2c-x+f}\right)^2}}+d,(x<c+f)\\ \dfrac{a-d}{\sqrt{1+b^2\left(\dfrac{x-f}{c}-\dfrac{c}{x-f}\right)^2}}+d,(x\geq c+f)\end{cases}\quad(2)$$

Spectrum Function Modeling of Multi-bunch Mode

Considering parameters b, c, f will be related to bunch charge, for simplicity, suppose b, c, f and bunch charge are a linear relationship.

In the injection process of electron storage ring, there are only two kinds of charge amount bunches at the same time from a macro point of view. And assume that each bunch wakefield effects the entire storage ring. Thus in the operating mode of the multi-beam group, the spectrum function of the bunch position can be regarded as the combined effect caused by two interacting single bunch.

Assume there are two kind of bunches with charge quantity q1, q2 number n1, n2 in the storage ring, and q1> q2.

Suppose two single-bunch interaction does not affect parameters f, c, and only affects the curve width b and peak a.

For the curve width:

The front has the assumption that b and single bunch charge are a linear relationship.

* Work supported by National Nature Science Foundationof China (11075198)

lengyongbin@sinap.ac.cn

ISBN 978-3-95450-119-9

THEORETICAL AND EXPERIMENTAL INVESTIGATION ON RESOLUTION OF OPTICAL TRANSITION RADIATION TRANSVERSE BEAM PROFILE MONITOR

A.S. Aryshev, N. Terunuma, J. Urakawa [KEK, Ibaraki, Japan]
B. Bolzon, E. Bravin, T. Lefevre (T. LefÃ¨vre) [CERN, Geneva, Switzerland]
S.T. Boogert, V. Karataev [Royal Holloway, University of London, Surrey, United Kingdom]
L.J. Nevay [Oxford University, Physics Department, Oxford, Oxon, United Kingdom]

Abstract

Optical Transition Radiation (OTR) appearing when a charged particle crosses an interface between two media with different dielectric constants has widely been used as a tool for transverse profile measurements of charged particle beams in numerous facilities worldwide. The basic tuning methods and operation of conventional OTR monitors are well established for transverse beam sizes not smaller than 3-5 um. Since the Point Spread Function (PSF) dimension defines the resolution of the conventional monitors, for small electron beam dimensions the PSF form significantly depends on a presence of OTR tails diffraction and aberrations in the optical system. In our experiment we have managed to squeeze the electron beam such that we can practically measure PSF distribution in one direction. The revealed PSF structure is such that the visibility depends on the transverse beam size on micron scale. We developed an empirical calibration technique and successfully overcame the resolution limit of the common OTR monitor reaching sub-micron level. Here we represent the recent developments and upgrades in both setup and data analysis of a sub-micrometer electron beam profile monitor.

CONTRIBUTION NOT RECEIVED

ISBN 978-3-95450-119-9

LEARNING FROM BEAMS - BEAM INSTRUMENTATION, SIGNAL PROCESSING, AND (MIS) APPLICATIONS OF LINEAR TIME INVARIANT SYSTEM FORMALISMS

J.D. Fox [SLAC, Menlo Park, California, USA]

Abstract

Almost all particle accelerators measure and control beam properties. This talk looks at the signals from bunched beams using time domain and frequency domain formalisms. The signatures of bunch charge and bunch structure, motion in the longitudinal and transverse planes are reviewed and illustrated with examples from various types of beam pick-ups and monitors. Common control room diagnostics, instruments and measurement techniques are highlighted via techniques in use at selected accelerators and light sources. This tutorial is intended to help engineers and accelerator physicists interpret signals in the control room, and specify and understand the fundamental and technological limits of beam measurements. Examples are presented for position monitor techniques, pickups and the signal processing required for tune measurements, multi-bunch and intra-bunch instability control systems. The significance of technical implementation choices, and important lessons in understanding the impact of non-linear effects (such as in amplifiers) are presented.

CONTRIBUTION NOT RECEIVED

ISBN 978-3-95450-119-9

OVERVIEW OF ESS BEAM DIAGNOSTICS

A. Jansson, C. Böhme, B. Cheymol, H. Hassanzadegan, M. Jarosz, T. Shea, L. Tchelidze,
European Spallation Source ESS AB, Lund, Sweden

Abstract

The European Spallation Source (ESS) will use a 2.5GeV superconducting proton linac with a 5MW average beam power to produce the world's most powerful neutron source. The project, sited in the south of Sweden, is approaching the end of the pre-construction phase, and is expected to enter the construction phase in 2013. This paper gives an overview of the ESS accelerator and the planned beam diagnostics systems, as well as the associated challenges.

THE ESS ACCELERATOR

The European Spallation Source (ESS) is a 5MW linac-based neutron source, which will be built in Lund, Sweden. It has a pulse repetition rate of 14Hz, a nominal beam current of 50mA and a pulse length of 2.86ms.Acceleration is provided by a warm RFQ and DTL operating at 352MHz, followed by superconducting spoke cavities (also at 352MHz), and two types of elliptical cavities operating at 704MHz. The overall length of the linac is about 400m, followed by and additional 160m of upgrade space and transfer line.

Figure 1: ESS linac layout overview.

The project is currently in a pre-construction phase. A conceptual design report[1] was recently released, and a Technical Design Report (TDR) along with an updated cost estimate is planned for the beginning of 2013. An overview of the current project status has been presented in recent conference proceedings [2].

PLANNED DIAGNOSTICS SUITE

The ESS LINAC optics is under configuration control since since 2010, with biannual updates. The discussion below is based on the October 2012 lattice release. This lattice is also the one that used in the Technical Design Report.

Warm Linac

The LEBT (see Fig. 2) consists of two solenoids for focussing (each equipped with a steering magnet) plus a chopper to trim the beginning and end of the ion source pulse. In the LEBT, the source emittance will be measured using a slit and one of two sets of SEM grids. The SEM grids also allow measurement of the beam profile and position directly. The beam current will be measured at the entry and exit using beam current transformers. An insertable Faraday cup also allow for beam current measurement and double as a temporary beam stop. An inclined viewport to determine ion species fraction by observing Doppler shifted luminescence light is also foreseen.

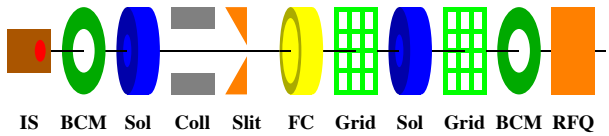

Figure 2: LEBT diagnostics layout.

The MEBT[3] will have 10 quadrupoles, three buncher cavities and a fast chopper (see Fig. 3). Here, the transverse emittance from the RFQ will be measured with a slit and grid system, employing a slit design similar to LINAC4. In addition, a set of 4 wire scanners will be used to measure the beam profile. Two of these are co-located with viewports for non-invasive profile measurement based on luminescense, and two are co-located with transverse halo measurement stations. Six BPMs will be used for TOF and position measurement, and two BCT will be inserted at the beginning and at the end of the line for intensity and transmission measurement. A movable Faraday cup allow for beam current measurement and double as a tune-up beam dump. Longitudinal beam profile measurement will be performed with a Beam Shape Monitor (BSM).

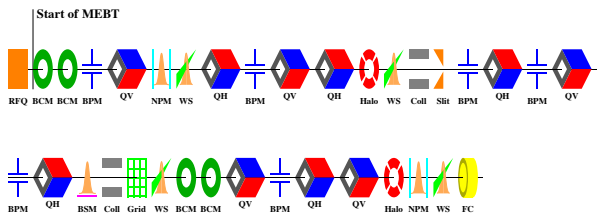

Figure 3: MEBT diagnostics layout.

The Drift Tube Linac (DTL) consists of four tanks (see Fig. 4). It employs a permanent magnet FODO lattice leaving empty drift tubes for diagnostics. The first tank will have two BPMs, and the following tanks one BPM each. The SNS-like inter-tank regions will each house a wire scanner, a Faraday cup, and viewports for non-invasive profile monitoring. In addition, each tank will have a BCT incorporated in the end wall.

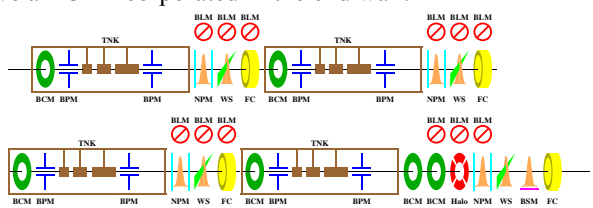

Figure 4: DTL diagnostics layout.

ISBN 978-3-95450-119-9

REVIEW OF RELIABILITY CONCEPTS APPLIED TO BEAM LOSS MONITORING SYSTEMS

Bernd Dehning, CERN, Geneva, Switzerland

Abstract

Beam loss measurement systems are often used for the protection of equipment against the damage caused by impacting particles creating secondary showers and their energy dissipation in the matter. Depending on the acceptable consequences and the frequency of particle impact events on equipment reliability requirements are scaled accordingly. Increasing reliability often leads to more complex systems. The downside of complexity is a reduction of availability, therefore an optimum has to be found for these conflicting requirements. A detailed review of selected concepts and solutions from real-life examples will be given to show approaches used in various parts of the system from the sensors, signal processing, and software implementations up to the requirements for operation and documentation.

SAFETY SYSTEM DESIGN APPROACH

All considerations start with the recognition that the probable frequency and probable magnitude of a non conformal behaviour could lead to a damage of the system integrity. The combined likelihood of frequency and magnitude determines the risk for a certain system (see Fig. 1, first column). A reduction of the risk could be reached with a safety system providing protection, but larger complexity reduces the availability of the protected system (see Fig. 1, first row). To come to a quantitative demand for a safety level the probable frequency of events and probable magnitude of its consequence are used by the SIL (Safety Integrity Level) approach [1] or by the As Low As Reasonably Practicable (ALARP) approach. For both approaches

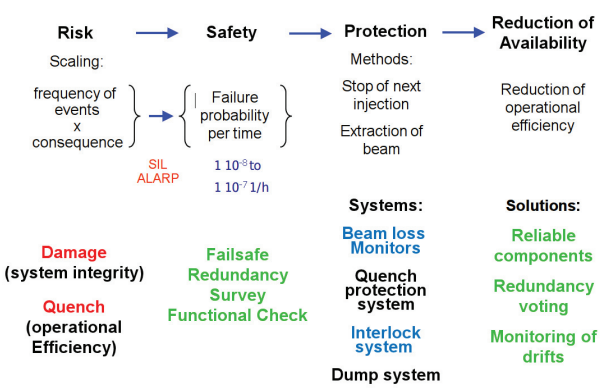

Figure 1: Schematic of the LHC protection system design approach (items in green are discussed in this paper).

a failure probability per time is estimated by the calculation of the risk of a damage and the resulting down time

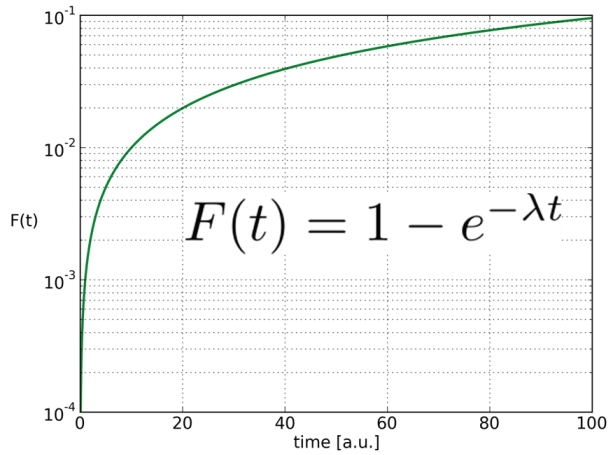

Figure 2: Exponential failure probability.

of the equipment [2]. In the case of a failure in the safety system itself, it should fall in a failsafe state with the consequence of reducing the operation efficiency. The main design criteria for the safety system are listed in the safety column: failsafe, redundancy, survey, functional check. In the protection column the methods for the protection of an accelerator are listed: stop of next injection applicable for a one path particle guiding system (linac, transfer line) and extraction of the beam for a multi path system (storage ring). The accelerator safety system is consisting of a beam loss measurement system, an interlock system and a beam dump system. If superconducting magnets are used, some beam loss protection could also be provided by the quench protection system. The availability column lists the means used in the design of the safety system to decrease the number of transitions of the system into the failsafe state. The effect of the number components added to a system to increase the probability of a safe operation results in a reduction of the availability of the system. This negative consequence of the safety increasing elements are partially compensated by the choice of reliable components, by redundancy, voting and the monitoring of drifts of the safety system parameters.

FAILURE PROBABILITY AND FAILURE RATE REDUCTION

To illustrate the available means to increase the safety of systems basic functional dependencies are discussed. A often valid assumption is given by the exponential time dependence of the failure probability $F(t)$ (see Fig. 2). With increasing time the probability of the occurrence of a failure in a system approaches 1. The failure rate λ is assumed

ISBN 978-3-95450-119-9

IFMIF-LIPAc DIAGNOSTICS AND ITS CHALLENGES

J. Marroncle, P. Abbon, J.F. Denis, J. Egberts, F. Jeanneau, J.F. Gournay, A. Marchix, J.P. Mols, T. Papaevangelou, M. Pomorski, CEA Saclay, France
J. Calvo, J.M. Carmona, P. Fernández, A. Guirao, D. Iglesias, C. Oliver, I. Podadera, A. Soleto, CIEMAT Madrid, Spain
M. Poggi, INFN Legnaro, Italy

Abstract

The International Fusion Materials Irradiation Facility (IFMIF) aims at providing a very intense neutron source (10^{17} neutron/s) to test the structure materials for the future fusion reactors beyond ITER (International Thermonuclear Experimental Reactor). Such a source will be driven using 2 deuteron accelerators of 125 mA cw each up to 40 MeV impinging into a lithium liquid curtain, thus producing very high neutron flux with a similar spectrum as those expected in fusion reactors. A validation phase was decided for this 10 MW facility consisting in the construction of part of the accelerator facility, the so-called LIPAc (Linear IFMIF Prototype Accelerator).

LIPAc, which is in construction phase, will accelerate a 125 mA cw beam deuteron up to the first of the four superconductive modules foreseen for IFMIF. The 9 MeV beam will be driven through the HEBT to the beam dump. This facility is currently under construction at Rokkasho (Japan).

In this contribution, we describe the beam diagnostics foreseen for this 1.125 MW prototype accelerator emphasizing the challenges encountered and present solutions how to overcome them.

IFMIF-EVEDA

The International Fusion Materials Irradiation Facility (IFMIF) [1], a project involving Japan and Europe in the framework of the "Broader Approach", aims at producing an intense flux of neutrons, in order to characterize materials envisaged for future fusion reactors. That should be done with 2 deuteron beam accelerators (125 mA - 40 MeV) impinging a liquid lithium target, producing a huge neutron flux (10^{17} neutrons/s) [2]. Downstream to this huge neutron source, cells will be implemented to test the responses of material samples submitted to mechanical and thermal stresses in these very harsh conditions.

Such a powerful 10 MW facility, sketched in Fig. 1, poses unprecedented challenges. Therefore, it was decided to perform a validation phase, EVEDA (Engineering Validation and Engineering Design Activities) consisting of designing and manufacturing a prototype accelerator, a 1/3-scaled Li loop target and part of test cells.

The LIPAc accelerator prototype (Linear IFMIF Prototype Accelerator) [3] is in designing and manufacturing phases; it will be installed at Rokkasho (Japan). LIPAc will accelerate 125 mA of deuterons up to 9 MeV. It is a 1-scaled IFMIF accelerator up to the first accelerating cryomodule. The huge space charge effect is a major challenge at this very high power beam (1.125 MW), which is particularly tricky for the beam transportation at low energy.

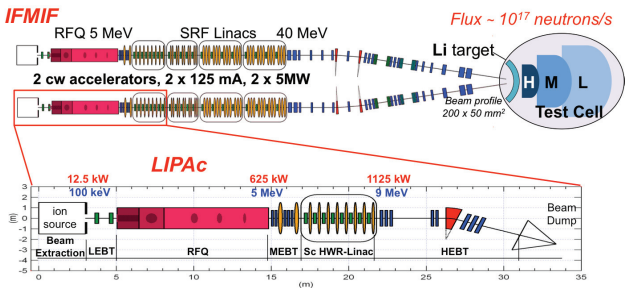

Figure 1: IFMIF facility (top) and LIPAc (bottom) [4].

In this paper, we will introduce a few challenges that LIPAc has to cope with as well as their impact on diagnostics. Then, a quick diagnostic overview will be given before to focus on the most challenging one.

IFMIF & LIPAc CHALLENGES

D^+ particles will be accelerated firstly by the source extraction system up to 100 keV [5] and then injected into the RFQ. At the RFQ exit [6], the 125 mA cw beam is bunched at 175 MHz with deuteron energy of 5 MeV. The first accelerating cryomodule (Superconductive Radio Frequency Linac or SRF Linac) with its half wave resonators (HWR) will give a last kick to reach the final LIPAc energy of 9 MeV [7]. Up to here, both LIPAc and IFMIF accelerators are identical. For IFMIF, three additional accelerating cryomodules will be added to reach 40 MeV.

Figure 2 [4] summarize the average beam power versus the beam energy for various linear facilities showing that IFMIF is the most powerful accelerator at given beam energy.

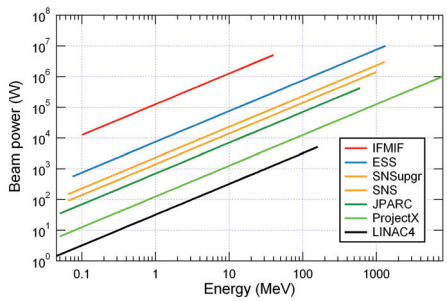

Figure 2: Average beam power for various linear facilities versus beam energy.

ISBN 978-3-95450-119-9

INTENSITY IMBALANCE OPTICAL INTERFEROMETER BEAM SIZE MONITOR*

M.J. Boland, Australian Synchrotron, Clayton, Victoria, Australia
T. Mitsuhashi, T. Naito, KEK, Ibaraki, Japan
K.P. Wootton, The University of Melbourne, Victoria, Australia

Abstract

The technique of measuring the beam size in a particle accelerator with an optical interferometer with the Mitsuhashi apparatus is well established and one of the only direct measurement techniques available. However, one of the limitations of the technique is the dynamic range and noise level of CCD cameras when measuring ultra low emittance beams and hence visibilities close to unity. A new design has been successfully tested to overcome these limitations by introducing a known intensity imbalance in one of the light paths of the interferometer. This modification reduces the visibility in a controlled way and lifts the measured interference pattern out of the noise level of the CCD, thus increasing the dynamic range of the apparatus. Results are presented from tests at the ATF2 at KEK and on the optical diagnostic beamline at the Australian Synchrotron storage ring.

OPTICAL INTERFEROMETRY

The Mitsuhashi apparatus [1] for measuring the first order spatial coherence of a beam of charged particles that emit synchrotron radiation is well established and used on many accelerators. The technique samples two parts of the diverging visible light beam using a double slit type configuration.

Using a focussing mirror the beams from each slit are brought together to form an interference pattern that is recorded with a CCD camera. A mirror is currently used to focus the beams since mirrors can be constructed with a larger aperture and with better roughness and dig-scratch performance than a lens of the same aperture. A parabolic mirror can be made with relatively few aberrations drawing on the experience of astronomical mirrors for telescopes. In essence to start to construct an interferometer the first step is to build a telescope to image the beam. Once a good optical path has been established the interferometer components can be added step by step to construct the Mitsuhashi apparatus for measuring the first order spatial coherence. A narrow bandpass filter is added to simplify the analysis, for example $\omega = 500$ nm, $\Delta\omega = 10$ nm. A polariser is used to select the σ-mode of the synchrotron radiation so as to distinguish it from the π-mode which produces a interference pattern with a phase shift that washes out the interferogram. If more intensity is needed for low beam currents it is possible to use a wider bandpass filer of 80 nm to increase the light, however the analysis of the data will have to take this into account.

* Work supported by a JSPS Travel Fellowship.

A typical example of an interference pattern produced with the Mitsuhashi apparatus is shown in Fig. 1:

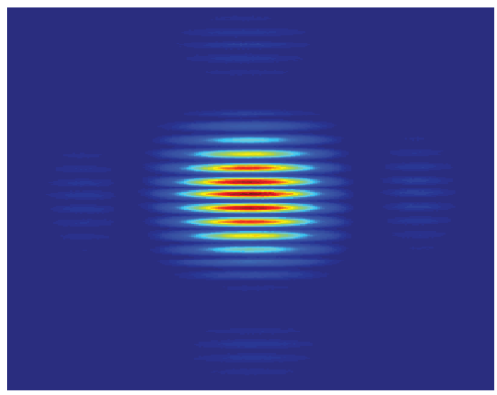

Figure 1: A typical interference pattern created by the Mitsuhashi apparatus for measuring beam sizes.

LIMITATIONS OF A CONVENTIONAL INTERFEROMETER

In modern accelerators where the vertical emittance is being pushed lower and lower, towards sub-picometre radian level, the beam size becomes very small and is highly spatially coherent. This means that the visibility of the interference pattern is very close to unity and the troughs dip down into the noise floor of the CCD that is recording the pattern. As a consequence the Mitsuhashi apparatus is practically limited by the signal to noise ratio of the CCD camera. At ATF2 optical beamline in the injection area the beam size was measured by the interferometer to be 5 µm with an error of less than 1 µm [2], which was mostly due to the CCD noise. The CCD by Hamamatsu [3] is one of the best performing on the market, with a low noise level and a very linear response across the range required for the interferometer, so a modification of the technique was required to improve the performance at very high spatial coherence.

INTENSITY IMBALANCE TECHNIQUE

The intensity distribution of the interference pattern created by light of wavelength λ passing through a double slit of hieght a, slit separation D and a distance R from the source with a certain polarisation is given by [2]

$$I(y) = I_0 \mathrm{sinc}\left(\frac{2\pi a}{\lambda R} y\right)^2 \left[1 + |\mathcal{V}| \cos\left(\frac{2\pi D}{\lambda R} y + \phi\right)\right],$$

ISBN 978-3-95450-119-9

ANALYSIS OF THE ELECTRO-OPTICAL FRONT END FOR THE NEW 40 GHz BUNCH ARRIVAL TIME MONITOR*

A. Kuhl†, J. Rönsch-Schulenburg, J. Roßbach, Universität Hamburg, Germany
M.K. Czwalinna (née Bock), M. Bousonville, H. Schlarb, C. Sydlo, DESY, Hamburg, Germany
S.M. Schnepp, Laboratory for Electromagnetic Fields and Microwave Electronics (IFH), ETH Zurich, Switzerland
T. Weiland, Institut für Theorie Elektromagnetischer Felder, Technische Universität Darmstadt, Germany
A. Angelovski, R. Jakoby, A. Penirschke, Institut für Mikrowellentechnik und Photonik, Technische Universität Darmstadt, Germany

Abstract

The Free-electron LASer in Hamburg (FLASH) is currently equipped with four Bunch Arrival time Monitors (BAMs) which achieve a measurement accuracy below 10 fs for bunch charges higher than 500 pC. In order to achieve single spike FEL pulses at FLASH, electron bunch charges down to 20 pC are required. To achieve a measurement accuracy of 10 fs also at such a small bunch charge a new BAM containing new pickups with a bandwidth of up to 40 GHz has been designed and manufactured. The signal of the pickups will be evaluated using a time-stabilized reference laser pulse which is modulated with an Electro-Optical intensity Modulator (EOM). The theoretical measurement accuracy depends on several parameters and their fluctuations. The impact of these fluctuations on the measurement accuracy will be discussed.

INTRODUCTION

The Free-electron LASer in Hamburg (FLASH) is a source of short photon pulses tunable within a wavelength range from 4.12 to 45 nm [1]. It is equipped with four Bunch Arrival time Monitors (BAMs), which provide a measurement accuracy below 10 fs for bunch charges above 0.5 nC [2]. In order to reach FEL pulses with a duration of a single mode only low bunch charges are required. For FLASH a bunch charge down to 20 pC is necessary [3]. Thus a BAM is required which allows the determination of the arrival time with a precision of 10 fs for bunch charges down to 20 pC. Therefore, a new pickup with a bandwidth of 40 GHz has been developed [4, 5, 6] and installed at FLASH. Besides the new pickup, a new electro-optical front-end is required for such a new BAM. The new front-end will use an electro-optical modulator (EOM) with a bandwidth of 40 GHz which corresponds to the bandwidth of the new pickup. Also a new readout electronic based on μTCA 4 [7] will be used. In order to preserve the large operating range of the bunch charges up to 3 nC a special wiring scheme is needed.

* The work is supported by Federal Ministry of Education and Research of Germany (BMBF) within FSP 301 under the contract numbers 05K10GU2 and 05K10RDA.

† alexander.kuhl@desy.de

PRINCIPLE OF MEASUREMENT

The arrival times of the electron bunches are detected with a pickup and compared with the timing of a laser pulse which is synchronized to a reference master oscillator. The new 40 GHz pickup contains four cone-shaped pick-up electrodes [4]. The electro-magnetic field of an electron bunch passing the BAM induces a short bipolar RF signal in each of the four pick-up electrodes. The RF signals of opposite pickup electrodes are combined to increase the amplitude and to reduce the influence on the orbit position of the electron bunches of the measured arrival time. One of these RF signals is directed to a 40 GHz EOM. This branch will be used as a fine channel with a high accuracy for the low bunch charge operation mode, but for high charges the amplitude of the pickup signal rises above the usable range of the EOM. The other branch is carried to a 10 GHz EOM (see Fig. 1). This branch will be used as coarse channel in low bunch charge mode and as standard channel for the high charge operation at FLASH. The laser pulse from the synchronisation system is approximately 100 times shorter than the RF signal pulse and the ratio of the laser amplitude of the output signal of the EOM (I_{out}) and the input signal (I_{in}) is given by the following equation [8]:

$$\begin{aligned} M_{\text{signal}} &= \frac{I_{\text{out}}}{I_{\text{in}}} \\ &= \cos^2\left(2\delta_0 + \frac{2\pi U_{\text{bias}}}{U_{\pi,\text{bias}}} + \frac{2\pi U_{\text{RF}}(t)}{U_{\pi,\text{RF}}}\right) \\ &= \frac{1}{2} + \frac{1}{2}\cos\left(\delta_0 + \frac{\pi U_{\text{bias}}}{U_{\pi,\text{bias}}} + \frac{\pi U_{\text{RF}}(t)}{U_{\pi,\text{RF}}}\right) \end{aligned} \quad (1)$$

The parameters δ_0, $U_{\pi,\text{bias}}$, and $U_{\pi,\text{RF}}$ are device specific constants of the EOM. The intrinsic operation point is presented by δ_0. $U_{\pi,\text{bias}}$ and $U_{\pi,\text{RF}}$ are the voltages to change the modulation M between 0 and 1 at the bias port respectively at the RF port. By setting the modulation to $M = 0.5$ with a DC bias voltage U_{bias} an optimized determination of the timing difference between the RF and the laser pulse at the EOM are feasible. With a correct timing of the electron bunch, the zero-crossing of the RF signal reaches the EOM at the same time as the reference laser pulse and the output of the EOM will be $M = 0.5$. When the electron

ISBN 978-3-95450-119-9

RECENT PROGRESS IN SR INTERFEROMETER

T. Mitsuhashi#, KEK, Tsukuba, Japan

Abstract

Beam size measurement in accelerator is very important to evaluate beam emittance. SR interferometer has been used as one of powerful tools for measurement of small beam size through special coherence of visible SR. Recent progresses in this technique improve measurable range for smaller beam size less than 10μm. An application of reflective optics to eliminate chromatic aberration in focus system in SR interferometer makes it possible to measure the beam size down to 3μm range. In recent few years an imbalance input technique is developed to introducing magnification into the interferometer.

INTRODUCTION

The synchrotron radiation (SR) monitor based on visible optics is one of the most fundamental diagnostic tools in the high energy accelerators. The monitor gives a static and dynamic observation for visible beam profile, beam size, longitudinal profile, etc. These greatly improve the efficiency of commissioning and operation of the accelerator. In this monitor, the visible SR is extracted by a mirror from the SR source such as bending magnet in accelerator, then the SR guided into the optical diagnostics systems. During these years, the development of the SR interferometer has been the most significant topic. The idea of the SR interferometer for measurement of beam profile and size struck me while I was performing experiments to investigate the coherence of synchrotron radiation in 1997 [1]. Nowadays, the SR interferometer is recognized as a powerful tool for easily measuring small beam sizes [2]. Recent progresses in improve measurable range for smaller beam size. An application of reflective optics to eliminate chromatic aberration in focus system makes it possible to measure the beam size down to 3μm range [3]. In recent few years, an imbalance input technique is developed to introducing magnification into the interferometer [4]. A simple introduction for interferometry, and results are introduced in the first half, and in the second half, recent progresses on SR interferometer are introduced in this paper.

BEAM PROFILE AND SIZE MEASUREMENT WITH INTERFEROMETRY

The measurements of beam profile and size are most important issues in optical monitor. The most conventional method to observe the beam profile is making an optical image of the beam. The resolution of this method is generally limited by diffraction phenomena. In the usual configuration of the imaging system, the RMS size of diffraction (1σ of the point spread function) is not smaller than 50 μm. Since, research and development in electron storage rings (especially in reducing the beam emittance) has been very remarkable in last few ten years, the above-mentioned profile monitor via imaging system becomes ineffective in precise quantitative measurements of the beam profile and size due to the diffraction resolution limit.

In visible optics, the interferometry is one of the standard methods for measuring the profile or size of very small objects such as angular dimension of the star. The principle to measure the profile of an object by means of spatial coherency was first proposed by H. Fizeau in 1898 [5], and is now known as the Van Cittert-Zernike theorem [6] with their work in 1932 (Van Cittert) and 1933 (Zernike). It is well known that A. A. Michelson measured the angular dimension (extent) of a star with this concept [11] with his stellar interferometer in 1935. The SR interferometry for the measurement of the spatial coherence of visible region of the SR beam was first performed by author in 1997 [1]. And in the same time, the author demonstrated that this method is applicable to measure the beam profile and size. Since the SR beam from a small electron beam has better spatial coherence, this method is suitable for measuring a small beam size. The characteristics of this method are: 1) one can measure beam sizes as small as 10 μm range with 1-μm resolution in a non-destructive manner using visible light (typically 500 nm); 2) the measurement time is a 1-2 seconds for size measurement; 3) due to self-consistency in interferometry, this method is classified in an absolute measurement. For the point 3), the absolute measurement means all the free parameters in interferometry such as wavelength are measured by interferometry and a ruler. In this meaning, interferometry is classified into one of most fundamental measurement method. Otherwise, other methods, such as imaging always use information from interferometry, such as wavelength.

THEORETICAL BACKGROUND OF THE INTERFEROMETRY

According to the work of H. Fizeau in 1868 [5], the visibility (contrast) of the interference fringe taken by an interferometer, is higher for a small light source and lower for a large light source. As the smallest limit of light source, a point source gives an interferogram with visibility 1. We now interpret the point source as the single mode of a photon which gives an interferogram of visibility 1. We can represent the general light source by an ensemble of point sources. Let us assume each point source has no 1st order temporal coherence. The interferogram given by such an ensemble of point sources are superimposed and the interference fringe is smeared. Then, the visibility of the obtained

#toshiyuki.mitsuhashi@kek.jp

ISBN 978-3-95450-119-9

BIW 2012 HIGHLIGHTS & HISTORY

K. Jordan [JLAB, Newport News, Virginia, USA]

Abstract

The final Beam Instrumentation Workshop, hosted by Jefferson Lab, was held in Newport News Virginia, April 15 - 19, 2012. The series of 15 meetings, spanning 23 years began at Brookhaven National Lab, adopted the Faraday Cup Award to recognize excellence in particle beam diagnostics instruments, and culminated in a transition to a 3 year cycle with DIPAC & a new Asian meeting; the IBIC. This presentation gives highlights of the spring meeting and a bit of nostalgia of the past events.

CONTRIBUTION NOT RECEIVED

ISBN 978-3-95450-119-9

OPERATION OF A SINGLE PASS, BUNCH-BY-BUNCH X-RAY BEAM SIZE MONITOR FOR THE CESR TEST ACCELERATOR RESEARCH PROGRAM*

N.T. Rider, M. G. Billing, M.P. Ehrlichman, D.P. Peterson, D. Rubin, J.P. Shanks, K. G. Sonnad,
CLASSE, Cornell University, Ithaca, NY 14853, U.S.A.
M. A .Palmer, Fermilab, Batavia, IL 60510, U.S.A.
J.W. Flanagan, KEK, Ibaraki 305-0801, Japan

Abstract

The CESR Test Accelerator (CESRTA) program targets the study of beam physics issues relevant to linear collider damping rings and other low emittance storage rings. This endeavour requires new instrumentation to study the beam dynamics along trains of ultra low emittance bunches. A key element of the program has been the design, commissioning and operation of an x-ray beam size monitor capable, on a turn by turn basis, of collecting single pass measurements of each individual bunch in a train over many thousands of turns. This new instrument utilizes custom, high bandwidth amplifiers and digitization hardware and firmware to collect signals from a linear InGaAs diode array. The instrument has been optimized to allow measurements with $3x10^9$ to $1x10^{11}$ particles per bunch. This paper reports on the operational capabilities of this instrument, improvements for its performance, and the methods utilized in data analysis. Examples of key measurements which illustrate the instrument's performance are presented. This device demonstrates measurement capabilities applicable to future high energy physics accelerators and light sources.

INTRODUCTION

The X-ray Beam Size Monitor (xBSM) provides experimenters in the CESRTA program with the ability to measure the vertical beam size of individual particle bunches on a turn-by-turn, single pass basis. At present two xBSM instruments have been installed in experimental areas of the Cornell High Energy Synchrotron Source (CHESS). One is used for positrons and the other is used for electrons. Each setup has its own x-ray source, which is a dipole magnet within the Cornell Electron Storage Ring (CESR). The critical energy is 0.6 keV during 2 GeV CESRTA operations. A set of in-vacuum optics focuses the photon flux onto the detector. The geometry of the beam line provides an optical magnification of 2.34 for the positron line and 2.52 for the electron line. A continuous vacuum vessel, containing optics elements and filters which are inserted into the x-ray beam, extends from the x-ray source to the detector. Images are collected via a custom data acquisition system. Figure 1 shows the functional layout of the positron line. The electron line is a near mirror image.

*Work supported by NSF grant PHY-0734867, PHY-1002467 and DOE grant DE-FC02-08ER41538, DE-SC0006505

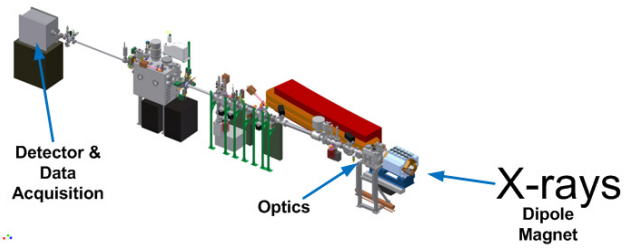

Figure 1: Layout of the xBSM positron line

VACUUM

A multi-stage differential pumping scheme has been implemented to allow "windowless" transmission path from the x-ray source to the detector. The scheme features a series of apertures, turbo pumps and gate valves along the x-ray beam line. This setup allows us to have electronics (printed circuit board, cables, etc) which are not vacuum compatible within the detector box without contaminating CESR. This is critical for the proper operation of the instrument. The vacuum system pressure is automatically controlled and monitored via programmable logic controllers.

DETECTOR

The detector is a vertical linear array of 32 InGaAs diodes with a 50 μm pitch and horizontal width of 400 μm. The InGaAs layer is 3.5 μm thick, and absorbs 73% of photons at 2.5 keV. The time response of the detector is sub-nanosecond.

OPTICS

The xBSM utilizes four different optical elements. For all beam energies, a vertically limiting slit (referred to as a pinhole) is available. For beam energies less than 2.5 GeV, a low energy Fresnel zone plate and a coded aperture are available. At 4 GeV and greater, a high power coded aperture can be inserted into the x-ray beam. The low energy optics are contained on one "chip" which is made from a 2.5 μm silicon substrate with a 0.7 μm layer of gold forming the optical features. The high energy coded aperture is made from a 625 μm silicon substrate with a 10 μm layer of gold. The coded aperture features of the high energy optics are the same but one half the scale of the low energy optics. Figure 2 shows the coded aperture features.

ISBN 978-3-95450-119-9

BEAM POSITION MONITORS FOR CIRCULAR ACCELERATORS

Shigenori Hiramatsu
KEK, 1-1 Oho, Tsukuba, Ibaraki, 305-0801, Japan

Abstract

Beam position monitor (BPM) systems are one of the most important system for tuning up accelerators to accelerate charged particle beams in a good condition. BPMs measure the betatron orbit or the closed orbit of the circulating beam in the accelerator, and beam optics parameters $\beta(s)$, betatron phase advance $\phi(s)$, etc. can be evaluated from the BPM data. For tuning up accelerators, it is required that BPMs can measure beam orbits accurately. To realize BPM system with good accuracy, we have to concern many issues related to the BPM system.

BEAM INDUCED CHARGE DISTRIBUTION ON BEAM CHAMBERS

Electrostatic type BPM pickups detect the beam induced charge imbalance among pickup electrodes. To investigate induced charge on pickup electrodes, it is helpful to investigate the beam induced charge distribution on the beam chamber surface. For the case of the beam chamber with circular cross section, the pencil beam located at

$$(x, y) = (r\cos\theta, r\sin\theta)$$

induces the surface charge density distribution on the chamber surface expressed as

$$\sigma(R,\phi) = -\frac{\lambda}{2\pi R}\cdot\frac{R^2 - r^2}{R^2 + r^2 - 2rR\cos(\phi-\theta)} = -\frac{\lambda}{2\pi R}\left\{1 + 2\sum_{n=1}^{\infty}\left(\frac{r}{R}\right)^n \cos n(\phi-\theta)\right\}, \quad (1)$$

where λ is the line charge density of the beam, R is the radius of the chamber, and ϕ is the azimuth.

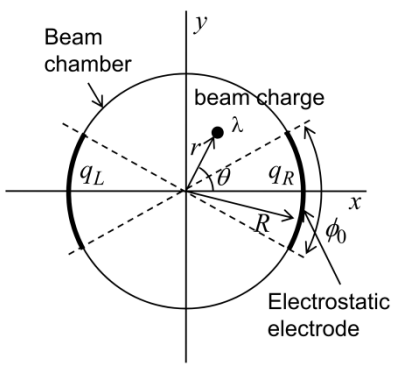

Figure 1: Cross section of BPM pickup model.

When two pickup electrodes with angular width ϕ_0 are placed at 0° and 180° as shown in Fig. 1, the induced charge on the electrodes q_R and q_L are given by the integration of Eq. (1) in the region of $(-\phi_0/2, \phi_0/2)$ and $(\pi-\phi_0/2, \pi+\phi_0/2)$ for ϕ. The response of the difference q_R-q_L normalized by the sum q_R+q_L for the beam position x is shown in Fig. 2. The difference-over- sum ratio (Δ/Σ) of the induced charge on two electrodes is proportional to the beam position displacement in x-direction from the chamber center [1] in the vicinity of the camber center (r<<R),

$$\frac{q_R - q_L}{q_R + q_L} = \kappa x, \quad (2)$$

where the sensitivity factor κ is given by

$$\kappa = \frac{2\sin(\phi_0/2)}{R\phi_0/2}. \quad (3)$$

Figure 2 shows dependence of Δ/Σ on the beam position x for y=0. It is noted that the dependence of $\log(q_R/q_L)$ is more linear than that of Δ/Σ.

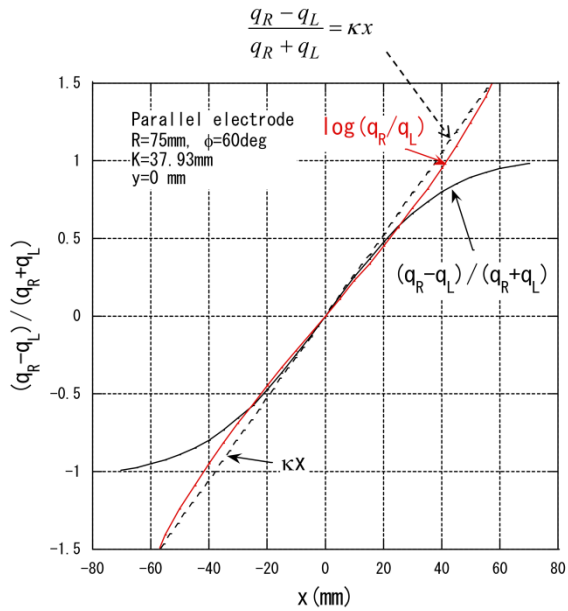

Figure 2: Response of Δ/Σ of the induced charge on the electrodes for the beam position x with the assumption of y=0.

Finite Boundary Element Methods

For the arbitrary shape of the chamber cross section, the beam induced charge can be calculated using the finite boundary element method [2]. The two dimensional potential $\phi(\boldsymbol{r})$ in the beam chamber is given by

$$\phi(\boldsymbol{r}) = \oint_{\text{surface}} \ln\left(\frac{1}{|\boldsymbol{r} - \boldsymbol{r}'(s)|}\right)\sigma(s)ds + \lambda\ln\left(\frac{1}{|\boldsymbol{r} - \boldsymbol{r}_0|}\right). \quad (4)$$

In the right hand side, the 1st term and 2nd term are the potential caused by the induced charge density $\sigma(s)$ on the chamber surface and the beam charge λ, respectively.

ISBN 978-3-95450-119-9

ELECTRON-LENS TEST STAND INSTRUMENTATION PROGRESS*

T. A. Miller†, J. Aronson, D. M. Gassner , X. Gu, A. Pikin, P. Thieberger,
C-AD, BNL, Upton, NY, 11973, U.S.A.

Abstract

In preparation for installation of Electron Lenses [1] into RHIC, planned for late 2012, a working test stand (or "test bench") is in use testing the performance of the gun, collector, modulator, instrumentation and controls. While testing & operating the instrumentation, both progress and pitfalls were encountered. Results are presented from issues including ground loop signals generated by the DCCTs, static magnetic field interference, competing YAG screen illumination techniques, YAG crystal damage during beam operation, performance of the four quadrant beam scraper electrodes, and challenges in measuring beam current in conductors. Working knowledge and insight into each of these systems has been gained through difficulties leading to success. These insights are presented with supporting data and images.

INTRODUCTION

The major components of this test bench [2] include an electron gun (tested from 500ns to DC, 1.0A, 5keV) and an electron collector, normal & superconducting solenoids, a 5kV collector power supply (CPS) between gun & collector, and a 10kV fast modulator controlling the gun's anode. The system is equipped with pulse & DC current transformers at the gun and collector power supply, a beam profile monitor composed of both YAG crystal screen & camera and a pin hole Faraday cup intercepting the scanned electron beam, a four quadrant halo monitoring electrode array mounted just upstream of the collector, and an ion collecting Faraday cup electrode within the collector just downstream of the electron reflector [3]. As a complete overview of the diagnostics used was presented last year [4], details and experiences learned during recent system tests are presented in their respective sections below.

CURRENT MEASUREMENT

Beam current measurement is made with both DCCTs and pulse CTs placed on the conductors near the gun and collector connections, as shown in Fig. 1. The DCCT is a Bergoz IPCT-C-02 providing a resolution of 10uA over a range of 1-2000mA through a 2.7" aperture. It is sensitive from DC down to 100us pulses. The pulse CT is a Pearson model 6585 with 1V/A ratio, 50Ω output, 1.5ns rise time and a 0.3%/µs droop. This arrangement provides measurement of 1 – 5µs pulses without a noticeable droop and pulses longer than 100µs out to DC. However, ringing of the current pulse edges in the conductors obscures pulse shapes over the first 15µs.

* Work supported by B.S.A, LLC under contract No. DE-AC02-98CH10886 with the U.S. Department of Energy.
†tmiller@bnl.gov

Ground Current Problems in Pulsed Mode

As the 5kV CPS has its collector side grounded, a current transformer was installed in the ground connection in an attempt to measure ground return currents from beam loss to the grounded vacuum structure. Aside from the ringing on the pulses (discussed in the next section), a large distortion of the pulse was measured in the gun CT that was exactly compensated by an opposite distortion in the ground CT. Note that in the waveforms shown in Fig. 1, the summation (gold) of the gun (red) and ground (blue) current pulses exactly equaled that measured at the collector (yellow).

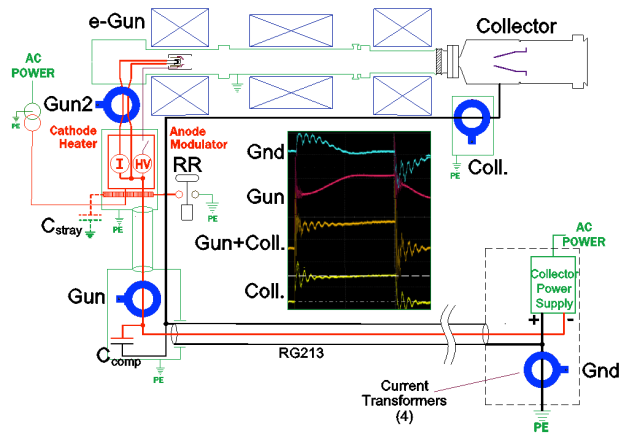

Figure 1: Current measurement system layout. Ground return currents found during pulsed beam operation impede attempts to measure beam loss currents.

The onset of the beam pulse current is believed to be supplied by stray capacitance of the floating instrument racks containing the gun power electronics on the cathode HV deck. This capacitance is shown in Fig. 1 as C_{stray}. An attempt to compensate for this undesired return path to the CPS via ground was made by installing a 5µF HV storage capacitor just before the gun CT, as shown in Fig. 1 as C_{comp}. This completely eliminated the ground coupled beam pulse current, except for the ringing, and brought agreement between the gun and collector CTs.

Ringing in Pulsed Beam Current Measurements

Initially, the fast edges (~50ns) of the beam pulse caused ringing in the currents measured by the gun, collector as well as ground CTs. Attempts were made to mitigate this ringing by adding RC filters (0.1µF, 50Ω) to either side of the 50Ω RG213 HV coaxial cable bringing power from the CPS to the cathode deck. However, these attempts have proved unfruitful.

Further attempts were made, such as providing a capacitive bypass around the ceramic break, shown in Fig.

ISBN 978-3-95450-119-9

TWISTING WIRE SCANNER

V. Gharibyan*, A. Delfs, I. Krouptchenkov, D. Noelle, H. Tiessen, M. Werner, K. Wittenburg
Deutsches Elektronen-Synchrotron DESY, Hamburg, Germany

Abstract

A new type of 'two-in-one' wire scanner is proposed. Recent advances in linear motors' technology make it possible to combine translational and rotational movements. This will allow to scan the beam in two perpendicular directions using a single driving motor and a special fork attached to it. Vertical or horizontal mounting will help to escape problems associated with the 45 deg scanners. Test results of the translational part with linear motors will be presented.

INTRODUCTION

Wire scanners serve as an essential part of accelerator diagnostic systems and are used mostly for beam transverse profile measurements (for a review see [1]). Depending on scanning wire trajectory the profilers could be classified as rotational [2] or linear [3]. When its necessary to measure vertical and horizontal beam profiles at the same longitudinal position one has to use two independent scanners. Alternatively two profiles could be sampled by using a single driver mounted at 45deg with two wires stretched horizontally and vertically over a fork attached to this linear driver. However, wire vibration in the scanning direction is a known problem for the 45deg scanners [4, 5]. Different types of driver motors have been employed in order to move and control scanning wires which are normally mounted on cards or forks connected to the motors. Stepper or servo rotating motors are among the most popular drivers and linear motors are at developing stage. Here we explore commercially available translational-rotational motor units to propose a wire scanner solution which will perform beam scans in mutually perpendicular directions using a single linear-rotary motor and a simple wire hosting construction attached to it. The construction is a key-like wire holder which makes twisting (helical) motion during a 2-D scan. Next will follow a more detailed description of the translational part with linear motors. In conclusion we will estimate technical feasibility of the proposed twisting scanner.

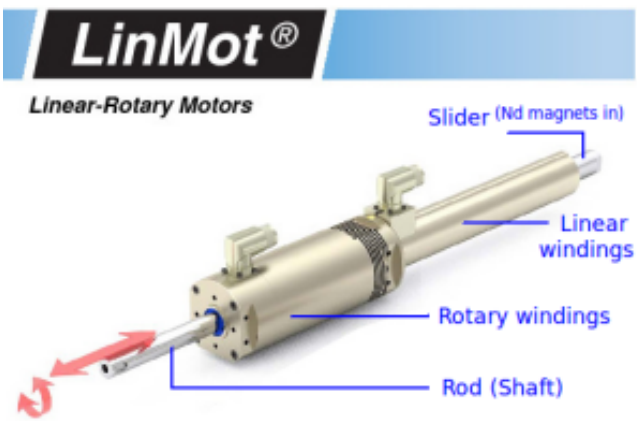

Figure 1: Linear-rotary motor from LinMot company.

LINEAR-ROTARY MOTORS

A linear-rotary motor produced by company LinMot [6] is shown in Fig. 1. The motor consists of a linear and a rotary part merged together. Translational and rotational motions are decoupled and organized independently. However, linear and rotary motion synchronization is foreseen by motor controller logic. The motors are provided in different configurations with variable sizes and strengths reaching up to 1 kN linear force and 7.5 Nm rotating torque. Motor controllers use advanced and flexible software/firmware which should help to perform slow or fast scans with minimal programming efforts. An operational voltage of 72VDC and maximal current of 15A complies to general Electro-Magnetic Interference (EMI) requirements in accelerator environments. Described features make the linear-rotary motor as an attractive tool for driving the proposed twisting wire scanner. A closer

Table 1: LinMot PR01-52x60-R/37x120F-HP-100 Linear-rotary Motor Parameters

Parameter	Value
Linear Motion	
Extended Stroke ES mm (in)	100 (3.94)
Standard Stroke SS mm (in)	100 (3.94)
Peak Force E12x0 - UC N (lbf)	255 (57.3)
Cont. Force N (lbf)	51 (11.5)
Cont. Force Fan cooling N (lbf)	92 (20.7)
Force Constant N/A (lbf/A)	17 (3.8)
Max. Current @ 72VDC A	15
Max. Velocity m/s (in/s)	3.9 (154)
Position Repeatability mm (in)	$\pm$0.05 ($\pm$0.0020)
Linearity %	$\pm$0.10
Rotary Motion	
Peak Torque Nm (lbfin)	2 (17.7)
Constant Torque (Halt) Nm (lbfin)	0.5 (4.4)
Max. Number of revolutions Rpm	1500
Torque Constant Nm/Arms (lbfin/Arms)	0.46 (4.07)
Max. Current @ 72VDC Arms	6.2
Repeatability deg	$\pm$0.05

* vahagn.gharibyan@desy.de

ISBN 978-3-95450-119-9